# MULTIUSER DEMODULATION FOR DS-CDMA SYSTEMS IN FADING CHANNELS

*MARKKU JUNTTI*

Department of Electrical Engineering

OULU 1998

*MARKKU JUNTTI*

# MULTIUSER DEMODULATION FOR DS-CDMA SYSTEMS IN FADING CHANNELS

Academic Dissertation to be presented with the assent of The Faculty of Technology, University of Oulu, for public discussion in Raahensali (Auditorium L 10), Linnanmaa, on October 17th, 1997, at 12 noon.

OULUN YLIOPISTO, OULU 1998

Manuscript received 16 Sebtember 1997
Accepted 18 Sebtember 1997

Communicated by
Professor Timo Laakso
Professor Sergio Verdú

ISBN 951-42-4755-8
(URL: http://herkules.oulu.fi/isbn9514247558/)

ALSO AVAILABLE IN PRINTED FORMAT

ISBN 951-42-4632-2
ISSN 0355-3213 (URL: http://herkules.oulu.fi/issn03553213/)

OULU UNIVERSITY LIBRARY
OULU 1998

*Dedicated to my family.*

**Juntti, Markku**, **Multiuser demodulation for DS-CDMA systems in fading channels**
Department of Electrical Engineering, University of Oulu, FIN-90570 Oulu, Finland
*Acta Univ. Oul. C 106, 1997*
Oulu, Finland

(Manuscript received 16 September, 1997)

***Abstract***

Multiuser demodulation algorithms for centralized receivers of asynchronous direct-sequence (DS) spread-spectrum code-division multiple-access (CDMA) systems in frequency-selective fading channels are studied. Both DS-CDMA systems with short (one symbol interval) and long (several symbol intervals) spreading sequences are considered.

Linear multiuser receivers process ideally the complete received data block. The approximation of ideal infinite memory-length (IIR) linear multiuser detectors by finite memory-length (FIR) detectors is studied. It is shown that the FIR detectors can be made near-far resistant under a given ratio between maximum and minimum received power of users by selecting an appropriate memory-length. Numerical examples demonstrate the fact that moderate memory-lengths of the FIR detectors are sufficient to achieve the performance of the ideal IIR detectors even under severe near-far conditions.

Multiuser demodulation in relatively fast fading channels is analyzed. The optimal maximum likelihood sequence detection receiver and suboptimal receivers are considered. The parallel interference cancellation (PIC) receiver is demonstrated to achieve better performance in known channels than the decorrelating receiver, but it is observed to be more sensitive to channel coefficient estimation errors than the decorrelator. At high channel loads the PIC receiver suffers from bit error rate (BER) saturation, whereas the decorrelating receiver does not. Choice of channel estimation filters is shown to be crucial if low BER is required. Data-aided channel estimation is shown to be more robust than decision-directed channel estimation, which may suffer from BER saturation caused by hang-ups at high signal-to-noise ratios.

Multiuser receivers for dynamic CDMA systems are studied. Algorithms for ideal linear detector computation are derived and their complexity is analyzed. The complexity of the linear detector computation is a cubic function of $KL$, where $K$ and $L$ are the number of users and multipath components, respectively. Iterative steepest descent, conjugate gradient, and preconditioned conjugate gradient algorithms are proposed to reduce the complexity. The computational requirements for one iteration are a quadratic function of $KL$. The iterative detectors are also shown to be applicable for parallel implementation. Simulation results demonstrate that a moderate number of iterations yields the performance of the corresponding ideal linear detectors. A quantitative analysis shows that the PIC receivers are significantly simpler to implement than the linear receivers and only moderately more complex than the conventional matched filter bank receiver.

*Keywords:* channel estimation, interference cancellation, decorrelation, iterative detection

# Preface

Research for this thesis has been carried out mostly in the spread-spectrum research group in the Telecommunication Laboratory, Department of Electrical Engineering, University of Oulu, Oulu, Finland. The work towards the thesis was initialized in August 1993 after I had completed the Master's thesis in May 1993. The first year of the research included mostly literature study. From September 1994 to October 1995 I was a visiting scholar at Department of Electrical and Computer Engineering, Rice University, Houston, Texas, USA in Professor Behnaam Aazhang's research group. During that time the major part of the research leading to the results in Chapters 3 and 5 was conducted. After completing the work carried out at Rice University the research for the results in Chapter 4 was performed at the University of Oulu in the second half of the year 1996.

I wish to express my gratitude to my advisors Docent Jorma Lilleberg and Professor Behnaam Aazhang for their comments and guidance throughout the work. My warmest thanks are also due to my supervisor Associate Professor Pentti Leppänen for providing me the opportunities to work on this interesting topic and for guidance in my postgraduate studies. The help provided by Professor Savo Glisic, Professor Emeritus Juhani Oksman and Dr. Juha Ylitalo on various issues and especially in getting the necessary financial support has also been invaluable. I am grateful to the reviewers of the thesis Professor Timo Laakso from Helsinki University of Technology, Espoo, Finland, and Professor Sergio Verdú from Princeton University, Princeton, New Jersey, USA.

I would like to thank numerous members of the spread-spectrum research group at the Telecommunication Laboratory of University of Oulu, as well as the faculty and students at Department of Electrical and Computer Engineering of Rice University for the challenging environments to pursue research. The co-operation and joint work with Matti Latva-aho has proven to be very fruitful. I am also grateful to Markku Heikkilä, who performed the simulations for Chapter 4. The discussions with Dr. Kishore Kota and Dr. Markus Lang have been of great value. Thanks are due to Jari Iinatti, Pertti Järvensivu, Matti Latva-aho, Harri Saarnisaari, Pekka Kaasila, and Tero Ojanperä who read and commented the manuscript. The help on various computer problems provided by Veikko Hovinen, Dr. Markus Lang, Pekka Nissinaho, Dr. Jan Erik Odegard, Harri Saarnisaari, and Jari Sillanpää has been

invaluable.

The financial support provided by the Academy of Finland, Elektrobit, Ltd., the Graduate School in Electronics, Telecommunications, and Automation, Finnish Air Force, Nokia Mobile Phones, Ltd., Nokia Telecommunications, Ltd., Rice University, the Technology Development Centre of Finland, the University of Oulu, as well as the following Finnish foundations: Emil Aaltosen Säätiö, Jenny ja Antti Wihurin Rahasto, Oy Nokia Ab:n Säätiö, Tauno Tönningin Säätiö, and Tekniikan Edistämissäätiö enabled this work and is thus gratefully acknowledged.

I am grateful to my father Aarno and to my late mother Kaija for the help, support, and love they have provided for me throughout my life. The positive attitude towards education in our home has been an important driving force for my later studies.

I wish to express my deepest thanks to my family, my wife Hanna for the love and support she has shown to me, and to my children Tuomas (three years) and Kaisa (one year) for the understanding they have shown in their own ways. Without Hanna's highly positive attitude the thesis would not have been completed.

Oulu, September 15, 1997 Markku Juntti

# List of original publigations

The thesis is in part based on the following original publications, which are referred in the text by Roman numerals:

I Juntti M & Glisic S (1997) Advanced CDMA for wireless communications. In: Glisic SG & Leppänen PA (eds) Wireless Communications: TDMA Versus CDMA, Kluwer Academic Publishers, Chapter 4, p 447–490.

II Juntti MJ & Aazhang B (1995) Linear finite memory-length multiuser detectors. Proc. Communication Theory Mini-Conference (CTMC'95) in conjunction with IEEE Global Telecommunications Conference (GLOBECOM'95), Singapore, November 13–17, p 126–130.

III Juntti MJ, Aazhang B & Lilleberg JO (1996) Linear multiuser detection for R-CDMA. Proc. Communication Theory Mini-Conference (CTMC'96) in conjunction with IEEE Global Telecommunications Conference (GLOBECOM'96) London, U.K., November 18–22, p 127–131.

IV Juntti MJ & Aazhang B (1997) Finite memory-length linear multiuser detection for asynchronous CDMA communications. IEEE Transactions on Communications 45(5): p 611–622.

V Juntti MJ (1997) Performance of decorrelating multiuser receiver with data-aided channel estimation. Proc. Communication Theory Mini-Conference (CTMC'97) in conjunction with IEEE Global Telecommunications Conference (GLOBECOM'97), Phoenix, Arizona, USA, November 5–7.

VI Juntti MJ, Latva-aho M & Heikkilä M (1997) Performance Comparison of PIC and Decorrelating Multiuser Receivers in Fading Channels. Proc. IEEE Global Telecommunications Conference (GLOBECOM'97), Phoenix, Arizona, USA, November 3–8.

VII Juntti MJ (1995) Linear multiuser detector update in synchronous dynamic CDMA systems. Proc. IEEE International Symposium on Personal, Indoor and Mobile Radio Communications (PIMRC'95) Toronto, Ontario, Canada, September 27–29, 3: p 980–984.

VIII Juntti MJ, Aazhang B & Lilleberg JO (1996) Iterative implementation of linear multiuser detection. Proceedings of Conference on Information Sciences and Systems (CISS'96), Princeton University, Princeton, New Jersey, USA, March 20–22, 1: p 343–348.

IX Juntti MJ & Lilleberg JO (1996) Implementation aspects of linear multiuser detectors in asynchronous CDMA systems. Proceedings of IEEE International Symposium on Spread Spectrum Techniques and Applications (ISSSTA'96) Mainz, Germany, September 22–25, 2: p 842–846.

X Juntti MJ, Aazhang B & Lilleberg JO (1996) Iterative implementation of linear multiuser detectors for dynamic CDMA systems. IEEE Transactions on Communications, preliminarily accepted.

For clarity, the thesis is presented as a monograph and the original publications are therefore not reprinted.

# List of symbols and abbreviations

| | |
|---|---|
| $\mathbf{A}$ | diagonal matrix of transmitted complex amplitudes of all users at one symbol interval $(K \times K)$ |
| $A_k$ | transmitted complex amplitude of user $k$ |
| $\mathcal{A}$ | diagonal matrix of transmitted complex amplitudes of all users over all symbol intervals $(N_b K \times N_b K)$ |
| $\mathcal{A}^{(n)}$ | diagonal matrix of transmitted complex amplitudes of all users over symbol intervals inside the processing window $(NK \times NK)$ |
| $\bar{\mathcal{A}}^{(n)}$ | diagonal matrix of transmitted complex amplitudes of all users over symbol intervals inside the processing window plus the edge symbol intervals $((N+4)K \times (N+4)K)$ |
| $\mathcal{A}_e^{(n)}$ | diagonal matrix of transmitted complex amplitudes of all users over the edge symbol intervals $(4K \times 4K)$ |
| $\boldsymbol{b}$ | vector of data symbols of all users over all symbol intervals $(N_b K \times 1)$ |
| $\boldsymbol{b}^{(n)}$ | vector of data symbols of all users over symbol intervals inside the processing window $(NK \times 1)$ |
| $\bar{\boldsymbol{b}}^{(n)}$ | vector of data symbols of all users over symbol intervals inside the processing window plus the edge symbol intervals $((N+4)K \times 1)$ |
| $\mathbf{b}^{(n)}$ | vector of data symbols of all users at symbol interval $n$ $(K \times 1)$ |
| $\boldsymbol{b}_e^{(n)}$ | vector of data symbols of all users over the edge symbol intervals $(4K \times 1)$ |
| $b_k^{(n)}$ | data symbol of user $k$ at symbol interval $n$ |
| $\boldsymbol{c}$ | vector of the channel coefficients of all users over all symbol intervals $(N_b KL \times 1)$ |
| $\mathbf{c}^{(n)}$ | vector of the channel coefficients of all users at symbol interval $n$ $(KL \times 1)$ |
| $\mathbf{c}_k^{(n)}$ | vector of the channel coefficients of user $k$ at symbol interval $n$ $(L \times 1)$ |
| $\tilde{\mathbf{c}}_k^{(n)}$ | combining vector $(L \times 1)$ |

| | |
|---|---|
| $c_k^{(n)}(t)$ | channel impulse response of user $k$ at symbol interval $n$ |
| $c_{k,l}^{(n)}$ | channel complex coeffcient (gain) of $l$th multipath of user $k$ at symbol interval $n$ |
| $\mathbf{C}^{(n)}$ | matrix of the channel coefficient vectors of all users at symbol interval $n$ $(KL \times K)$ |
| $\tilde{\mathbf{C}}^{(n)}$ | combining matrix |
| $\mathcal{C}$ | matrix of the channel coefficient vectors of all users over all symbol intervals $(N_b KL \times N_b K)$ |
| $\mathcal{C}^{(n)}$ | matrix of the channel coefficient vectors of all users over symbol intervals inside the processing window $(NKL \times NK)$ |
| $\bar{\mathcal{C}}^{(n)}$ | matrix of the channel coefficient vectors of all users over symbol intervals inside the processing window plus the edge symbol intervals $((N+4)KL \times (N+4)K)$ |
| $\mathcal{C}_e^{(n)}$ | matrix of the channel coefficient vectors of all users over the edge symbol intervals $(4KL \times 4K)$ |
| $CAP_k$ | channel capacity of user $k$ |
| $\mathbb{C}$ | set of complex numbers |
| $\mathbf{D}(i)$ | detector block $(KL \times KL)$ |
| $\mathbf{D}(z)$ | $z$-transform of a linear detector $(KL \times KL)$ |
| $\mathcal{D}$ | linear infinite memory-length multiuser detector |
| $\mathcal{D}_N$ | truncated linear finite memory-length multiuser detector of length $N$ $(NKL \times KL)$ |
| $\bar{\mathcal{D}}_N$ | optimal linear finite memory-length multiuser detector of length $N$ $(NKL \times KL)$ |
| $E_k$ | transmitted energy per symbol of user $k$ |
| $\mathcal{F}$ | convolution of the multiuser channel impulse response and multiuser detector $(NKL \times KL)$ |
| $\boldsymbol{h}$ | vector of data-amplitude products of all users over all symbol intervals $(N_b K \times 1)$ |
| $\boldsymbol{h}^{(n)}$ | vector of data-amplitude products of all users over symbol intervals inside the processing window $(NK \times 1)$ |
| $\bar{\boldsymbol{h}}^{(n)}$ | vector of data-amplitude products of all users over symbol intervals inside the processing window plus the edge symbol intervals $((N+4)K \times 1)$ |
| $\mathbf{h}^{(n)}$ | vector of data-amplitude products of all users at symbol interval $n$ $(K \times 1)$ |
| $\boldsymbol{h}_e^{(n)}$ | vector of data-amplitude products of all users over the edge symbol intervals $(4K \times 1)$ |
| $h_k^{(n)}$ | data-amplitude product of user $k$ at symbol interval $n$ |
| $\mathbf{I}$ | identity matrix |
| $\mathbf{I}_L$ | identity matrix $(L \times L)$ |
| $J$ | distance of channel estimation filter taps in symbol intervals |
| $\mathcal{J}_0$ | zero-order Bessel function of the first kind |
| $k$ | user index |
| $K$ | number of active users |

| | |
|---|---|
| $l$ | propagation path index |
| $L$ | number of propagation paths |
| $\tilde{\mathbf{L}}$ | Cholesky factor of the correlation matrix $\mathbf{R}(0)$ |
| $\mathcal{L}^{(n)}$ | Cholesky factor of the correlation matrix $\mathcal{R}^{(n)}$ |
| $n$ | discrete symbol interval index |
| $N$ | number of symbols in the processing window |
| $N_b$ | number of symbols in the data packet |
| $N_c$ | processing gain |
| $N_p$ | distance of the pilot symbols |
| $N_s$ | number of samples in symbol interval |
| $P$ | "half" of the processing window length |
| $P_k$ | probability of bit error for user $k$ |
| $P_{pr}$ | number of coefficients in the prediction part of the channel estimation filter |
| $P_{sm}$ | number of coefficients in the smoothing part of the channel estimation filter |
| $\mathbf{q}_{k,l}^{(n)}$ | channel estimation filter input vector |
| $\boldsymbol{r}$ | discrete-time sampled received signal vector over all symbol intervals ($N_bN_s \times 1$) |
| $\boldsymbol{r}^{(n)}$ | discrete-time sampled received signal vector over symbol intervals inside the processing window ($NN_s \times 1$) |
| $r(t)$ | complex envelope of received continuous-time signal |
| $\mathbf{R}_{k,k'}^{(n)}(i)$ | matrix of crosscorrelations of signature waveforms for all multipath components of users $k$ and $k'$ with delay of $i$ symbols at symbol interval $n$ ($L \times L$) |
| $\mathbf{R}^{(n)}(i)$ | matrix of crosscorrelations of signature waveforms for all multipath components of all users with delay of $i$ symbols at symbol interval $n$ ($KL \times KL$) |
| $\mathcal{R}$ | matrix of crosscorrelations of signature waveforms for all multipath components of all users over all symbol intervals ($N_bKL \times N_bKL$) |
| $\mathcal{R}^{(n)}$ | matrix of crosscorrelations of signature waveforms of multipath components of all users over symbol intervals inside the processing window ($NKL \times NKL$) |
| $\bar{\mathcal{R}}^{(n)}$ | matrix of crosscorrelations of signature waveforms of multipath components of all users over symbol intervals inside the processing window plus the edge symbol intervals ($NKL \times (N+4)KL$) |
| $\mathcal{R}_e^{(n)}$ | matrix of crosscorrelations of signature waveforms of multipath components of all users over the edge symbol intervals ($NKL \times 4KL$) |
| $\mathbb{R}$ | set of real numbers |
| $s_k^{(n)}(t)$ | signature waveform of user $k$ at symbol interval $n$ |
| $s_{k,m}^{(n)}$ | chip $m$ of user $k$ at symbol interval $n$ |
| $\mathbf{S}^{(0)}(0)$ | matrix of samples of signature waveforms ($N_s \times KL$) |

| | |
|---|---|
| $\mathcal{S}$ | matrix of samples of signature waveforms ($(N+2)N_s \times NKL$) |
| $t$ | continuous-time index |
| $T$ | length of a symbol period |
| $T_m$ | delay spread |
| $T_c$ | length of a chip period |
| $\mathcal{T}$ | detector matrix; inverse of $\mathcal{R}$ or $\mathcal{R}^{(n)}$ |
| $\mathcal{U}_N$ | block column of inverse matrix ($NKL \times KL$) |
| $\mathbf{v}_{k,l}^{(n)}$ | channel estimation filter vector |
| $\boldsymbol{w}$ | vector of the matched filter output noise components of all users over all symbol intervals ($N_bKL \times 1$) |
| $\boldsymbol{w}^{(n)}$ | vector of the matched filter output noise components of all users over symbol intervals inside the processing window ($NKL \times 1$) |
| $\mathbf{w}^{(n)}$ | vector of the matched filter output noise components of all users at symbol interval $n$ ($KL \times 1$) |
| $\mathbf{w}_k^{(n)}$ | vector of the matched filter output noise components of user $k$ at symbol interval $n$ ($L \times 1$) |
| $w_{k,l}^{(n)}$ | noise component of the sampled output of the matched filter for the $l$th multipath of user $k$ at symbol interval $n$ |
| $\boldsymbol{y}$ | vector of matched filter outputs of all users over all symbol intervals ($N_bKL \times 1$) |
| $\boldsymbol{y}^{(n)}$ | vector of matched filter outputs of all users over symbol intervals inside the processing window ($NKL \times 1$) |
| $\mathbf{y}^{(n)}$ | vector of matched filter outputs of all users at symbol interval $n$ ($KL \times 1$) |
| $\mathbf{y}_k^{(n)}$ | vector of matched filter outputs of multipath components of user $k$ at symbol interval $n$ ($L \times 1$) |
| $y_{k,l}^{(n)}$ | sampled output of the filter matched to the $k$th users $l$th multipath component at symbol interval $n$ |
| $\boldsymbol{y}_{[MUD]}$ | multiuser detector output vector over all symbol intervals ($N_bKL \times 1$) |
| $\boldsymbol{y}_{[MUD]}^{(n)}$ | multiuser detector output vector over symbol intervals inside the processing window ($NKL \times 1$) |
| $\boldsymbol{y}_{[MUD]}^{(n)}(m)$ | multiuser detector output vector over symbol intervals inside the processing window at iteration $m$ ($N_bKL \times 1$) |
| $\mathbf{y}_{[MUD]}^{(n)}$ | multiuser detector output vector at symbol interval $n$ ($KL \times 1$) |
| $\boldsymbol{z}$ | complex discrete-time sampled zero mean additive white Gaussian noise vector over all symbol intervals ($N_bN_s \times 1$) |
| $z(t)$ | complex continuous-time zero mean additive white Gaussian noise |
| $\mathbf{0}_L$ | zero matrix ($L \times L$) |
| $\delta_{k,k'}$ | Kronecker delta function |

| | |
|---|---|
| $\delta(t)$ | Dirac's delta function |
| $\boldsymbol{\zeta}_1^{(n)}$ | matrix of the past edge correlations ($NKL \times 2KL$) |
| $\boldsymbol{\zeta}_2^{(n)}$ | matrix of the future edge correlations ($NKL \times 2KL$) |
| $\eta_k$ | asymptotic multiuser efficiency of user $k$ |
| $\bar{\eta_k}$ | power-limited near-far resistance of user $k$ |
| $\lambda_i$ | eigenvalue of a matrix |
| $\boldsymbol{\mu}^{(n)}$ | response of the edge symbols at linear detector output |
| $\Xi$ | modulation symbol alphabet |
| $\phi_k$ | transmitted carrier phase |
| $\varphi_{k,l}(.)$ | channel autocorrelation (autocovariance) function |
| $\sigma^2$ | two-sided power spectral density of the noise |
| $\boldsymbol{\Sigma_c}$ | covariance matrix of vector $\boldsymbol{c}$ |
| $\tau_k$ | delay of $k$th user's transmitted signal |
| $\tau_{k,l}$ | delay of $l$th multipath component of user $k$ |
| $\psi(t)$ | chip waveform |
| $\hat{\boldsymbol{\Psi}}$ | multiple-access interference estimate |
| $\Omega(.)$ | log-likelihood function |
| AME | asymptotic multiuser efficiency |
| AWGN | additive white Gaussian noise |
| BEP | bit error probability |
| BER | bit error rate |
| BPSK | binary phase shift keying |
| CG | conjugate gradient |
| CGL | conjugate gradient for solving least squares problems |
| CDMA | code-division multiple-access |
| DA | data-aided |
| DD | decision-directed |
| DF | decision-feedback |
| DFE | decision-feedback equalizer |
| DS | direct-sequence |
| DSP | digital signal processing |
| D-CDMA | deterministic code-division multiple-access |
| EM | expectation-maximization |
| FDMA | frequency-division multiple-access |
| FH | frequency-hopping |
| FIR | finite impulse response |
| flop | floating point operation |
| GPIC | groupwise parallel interference cancellation |
| GSIC | groupwise serial interference cancellation |
| HD | hard decision |
| IC | interference cancellation |
| IIR | infinite impulse response |
| ISI | intersymbol interference |
| LMMSE | linear minimum mean squared error |
| MAI | multiple-access interference |
| MC | multicarrier |

| | |
|---|---|
| MF | matched filter |
| ML | maximum likelihood |
| MLSD | maximum likelihood sequence detection |
| MMSE | minimum mean squared error |
| MOE | minimum output energy |
| MPSK | M-ary phase shift keying |
| MRC | maximal ratio combining |
| MSE | mean squared error |
| MUD | multiuser demodulation |
| NDA | non-data-aided |
| NFR | near-far resistance |
| PCG | preconditioned conjugate gradient |
| pdf | probability density function |
| PDMA | polarization-division multiple-access |
| PIC | parallel interference cancellation |
| PSK | phase shift keying |
| R-CDMA | random code-division multiple-access |
| SAGE | space alternating generalized expectation-maximization |
| SIC | serial interference cancellation |
| SD | soft decision; steepest descent |
| SINR | signal-to-interference-plus-noise ratio |
| SNR | signal-to-noise ratio |
| TDMA | time-division multiple-access |
| SDMA | space-division multiple-access |
| WSSUS | wide-sense stationary uncorrelated scattering |
| W-CDMA | wideband code-division multiple-access |
| $*$ | convolution |
| $(\cdot)^*$ | complex conjugation |
| $(\cdot)_{max}$ | maximum of the argument |
| $(\cdot)_{min}$ | minimum of the argument |
| $(\cdot)_{[d]}$ | decorrelating detector applied to the argument |
| $(\cdot)_{[HD-PIC]}$ | hard decision parallel interference cancellation detector applied to the argument |
| $(\cdot)_{[LIN]}$ | linear detector applied to the argument |
| $(\cdot)_{[MRC]}$ | maximal ratio combining applied to the argument |
| $(\cdot)_{[ms]}$ | linear minimum mean squared error detector applied to the argument |
| $(\cdot)_{[nw]}$ | noise-whitening detector applied to the argument |
| $(\cdot)_{[PIC]}$ | parallel interference cancellation detector applied to the argument |
| $\hat{(\cdot)}$ | estimate of the argument |
| arg | argument |
| $\mathbf{A}^{\mathrm{H}}$ | conjugate transpose of $\mathbf{A}$ |
| $\mathbf{A}^{-1}$ | inverse of $\mathbf{A}$ |
| $\mathbf{A}^{\top}$ | transpose of $\mathbf{A}$ |
| $\mathrm{diag}(\cdots)$ | diagonal matrix with elements $\cdots$ on main diagonal |

| | |
|---|---|
| $\mathrm{E}(\cdot)$ | expectation |
| $\inf(\cdot)$ | largest lower bound (infimum) |
| $\ln(\cdot)$ | natural logarithm |
| $\max(\cdot)$ | maximum |
| $\mathrm{mbc}(\cdot)$ | middle block column |
| $\min(\cdot)$ | minimum |
| $\mathrm{Q}(.)$ | normalized and scaled Gaussian complementary error function |
| $\mathrm{Re}(\cdot)$ | real part |
| $\mathrm{sgn}(\cdot)$ | signum function |
| $\sup$ | smallest upper bound (supremum) |
| $\lvert \cdot \rvert$ | magnitude |
| $\lVert \cdot \rVert$ | Euclidean norm |
| $\lceil x \rceil$ | smallest integer larger than or equal to $x$ |
| $(\mathbf{A})_{ij}$ | element at the $i$th row and $j$th column of matrix $\mathbf{A}$ |
| $\frac{\partial}{\partial \mathbf{x}}$ | gradient vector with respect to $\mathbf{x}$ |

# Contents

# 1. Introduction

Transmission of information has become a key feature of the modern way of life. The possibilities offered by telecommunications are changing the way how people work, shop, spend their leisure time etc. The advancing communication and information processing technologies create more markets for new communication services and products. In particular, the demand for wireless communication services has increased rapidly and the trend is excepted to continue. Therefore, stringent requirements on the capacity of communication systems are posed in terms of the number of users a system can serve simultaneously. In other, and more appropriate, words, as much information as possible should be transferred. This goal can be achieved by designing efficient source coding methods to compress the non-systematic redundancies in the information, by using smaller cells in cellular systems, by utilizing spatial signal processing techniques, and by designing efficient multiple-access techniques and transceivers for them.

The topic of this thesis is to analyze demodulation techniques which demodulate multiple users of a communications system jointly increasing the capacity of communication systems. The approach is called *multiuser demodulation* (MUD) or *multiuser detection*. Receivers applying multiuser demodulation are called *multiuser receivers*. As an introduction to the topic, multiple-access techniques, their features, as well as pros and cons are discussed in Section 1.1. In Section 1.2 facts motivating the need for the multiuser receivers are considered, and short historical overview of the multiuser demodulation is also presented. The aims and outline of the thesis is described in Section 1.3.

## 1.1. Multiple-access techniques

Multiple-access refers to a technique to share a common communications channel between multiple users. The freedoms in use when designing multiuser communication systems include space, time, and frequency. Time and frequency domains are duals of each other via the Fourier transform so that the actual options to use are

space domain and time-frequency domain designs. In the space domain users can be separated by making their distance large enough. An example is to use cables to separate communication signals in wireline communication. Another example is to separate transmitters geographically to have large enough distances attenuating the signals so that they do not interfere significantly. More advanced techniques include polarization-division multiple-access (PDMA) and space-division multiple-access (SDMA) [1]. In PDMA two users can be separated by using electromagnetic waves with different polarization. In SDMA sectorized antennas are usually applied to separate users at the same frequency.

In time-frequency domain multiple-access each users' transmitted data signal is modulated by a *signature waveform*. The receiver can demodulate each users data, if the signature waveforms of the users are different enough. Various signature waveform designs result in different multiple-access techniques.

The oldest multiple-access technique is frequency-division multiple-access (FDMA). In FDMA each users' signature waveform occupies its own frequency band and the receiver can separate the users' signals by simple bandpass filtering. FDMA is a simple scheme and applicable to both analog and digital modulation. It is not, however, very flexible for providing variable bit rates, which is an important requirement in future communication services. Making the bit rate higher requires more frequency channels to be allocated for a user. This implies a need for several bandpass filters.

The introduction of digital modulations enabled the appearance of time-division multiple-access (TDMA), in which each users' signature waveform is limited to a predetermined time interval. TDMA is relatively simple to implement and it is very flexible for providing variable bit rates. Increasing the bit rate can be implemented by assigning to a user more transmission intervals. However, the transmissions of all the users must be exactly synchronized to each other. Due to simpler implementation of more complicated modulation schemes in TDMA than in FDMA the capacity of TDMA systems is usually significantly higher than that of the FDMA systems.

The invention of spread-spectrum techniques for communication systems with anti-jamming and low probability of undesired interception capabilities lead to the idea of code-division multiple-access (CDMA). A review of the spread-spectrum techniques can be found in papers by Scholtz [2] and Pickholtz *et al.* [3]. More detailed treatments can be found in the books by Simon *et al.* [4], Dixon [5], Peterson *et al.* [6], and Viterbi [7]. The history of spread-spectrum has been reviewed in [8, 9, 10] and [4, Part 1, Chap. 2].

CDMA can be implemented in numerous ways including frequency-hopping (FH), time-hopping (TH), and direct-sequence (DS) spread-spectrum techniques [4] as well as multicarrier (MC) techniques [11]. Design of CDMA signature waveforms based on wavelets [12, 13, 14, 15] or overlapping signature waveforms (spread-signature CDMA) counteracting fading [16, 17] have also been proposed. Hybrid CDMA systems based on combining all or some of the techniques are also possible. In FH-CDMA users' signature waveforms are centered on different carrier frequencies at different time intervals. The hopping from a frequency to another is controlled according to a pseudo-random spreading sequence. In DS-CDMA sys-

tems each users' signature waveforms are continuous in the time domain and have a relatively flat spectrum. Therefore, in DS-CDMA systems users are separated neither in time nor in frequency domains, but all signature waveforms occupy the whole frequency band allocated for the transmission at all times. However, the data of users can be separated in the receivers, since the signature waveforms of DS-CDMA are formed by spreading sequences which are unique to all users. In multicarrier modulation each user's data is transmitted using different carrier frequencies [18]. In MC-CDMA the data signal is also spread in the frequency domain as in DS-CDMA [11].

Traditional FDMA and TDMA are designed to be orthogonal in the sense that the signature waveforms are mutually orthogonal. DS-CDMA, on the other hand, can be designed to be either orthogonal or non-orthogonal. The spreading sequences can be designed to be orthogonal. If the signals of all users arrive at the receiver with the same time delay (spreading sequence phase) and if the transmission medium does not cause time dispersion, the signature waveforms appear as orthogonal at the receiver. With unequal timing offsets, the signature waveforms are non-orthogonal at the receiver.[1] The spreading sequences may also be designed to be non-orthogonal. Orthogonal CDMA is in many respects similar to FDMA or TDMA. The non-orthogonal CDMA is more flexible than orthogonal multiple-access techniques, since there is no hard limit on the number of users, as there is in orthogonal multiple-access techniques due to the finite dimensionality of the signal space.

The debate on the question which multiple-access technique gives the maximal system capacity is very controversial[2]. One significant answer is given by information theory. In the so called Gaussian multiple-access channel, i.e., in a time-frequency channel distorted by additive white Gaussian noise (AWGN) with several transmitters and one centralized receiver, the maximum Shannon capacity is obtained by letting all the users to use all the bandwith at all time instants [22]. A DS-CDMA system is clearly a good approximation of such a system. Another answer for cellular systems is provided by the fact that a DS-CDMA system can provide a frequency reuse factor of one [7], whereas TDMA has so far been limited to a reuse factor of three or four. However, antenna diversity may push the reuse factor for TDMA lower in the future. With a frequency reuse factor of one FH-CDMA cannot avoid frequency hits between users at the same frequencies in adjacent cells causing a severe performance degradation. Furthermore, coherent demodulation is not practical in FH systems, which causes a performance penalty in comparison to DS systems with coherent demodulation. The CDMA signature waveforms have usually a significantly larger bandwith than FDMA or TDMA waveforms. Thus, CDMA signature waveforms offer protection against fading, which is an impairment of mobile radio channels [23]. The advantages of TDMA in comparison to CDMA include its simpler implementation in many cases and the infrastructure of some existing systems.

[1] Similar nonidealities, such as time- or frequency-dispersive channel, often remove also the orthogonality of FDMA, TDMA, or FH-CDMA.

[2] As an example, for DS-CDMA applied to cellular mobile communications contrary views are presented, e.g., by Viterbi & Vembu [19, 20] and by Verdú [21].

CDMA has reached most interest in application to wireless cellular terrestrial [1, 24, 25, 26, 27, 7] or satellite [28] communications. The IS-95 cellular system [29, 30] is a second generation cellular wireless communication system applying CDMA technology. Since the bandwith of IS-95 is relatively narrow (1.25 MHz), IS-95 is often called a narrowband CDMA system. There are several third generation systems under development, which utilize the DS-CDMA technique. One of them is a CDMA system utilizing multiuser detection [31, 32] proposed in a European research project FRAMES [33, 34]. Another developing DS-CDMA system is the so called wideband CDMA (W-CDMA) system proposed for Japan [35, 36]. The modified IS-95 standard IS-665 introduces also a wideband CDMA system [37]. All the above mentioned third generation CDMA systems are proposed to utilize multiuser receivers, namely some form of multiple-access interference (MAI) cancellation.

## 1.2. Multiuser demodulation

As discussed in the previous section, non-orthogonal multiple-access can potentially offer better system capacity than orthogonal schemes. The price to be paid for non-orthogonal signature waveforms is the fact that the conventional single-user matched filter or correlator receiver is not optimal for demodulation. Actually, obtaining the maximum Shannon capacity requires joint decoding of the data of all users [22]. The problem becomes increasingly significant if the received power levels of the users are dissimilar. This is the so called near-far problem. Strong signals may completely bury the weak ones if the conventional receiver is applied. Therefore, the design of conventional CDMA systems relies on accurate power control [7, 38] to alleviate the near-far problem, and spreading sequence design [4, 5, 6, 7, 39] to reduce crosscorrelations between the signature waveforms of the users. If the number of users is large, the performance of the conventional single-user receiver is poor even in the absence of the near-far problem due to the large level of MAI.

An alternative to the conventional receiver is to apply a receiver designed to take the multiple-access interference into consideration, i.e., multiuser demodulation. The multiuser demodulation is related to co-channel interference rejection [40]. Co-channel interference is caused by signals of users transmitting at the same frequency band, and it is usually rejected by adaptive filtering [41, 42]. This can be seen as a special case of multiuser demodulation. A multiuser detector can also make a joint detection of the data of all users.

The first publication on multiuser detection was presented by Schneider [43], who studied the zero-forcing decorrelating detector. Later Kashihara [44] and Kohno *et al.* [45] studied multiple-access interference cancellation receivers. Both Schneider and Kohno also suggested the use of the Viterbi algorithm for optimal detection in asynchronous multiuser communications. The real trigger to the increasing interest in multiuser detection was Verdú's work on multiuser detection [46, 47, 48], where the application of the Viterbi algorithm for optimal maximum likelihood sequence

detection (MLSD) was developed, and its performance was analyzed. Verdú showed that the CDMA systems are neither interference nor near-far limited, but both are actually limitations of the conventional single-user receiver.

Since the optimal multiuser detection is prohibitively complex to implement for many practical applications, numerous suboptimal schemes have been investigated. A review of multiuser demodulation literature will be presented in Chapter 2. Tutorial reviews can also be found in [49, 50, 51] and an overview in [52]. The work on multiuser receivers has demonstrated that even suboptimal detector with a significantly lower implementation complexity than the optimal detector can greatly improve the detection performance and capacity of multiuser communication systems. Furthermore, robust detection in the presence of a near-far problem was shown to be possible.

## 1.3. Aim and outline of the thesis

In spite of the major research effort invested in multiuser demodulation techniques, several practical as well as theoretical open problems still exist in the field of multiuser receivers. Some of them are considered in more detail in this thesis. The aim of the thesis is to develop practical multiuser demodulation algorithms for mobile communication systems with frequency-selective fading channels, and to analyze their implementation complexity. The emphasis is restricted to the uplink (i.e., reverse link) of asynchronous DS-CDMA systems where users transmit in an uncoordinated manner and are received by one centralized receiver.

The thesis is presented as a monograph for clarity and to make it easier to read. However, parts of the literature review in Chapter 2 and parts of the main contributions in Chapters 3–5 have been published earlier or submitted for publication. The rest of the thesis is organized as follows.

Chapter 2, literature review of which is in part included in Paper I, presents the background knowledge for the main contributions of the thesis. Notations and a mathematical model of a CDMA system utilized in the later chapters are introduced. Relevant literature on single-user fading channel receivers as well as on multiuser demodulation is reviewed. Based on the literature review, open problems to be considered in Chapters 3–5 are pointed out.

Chapter 3, results of which are in part included in Papers II–IV, considers the approximation of ideal infinite memory-length (infinite impulse response, IIR) linear multiuser detectors by finite memory-length (finite impulse response, FIR) detectors in asynchronous CDMA systems. The stability and performance of the FIR detectors are analyzed and numerical examples are presented.

Chapter 4, results of which are in part included in Papers V–VI, considers multiuser demodulation in relatively fast fading channels. An optimal multiuser receiver is derived, and the performance of two suboptimal receivers, namely the decorrelating and parallel interference cancellation receivers, is studied. In particular, the performance of different channel estimation filters, data-aided (DA) and decision-directed (DD) channel estimation, and the bit error rates of the decorre-

lating and the parallel interference cancellation receivers are compared.

Chapter 5, results of which are in part included in Papers III, VII–X, focuses on the implementation issues of the linear receivers. The computational complexity of updating the receivers to changes in communication scenario is analyzed and compared to the parallel interference cancellation receivers.

Chapter 6 concludes the thesis. The results and contributions are summarized and discussed. Furthermore, some open problems for future research are pointed out.

## 1.4. Author's contribution to publications

The thesis is in part based on the ten original publications. The author has had the main responsibility for making the analysis and writing all the Papers I–X. The author has also implemented the software to perform the numerical analysis and computer simulations except in Paper VI, where Markku Heikkilä compiled the software in the guidance of the author and Matti Latva-aho.

In Paper I, the author has compiled the literature review of multiuser demodulation utilized in Chapter 2. In Papers, II–III, the author invented the main ideas, developed the analysis, and produced the examples. The second author provided help, ideas, and criticism during the process. In Papers IV and VIII–X, the idea of application of the conjugate gradient algorithm to multiuser detection is due to Jorma Lilleberg. The author developed the idea and the analysis, as well as produced the examples. The second and third authors provided help, ideas, and criticism during the process. Papers V and VII are author's own work. In Paper VI, the author developed the ideas and analysis together with the help of the other authors.

# 2. Preliminaries

Some preliminaries necessary for analysis in the following chapters are presented in this chapter. In Section 2.1 a multiuser CDMA system is defined in mathematical terms. A review of the earlier and parallel work regarding receiver design for fading channel communications and multiuser demodulation is presented in Section 2.2. The open problems addressed in this thesis are defined in Section 2.3.

## 2.1. System model

A general multiuser CDMA system is illustrated in Fig. 2.1. The so called multiple-access channel [22, Chap. 14] is considered in this thesis. In this model $K$ users share the same communication media and the signals transmitted by the users pass through separate and independent channels. The outputs of the channels are added to a common noise process. The transmitted data is demodulated in a centralized multiuser receiver, which makes a joint decision of the data of all users. In a mobile communication system, for example, the setup is valid for the uplink. The mathematical formulation of the transmission system presented in this section has been inspired by several earlier papers, e.g., [53, 47, 54, 55, 56, 57]. In Section 2.1.1, the system model is defined in a conventional way with continuous-time variables. The corresponding discrete-time model, which is more suitable for algorithm derivations than the continuous-time one, is defined in Section 2.1.2. In Section 2.1.3, the system model for a truncated observation window is presented. The statistical model of the fading channel is described in Section 2.1.4. To ease the reading of the thesis some notational principles are summarized in Section 2.1.5.

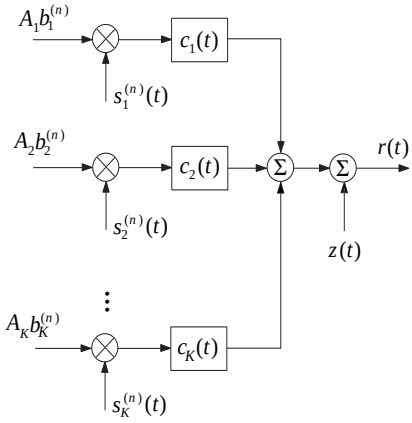


**Fig. 2.1. CDMA system.**

### *2.1.1. Continuous-time model*

A user $k \in \{1, 2, \ldots, K\}$ transmits in the $n$th symbol interval $t \in \Big[(n-1)T, nT\Big)$ complex signal

$$b_k^{(n)} A_k s_k^{(n)}(t - \tau_k), \tag{2.1}$$

where $T$ is the length of the symbol period, $b_k^{(n)} \in \Xi$ is the transmitted complex data symbol[1], $\Xi$ is the modulation symbol alphabet, $A_k = \sqrt{E_k} e^{j\phi_k}$ is the transmitted complex amplitude of user $k$ (assumed to be constant over the transmission), $E_k$ is the energy per symbol of the corresponding real bandpass signal, $\phi_k$ is the carrier phase, $\tau_k \in [0, T)$ is the delay of $k$th user's transmitted signal, and $s_k^{(n)}(t)$ is the signature waveform of user $k$. For convenience, $s_k^{(n)}(t)$ is assumed to be real (the analysis can be straightforwardly generalized to the complex case) and normalized so that $s_k^{(n)}(t) = 0$, if $t \notin [0, T)$, and $\int_0^T \mid s_k^{(n)}(t) \mid^2 dt = 1$. In a DS-CDMA system the signature waveforms are of the form

$$s_k^{(n)}(t) = \sum_{m=0}^{N_c - 1} s_{k,m}^{(n)} \psi(t - mT_c), \tag{2.2}$$

where $s_{k,m}^{(n)}$ is the $m$th chip of user $k$ on the symbol interval $n$, $T_c$ is the length of the chip period, $N_c = T/T_c$ is the processing gain, and $\psi(t)$ is the chip waveform.

[1] Uncoded transmission is studied in this thesis, i.e., the data symbols $b_k^{(n)}$, $\forall\, k, n$ are assumed to be i.i.d. random variables with uniform distribution into $\Xi$.

In this work the chips are assumed binary, i.e., $s_{k,m}^{(n)} \in \{-1, 1\}$. If the signature waveforms are periodic with period $T$, i.e., $s_k^{(n)}(t) = s_k^{(i)}(t)\ \forall\, n, i$ or for DS signals $s_{k,m}^{(n)} = s_{k,m}^{(i)}\ \forall\, n, i$, they will be called *time-invariant*, otherwise *time-varying*. Constant envelope modulation (e.g., MPSK) is assumed, therefore, $|b| = 1,\ \forall\, b \in \Xi$. It is assumed that the CDMA system under investigation is *asynchronous* in the sense that the delays are uniformly distributed into the interval $\tau_k \in \big[0, T\big)\ \forall\, k, l$. The CDMA system is called *synchronous* if the delays are equal (and, thus, normalized to zero), i.e., $\tau_1 = \tau_2 = \ldots = \tau_K = 0$, and *quasi-synchronous* if the delays are small compared to the symbol interval.

It is assumed that the channel of user $k$ appears as a linear filter with impulse response $c_k^{(n)}(t)$ (Fig. 2.1). It is further assumed that the channel impulse responses consists of discrete multipath components [23, Chap. 14] so that they can be expressed as

$$c_k^{(n)}(t) = \sum_{l=1}^{L} c_{k,l}^{(n)} \delta\Big(t - \tau_{k,l}^{(n)}\Big), \tag{2.3}$$

where $L$ is the number of multipath components[2] of the channel, $c_{k,l}^{(n)}$ is the complex coefficient (gain) of the $l$th multipath component of user $k$ at symbol interval $n$, $\tau_{k,l}^{(n)} \in \big[0, T_m\big)$ is the delay of the $l$th multipath component of user $k$ at symbol interval $n$, $T_m$ is the delay spread of the channel and $\delta(t)$ is the Dirac's delta function. The effect of time-varying delays is not analyzed in this thesis and the delays are assumed to be perfectly tracked. Thus, they will be denoted by $\tau_{k,l}$ in the forthcoming analysis. Furthermore, it is assumed that the delay spread of the channel is less than the symbol interval, i.e., $T_m < T$.

The received CDMA signal is the convolution of the transmitted signal (2.1) and the channel impulse response (2.3) plus the additive channel noise. Thus, the complex envelope of the received signal can be expressed as

$$\begin{aligned} r(t) &= \sum_{n=0}^{N_b-1} \sum_{k=1}^{K} b_k^{(n)} A_k s_k^{(n)}(t - nT - \tau_k) * c_k^{(n)}(t) + z(t) \\ &= \sum_{n=0}^{N_b-1} \sum_{k=1}^{K} b_k^{(n)} A_k \sum_{l=1}^{L} c_{k,l}^{(n)} s_k^{(n)}(t - nT - \tau_k - \tau_{k,l}) + z(t), \end{aligned} \tag{2.4}$$

where $N_b$ is the number of symbols in the data packet, the asterix $*$ denotes convolution, $z(t)$ is complex zero mean additive white Gaussian noise process with two-sided power spectral density $\sigma^2$.

It has been shown that the set of matched filter (MF) outputs sampled once in a symbol interval forms sufficient statistics for the detection of the transmitted data[3] [47, 56]. The sampled output of the filter matched to the $k$th users $l$th multipath

[2] The number of propagation paths is assumed to be equal for all users for notational simplicity.

[3] This is true due to the key assumption that the channel noise $z(t)$ has Gaussian complex amplitude distribution and the delays are known so that the MF outputs can be sampled at correct times.

component is

$$y_{k,l}^{(n)} = \int_{nT+\tau_k+\tau_{k,l}}^{(n+1)T+\tau_k+\tau_{k,l}} r(t) s_k^{(n)}(t - nT - \tau_k + \tau_{k,l}) dt. \tag{2.5}$$

Let the vectors of MF output samples for the $n$th symbol interval be defined as

$$\mathbf{y}_k^{(n)} = (y_{k,1}^{(n)}, y_{k,2}^{(n)}, \ldots, y_{k,L}^{(n)})^\top \in \mathbb{C}^L \tag{2.6}$$

$$\mathbf{y}^{(n)} = (\mathbf{y}_1^{\top(n)}, \mathbf{y}_2^{\top(n)}, \ldots, \mathbf{y}_K^{\top(n)})^\top \in \mathbb{C}^{KL} \tag{2.7}$$

and their concatenation over the whole data packet

$$\boldsymbol{y} = \begin{pmatrix} \mathbf{y}^{\top(1)} & \mathbf{y}^{\top(2)} & \cdots & \mathbf{y}^{\top(N_b)} \end{pmatrix}^\top \in \mathbb{C}^{N_b KL}. \tag{2.8}$$

Let $\mathbf{R}^{(n)}(i) \in (-1,1]^{KL \times KL}$ be a crosscorrelation matrix[4] with the partitioning

$$\mathbf{R}^{(n)}(i) = \begin{pmatrix} \mathbf{R}_{1,1}^{(n)}(i) & \mathbf{R}_{1,2}^{(n)}(i) & \cdots & \mathbf{R}_{1,K}^{(n)}(i) \\ \mathbf{R}_{2,1}^{(n)}(i) & \mathbf{R}_{2,2}^{(n)}(i) & \cdots & \mathbf{R}_{2,K}^{(n)}(i) \\ \vdots & \vdots & \ddots & \vdots \\ \mathbf{R}_{K,1}^{(n)}(i) & \mathbf{R}_{K,2}^{(n)}(i) & \cdots & \mathbf{R}_{K,K}^{(n)}(i) \end{pmatrix} \in \mathbb{R}^{KL \times KL}, \tag{2.9}$$

where matrices $\mathbf{R}_{k,k'}^{(n)}(i) \in \mathbb{R}^{L \times L}$, $\forall\, k, k' \in \{1, 2, \ldots, K\}$ have elements

$$\left(R_{k,k'}^{(n)}(i)\right)_{l,l'} = \int_{-\infty}^{\infty} s_k^{(n)}(t - \tau_k - \tau_{k,l}) s_{k'}^{(n-i)}(t + iT - \tau_{k'} - \tau_{k',l'}) dt,$$

$$\forall\, l, l' \in \{1, 2, \ldots, L\} \tag{2.10}$$

The vector (2.7) can be expressed as [54]

$$\begin{aligned} \mathbf{y}^{(n)} = {} & \mathbf{R}^{(n)}(2)\mathbf{C}^{(n-2)}\mathbf{A}\mathbf{b}^{(n-2)} + \mathbf{R}^{(n)}(1)\mathbf{C}^{(n-1)}\mathbf{A}\mathbf{b}^{(n-1)} \\ & + \mathbf{R}^{(n)}(0)\mathbf{C}^{(n)}\mathbf{A}\mathbf{b}^{(n)} + \mathbf{R}^{(n)}(-1)\mathbf{C}^{(n+1)}\mathbf{A}\mathbf{b}^{(n+1)} \\ & + \mathbf{R}^{(n)}(-2)\mathbf{C}^{(n+2)}\mathbf{A}\mathbf{b}^{(n+2)} + \mathbf{w}^{(n)}, \end{aligned} \tag{2.11}$$

where

$$\mathbf{A} = \mathrm{diag}\,(A_1, A_2, \ldots, A_K) \in \mathbb{C}^{K \times K} \tag{2.12}$$

is a diagonal matrix of transmitted amplitudes,

$$\mathbf{C}^{(n)} = \mathrm{diag}\left(\mathbf{c}_1^{(n)}, \mathbf{c}_2^{(n)}, \ldots, \mathbf{c}_K^{(n)}\right) \in \mathbb{C}^{KL \times K}, \tag{2.13}$$

is the matrix of channel coefficient vectors

$$\mathbf{c}_k^{(n)} = \left(c_{k,1}^{(n)}, c_{k,2}^{(n)}, \ldots, c_{k,L}^{(n)}\right)^\top \in \mathbb{C}^L, \tag{2.14}$$

[4]For notational compactness, the discrete-time index $n$ will be left out from $\mathbf{R}^{(n)}(i)$, when possible without confusion.

$$\mathbf{b}^{(n)} = \left(b_1^{(n)}, b_2^{(n)}, \ldots, b_K^{(n)}\right)^\top \in \Xi^K, \tag{2.15}$$

is the vector of the transmitted data and $\mathbf{w}^{(n)} \in \mathbb{C}^{KL}$ is the output vector due to noise. As in the case of time-invariant signature waveforms [54], it is easy to show that $\mathbf{R}^{(n)}(i) = \mathbf{0}_{KL}$, $\forall\, |i| > 2$ and $\mathbf{R}^{(n)}(-i) = \mathbf{R}^{\top(n+i)}(i)$, where $\mathbf{0}_{KL}$ is an all-zero matrix of size $KL \times KL$.

The concatenation vector of the matched filter outputs (2.8) has the expression

$$\boldsymbol{y} = \mathcal{R}\mathcal{C}\mathcal{A}\boldsymbol{b} + \boldsymbol{w} = \mathcal{R}\mathcal{C}\boldsymbol{h} + \boldsymbol{w}, \tag{2.16}$$

where

$$\mathcal{R} = \begin{pmatrix} \mathbf{R}^{(0)}(0) & \mathbf{R}^{\top(1)}(1) & \mathbf{R}^{\top(2)}(2) & \cdots & \mathbf{0}_{KL} \\ \mathbf{R}^{(1)}(1) & \mathbf{R}^{(1)}(0) & \mathbf{R}^{\top(2)}(1) & \cdots & \mathbf{0}_{KL} \\ \mathbf{R}^{(2)}(2) & \mathbf{R}^{(2)}(1) & \mathbf{R}^{(2)}(0) & \cdots & \mathbf{0}_{KL} \\ \vdots & \vdots & \vdots & \ddots & \vdots \\ \mathbf{0}_{KL} & \mathbf{0}_{KL} & \mathbf{0}_{KL} & \cdots & \mathbf{R}^{(N_b-1))}(0) \end{pmatrix}$$

$$\in \mathbb{R}^{N_b KL \times N_b KL}, \tag{2.17}$$

$$\mathcal{C} = \operatorname{diag}\left(\mathbf{C}^{(0)}, \mathbf{C}^{(1)}, \ldots, \mathbf{C}^{(N_b-1)}\right) \in \mathbb{C}^{N_b KL \times N_b K}, \tag{2.18}$$

$$\mathcal{A} = \operatorname{diag}\left(\mathbf{A}, \mathbf{A}, \ldots, \mathbf{A}\right) \in \mathbb{C}^{N_b K \times N_b K}, \tag{2.19}$$

$$\boldsymbol{b} = \left(\mathbf{b}^{\top(0)}, \mathbf{b}^{\top(1)} \ldots, \mathbf{b}^{\top(N_b-1)}\right)^\top \in \Xi^{N_b K}, \tag{2.20}$$

$\boldsymbol{h} = \mathcal{A}\boldsymbol{b}$ is the data-amplitude product vector, and $\boldsymbol{w}$ is the Gaussian noise output vector with zero mean and covariance matrix $\sigma^2\mathcal{R}$.

The emphasis in this thesis is on centralized multiuser detectors that process the matched filter output to provide statistics for both channel amplitude estimation and data detection. The multiuser detector output for the $n$th symbol interval is denoted by $\mathbf{y}_{[MUD]}^{(n)} \in \mathbb{C}^{KL}$. Similarly, as in (2.8), the concatenation of the detector outputs over the whole data symbol packet is denoted by $\boldsymbol{y}_{[MUD]} \in \mathbb{C}^{N_b KL}$.

### *2.1.2. Discrete-time model*

The received continuous-time signal is assumed to be sampled after front-end filtering with $N_s$ samples per symbol interval. The received signal vector for the whole data packet over time interval $t \in \big[0, (N_b+1)T\big)$, is

$$\boldsymbol{r} = \mathcal{S}\mathcal{C}\mathcal{A}\boldsymbol{b} + \boldsymbol{z}, \tag{2.21}$$

where $\boldsymbol{z}$ is the received complex white Gaussian noise sequence, and $\mathcal{S}$ is a matrix of samples of signature waveforms of the form

$$\mathcal{S} = \begin{pmatrix} \mathbf{S}^{(0)}(0) & \mathbf{0} & \mathbf{0} & \cdots & \mathbf{0} \\ \mathbf{S}^{(0)}(-1) & \mathbf{S}^{(1)}(0) & \mathbf{0} & \cdots & \mathbf{0} \\ \mathbf{S}^{(0)}(-2) & \mathbf{S}^{(1)}(-1) & \mathbf{S}^{(2)}(0) & \cdots & \mathbf{0} \\ \vdots & \vdots & \vdots & \ddots & \vdots \\ \mathbf{0} & \mathbf{0} & \mathbf{0} & \cdots & \mathbf{S}^{(N_b-1)}(0) \\ \mathbf{0} & \mathbf{0} & \mathbf{0} & \cdots & \mathbf{S}^{(N_b-1)}(-1) \\ \mathbf{0} & \mathbf{0} & \mathbf{0} & \cdots & \mathbf{S}^{(N_b-1)}(-2) \end{pmatrix}$$

$$\in \mathbb{R}^{(N+2)N_s \times NKL}, \tag{2.22}$$

where matrix $\mathbf{S}^{(n)}(0) \in \mathbb{R}^{N_s \times KL}$ includes the first $N_s$ samples, $\mathbf{S}^{(n)}(-1) \in \mathbb{R}^{N_s \times KL}$ includes the middle $N_s$ samples, and $\mathbf{S}^{(n)}(-2) \in \mathbb{R}^{N_s \times KL}$, includes the last $N_s$ samples of signature waveforms of the users in the $n$th symbol interval due to the delay differences of users. Assuming $0 = \tau_1 < \tau_2 < \cdots < \tau_K < T$ the element matrices have the structure

$$\begin{bmatrix} \mathbf{S}^{(n)}(0) \\ \hline \mathbf{S}^{(n)}(-1) \\ \hline \mathbf{S}^{(n)}(-2) \end{bmatrix} = \begin{bmatrix} \begin{array}{|c|c|c|} \hline & & 0 \\ \hline & \iddots & \\ \hline 0 & & \\ \hline \end{array} \end{bmatrix} \in \mathbb{R}^{3N_s \times KL}.$$

A column bar in the matrix above describes the non-zero sampled signature waveform of a particular user, and the zeros at the top are used to represent the delays of a propagation path of the particular user.

The matched filter output vector has the expression

$$\boldsymbol{y} = \mathcal{S}^{\mathrm{H}}\boldsymbol{r} = \mathcal{R}\mathcal{C}\mathcal{A}\boldsymbol{b} + \boldsymbol{w} = \mathcal{R}\mathcal{C}\boldsymbol{h} + \boldsymbol{w}, \tag{2.23}$$

where the correlation matrix $\mathcal{R}$ in (2.17) has the expression

$$\mathcal{R} = \mathcal{S}^{\top}\mathcal{S} \in (-1, 1]^{NKL \times NKL}. \tag{2.24}$$

Therefore the blocks of $\mathcal{R}$ have the expressions

$$\begin{aligned} \mathbf{R}^{(n)}(0) &= \mathbf{S}^{\top(n)}(0)\mathbf{S}^{(n)}(0) + \mathbf{S}^{\top(n)}(-1)\mathbf{S}^{(n)}(-1) + \mathbf{S}^{\top(n)}(-2)\mathbf{S}^{(n)}(-2) \\ \mathbf{R}^{(n)}(1) &= \mathbf{S}^{\top(n)}(0)\mathbf{S}^{(n-1)}(-1) + \mathbf{S}^{\top(n)}(-1)\mathbf{S}^{(n-1)}(-2) \\ \mathbf{R}^{(n)}(2) &= \mathbf{S}^{\top(n)}(0)\mathbf{S}^{(n-2)}(-2). \end{aligned}$$

### *2.1.3. Finite processing window model*

In purely asynchronous, unslotted CDMA systems the data packet lengths $N_b$ are very large. Actually, each user activates and deactivates its terminal independently

from each other. Thus, it is not practical to assume that the whole received signal $\boldsymbol{r}$ or the matched filter output vector $\boldsymbol{y}$ would be processed in a receiver. Therefore, a finite processing window model will be defined.

The received signal will be processed in *processing windows* of length $N = 2P+1$, where $P$ is a positive integer and $N$ is the window length measured in symbol durations $T$. A concatenation of symbols over a processing window is denoted by

$$\boldsymbol{b}^{(n)} = \left(\mathbf{b}^{\top(n-P)}, \ldots, \mathbf{b}^{\top(n-1)}, \mathbf{b}^{\top(n)}, \mathbf{b}^{\top(n+1)}, \ldots, \mathbf{b}^{\top(n+P)}\right)^{\top} \in \Xi^{NK}. \quad (2.25)$$

Similarly, the concatenation of the matched filter outputs over the processing window is defined as

$$\boldsymbol{y}^{(n)} = \left(\mathbf{y}^{\top(n-P)}, \ldots, \mathbf{y}^{\top(n-1)}, \mathbf{y}^{\top(n)}, \mathbf{y}^{\top(n+1)}, \ldots, \mathbf{y}^{\top(n+P)}\right)^{\top} \in \mathbb{C}^{NKL}. \quad (2.26)$$

The vector of the matched filter outputs has the expressions

$$\begin{aligned} \boldsymbol{y}^{(n)} &= \mathcal{R}^{(n)}\mathcal{C}^{(n)}\mathcal{A}^{(n)}\boldsymbol{b}^{(n)} + \mathcal{R}_e^{(n)}\mathcal{C}_e^{(n)}\mathcal{A}_e^{(n)}\boldsymbol{b}_e^{(n)} + \boldsymbol{w}^{(n)} && (2.27)\\ &= \bar{\mathcal{R}}^{(n)}\bar{\mathcal{C}}^{(n)}\bar{\mathcal{A}}^{(n)}\bar{\boldsymbol{b}}^{(n)} + \boldsymbol{w}^{(n)}, && (2.28) \end{aligned}$$

where the vector

$$\boldsymbol{b}_e^{(n)} = \left(\mathbf{b}^{\top(n-P-2)}, \mathbf{b}^{\top(n-P-1)}, \mathbf{b}^{\top(n+P+1)}, \mathbf{b}^{\top(n+P+2)}\right)^{\top} \in \Xi^{4K} \quad (2.29)$$

includes the symbols outside the processing window,

$$\bar{\boldsymbol{b}}^{(n)} = \left(\mathbf{b}^{\top(n-P-2)}, \mathbf{b}^{\top(n-P-1)}, \boldsymbol{b}^{\top(n)}, \mathbf{b}^{\top(n+P+1)}, \mathbf{b}^{\top(n+P+2)}\right)^{\top} \in \Xi^{(N+4)K}, \quad (2.30)$$

includes the symbols both inside and outside the processing window,

$$\mathcal{C}^{(n)} = \operatorname{diag}\left(\mathbf{C}^{(n-P)}, \mathbf{C}^{(n-P+1)}, \ldots, \mathbf{C}^{(n+P)}\right) \in \mathbb{C}^{NKL\times NK}, \quad (2.31)$$

$$\mathcal{C}_e^{(n)} = \operatorname{diag}\left(\mathbf{C}^{(n-P-2)}, \mathbf{C}^{(n-P-1)}, \mathbf{C}^{(n+P+1)}, \mathbf{C}^{(n+P+2)}\right) \in \mathbb{C}^{4KL\times 4K}, \quad (2.32)$$

$$\begin{aligned} \bar{\mathcal{C}}^{(n)} &= \operatorname{diag}\left(\mathbf{C}^{(n-P-2)}, \mathbf{C}^{(n-P-1)}, \mathcal{C}^{(n)}, \mathbf{C}^{(n+P+1)}, \mathbf{C}^{(n+P+2)}\right)\\ &\in \mathbb{C}^{(N+4)KL\times(N+4)K}, && (2.33)\\ \mathcal{A}^{(n)} &= \operatorname{diag}\left(\mathbf{A}, \mathbf{A}, \ldots, \mathbf{A}\right) \in \mathbb{C}^{NK\times NK}, && (2.34)\\ \mathcal{A}_e^{(n)} &= \operatorname{diag}\left(\mathbf{A}, \mathbf{A}, \mathbf{A}, \mathbf{A}\right) \in \mathbb{C}^{4K\times 4K}, && (2.35)\\ \bar{\mathcal{A}}^{(n)} &= \operatorname{diag}\left(\mathbf{A}, \mathbf{A}, \mathcal{A}, \mathbf{A}^{(n)}, \mathbf{A}\right) \in \mathbb{C}^{(N+4)K\times(N+4)K}, && (2.36) \end{aligned}$$

$$\mathcal{R}^{(n)} = \begin{pmatrix} \mathbf{R}^{(n-P)}(0) & \mathbf{R}^{\top(n-P+1)}(1) & \mathbf{R}^{\top(n-P+2)}(2) & \cdots & \mathbf{0}_{KL} \\ \mathbf{R}^{(n-P+1)}(1) & \mathbf{R}^{(n-P+1)}(0) & \mathbf{R}^{\top(n-P+2)}(1) & \cdots & \mathbf{0}_{KL} \\ \mathbf{R}^{(n-P+2)}(2) & \mathbf{R}^{(n-P+2)}(1) & \mathbf{R}^{(n-P+2)}(0) & \cdots & \mathbf{0}_{KL} \\ \vdots & \vdots & \vdots & \ddots & \vdots \\ \mathbf{0}_{KL} & \mathbf{0}_{KL} & \mathbf{0}_{KL} & \cdots & \mathbf{R}^{(n+P)}(0) \end{pmatrix}$$

$$\in \mathbb{R}^{NKL \times NKL}, \tag{2.37}$$

$$\begin{aligned} \mathcal{R}_e^{(n)} &= \left(\boldsymbol{\zeta}_1^{(n)}, \boldsymbol{\zeta}_2^{(n)}\right) \\ &= \begin{pmatrix} \mathbf{R}^{(n-P)}(2) & \mathbf{R}^{(n-P)}(1) & \mathbf{0}_{KL} & \mathbf{0}_{KL} \\ \mathbf{0}_{KL} & \mathbf{R}^{(n-P+1)}(2) & \mathbf{0}_{KL} & \mathbf{0}_{KL} \\ \mathbf{0}_{KL} & \mathbf{0}_{KL} & \mathbf{R}^{\top(n+P+1)}(2) & \mathbf{0}_{KL} \\ \mathbf{0}_{KL} & \mathbf{0}_{KL} & \mathbf{R}^{\top(n+P+2)}(1) & \mathbf{R}^{\top(n+P+3)}(2) \end{pmatrix} \\ &\in \mathbb{R}^{NKL \times 4KL}, \end{aligned} \tag{2.38}$$

i.e., $\boldsymbol{\zeta}_1^{(n)} \in \mathbb{R}^{NKL \times 2KL}$ includes the first and $\boldsymbol{\zeta}_2^{(n)} \in \mathbb{R}^{NKL \times 2KL}$ the last $2KL$ columns of $\mathcal{R}_e^{(n)}$, and

$$\bar{\mathcal{R}}^{(n)} = \left(\boldsymbol{\zeta}_1^{(n)}, \mathcal{R}^{(n)}, \boldsymbol{\zeta}_2^{(n)}\right) \in \mathbb{R}^{NKL \times (N+4)KL}. \tag{2.39}$$

In (2.27) the first term is the response due to symbols $\boldsymbol{b}$ inside the processing window and the second is the response due to symbols $\boldsymbol{b}_e$ outside the processing window. The third term $\boldsymbol{w} \in \mathbb{C}^{NKL}$ is the response due to noise, which is a zero mean Gaussian random vector with covariance matrix $\sigma^2\mathcal{R}$. Expression (2.28) is obtained by writing the first two terms in (2.27) as one matrix-vector product. It is assumed in this work that matrices $\mathcal{R}$ and $\mathcal{R}^{(n)}$ are positive definite and therefore nonsingular. This is ideally the case with probability one [54]. In practice, $\mathcal{R}$ and $\mathcal{R}^{(n)}$ become singular (positive-semidefinite) if the product $KL$ is large in comparison to the processing gain of a DS-CDMA system. The reason is that practical bandwith constraints pose upper limits to the dimensionality of signal space spanned by the columns of $\mathcal{S}$. It has been observed by the author that the number of users and multipath components up to $KL \approx 3N_c$ can be tolerated in asynchronous DS-CDMA systems so that the matrix $\mathcal{R}$ is still nonsingular.

### *2.1.4. Statistical fading channel model*

The channel coefficient vector

$$\boldsymbol{c} = \left(\mathbf{c}^{\top(0)}, \mathbf{c}^{\top(1)}, \ldots, \mathbf{c}^{\top(N_b-1)}\right)^\top, \tag{2.40}$$

where $\mathbf{c}^{(n)} = \left(\mathbf{c}_1^{\top(0)}, \mathbf{c}_2^{\top(0)}, \ldots, \mathbf{c}_K^{\top(0)}\right)^\top$ is assumed to be complex Gaussian random vector with zero mean and covariance matrix $\boldsymbol{\Sigma}_{\boldsymbol{c}}$. It is assumed that the fading channel coefficients have a zero mean and variance normalized for convenience so that

$$\sum_{l=1}^{L} \mathrm{E}\left(|c_{k,l}^{(n)}|^2\right) = 1, \; \forall\, k. \tag{2.41}$$

The channel coefficients are assumed to be independent, i.e., $\mathrm{E}\left(c_{k,l}^{(n)}, c_{k',l'}^{*(n)}\right) = \sigma_{c_{k,l}}^2 \delta_{k,k'} \delta_{l,l'}$, where $\delta_{k,k'}$ is the discrete Kronecker delta function, and $\sigma_{c_{k,l}}^2 =$

$\mathrm{E}\Big(|c_{k,l}|^2\Big)$ is the power of the $l$th path of user $k$. The assumption is equivalent to the common uncorrelated scattering (US) model [23]. The channels are assumed to be stationary over the observation interval so that the channel autocorrelation (autocovariance) function $\varphi_{k,l}(n,n') = \mathrm{E}\Big(c_{k,l}^{(n)} c_{k,l}^{*(n')}\Big)$ is a function of the time difference $n'-n$ only. The assumption is equivalent to the common wide-sense stationary (WSS) model [23]. In other words, the channel autocorrelation becomes

$$\varphi_{k,l}(i) = \mathrm{E}\Big(c_{k,l}^{(n)} c_{k,l}^{*(n+i)}\Big). \tag{2.42}$$

The stationarity assumption is valid if the vehicle speed does not change during the transmission. The Doppler power spectrum is assumed to be the classical Jakes' spectrum [58, Sec. 5.4], which results in the Clarke's channel autocorrelation function

$$\varphi_{k,l}(i) = \sigma_{c_{k,l}}^2 \mathcal{J}_0(2\pi f_d \frac{i}{T}), \tag{2.43}$$

where $\mathcal{J}_0$ is the zero-order Bessel function of the first kind,

$$f_d = \frac{v}{c_{light}} f_c \tag{2.44}$$

is the maximum Doppler spread, $v$ is the speed of the vehicle, $c_{light}$ is the speed of light, and $f_c$ is the carrier frequency. The width of the channel autocorrelation function is called channel coherence time, denoted by $T_{coh}$. The coherence time satisfies $T_{coh} \approx 1/f_d$. Channel is said to be slowly fading if $T_{coh} \gg T$ or $f_d T \ll 1$, and fast fading if $T_{coh} < T$ or $f_d T > 1$. In the intermediate case $T_{coh} > T$ or $f_d T < 1$, the channel will be termed *relatively fast fading*. This is often the case in current mobile communication systems with high vehicle speeds.

The covariance matrix of the channel can be partitioned as

$$\mathbf{\Sigma_c} = \begin{pmatrix} \mathbf{\Sigma}_{\mathbf{c}^{(0)}} & \mathbf{\Sigma}_{\mathbf{c}^{(0)},\mathbf{c}^{(1)}} & \cdots & \mathbf{\Sigma}_{\mathbf{c}^{(0)},\mathbf{c}^{(N_b-1)}} \\ \mathbf{\Sigma}^{\mathrm{H}}_{\mathbf{c}^{(0)},\mathbf{c}^{(1)}} & \mathbf{\Sigma}_{\mathbf{c}^{(1)}} & \cdots & \mathbf{\Sigma}_{\mathbf{c}^{(1)},\mathbf{c}^{(N_b-1)}} \\ \vdots & \vdots & \ddots & \vdots \\ \mathbf{\Sigma}^{\mathrm{H}}_{\mathbf{c}^{(0)},\mathbf{c}^{(N_b-1)}} & \mathbf{\Sigma}^{\mathrm{H}}_{\mathbf{c}^{(1)},\mathbf{c}^{(N_b-1)}} & \cdots & \mathbf{\Sigma}_{\mathbf{c}^{(N_b-1)}} \end{pmatrix}. \tag{2.45}$$

With the WSSUS channel model the blocks in (2.45) can be expressed as

$$\mathbf{\Sigma}_{\mathbf{c}^{(n)},\mathbf{c}^{(n+i)}} = \begin{pmatrix} \mathbf{\Sigma}_{\mathbf{c}_1^{(n)},\mathbf{c}_1^{(n+i)}} & \mathbf{0}_L & \cdots & \mathbf{0}_L \\ \mathbf{0}_L & \mathbf{\Sigma}_{\mathbf{c}_2^{(n)},\mathbf{c}_2^{(n+i)}} & \cdots & \mathbf{0}_L \\ \vdots & \vdots & \ddots & \vdots \\ \mathbf{0}_L & \mathbf{0}_L & \cdots & \mathbf{\Sigma}_{\mathbf{c}_K^{(n)},\mathbf{c}_K^{(n+i)}} \end{pmatrix}, \tag{2.46}$$

and

$$\mathbf{\Sigma}_{\mathbf{c}_k^{(n)},\mathbf{c}_k^{(n+i)}} = \begin{pmatrix} \varphi_{k,1}(i) & 0 & \cdots & 0 \\ 0 & \varphi_{k,2}(i) & \cdots & 0 \\ \vdots & \vdots & \ddots & \vdots \\ 0 & 0 & \cdots & \varphi_{k,L}(i) \end{pmatrix}. \tag{2.47}$$

### *2.1.5. Summary of notational conventions*

A boldface, lower-case non-*italic* symbol with discrete-time index as a superscript, e.g., $\mathbf{b}^{(n)} \in \Xi^K, \mathbf{h}^{(n)} \in \mathbb{C}^K, \mathbf{y}^{(n)} \in \mathbb{C}^{KL}, \mathbf{w}^{(n)} \in \mathbb{C}^{KL}$, denotes a vector of $K$ or $KL$ variables over the $n$th symbol interval. A boldface, lower-case, *italic* symbol, e.g., $\boldsymbol{b} \in \Xi^{N_b K}, \boldsymbol{h} \in \mathbb{C}^{N_b K}, \boldsymbol{y} \in \mathbb{C}^{N_b KL}, \boldsymbol{w} \in \mathbb{C}^{N_b KL}$, denotes a vector of $N_b K$ or $N_b KL$ variables concatenated over the whole data packet of $N_b$ symbol intervals. A boldface, lower-case, *italic* symbol with discrete-time index as a superscript, e.g., $\boldsymbol{b}^{(n)} \in \Xi^{NK}, \boldsymbol{h}^{(n)} \in \mathbb{C}^{NK}, \boldsymbol{y}^{(n)} \in \mathbb{C}^{NKL}, \boldsymbol{w}^{(n)} \in \mathbb{C}^{NKL}$, denotes a vector of $NK$ or $NKL$ variables concatenated over the observation window of $N$ symbol intervals. A boldface, lower-case *italic* symbol with discrete-time index as a superscript and symbol $e$ (denoting for edge) as a subscript, e.g., $\boldsymbol{b}_e^{(n)} \in \Xi^{4K}, \boldsymbol{h}_e^{(n)} \in \mathbb{C}^{4K}, \boldsymbol{y}_e^{(n)} \in \mathbb{C}^{4KL}, \boldsymbol{w}_e^{(n)} \in \mathbb{C}^{4KL}$, denotes a vector of $4K$ or $4KL$ variables over the symbol intervals $n-P-2$, $n-P-1$, $n+P+1$, $n+P+2$. A boldface, lower-case, *italic* symbol with a bar above and discrete-time index as a superscript, e.g., $\bar{\boldsymbol{b}}^{(n)} \in \Xi^{(N+4)K}, \bar{\boldsymbol{h}}^{(n)} \in \mathbb{C}^{(N+4)K}, \bar{\boldsymbol{y}}^{(n)} \in \mathbb{C}^{(N+4)KL}, \bar{\boldsymbol{w}}^{(n)} \in \mathbb{C}^{(N+4)KL}$, denotes a vector of $(N+4)K$ or $(N+4)KL$ variables concatenated over the observation window of $N$ symbol intervals and the previous and following two symbol intervals causing the edge effect.

Corresponding conventions apply to matrices as well. The boldface, upper-case symbols denote matrices for one symbol interval, and the boldface, upper-case, calligraphic symbols, e.g., $\mathcal{R}$, denote matrices concatenated over several symbol intervals. If the discrete-time index as a superscript is included to the calligraphic symbol, the concatenation is over a processing window of length $N$, otherwise over data packet length $N_b$. If there is the bar above the calligraphic symbol, the concatenation is over $N+4$ symbols including the edge effect. The symbol $e$ as a subscript refers to concatenation over the edge symbols only.

## 2.2. Review of earlier and parallel work

The relevant background literature is reviewed in this section. The main emphasis is on multiuser demodulation techniques for DS-CDMA systems[5], which are most important either from a practical or theoretical point of view. Most centralized[6] multiuser receivers can be illustrated as in Figs. 2.2(a) or 2.2(b). The multiuser signal processing can be performed either before the multipath combining, by processing the matched filter bank output vector $\boldsymbol{y}$, or after the multipath combining,

[5] Although the multiuser receivers have gained most interest in conjunction with DS-CDMA systems, they can be applied in any non-orthogonal multiple-access scheme. They have been considered for TDMA [59], hybrid DS-CDMA/TDMA [60, 61], FH-CDMA [62, 63], MC-CDMA [64, 65, 66, 67], wavelet packet CDMA [15], and spread-signature CDMA [68] communications.

[6] *Centralized* multiuser detectors (called sometimes also joint detectors) make a joint detection of the symbols of different users. *Decentralized* multiuser detectors (called sometimes also single-user detectors) demodulate a signal of one desired user only.

by processing the maximal ratio combined matched filter bank output vector

$$\boldsymbol{y}_{[MRC]} = \mathcal{C}^{\mathrm{H}}\boldsymbol{y}. \tag{2.48}$$

It should be noted, however, that the block diagrams in Figs. 2.2 are simplified and cannot fit all multiuser receivers into their framework. Most multiuser receivers can also be implemented before matched filtering, i.e., by processing the received spread-spectrum signal samples $\boldsymbol{r}$. It should also be noted that most multiuser receivers alleviate not only the detrimental effects of multiple-access interference, but the intersymbol interference as well.

The performance of multiuser receivers can be measured by *bit error probability* (BEP) or *bit error rate* (BER), as well as by *mean squared error* (MSE) of the detector output or channel estimates. Furthermore, other performance criteria yielding simpler analysis than the bit error probability have also been considered. They include the *asymptotic multiuser efficiency* (AME) [47, 48], and the *near-far resistance* (NFR) [69, 70, 54]. The AME describes the asymptotic limit of the loss in the signal-to-noise ratio (SNR) as the power spectral density of the noise approaches zero. For coherent BPSK modulation in AWGN channels, AME is defined as

$$\eta_k = \sup_{\varrho\in[0,1]} \lim_{\sigma^2\to 0} \frac{P_k}{\mathrm{Q}\left(\sqrt{\frac{\varrho E_k}{\sigma^2}}\right)} < \infty, \tag{2.49}$$

where sup denotes the smallest upper bound, $\mathrm{Q}(x) = \frac{1}{\sqrt{2\pi}}\int_x^\infty e^{-t^2/2}dt$ is the normalized and scaled Gaussian complementary error function, and $P_k$ is the bit error probability of user $k$ with the particular multiuser detector. The AME for multiuser detectors in Rayleigh fading channels has been defined in [56, 71, 72]. The Rician fading case has been considered in [73, 74]. The near-far resistance is the value of the AME for the worst possible interfering energy combination and is defined as

$$\bar{\eta_k} = \inf_{E_l\geq 0, l\neq k} \eta_k. \tag{2.50}$$

The detector for user $k$ is said to be near-far resistant if $\bar{\eta_k} > 0$.

In Section 2.2.1, some of the key results on single-user fading channel receiver techniques are reviewed. Optimal multiuser receivers are considered in Section 2.2.2 and suboptimal ones in Section 2.2.3.

### *2.2.1. Receivers for fading channel communications*

Some key aspects of the receivers for single-user ($K = 1$) fading channel communications will be reviewed in short in this section. Tutorial expositions of fading channel communications have been presented by Turin [75] and Stein [76]. More complete treatments can be found in books by Proakis [23], and Schwartz et al. [77]. A treatment of the mobile radio channel can be found in [58]. A comprehensive survey of the literature on fading channel communications is included in the thesis of Mämmelä [78].

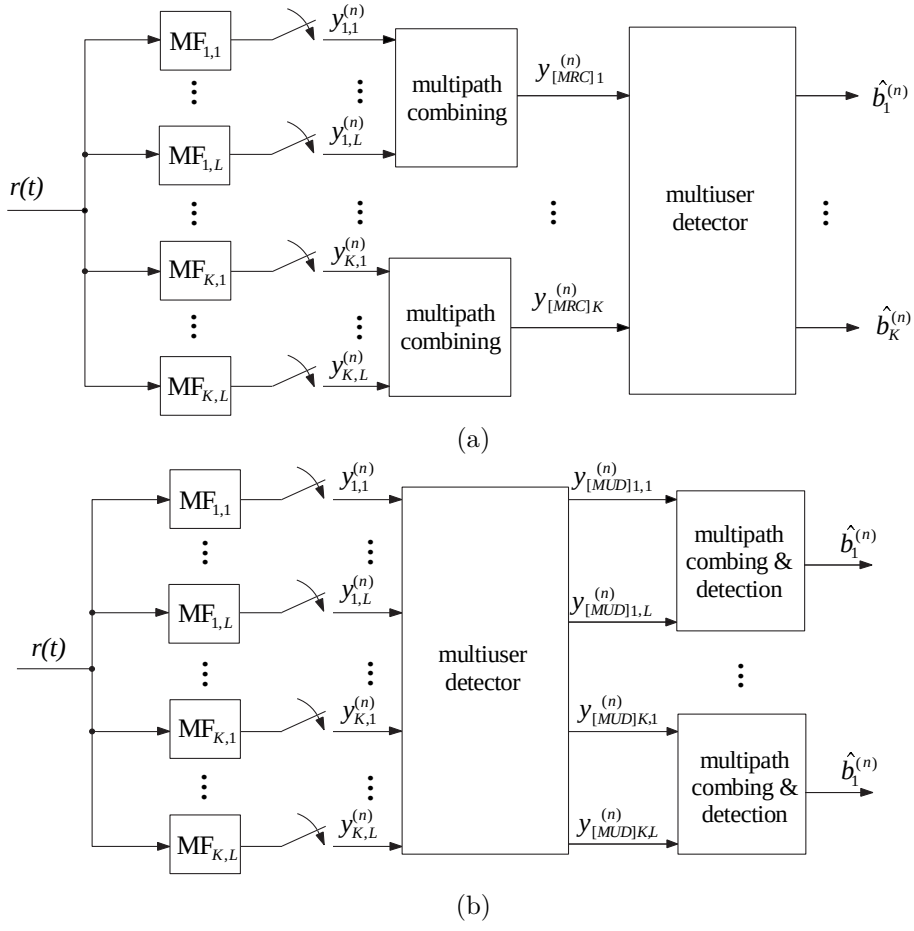


**Fig. 2.2**. **Multiuser receiver structures.**

For slowly fading channels the channel impulse response can be estimated precisely and the channel impulse response can be assumed to be known. In that case the optimal receiver (yielding lowest probability of symbol error) for the single user $k$ includes a filter matched to the convolution of the signature waveform $s_k^{(n)}(t)$ and the channel impulse response $c_k^{(n)}(t)$. In multipath channels such a matched filter is called a coherent RAKE receiver [79, 23]. The output of the coherent RAKE receiver for user $k$ is obtained by maximal ratio combing (MRC) the MF outputs

for different propagation paths, i.e., by

$$y_{[MRC]k}^{(n)} = \mathbf{c}_k^{\mathrm{H}(n)} \mathbf{y}_k^{(n)} = \sum_{l=1}^{L} c_{k,l}^{*(n)} y_{k,l}^{(n)}. \tag{2.51}$$

If the delay spread is significantly smaller than the symbol interval ($T_m \ll T$), the intersymbol interference (ISI) can be assumed to be negligible and a hard decision on the RAKE output $y_{[MRC]k}^{(n)}$ yields (near)optimal decision. If the channel introduces ISI, the receiver minimizing the error probability is significantly more complicated to implement. Thus, another optimization criterion, namely the minimum symbol sequence error probability, is selected. The optimum receiver then performs maximum likelihood sequence detection [23] in the presence of ISI. The MLSD can be implemented efficiently by applying the Viterbi algorithm [23, 80, 81]. Suboptimal receivers, which are simpler than MLSD and do not require separate channel estimator, for ISI channels include linear and decision-feedback (DF) equalizers (DFE) [23]. The DFE's can be applied also in frequency-selective channels [75]. Their overall impulse response should be such that the equalizer implicitly performs both maximal ratio combining and ISI reduction. The equalizers can be made adaptive so that they automatically tune their impulse response to approximate the desired one [23] or the impulse response can be computed by utilizing a channel impulse response estimate [82].

In fast or relatively fast fading channels, the channel impulse response cannot be assumed to be known. Thus, the optimal receiver is somewhat different from that in the slowly fading channels. The receiver minimizing the symbol error probability is again complex to implement and difficult to analyze [83]. Therefore, the MLSD is usually selected to be the optimal reference receiver. The MLSD receiver consists of an estimator, which estimates the received noiseless signal, and a correlator, which correlates (multiplies) the received signal with the signal estimate [84, 85, 86, 78]. The receiver structure is called *estimator-correlator* [85]. The optimal received noiseless signal estimator with known delays according to the MLSD criterion is the estimator which minimizes the mean squared error at the estimator output. The estimator is thus called minimum mean squared error (MMSE) estimator. Since the channel noise as well as the complex channel coefficients are assumed to have a Gaussian distribution, the MMSE estimator is a linear filter. The estimation and correlation must be performed for all possible transmitted data sequences. The data sequence yielding the largest correlator output is selected as the maximum likelihood sequence decision. Therefore, the computational complexity of the MLSD receiver depends exponentially on the transmitted data packet size. For that reason the MLSD is not feasible for most practical applications.

Suboptimal receivers which are simpler to implement can be obtained by applying differentially coherent or noncoherent receivers [77], or by decoupling the channel estimation and data detection. Blind sequence detectors not needing explicit channel estimation have also been proposed [87]. However, their applicability to time-varying channels has not been studied. The channel coefficients can be estimated by filtering the MF outputs by a *channel estimation filter* if the effect of data symbols is removed from them. The channel estimation filter can in principle

be either a *predictor*[7], a *filter*[8], or a *smoother* [88, p. 400]. A predictor uses only the past samples to estimate the current channel coefficient, whereas a "filter" uses also the current sample. A smoother uses the past, current, and future samples. The removal of the data modulation can be accomplished either in a data-aided, decision-directed[9], or non-data-aided (NDA) manner [89]. The DA channel estimators utilize MF output samples for which the data is known. This can be accomplished by transmitting a separate channel sounding reference signal (pilot signal) from which the channel is estimated [90, 91, 92]. For example, code-division duplexed pilot signal is utilized in the IS-95 CDMA system downlink [29]. Another way of implementing DA channel estimation is to utilize known pilot symbols time-division multiplexed in the transmitted data stream [93, 94, 95, 96, 97, 98, 99]. The channel needs to be interpolated between the pilot symbol intervals. The DD channel estimators utilize the decisions of the receiver to remove the effect of data modulation [100, 101, 102, 103]. The DD channel estimation often applies prediction of the complex channel coefficients, since only the past decisions are available for channel estimator [100, 101, 102]. By using tentative decisions smoother type channel estimation filters can also be applied [103]. The NDA channel estimators (also called blind channel estimators) estimate the channel without utilizing data or decisions. There has been an increasing interest in blind channel identification [104, 105, 106]. Their application to fast or relatively fast fading channels has gained very little attention [107].

### *2.2.2. Optimal multiuser demodulation*

The centralized multiuser receiver minimizing the bit error probability of one symbol of a particular user has been studied by Verdú [46] for the known channel case. The minimum error probability receiver must find the most probably transmitted data symbol for all users for all symbol intervals. In other words, $N_bK$ separate minimizations need to be performed. Each minimization computes a metric for all possible $|\Xi|^{N_b(K-1)}$ interfering data symbol combinations, where $|\Xi|$ denotes the cardinality of the set $\Xi$. Although a dynamic programming algorithm can be devised to implement the minimum probability of error detector, the required number of operations grow exponentially with the number of users. Furthermore, the performance of the minimum probability of error detector is difficult to analyze. Therefore, similarly to the single-user ISI channels, the minimum symbol sequence error probability is selected to be the optimization criterion. Thus, the maximum

[7] Only forward predictors are considered in this thesis.

[8] The term "filter" has here unavoidably two meanings: it denotes a general channel estimation filter or it denotes a certain type of filter as in [88, p. 400]. In nearly all cases the term "filter" has the former meaning in this thesis. In the case of the latter meaning, the word will be given in quotes in the sequel.

[9] Decision-feedback (DF) and decision-directed are synonyms. In this thesis, however, the term decision-directed is used in conjunction with removal of the effect of the data symbols in the channel estimation, whereas the term decision-feedback is used in conjunction with the decisions utilized in intersymbol interference or multiple-access interference cancellation.

likelihood sequence detector will be the optimal multiuser detector.

The MLSD multiuser receiver minimizes the probability of an erroneous decision on the bit vector $\boldsymbol{b}$ including the data symbols of all users on all symbol intervals. If the channel is known, the decision can be expressed in the form [47, 71, 108]

$$\hat{\boldsymbol{b}}_{[MLSD]} = \arg \min_{\boldsymbol{b} \in \Xi^{N_b K}} \Omega(\boldsymbol{b}), \tag{2.52}$$

where the log-likelihood function $\Omega(\boldsymbol{b})$ is

$$\Omega(\boldsymbol{b}) = 2\mathrm{Re}\big(\boldsymbol{b}^{\mathrm{H}} \mathcal{A}^{\mathrm{H}} \mathcal{C}^{\mathrm{H}} \boldsymbol{y}\big) - \boldsymbol{b}^{\mathrm{H}} \mathcal{A}^{\mathrm{H}} \mathcal{C}^{\mathrm{H}} \mathcal{R} \mathcal{C} \mathcal{A} \boldsymbol{b}. \tag{2.53}$$

The maximum likelihood detector admits the structure of the receiver in Fig. 2.2(a). If the signature waveforms are time-invariant, the minimization can be implemented by a dynamic programming algorithm so that the implementation complexity depends exponentially on the number of users only, not on the data packet length [46, 47]. However, the implementation complexity makes the MLSD infeasible for many practical applications. The asymptotic multiuser efficiency of the MLSD has been analyzed in [48, 109, 110]. MLSD for trellis-coded modulated CDMA transmissions in AWGN channels has been studied in [111], and for convolutionally encoded transmissions in [112]. The effect of delay estimation errors to MLSD has been considered in [113]. Joint maximum likelihood sequence detection and amplitude estimation in AWGN channels has been analyzed in [114, 115]. MLSD for flat Rician fading channels with synchronous CDMA have been considered in [73] and two path Rician fading channels with asynchronous CDMA in [74]. MLSD in unknown slowly fading channels has been considered in [116].

The performance of the MLSD is analyzed in [47, 48]. It turned out to be impossible to derive a closed form bit error probability expression for the MLSD. Upper and lower bounds, most of which are complicated to calculate, were found. The simplest lower bound is the *single-user bound* (or matched filter bound), which is the performance of a communication system with one active user ($K = 1$). The performance results on the MLSD demonstrate that significant performance gains can be obtained over the conventional single-user receiver. It has been demonstrated that the CDMA systems are not inherently interference limited, but that is the limitation of the conventional detector.

The maximum likelihood sequence detection for relatively fast fading channels has also been analyzed. MLSD for synchronous CDMA in Rayleigh fading channels has been presented in [72, 117]. The resulting MLSD receiver consists of the received noiseless signal estimator for all possible data sequences and a correlator, which multiplies the received signal with the estimated received noiseless signal (estimator-correlator receiver).

The optimal MLSD receiver for channels with unknown user and multipath delays $\tau_k$ and $\tau_{k,l}$ is significantly more difficult to derive. The reason is the fact that the received signal depends nonlinearly on the delays, and the MLSD receiver does not admit a simple estimator-correlator interpretation. One way to approximate the MLSD for the reception of a signal with unknown delays is to perform joint maximum likelihood estimation on the data, received complex amplitude, and the delays [118]. The joint ML estimation has clearly extremely high computational

complexity, which is exponential in the product of the number of users $K$, number of propagation paths $L$, and number of samples per symbol interval $N_s$.

Optimal decentralized multiuser detectors for AWGN channels have been considered in [119], where the multiple-access interference was modeled as non-Gaussian noise. The optimal decentralized multiuser detectors can also admit the utilization of the knowledge of a subset of the $K-1$ interfering signature waveforms. The optimal decentralized multiuser detector has also computational complexity which depends exponentially on the number of users.

### *2.2.3. Suboptimal multiuser demodulation*

Due to the prohibitive computational complexity of the optimal MLSD multiuser receiver suboptimal solutions have been studied extensively. They somehow approximate the optimal MLSD receiver. Most receivers can process either the matched filter bank output (Fig. 2.2(b)) or its maximal ratio combined version (Fig. 2.2(a)). The latter receivers do not eliminate the effect of MAI on channel estimation. Therefore, the multiuser detectors processing the MF bank output are often more desirable in practice, and the discussion in this thesis will focus on such receivers. Section 2.2.3.1 concentrates on linear equalizer type receivers, whereas interference cancellation receivers are considered in Section 2.2.3.2. Other suboptimal receivers are reviewed in Section 2.2.3.3.

#### *2.2.3.1. Linear equalizer type multiuser demodulation*

Linear equalizer type multiuser receivers process the matched filter output vector $\boldsymbol{y}$ (or the maximal ratio combined vector $\boldsymbol{y}_{[MRC]}$) by a linear operation. In other words, the output $\boldsymbol{y}_{[LIN]}$ of a linear multiuser detector $\mathcal{T} \in \mathbb{C}^{N_b KL \times N_b KL}$ is

$$\boldsymbol{y}_{[LIN]} = \mathcal{T}^{\top} \boldsymbol{y}. \tag{2.54}$$

Different choices of the matrix $\mathcal{T}$ yield different multiuser receivers. The identity matrix $\mathcal{T} = \mathbf{I}_{N_b KL}$, is equivalent to the conventional single-user receiver. The linear equalizer type receivers apply the principles of linear equalization, which has been used in ISI reduction [23].

The decorrelating or zero-forcing receiver, which completely removes the MAI, corresponds to the choice [54, 120]

$$\mathcal{T} = \mathcal{R}^{-1}. \tag{2.55}$$

Performance of the decorrelating detector in AWGN channels has been analyzed in [70, 54, 121, 122]. It has been shown that the decorrelating detector is optimally near-far resistant in the sense that it achieves the same NFR as the MLSD.

The performance of the decorrelator in known, slowly fading channels has been analyzed in [120, 71, 123, 108, 124]. Differentially coherent case has been considered in [125]. The corresponding analysis for estimated, relatively fast fading channels has been presented in [73, 74, 72, 126, 127]. The performance of the decorrelator utilizing the matched filter bank output $\boldsymbol{y}$ or the maximal ratio combined MF bank output $\boldsymbol{y}_{[MRC]}$ has been compared in [128, 129]. The principle of the decorrelating receiver has been extended to receivers utilizing antenna arrays [130, 131, 132, 133, 134, 135, 129], multiple base stations [136, 137, 138], or multiple data rates [139, 140]. Adaptive implementations of the decorrelating receiver for synchronous CDMA systems have been considered in [141, 142] and for asynchronous CDMA systems in [143]. The decorrelating receiver for convolutionally encoded CDMA transmissions in AWGN channels has been studied in [144]. Decorrelating receivers for quasi-synchronous CDMA systems in AWGN channels without precise delay estimation has been proposed in [145, 146, 147, 148], and for code acquisition in quasi-synchronous CDMA in [149]. The effect of delay estimation errors to the decorrelator performance has been analyzed in [150, 151]. The impact of quantization due to the finite precision presentation of the numbers in the receiver has been considered in [152, 153].

A partial decorrelator, which also makes the additive channel noise component white, so called noise-whitening detector is defined as

$$\mathcal{T} = \mathcal{L}^{-1}, \tag{2.56}$$

where $\mathcal{L}$ is lower triangular Cholesky factor of $\mathcal{R}$ such that $\mathcal{R} = \mathcal{L}^{\top}\mathcal{L}$ [154][10]. The noise-whitening detector forces the MAI due to past symbols to zero. The MAI due to future symbols may be suppressed by interference cancellation utilizing decision-feedback [155, 154] or the MAI may be handled by some suboptimal tree-search algorithm [157, 158, 159].

If the information symbols $b_k^{(n)}$ are independent and uniformly distributed and the channel is known, the linear receiver which minimizes the mean squared errors at the detector outputs (so called LMMSE detector) is [88]

$$\mathcal{T} = \left[\mathcal{R} + \sigma^2\left(\mathcal{C}\mathcal{A}\mathcal{A}^{\mathrm{H}}\mathcal{C}^{\mathrm{H}}\right)^{-1}\right]^{-1}. \tag{2.57}$$

The LMMSE receiver is equal to the linear receiver maximizing the signal-to-interference-plus-noise ratio (SINR) [160]. Centralized LMMSE receivers have been proposed for AWGN channels in [161], for fading channels in [124, 162, 163], and for antenna array receivers [132, 133, 164, 165]. Bounds for the NFR and SINR of the LMMSE receiver in AWGN channels have been derived in [166], and the bit error probability has been analyzed in [167].

The LMMSE receivers have attracted most interest due to their applicability to decentralized adaptive implementation. Decentralized LMMSE multiuser receivers for AWGN or slowly fading channels suitable for adaptive implementation based on training have been considered in [168, 169, 160, 170]. The convergence of the

[10]The definition of Cholesky factorization used in this thesis is an *upper* triangular matrix times a *lower* triangular matrix [155, 154] as opposed to the usual lower triangular times upper triangular matrix [156].

adaptive algorithms for the LMMSE multiuser receivers has been considered in [171, 172, 173]. A modified adaptive multiuser receiver applicable to relatively fast fading frequency-selective channels with channel state information has been proposed in [174]. CDMA system capacity with LMMSE receivers has been studied in [175, 176], where the *spreading-coding tradeoff*[11] has been addressed for systems with multiuser receivers. An improved LMMSE receiver, less sensitive to the time delay estimation errors, has been proposed in [177]. Receivers suitable for blind adaptation utilizing the minimum output energy (MOE) criterion have been studied in [178, 179, 180, 181]. It has been shown that the linear filter optimal in the MOE sense is equal to the linear filter optimal in the MMSE sense [178]. A blind receiver performing both the MOE filtering and timing estimation has been studied in [182]. Another blind algorithm, namely a linearly constrained constant modulus algorithm, has been applied in [183].

Decentralized linear receivers include MAI-whitening filters, which model the multiple-access interference as colored noise. The filters are then designed to whiten the colored MAI-noise plus the AWGN. The MAI-whitening filters have been studied in [184, 185, 186, 187, 188]. The implemention of the MAI-whitening filters is difficult, since it requires information on the MAI covariance. Approximate implementation results in adaptive receivers similar to their LMMSE counterparts [186].

The linear multiuser receivers process ideally the complete received data block, the length of which approaches infinity in asynchronous CDMA systems. In other words, the memory-length of the linear equalizer type receivers is infinite. In [54] it was shown that as $N_b \to \infty$ the decorrelating detector approaches a time-invariant, stable digital multichannel infinite impulse response (IIR) filter with $z$-domain transfer function

$$\mathbf{D}_d(z) = \left[\mathbf{R}(2)z^{-2} + \mathbf{R}(1)z^{-1} + \mathbf{R}(0) + \mathbf{R}(-1)z + \mathbf{R}(-2)z^2\right]^{-1}. \tag{2.58}$$

The input of $\mathbf{D}_d(z)$ is the matched filter bank output vector sequence $\mathbf{y}^{(n)}$. Since the matrix algebraic structure of the LMMSE detector is similar to that of the decorrelating detector, (2.58) can be generalized for it. The corresponding result applies for the noise-whitening detector as well [154]. The detectors can be presented in the form of (2.58) in systems with time-invariant signature waveforms only. The implementation of the multichannel IIR filter of the form (2.58) is not straightforward due to the symbolic computation of the inverse. Any multichannel IIR filter of the form (2.58) can also be represented in the form

$$\mathbf{D}(z) = \sum_{i=-\infty}^{\infty} \mathbf{D}(-i)z^i, \tag{2.59}$$

where the blocks $\mathbf{D}(-i) \in \mathbb{R}^{KL\times KL}$ define the filter coefficients. Truncation of (2.59) to obtain finite impulse response (FIR) filters has been suggested in [54] for

[11] The spreading-coding tradeoff deals with the question how much of the bandwith expansion should be invested in forward error-correcting encoding and how much should be invested in spreading.

the decorrelating detector. However, the effect of such a truncation on the detector performance was not analyzed. The truncation of the noise-whitening detector has been studied independently in [158], but the effect of detector memory-length to the performance has not been analyzed.

Several other ways to obtain finite memory-length multiuser detectors have been proposed. The most natural way is to leave symbol intervals regularly without transmission. This will result in finite blocks of transmitted symbols and obviously the detectors would then have finite memory-length [189, 190]. In [189], such an approach was called "isolation bit insertion". This, however, degrades the bandwith efficiency and requires some form of synchronism between users. Other approaches to obtain finite memory-length multiuser detectors include nonlinear subtraction of estimated multiple-access interference ("edge correction") [191], and hard decision approximation of decorrelator [161], which ends up with the decision directed, nonlinear MAI canceler. One-shot detection [49, 192] has also been studied. FIR designs have been considered in [193].

In addition to the infinite memory, the linear multiuser receivers have relatively high implementation complexity due to the matrix inversion as in (2.55), (2.56), or (2.57). An approximate update algorithm has been proposed in [194, 191]. However, the algorithm is restricted to track only small changes in the correlations caused by minor delay changes. Approximate multistage linear equalizer type detectors have been proposed in [190]. Their computational requirements are still a cubic function of the number of users. Another approach called $\delta$-adjusted multiuser detection has been proposed in [195], but its near-far resistance is still an open problem.

#### *2.2.3.2. Interference cancellation*

The idea of *interference cancellation* (IC) receivers is to estimate the multiple-access and multipath induced interference and then subtract the interference estimate from the MF bank (or MRC) output. The interference cancellation can be derived as an approximation of the MLSD receiver with the assumption that the data, amplitude, and delays of the interfering users (or a subset of them) are known [55]. There are several principles of estimating the interference leading to different IC techniques. The interference can be canceled simultaneously from all users leading to *parallel* interference cancellation (PIC), or on a user by user basis leading to *serial* (successive) interference cancellation (SIC). Also *groupwise* serial (GSIC) or parallel (GPIC) interference cancellation are possible. The interference estimation can utilize tentative data decisions. The scheme is called hard decision (HD) interference cancellation. If tentative data decisions are not used, the scheme is called soft decision (SD) interference cancellation. The interference cancellation can also iteratively improve the interference estimates. Such a technique is utilized in multistage receivers.

The multistage hard-decision parallel interference cancellation (HD-PIC) output

at the $m$th stage can be presented as [55]

$$\boldsymbol{y}_{[HD-PIC]}(m) = \boldsymbol{y} - \big(\mathcal{R} - \mathbf{I}_{N_b KL}\big)\hat{\mathcal{C}}(m-1)\mathcal{A}\hat{\boldsymbol{b}}(m-1), \tag{2.60}$$

where $\hat{\mathcal{C}}(m-1)$ and $\hat{\boldsymbol{b}}(m-1)$ denote the tentative channel and data estimates provided by the stage $m-1$ of the multistage HD-PIC receiver. The multistage PIC can be initialized by any linear equalizer type receiver. In the soft-decision parallel interference cancellation (SD-PIC) the amplitude-data product is estimated linearly without making an explicit data decision, or a tentative data decision with a soft nonlinearity (such as hyperbolic tangent of linear clipper) is made. In other words, the product $\hat{\mathcal{C}}(m-1)\mathcal{A}\hat{\boldsymbol{b}}(m-1)$ of the estimates $\hat{\mathcal{C}}(m-1)$, $\hat{\boldsymbol{b}}(m-1)$, and $\mathcal{A}$ in (2.60) is replaced by an estimate $(\widehat{\mathcal{C}\mathcal{A}\boldsymbol{b}})(m-1)$ of the product $\mathcal{C}\mathcal{A}\boldsymbol{b}$. In contrast to the linear equalizer type multiuser receivers, the PIC receivers have inherently finite memory. The output of the HD-PIC receiver for the $n$th symbol interval is

$$\mathbf{y}^{(n)}_{[PIC]}(m) = \mathbf{y}^{(n)} - \hat{\mathbf{\Psi}}^{(n)}_{[PIC]}(m). \tag{2.61}$$

The multiple-access interference estimate $\hat{\mathbf{\Psi}}^{(n)}_{[PIC]}(m)$ has the form

$$\hat{\mathbf{\Psi}}^{(n)}_{[PIC]}(m) = \sum_{i=-P_{PIC}}^{P_{PIC}} \left(\mathbf{R}(-i) - \delta_{i,0}\mathbf{I}_{KL}\right)\hat{\mathbf{C}}^{(n+i)}(m-1)\mathbf{A}\hat{\mathbf{b}}^{(n+i)}(m-1), \tag{2.62}$$

where $\delta_{i,j}$ is the Kronecker delta, $P_{PIC} = \lceil \frac{T+T_m}{T} \rceil$, and $\lceil x \rceil$ denotes the smallest integer larger than or equal to $x$. The tentative estimates and decisions may be replaced by final ones at those symbol intervals for which they are available [161]. The result is decision-feedback HD-PIC receiver.

The multistage HD-PIC receiver has been proposed and analyzed for AWGN channels in [196, 55, 197, 198, 199, 200, 201]. The corresponding receivers for slowly fading channels have been studied in [202, 203, 204, 205, 206, 207, 208], and for relatively fast fading channels in [209, 210, 211, 57]. The HD-PIC receivers for transmissions with diversity encoding has been analyzed in [212], and for systems with multiple data rates has been studied in [213]. HD-PIC receivers for trellis-coded modulated CDMA systems in AWGN channels have been studied in [111]. The application of the HD-PIC to multiuser delay estimation in relatively fast fading channels has been considered in [214, 215, 57]. The SD-PIC receivers with linear data-amplitude product estimation for slowly fading channels have been considered in [216, 217], and for multicellular systems in [218]. The SD-PIC receivers with soft nonlinearity have been considered for AWGN channels in [219, 220, 221]. Modifications of the PIC receiver have also been presented. Replacing the matrix $\big(\mathcal{R} - \mathbf{I}_{N_b KL}\big)\hat{\mathcal{C}}(m-1)\mathcal{A}$ in (2.60) by an adaptively controlled weighting matrix for AWGN channels has been proposed in [219, 222, 223, 224, 225]. A partial PIC receiver with a weighting matrix in front of the matrix $\big(\mathcal{R} - \mathbf{I}_{N_b KL}\big)\hat{\mathcal{C}}(m-1)\mathcal{A}$ in (2.60) has been proposed in [226, 227, 228]. The weights were chosen in an *ad hoc* manner according to the reliability of the interference estimates. By applying the expectation-maximization (EM) or the space alternating generalized EM (SAGE) algorithm a class of iterative multistage receivers is obtained [229, 230, 231, 232].

The iterative EM or SAGE based receivers lead to the application different modified interference cancellation principles. The effect of delay estimation errors on the performance of the HD-PIC receiver has been considered in [113], and to the SD-PIC receiver in [216].

The serial interference cancellation is performed on user by user basis [233, 234]. In the SIC, the amplitude and data of user 1 are estimated first. Using the obtained estimates the MAI estimate of user 1 is subtracted from the MF outputs of the rest of the users. Then the amplitude and data of user 2 are estimated, and the MAI estimate of user 2 is subtracted from the MF outputs of the users $k = 3, 4, \ldots, K$ etc. The cancellation should start with the user with the largest average power (indexed as user 1), the second powerful user (indexed as user 2) should be canceled next etc. The ordering is a problem in relatively fast fading channels, since it must be updated frequently. SD-SIC has been considered in [234, 235, 217], and HD-SIC in [233, 236, 237, 238, 239]. The SIC for multirate CDMA communications has been studied in [240, 241]. The SIC has the inherent problem that in asynchronous CDMA systems the processing window of user 1 must ideally be $K$ symbols so that the MAI caused by users $1, 2, \ldots, K-1$ can be canceled from the MF output of user $K$ [51]. Another problem with the SIC is that it may not yield good enough performance in heavily loaded CDMA systems, where the performance of the conventional receiver is poor. The reason for that is that the SIC is initialized by a conventional receiver for user 1. If the MAI estimate of the signal of user 1 is poor in the cancellations, the estimation errors propagate to all users. The SIC has good performance in systems where the powers of users differ significantly. This cannot be the case in systems with very large number of users. The effect of delay estimation errors to the SD-SIC has been considered in [242] and to the HD-SIC in [243]. The combination of the PIC and the SIC receivers has been studied in [244].

The groupwise interference cancellation receivers detect the symbols of the users within some group and form an estimate of the MAI caused by the users within that group based on the symbol decisions. The MAI estimate is then subtracted from the other users' MF outputs. The groupwise interference cancellation can be performed either serially or in parallel. The groupwise serial interference cancellation has been proposed in [245], and the groupwise parallel interference cancellation in [246, 247]. The grouping can also be performed on consecutive symbols of a particular user in time [246, 247]. The groupwise SIC has been proposed also for multiple data rate CDMA systems utilizing multiple processing gains [248, 249]. The detector for a group of users can, in principle, apply any known multiuser detector, such as the conventional detector, the decorrelating detector, the PIC detector, or the maximum likelihood sequence detector. The groupwise interference cancellation is a special case of more general groupwise multiuser receivers [250, 251].

The interference cancellation can also be combined to linear equalizer type reception. Most often that is based on decision-feedback of the detected symbols to perform a subtractive cancellation of part of the MAI. The DF-IC in conjunction with the noise-whitening detector has been considered in [155, 154], and in conjunction with an adaptive equalizer in [252, 253]. The DF-IC receiver for convolutionally encoded CDMA transmissions in AWGN channels has been studied in

[144].

### *2.2.3.3. Other multiuser receivers*

Most suboptimal multiuser receivers fit into the categories presented in Sections 2.2.3.1 and 2.2.3.2. The other most interesting techniques are reviewed briefly in this section.

In addition to the linear equalization or interference cancellation, the MLSD can be approximated by partial trellis-search algorithms. The log-likelihood metric (2.53) is computed for a subset of all possible data vectors $\boldsymbol{b}$. Different criteria to choose the subsets result in different partial trellis-search algorithms. The application of sequential decoding has been proposed in [254]. Some of the groupwise multiuser receivers discussed above in Section 2.2.3.2 can also be interpreted as partial trellis-search algorithms [246]. Other partial tree-search algorithms have been proposed in [255, 256]. A partial trellis-search algorithm for trellis-coded modulated CDMA transmissions in AWGN channels has been studied in [111], and for convolutionally encoded transmissions in [112].

Multiuser parameter estimation, i.e., the complex amplitude and delay estimation has gained increasing interest. Since there is usually no a priori distribution available for the delays, maximum likelihood estimation is usually selected to be the optimal technique for delay acquisition and tracking [257, 258, 118]. This approach has also been considered for amplitude estimation [259]. Suboptimal techniques include subspace estimators [258, 260, 261, 262, 263], a hierarchical ML estimation [264], large sample mean ML estimation [265], an extended Kalman filter [266, 267], recursive least squares algorithm [267], and sequential estimation [268, 269]. The amplitude estimation in AWGN channels with unknown delays has been the topic in [270]. The estimation of the number of active users in AWGN channels has been studied in [271, 272, 273, 274, 275].

Multiuser detection based on empirical distribution of the MAI has been proposed in [276, 277, 278]. The distribution of the MAI is estimated by forming a corresponding histogram, and the received symbol is selected so that it matches best into the histogram.

Neural networks have been proposed to approximate the decision regions of the optimal receivers. Multilayer perceptron networks both for centralized and decentralized detection in AWGN channels have been proposed in [279] and single-layer perceptron networks in [280]. Self-organizing maps for centralized detection in AWGN channels have been studied in [281]. Radial basis functions for decentralized detection in AWGN channels have been considered in [282]. Hopfield networks for centralized detection in AWGN channels have been proposed in [283, 284].

## 2.3. Problem formulation

Several interesting open problems exist in the field of multiuser receivers. From the practical point of view, one of the most important questions is, whether multiuser receivers are feasible in practical DS-CDMA systems or not. The question can also be posed as whether the price paid in terms of implementation complexity is worth the obtained performance improvement. The final answer is of course not only technical but also commercial and, thus, out of the scope of this thesis. To provide tools for the decision making process, some open problems related to the multiuser receivers which are considered to be most promising from the practical point of view, are addressed in this thesis. The multiuser receivers appearing possibly practical include the class of linear equalizer type and interference cancellation receivers[12]. As can be seen from the literature review in Section 2.2, the decorrelating multiuser receiver has received huge attention from the scientific community. The interference cancellation is popular in the proposed CDMA system standards mentioned at the end of Section 1.1. In the class of interference cancellation receivers the attention is focused on the HD-PIC receivers in this thesis. The PIC is applied due to problems associated with SIC in purely asynchronous DS-CDMA systems, and due to the potentially better performance of PIC as hard decisions are applied [51]. Hard decisions yield usually better performance than soft decisions, since HD receivers can utilize efficient channel estimators, whereas the SD receivers cannot [51]. The groupwise interference cancellation receivers are definitely promising and interesting, but they are neglected in this thesis to make the discussion clearer and simpler.

The key problems in the implementation of the linear equalizer type multiuser detectors are the infinite memory-length, and the need for matrix inversion in the detector update. The memory-length problem is the topic of Chapter 3, where finite memory-length detection is studied. The matrix inversion problem is considered in Chapter 5, where implementation algorithms for multiuser receivers are proposed. The implementation requirements of both the linear equalizer type and the HD-PIC receivers are also compared in Chapter 5. Emphasis is on detection in dynamic CDMA systems, where the detectors must be updated frequently due to changes in the number of users, in the signature waveforms, in the delays, or in the received amplitudes. The HD-PIC receivers are relatively straightforward to implement in principle, although a large variety of different modifications exist. The performance of the linear equalizer type and the HD-PIC multiuser receivers with real DA or DD channel estimation has been studied only very little. The performance analysis and comparisons of the decorrelating and HD-PIC in Rayleigh fading channels is therefore the topic of Chapter 4.

[12]Several other receiver techniques described in Section 2.2.3.3, may very well become practical after a while. However, most of them are currently rather immature.

# 3. Finite memory-length linear multiuser detection

Most of the linear equalizer type multiuser detectors can be characterized as an inverse of some form of correlation matrix, as discussed in Chapter 2. In an ideal implementation their memory equals the data packet length, which often can be assumed to approach infinity. The linear multiuser detectors for an asynchronous CDMA system can be presented as multichannel IIR filters. Although stable versions of the multiuser detector filters are known to exist in many cases, FIR filters are more robust in practical systems. Multichannel IIR filters are also complicated to update as a change in correlations occurs, whereas multichannel FIR filters admit easier update formulation. Variations in the number of users, in their signature waveforms (e.g., due to a hand-over in a cellular system), or in their delays change the correlations. In such a case, the multiuser detectors must be updated accordingly to match to the new received signal. In this chapter, it is shown that the infinite memory-length detectors can be accurately approximated by detectors with finite and also relatively short memory-length. In particular, it is shown that near-far resistance to a high degree can be obtained by moderate memory-lengths. This result provides a mechanism to implement near-far resistant linear multiuser detectors in systems in which the number of users or their propagation delays change over time.

The detectors studied in this chapter process the MF filter bank output vector and the multipath combining is performed after the multiuser processing. The analysis in this chapter assumes that the channel is constant, i.e., the effects due to fading are neglected. The assumption is justified since the effect of detector memory-length to the performance of the detection can be characterized equally in an additive white Gaussian noise as well as in a fading channel.

The chapter is organized as follows. Linear finite memory-length multiuser detectors are defined in Section 3.1. The results of the stability analysis of finite memory-length detectors are presented in Section 3.2. The effects of the finite memory-length on the bit error probability, the asymptotic multiuser efficiency, and the near-far resistance of the detectors are analyzed in Section 3.3. In Section 3.4, the results are illustrated by numerical examples. Finally, the results are summarized and discussed in Section 3.5.

## 3.1. Linear FIR multiuser detectors

The idea to be considered is to replace the $N_bKL \times N_bKL$ detector matrix $\mathcal{T}$ by a $NKL \times KL$ detector matrix. A *finite memory-length* linear multiuser detector of length $N = 2P + 1$ (referred to as an FIR detector for brevity) is defined as[1]

$$\mathcal{D}_N = \left( \begin{array}{ccccccccc} \mathbf{D}(P) & \cdots & \mathbf{D}(1) & \mathbf{D}(0) & \mathbf{D}(-1) & \cdots & \mathbf{D}(-P) \end{array} \right)^\top \in \mathbb{R}^{NKL \times KL}, \tag{3.1}$$

where the blocks $\mathbf{D}(i) \in \mathbb{R}^{KL \times KL}, i \in \{-P, \ldots, P\}$ define a partition of the detector $\mathcal{D}_N$. The *infinite memory-length* linear multiuser detector (referred to as an IIR detector) $\mathcal{D}$ corresponding to the FIR detector $\mathcal{D}_N$ is defined as

$$\mathcal{D} = \mathcal{D}_N, N \to \infty. \tag{3.2}$$

The linear multiuser FIR detector output

$$\mathbf{y}^{(n)}_{[LIN]} = \mathcal{D}_N^\top \boldsymbol{y}^{(n)} \in \mathbb{C}^{KL} \tag{3.3}$$

provides a decision statistic for the symbols $\mathbf{b}^{(n)}$. The output can be expressed by (2.27) and (2.28) as

$$\mathbf{y}^{(n)}_{[LIN]} = \mathcal{F}^\top \mathcal{A}^{(n)} \boldsymbol{b}^{(n)} + \boldsymbol{\mu}^{(n)}(\boldsymbol{b}^{(n)}_e) + \mathbf{w}^{(n)}_{[LIN]} = \bar{\mathcal{F}}^\top \bar{\mathcal{A}}^{(n)} \bar{\boldsymbol{b}}^{(n)} + \mathbf{w}^{(n)}_{[LIN]}, \tag{3.4}$$

where $\mathcal{F} = \mathcal{R}^{(n)}\mathcal{D}_N$ and $\bar{\mathcal{F}} = \bar{\mathcal{R}}^{\top(n)}\mathcal{D}_N$ are the convolutions of the multiuser channel impulse response $\mathcal{R}^{(n)}$ or $\bar{\mathcal{R}}^{(n)}$ and the multiuser detector $\mathcal{D}_N$,

$$\begin{aligned} \boldsymbol{\mu}^{(n)}(\boldsymbol{b}^{(n)}_e) &= \mathbf{D}(P)\mathbf{R}^{(n-P)}(2)\mathbf{C}^{(n-P-2)}\mathbf{A}\mathbf{b}^{(n-P-2)} \\ &+ \mathbf{D}(P)\mathbf{R}^{(n-P)}(1)\mathbf{C}^{(n-P-1)}\mathbf{A}\mathbf{b}^{(n-P-1)} \\ &+ \mathbf{D}(P-1)\mathbf{R}^{(n-P+1)}(2)\mathbf{C}^{(n-P-1)}\mathbf{A}\mathbf{b}^{(n-P-1)} \\ &+ \mathbf{D}(-P+1)\mathbf{R}^{\top(n+P+1)}(2)\mathbf{A}\mathbf{C}^{(n+P+1)}\mathbf{b}^{(n+P+1)} \\ &+ \mathbf{D}(-P)\mathbf{R}^{\top(n+P+2)}(1)\mathbf{A}\mathbf{C}^{(n+P+1)}\mathbf{b}^{(n+P+1)} \\ &+ \mathbf{D}(-P)\mathbf{R}^{\top(n+P+3)}(2)\mathbf{A}\mathbf{C}^{(n+P+2)}\mathbf{b}^{(n+P+2)} \end{aligned} \tag{3.5}$$

is the response of the symbols outside the processing window, i.e., the *edge effect* due to finite detector memory-length, and $\mathbf{w}^{(n)}_{[LIN]} = \mathcal{D}_N^\top \boldsymbol{w}^{(n)}$ is a zero mean Gaussian random vector with covariance matrix $\sigma^2 \mathcal{D}_N^\top \mathcal{R}^{(n)} \mathcal{D}_N$. In systems with time-varying signature waveforms the above formulation should be interpreted as a snap-shot of the time-varying detector on a particular symbol interval. Filtering interpretation of an arbitrary multichannel linear FIR detector is illustrated in Fig. 3.1.

To design FIR detectors, or in other words, to find in some sense good $NKL \times KL$ matrices $\mathcal{D}_N$, the truncation of IIR detectors is first considered. This was

[1]Note that the time index $n$ is left out for notational convenience, although the detector $\mathcal{D}_N$ and the convolution matrix $\mathcal{F}$ depend on $n$ if the signature waveforms are time-varying.

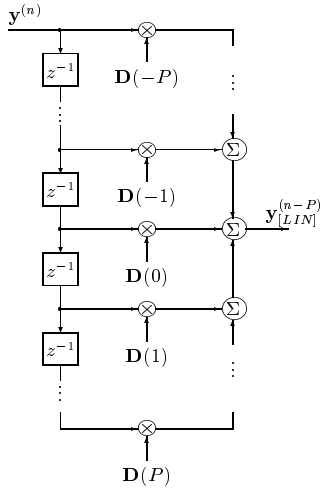


**Fig. 3.1. A FIR linear multiuser detector.**

suggested in [54] for the decorrelating detector. A linear multiuser detector $\mathcal{D}_{[d]N}$ satisfying

$$\mathcal{R}^{(n)}\mathcal{D}_{[d]N} = \mathcal{U}_N, \tag{3.6}$$

where $\mathcal{U}_N = (\mathbf{0}_{KL}, \ldots, \mathbf{0}_{KL}, \mathbf{I}_{KL}, \mathbf{0}_{KL}, \ldots, \mathbf{0}_{KL})^\top \in \{0,1\}^{NKL \times KL}$, will be called the *truncated decorrelating detector*. It is clear that $\mathcal{D}_{[d]N}$ is the $NKL \times KL$ *middle block column*, i.e., the middle $KL$ columns, of the inverse of $\mathcal{R}^{(n)}$. A linear multiuser detector $\mathcal{D}_{[ms]N}$ satisfying

$$[\mathcal{R}^{(n)} + \sigma^2(\mathcal{C}^{(n)}\mathcal{A}^{(n)}\mathcal{A}^{\mathrm{H}(n)}\mathcal{C}^{\mathrm{H}(n)})^{-1}]\mathcal{D}_{[ms]N} = \mathcal{U}_N, \tag{3.7}$$

will be called the *truncated LMMSE detector*.[2] A linear multiuser detector $\mathcal{D}_{[nw]N}$ satisfying

$$\mathcal{L}^{(n)}\mathcal{D}_{[nw]N} = \mathcal{U}_N, \tag{3.8}$$

will be called the *truncated noise-whitening detector*.

An alternative to truncation is to optimize detectors based on the finite processing-window length model (2.28). To generalize the decorrelating detector we should find a zero-forcing detector $\bar{\mathcal{D}}_{[d]N} \in \mathbb{R}^{NKL \times KL}$ satisfying

$$\bar{\mathcal{R}}^{\top(n)}\bar{\mathcal{D}}_{[d]N} = \mathcal{U}_N, \tag{3.9}$$

which does not have a unique solution. A unique detector can be found by selecting the pseudoinverse (i.e., Moore-Penrose generalized inverse), which yields the best

[2]Note that at high signal-to-noise ratios ($\sigma^2 \to 0$) or at high interference levels ($E_k \to \infty$) the LMMSE detector approaches the decorrelating detector.

least squares solution to (3.9). Since $\mathcal{R}^{(n)}$ is positive definite, $\bar{\mathcal{R}}^{(n)}$ has full rank with more columns than rows. Thus, the pseudoinverse solution defines the *optimal FIR decorrelating detector*

$$\bar{\mathcal{D}}_{[d]N} = \text{mbc}\left\{(\bar{\mathcal{R}}^{(n)}\bar{\mathcal{R}}^{\top(n)})^{-1}\bar{\mathcal{R}}^{(n)}\right\}, \tag{3.10}$$

where mbc denotes "middle block column of". It should be noted that the above detector is the optimal FIR decorrelator in the sense that it minimizes the least squares error in the solution of (3.9). However, there is no guarantee that the detector $\bar{\mathcal{D}}_{[d]N}$ would yield lower bit error probability than the truncated decorrelating detector $\mathcal{D}_{[d]N}$. Since the optimal FIR detector forces the MAI due to edge symbols $\boldsymbol{b}_e^{(n)}$ to minimum, it cannot any more force the MAI due to symbols $\boldsymbol{b}^{(n)}$ to zero. This trade-off can introduce a performance penalty in some cases.

The *optimal FIR LMMSE detector* is by (2.28) and [88, Sec. 12.5][3]

$$\begin{aligned}\bar{\mathcal{D}}_{[ms]N} &= \text{mbc}\quad\Big\{(\mathcal{R}^{(n)})^{-1}\bar{\mathcal{R}}^{(n)}[\bar{\mathcal{R}}^{\top(n)}(\mathcal{R}^{(n)})^{-1}\bar{\mathcal{R}}^{(n)} \\ &\qquad +\sigma^2(\mathcal{C}^{(n)}\mathcal{A}^{(n)}\mathcal{A}^{\mathrm{H}(n)}\mathcal{C}^{\mathrm{H}(n)})^{-1}]^{-1}\Big\}.\end{aligned} \tag{3.11}$$

If all diagonal values of $\sigma^2(\mathcal{C}^{(n)}\mathcal{A}^{(n)}\mathcal{A}^{\mathrm{H}(n)}\mathcal{C}^{\mathrm{H}(n)})^{-1}$ are non-zero, matrix

$$\bar{\mathcal{R}}^{\top(n)}(\mathcal{R}^{(n)})^{-1}\bar{\mathcal{R}}^{(n)} + \sigma^2(\mathcal{C}^{(n)}\mathcal{A}^{(n)}\mathcal{A}^{\mathrm{H}(n)}\mathcal{C}^{\mathrm{H}(n)})^{-1}$$

is nonsingular and (3.11) has a unique solution. If $\sigma^2 \to 0$, the inverse in (3.11) does not exist. In that case there is no noise term in the model in (2.28) and the problem can be viewed to be deterministic and underdetermined. In that case there is no LMMSE detector. It should be noted that, contrary to the optimal FIR decorrelator, the optimal FIR LMMSE detector is never inferior to the truncated LMMSE detector. Obviously, it is computationally simpler to update the truncated detectors than the optimal ones. What is more, computation of the truncated FIR detectors is numerically more stable in practical implementations. However, both classes of FIR detectors are studied for completeness.

It is clear that the use of FIR detectors instead of the IIR ones causes some performance loss. The performance analysis of the FIR detectors will be carried out in Section 3.3. However, to be able to quantify the performance loss, the stability of linear multiuser detectors is analyzed in the next section.

## 3.2. Stability of detectors

In this section, conditions for the stability of the multiuser detectors are first discussed. Although it proves to be impossible to find an easy test for detector

[3]The same result in a different form has been derived in [161]. The expression in (3.11) is more appropriate for further derivations in subsequent sections than the expression given in [161, Eq. (4.3)].

stability, the analysis gives insight into the problem. Furthermore, the analysis provides us with tools to derive two interesting results for stable detectors.

For notational simplicity, the analysis in this section is presented for an AWGN channel with one propagation path (i.e., $L = 1$, and $\mathcal{C} = \mathbf{I}_{N_b}$, $\mathbf{R}^{(n)}(2) = \mathbf{0}_K$, $\forall\, n$). However, the generalization of the analysis to the multipath channel case ($L \geq 2$) is straightforward.

A multiuser detector $\mathcal{D}_N$ is defined to be stable if and only if the impulse response of the IIR detector is decaying, i.e., $\mathbf{D}(-P)$, and $\mathbf{D}(P) \to \mathbf{0}_K$, as $N \to \infty$ (or equivalently $P \to \infty$). The above definition is a consequence of the standard stability definition of a digital IIR filter [285, pp. 81–82]. It is intuitively clear that, if a multiuser detector is stable, the IIR detector can be truncated to a FIR detector with little performance degradation if the memory-length $N$ is large enough. This can be predicted from (3.5), where the response of the symbols outside the processing window satisfies $\boldsymbol{\mu}^{(n)} \to \mathbf{0}$, as $N \to \infty$.

For systems with time-invariant signature waveforms, it was shown in [54] that the truncated decorrelating detector is stable if and only if[4]

$$\det[\mathbf{R}^{\top}(1)e^{j\omega} + \mathbf{R}(0) + \mathbf{R}(1)e^{-j\omega}] \neq 0,\ \forall\, \omega \in [0, 2\pi). \tag{3.12}$$

It is clear that (3.12) is difficult to evaluate for all possible delay combinations. Therefore, the most practical solution is to compute numerical examples to determine whether a detector is stable or not. This is particularly true for systems with time-varying signature waveforms, as will be discussed below.

The result (3.12) was derived via a $z$-domain approach, which is not applicable in systems with time-varying signature waveforms. For that reason a time-domain analysis is needed[5]. First a dimension symbol $N$ is added to $\mathcal{R}^{(n)}$ in (2.37) and the time interval index $(n)$ is dropped to yield $\mathcal{R}_N$. To simplify the notations, the non-zero blocks in $i$th block column of $\mathcal{R}_N$ are denoted by $\mathbf{R}_i^{\top}(1)$, $\mathbf{R}_i(1)$, and $\mathbf{R}_{i+1}(0)$ etc.[6]. Let the inverse of $\mathcal{R}_N$ be

$$\mathcal{T}_N = \mathcal{R}_N^{-1} = \begin{pmatrix} \mathbf{T}_{11}(N) & \mathbf{T}_{21}^{\top}(N) & \cdots & \mathbf{T}_{N,1}^{\top}(N) \\ \mathbf{T}_{21}(N) & \mathbf{T}_{22}(N) & \cdots & \mathbf{T}_{N,2}^{\top}(N) \\ \vdots & \vdots & & \vdots \\ \mathbf{T}_{N,1}(N) & \mathbf{T}_{N,2}(N) & \cdots & \mathbf{T}_{N,N}(N) \end{pmatrix} \in \mathbb{R}^{NK \times NK}, \tag{3.13}$$

where each $\mathbf{T}_{ij}(N) \in \mathbb{R}^{K \times K}$. The dependence on $N$ is included in the argument, since the blocks are different for different $N$. Note that $\mathbf{D}_d(-P) = \mathbf{T}_{N,P+1}(N)$. Thus, the stability of the truncated decorrelating detector is equivalent to $\mathbf{T}_{N,P+1}(N) \to \mathbf{0}_K$, as $N \to \infty$. The following recursive expressions (3.14) and (3.15), which are proved in Appendix 1, provide the tools to study the stability

[4]Time index $n$ is not needed in $\mathbf{R}(i)$, since the signature waveforms are time-invariant and the delays are assumed to be constant.

[5]The analysis will also apply to systems with time-invariant signature waveforms, since the time-invariant case can be viewed as a special case of a system with time-varying signature waveforms.

[6]In the second column, for example, $\mathbf{R}_2^{\top}(1) = \mathbf{R}^{\top(n-P+1)}(1)$, $\mathbf{R}_2(0) = \mathbf{R}^{(n-P+1)}(0)$, $\mathbf{R}_3(1) = \mathbf{R}^{(n-P+2)}(1)$ etc.

of the detectors. For any $i, j \in \{1, 2, \ldots, N-1\}$

$$\mathbf{T}_{i,j}(N) = \mathbf{T}_{i,j}(N-1) + \mathbf{T}^{\top}_{N-1,i}(N-1)\mathbf{R}^{\top}_{N}(1)\mathbf{T}_{N,N}(N)\mathbf{R}_{N}(1)\mathbf{T}_{N-1,j}(N-1), \tag{3.14}$$

$$\mathbf{T}_{N,j}(N) = \mathbf{T}_{N,N}(N)\mathbf{R}_{N}(1)\mathbf{T}_{N-1,j}(N-1). \tag{3.15}$$

For any $1 \leq i < N$ it is obtained by induction from (3.15) that

$$\mathbf{T}_{N,i}(N) = \prod_{j=i+1}^{N} [\mathbf{T}_{j,j}(j)\mathbf{R}_{j}(1)]\mathbf{T}_{i,i}(i). \tag{3.16}$$

A sufficient condition for the stability of the detector, that is for

$$\mathbf{T}_{N,i}(N) \to \mathbf{0}_{K}, \text{ as } N \to \infty, \tag{3.17}$$

is $\left|\lambda_{max}\left[\mathbf{R}^{\top}_{j}(1))\mathbf{T}^{-2}_{j,j}(j)\mathbf{R}_{j}(1)\right]\right| < 1, \forall\, j \in \{i+1, i+2, \ldots, N\}$ [286, p. 69], where $\lambda_{max}(\mathbf{A})$ denotes the eigenvalue of the argument matrix $\mathbf{A}$ with the largest absolute value. The above condition is, however, often overly stringent. It was not satisfied in most of the numerical examples computed, but still the detectors were stable in nearly all cases. In other words, it is very difficult to provide necessary conditions for detector stability. Numerical examples are often the only practical way to verify the stability of detectors.

For systems with time-invariant signature waveforms it has been shown via the $z$-domain approach that the stability of the decorrelating detector implies the uniqueness of the limiting IIR detector [54]. The corresponding result for systems with time-varying signature waveforms is posed in the following proposition and proved in Appendix 1.

**Proposition 1** *If the truncated decorrelating, LMMSE, or noise-whitening detectors are stable, the limiting IIR detectors are unique.*

The truncated detectors neglect the edge effect caused by the symbols outside the observation window, while the optimal FIR detectors take it into consideration. On the other hand, the stability of the detectors implies that the edge effect at the detector output approaches zero as $N$ is large. Thus, it is expected that the truncated and the optimal FIR detectors should approach the same limiting IIR detector, if they are stable. This is indeed the case under mild conditions as stated below and proved in Appendix 1.

**Proposition 2** *Assume that the received energies $E_k$ and noise power spectral density $\sigma^2$ satisfy $0 < \frac{E_k}{\sigma^2} < \infty$, $\forall\, k \in \{1, 2, \ldots, K\}$. Assume also that the decorrelating and LMMSE detectors are stable. Then both the truncated LMMSE detector $\mathcal{D}_{[ms]N}$ (3.7) and the optimal FIR LMMSE detector $\bar{\mathcal{D}}_{[ms]N}$ (3.11) converge to the same IIR LMMSE detector as the detector memory-length $N$ approaches infinity, i.e.,*

$$\bar{\mathcal{D}}_{[ms]} = \mathcal{D}_{[ms]}. \tag{3.18}$$

The corresponding result for the decorrelating detectors as in Proposition 2, does not have such simple formulation. However, both the truncated decorrelating detector $\mathcal{D}_{[d]N}$ (3.6) and the optimal FIR decorrelating detector $\bar{\mathcal{D}}_{[d]N}$ (3.10) converge to the same IIR decorrelating detector as the processing window length $N$ approaches infinity, i.e.,

$$\bar{\mathcal{D}}_{[d]} = \mathcal{D}_{[d]} \tag{3.19}$$

under mild conditions. The conditions are described at the end of Appendix 1.

It was noted in Section 3.1 that the truncated detectors are easier to compute than the optimal FIR detectors. Moreover, the above results justify the use of truncated detectors with a large enough memory-length.

## 3.3. Performance analysis

In the performance analysis it is assumed that BPSK data modulation is applied, and that the carrier phases satisfy $\phi_k = 0$. However, the extension to more general cases is straightforward. The delays are assumed to be fixed. For notational simplicity and clarity the analysis is performed for a single-path channel ($L = 1$) in Section 3.3.1. The extension to a multipath channel is presented in Section 3.3.2. The signature waveforms are assumed to be time-invariant for notational convenience so that the discrete-time index can be removed from the correlation matrices.

### *3.3.1. Single-path channel*

The $k$th user's average bit error probability of a linear FIR detector is obtained by averaging over all possible interfering symbol combinations [197]. Since in a single-path channel, $\mathcal{C} = I_{N_b K \times N_b K}$, the error probability can be expressed by using (3.4) in the forms

$$\begin{aligned} P_k &= \frac{1}{2^{(N+2)K-1}} \sum_{\substack{\bar{\boldsymbol{b}}^{(n)} \in \{-1,1\}^{(N+2)K} \\ b_k^{(n)}=0}} \\ &\quad \mathrm{Q}\left( \frac{\sqrt{E_k}(\mathcal{F})_{(P+1)K+k,k} - \bar{\boldsymbol{f}}_k^{\top} \bar{\mathcal{A}}^{(n)} \bar{\boldsymbol{b}}^{(n)}}{\sqrt{\sigma^2 [\mathcal{D}_N^{\top} \mathcal{R}^{(n)} \mathcal{D}_N]_{kk}}} \right) \\ &= \frac{1}{2^{(N+2)K-1}} \sum_{\substack{\bar{\boldsymbol{b}}^{(n)} \in \{-1,1\}^{(N+2)K} \\ b_k^{(n)}=0}} \end{aligned} \tag{3.20}$$

$$\mathrm{Q}\left(\frac{\sqrt{E_k}(\mathcal{F})_{(P+1)K+k,k} - \boldsymbol{f}_k^\top \mathcal{A}^{(n)} \boldsymbol{b}^{(n)} - \mu_k^{(n)}(\boldsymbol{b}_e^{(n)})}{\sqrt{\sigma^2 [\mathcal{D}_N^\top \mathcal{R}^{(n)} \mathcal{D}_N]_{kk}}}\right), \qquad (3.21)$$

where $\boldsymbol{f}_k$ and $\bar{\boldsymbol{f}}_k$ are the $k$th columns of $\mathcal{F}$ and $\bar{\mathcal{F}}$ defined after (3.4). The term $\sqrt{E_k}(\mathcal{F})_{(P+1)K+k,k}$ is the desired signal component, $\bar{\boldsymbol{f}}_k^\top \bar{\mathcal{A}}^{(n)} \bar{\boldsymbol{b}}^{(n)} = \boldsymbol{f}_k^\top \mathcal{A}^{(n)} \boldsymbol{b}^{(n)} + \mu_k^{(n)}(\boldsymbol{b}_e^{(n)})$ is the remaining MAI, and $\sigma^2 [\mathcal{D}_N^\top \mathcal{R}^{(n)} \mathcal{D}_N]_{kk}$ is the Gaussian noise variance at the detector output. Note that the bit error probability can also be expressed in a more compact form as

$$P_k = \frac{1}{2^{(N+2)K-1}} \sum_{\substack{\bar{\boldsymbol{b}}^{(n)} \in \{-1,1\}^{(N+2)K} \\ b_k^{(n)} = 1}} \mathrm{Q}\left(\frac{\bar{\boldsymbol{f}}_k^\top \bar{\mathcal{A}}^{(n)} \bar{\boldsymbol{b}}^{(n)}}{\sqrt{\sigma^2 [\mathcal{D}_N^\top \mathcal{R}^{(n)} \mathcal{D}_N]_{kk}}}\right). \qquad (3.22)$$

The expression for error probability of an IIR detector is as in (3.21) with $\mu_k^{(n)}(\boldsymbol{b}_e^{(n)}) = 0$, since there is no edge term with IIR detectors. It is easy to see from (3.5) and (3.21) that in the case of a stable detector the effect of the edge symbols $\mathbf{b}^{(n-P-1)}$ and $\mathbf{b}^{(n+P+1)}$ can be made arbitrarily small by selecting large enough memory-length $N$. In the case of the decorrelating detector this becomes even more clear. Since by (3.6) $(\mathcal{F})_{(P+1)K+k,k} = 1$, $\boldsymbol{f}_k = \mathbf{0}$ (except $(\boldsymbol{f}_k)_{(P+1)K+k} = 1$), and $[\mathcal{D}_N^\top \mathcal{R}^{(n)} \mathcal{D}_N]_{kk} = [\mathbf{D}_d(0)]_{kk}$, the error probability of the truncated decorrelator simplifies from (3.21) to

$$P_{[d]k} = \frac{1}{2^{2K}} \sum_{\boldsymbol{b}_e^{(n)} \in \{-1,1\}^{2K}} \mathrm{Q}\left(\frac{\sqrt{E_k} - \mu_{[d]k}^{(n)}(\boldsymbol{b}_e^{(n)})}{\sqrt{\sigma^2 [\mathbf{D}_d(0)]_{kk}}}\right). \qquad (3.23)$$

With a large enough $N$, $[\mathbf{D}_d(0)]_{kk}$ approaches the value of the IIR detector by Proposition 1, and $\mu_{[d]k}^{(n)}$ approaches zero if the decorrelator is stable. Thus, the stable decorrelator approaches the performance of the IIR detector with a large enough memory-length $N$.

In the following the asymptotic multiuser efficiency (2.49) and the near-far resistance (2.50) of the linear FIR detectors will be analyzed. With large argument values we can approximate $\mathrm{Q}(x) \approx \frac{\exp(-x^2/2)}{2}$. At high signal-to-noise ratios the worst case symbol combination dominates the value of the sum in the numerator of (3.20) or (3.21) [54]. Thus, using (3.21) the AME of an arbitrary linear FIR multiuser detector is

$$\eta_k = \frac{1}{E_k} \max^2 \left\{ 0, \min_{\substack{\bar{\boldsymbol{b}}^{(n)} \in \\ \{-1,1\}^{(N+2)K} \\ b_k^{(n)} = 0}} \frac{\sqrt{E_k}(\mathcal{F})_{(P+1)K+k,k} - \boldsymbol{f}_k^\top \bar{\mathcal{A}}^{(n)} \bar{\boldsymbol{b}}^{(n)}}{\sqrt{[\mathcal{D}_N^\top \mathcal{R}^{(n)} \mathcal{D}_N]_{kk}}} \right\} \qquad (3.24)$$

$$= \frac{1}{E_k}\max^2\left\{0, \min_{\substack{\bar{\boldsymbol{b}}^{(n)}\in\{-1,1\}^{(N+2)K} \\ b_k^{(n)}=1}} \frac{\bar{\boldsymbol{f}}_k^\top \bar{\mathcal{A}}^{(n)}\bar{\boldsymbol{b}}^{(n)}}{\sqrt{[\mathcal{D}_N^\top \mathcal{R}^{(n)}\mathcal{D}_N]_{kk}}}\right\}. \tag{3.25}$$

The minimum above is obtained from the worst possible interfering symbol combination, i.e., with symbols $(\bar{\boldsymbol{b}}^{(n)})_i = \text{sgn}[(\bar{\boldsymbol{f}}_k)_i]$, $\forall\, i \in \{1, 2, \ldots, (P+1)K + k - 1, (P+1)K + k + 1, \ldots, NK\}$.

After evaluating the square in (3.24), the AME for the truncated decorrelating detector becomes

$$\eta_{[d]k} = \begin{cases} 0, & \text{if } \mu_{[d]k}^{max} \geq \sqrt{E_k} \\ \frac{1-\rho_{[d]k}}{D_{kk}(0)}, & \text{if } \mu_{[d]k}^{max} < \sqrt{E_k} \end{cases}, \tag{3.26}$$

where $\rho_{[d]k} = \frac{2\sqrt{E_k}\mu_{[d]k}^{max} - (\mu_{[d]k}^{max})^2}{E_k}$ describes the degradation due to the edge effect, and

$$\begin{aligned} \mu_{[d]k}^{max} &= \max_{\boldsymbol{b}_e^{(n)}\in\{-1,1\}^{2K}} \mu_{[d]k}^{(n)}(\boldsymbol{b}_e^{(n)}) \\ &= \sum_{l\neq k} \left\{ \mid [\mathbf{D}_d(P)\mathbf{R}(1)]_{kl} \mid + \mid [\mathbf{D}_d(-P)\mathbf{R}^\top(1)]_{kl} \mid \right\} \sqrt{2E_l} \end{aligned} \tag{3.27}$$

is the maximum absolute value of $\mu_{[d]k}^{(n)}$. The AME of the IIR decorrelator is as in (3.26) with $\rho_{[d]k} = 0$, since the edge effect has reduced to zero.

It can be verified from (3.26) that $\eta_{[d]k} > 0$ if and only if $\mu_{[d]k}^{max} < \sqrt{E_k}$. In other words, the truncated decorrelating detector has a positive AME if and only if the maximum value of the remaining MAI component at the detector output is smaller than the desired users' amplitude. If any interfering amplitude approaches infinity, $\mu_{[d]k}^{max}$ at the output of a FIR detector also approaches infinity. Thus, it is clear that the FIR detectors cannot be near-far resistant in a strict sense[7]. For that reason *power limited near-far resistance* will be defined as

$$\bar{\eta_k} = \inf_{0\leq E_l\leq E_{max}, l\neq k} \eta_k, \tag{3.28}$$

where $E_{max}$ is finite. In wireless communication systems, for example, $E_{max}$ is determined by the accuracy of the power control of the CDMA system. If a FIR detector is stable, $\mu_k^{max}$ can be made arbitrarily small by selecting $N$ large enough for any $E_{max}$. This implies that the truncated decorrelating detector (and also LMMSE and data-aided noise-whitening detectors) with large enough (but finite) memory-length, can be made near-far resistant given an arbitrarily large (but finite) upper bound for the received powers of the interfering users. By (3.19) it is noted that, with $N$ large enough, the above discussion applies to the optimal FIR decorrelator as well.

[7]The use of truncated MF outputs [49] makes an FIR detector strictly near-far resistant. The price is that the data of only very small number of users can be detected.

From (3.24) it is seen that the power limited NFR for the FIR detectors can be computed by substituting $E_l = E_{max}\,\forall\, l \neq k$. Thus, the power limited NFR is a function of the ratio $E_{max}/E_k$ only. Let $E_{min}$ be the minimum received energy per symbol a user needs to have to be served by the CDMA system. The worst case power limited near-far resistance $\bar{\eta_k}$ can be computed by substituting $E_k = E_{min}$ and $E_l = E_{max}\,\forall\, l \neq k$ in (3.24). In practice $E_{max}$, $E_{min}$, and $N$ are design parameters of the CDMA system and a trade-off between them must be considered. The larger $N$ the more complicated the implementation of the detector is. On the other hand, large $N$ poses milder requirements for the power control of the system. In a digital signal processing (DSP) implementation large $N$ introduces more round-off errors and implementation noise so that in practice there is a finite optimal value for $N$ given the ratio $E_{max}/E_{min}$ and the implementation constraints (filter structure, floating point number word length etc.).

### *3.3.2. Multipath channel*

The performance analysis for a fixed, known multipath channel is conceptually similar to that of a single-path channel. The output vector of the linear detector $\mathbf{y}^{(n)}_{[LIN]}$ is multiplied by the complex conjugate of a multipath combining matrix. The optimal combining vector for user $k$ in the known multipath channel is [129, p. 20]

$$\tilde{\mathbf{c}}^{(n)}_k = \mathbf{D}^{-1}_{[d]k,k}(0)\mathbf{c}_k, \tag{3.29}$$

where $\mathbf{D}_{[d]k,k}(0)$ denotes the $k$th $L \times L$ diagonal block of the matrix $\mathbf{D}_{[d]}(0)$. The optimal combiner matrix $\tilde{\mathbf{C}}^{(n)}$ is then formed from the vectors $\tilde{\mathbf{c}}^{(n)}_k$ as in (2.13). Therefore, the maximal ratio combined vector is

$$\mathbf{y}^{(n)}_{[LIN,MRC]} = \tilde{\mathbf{C}}^{\mathrm{H}(n)}\mathbf{y}^{(n)}_{[LIN]} = \tilde{\mathbf{C}}^{\mathrm{H}(n)}\mathcal{F}^{\top}\bar{\mathcal{C}}^{(n)}\bar{\mathcal{A}}^{(n)}\bar{\boldsymbol{b}}^{(n)} + \tilde{\mathbf{C}}^{\mathrm{H}(n)}\mathbf{w}^{(n)}_{[LIN]}. \tag{3.30}$$

Let $(\tilde{\mathbf{C}}^{(n)})_k$ denote the $k$th column of $\tilde{\mathbf{C}}^{(n)}$. Then the bit error probability expression (3.22) can be generalized to the form

$$\begin{aligned} P_k \;=\; & \frac{1}{2^{(N+2)K-1}} \sum_{\substack{\bar{\boldsymbol{b}}^{(n)} \in \{-1,1\}^{(N+4)K} \\ b^{(n)}_k = 1}} \\ & \mathrm{Q}\left( \frac{(\tilde{\mathbf{C}}^{(n)})^{\mathrm{H}}_k \bar{\boldsymbol{f}}^{\top}_k \bar{\mathcal{C}}^{(n)} \bar{\mathcal{A}}^{(n)} \bar{\boldsymbol{b}}^{(n)}}{\sqrt{\sigma^2 (\tilde{\mathbf{C}}^{(n)})^{\mathrm{H}}_k \mathcal{D}^{\top}_N \mathcal{R}^{(n)} \mathcal{D}_N (\tilde{\mathbf{C}}^{(n)})_k}} \right). \end{aligned} \tag{3.31}$$

Similarly, the asymptotic multiuser efficiency expression (3.25) for the multipath channel case becomes

$$\eta_k = \frac{1}{E_k}\max^2 \left\{ 0, \min_{\substack{\bar{\boldsymbol{b}}^{(n)}\in\{-1,1\}^{(N+4)K} \\ b_k^{(n)}=1}} \frac{(\tilde{\mathbf{C}}^{(n)})_k^{\mathrm{H}} \boldsymbol{f}_k^{\top} \bar{\mathcal{C}}^{(n)} \bar{\mathcal{A}}^{(n)} \bar{\boldsymbol{b}}^{(n)}}{\sqrt{[(\tilde{\mathbf{C}}^{(n)})_k^{\mathrm{H}} \mathcal{D}_N^{\top} \mathcal{R}^{(n)} \mathcal{D}_N (\tilde{\mathbf{C}}^{(n)})_k]_k}} \right\}. \quad (3.32)$$

The near-far resistance analysis and the discussion of Section 3.3.1 can be applied to the multipath channel as well.

## 3.4. Numerical examples

The performance and stability of the detectors is studied by numerical examples. Direct-sequence spread-spectrum waveforms with BPSK data and spreading modulation as well as coherent detection are considered. The number of users is 33 or 20 with a processing gain of 31, i.e., the chip duration $T_c = T/31$. A length 31 Gold sequence family is used in the examples with time-invariant signature waveforms. A random code family of length 6200 chips is used in the examples with time-varying signature waveforms so that the results are averaged over $6200/31 = 200$ symbols. The carrier phases are assumed to be zero. The results are averaged over ten different, randomly selected delay combinations in the examples where time-invariant signature waveforms are applied. Two kinds of chip waveforms are considered. One is a rectangular chip waveform, the length of which is limited to one chip interval. The other chip waveform is a raised cosine waveform, the length of which is limited to two chip intervals (Fig. 3.2). Examples illustrating the detector stability are considered in Section 3.4.1, and the bit error probability as well as the power limited near-far resistance results in Section 3.4.2.

### *3.4.1. Detector stability*

The detector stability is illustrated by simulating the convergence of the edge blocks $\mathbf{D}(P)$ and $\mathbf{D}(-P)$ of the truncated decorrelating and LMMSE detectors versus the detector memory-length. Time-invariant signature waveforms are used. The mean absolute values of the elements of $\mathbf{D}(P)$ and $\mathbf{D}(-P)$ are presented in Figs. 3.3 and 3.4 for rectangular and raised cosine chip waveforms, respectively. The received energies are equal and the SNR is to be 10 dB with the LMMSE detector.

The results show that both detectors are stable in all cases, except the decorrelator is unstable, when $K = 33$, $L = 3$ and the rectangular chip waveform is applied. It should be noted that the decorrelating detector was not unstable with all delay combinations, but with one only. The one poor delay combination makes

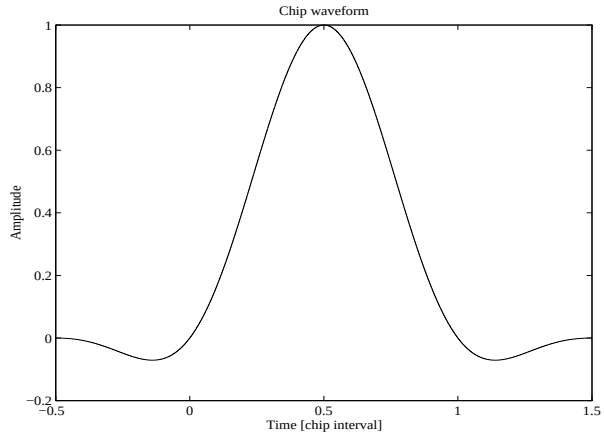


**Fig. 3.2**. **Raised cosine chip waveform.**

the decorrelating detector look unstable also in the average. Actually, the results in Figs. 3.3 and 3.4 are somewhat too pessimistic in the sense that averaging the absolute values of the edge blocks $\mathbf{D}(P)$ and $\mathbf{D}(-P)$ gives too much emphasis to the large values obtained with a poor delay combination. The conclusion will also be confirmed by the examples in the Section 3.4.2. However, the results demonstrate that the detector stability appears to be a mild assumption. Furthermore, it is seen that increasing the channel load $KL$ makes the detector to converge more slowly with increasing $P$. This applies in particular to the decorrelating detector, whereas the convergence of the edge blocks of the LMMSE detector suffer rather little penalty from increased channel load. The phenomenon is easy to understand by comparing (3.6) and (3.7). The matrix that needs to be inverted when computing the LMMSE detector in (3.7), is more diagonally dominant than the matrix to be inverted when computing the decorrelating detector in (3.6). Thus, the computation of the LMMSE detector is understandably numerically more robust than the computation of the decorrelating detector. Comparing Figs. 3.3 and 3.4 demonstrates that the filtering of the chip waveform has very minor impact to the convergence speed of the edge blocks $\mathbf{D}(P)$ and $\mathbf{D}(-P)$ versus the memory-length. Since the detectors are always stable with the raised cosine chip waveform, the filtering of the chip waveform makes the system more robust.

### *3.4.2. Detector performance*

The error probabilities are estimated for low signal-to-noise ratio by (3.22) or (3.31). Data-aided detection is assumed for the noise-whitening detector, which may not

be practical. However, the effect of finite memory-length can be well illustrated by examples assuming data aided detection. The performance at high signal-to-noise ratios is evaluated by computing AME's using expressions (3.25) or (3.32). The results are represented versus the half memory-length $P$. All the interfering users are assumed to have the same energy per symbol, which is denoted by $E_{max}$ in the figures. Correspondingly the energy per symbol of the desired user is denoted by $E_{min}$. The performance of the ideal IIR detector is estimated with the assumption that the edge symbols are zero, and the detector has a large enough block size.

The results of examples with time-invariant signature waveforms are presented in Figs. 3.5–3.6 and 3.9–3.10. Time-varying signature waveforms yield the results in Figs. 3.7–3.8. The performance of several detectors in a single-path channel is shown in Figs. 3.5–3.8. The performance of the truncated decorrelating detector for three numbers of propagation paths ($L = 1, 2, 3$) is shown in Figs. 3.9–3.10. The results in Fig. 3.10 assume that the chip waveform is the raised cosine waveform, in other examples the chip waveform is the rectangular waveform. The truncated decorrelating and the LMMSE detectors are considered only in the examples with time-varying signature waveforms, since the analysis of the optimal FIR and noise-whitening detectors would be computationally intensive. For clarity, the bit error probabilities of the ideal LMMSE detector have not been plotted for the cases $E_{max}/E_{min} = 10$ dB and $E_{max}/E_{min} = 20$ dB in Figs. 3.6 and 3.8, since they are very close to the bit error probability of the decorrelating detector.

It can be seen from Fig. 3.5 that the asymptotic loss in signal-to-noise ratio converges relatively fast. With $P = 6$ the performance is the same as with an ideal IIR detector even in the case $E_{max}/E_{min} = 20$ dB. With perfect power-control ($E_{max}/E_{min} = 0$ dB), value $P = 4$ is required. A 10 dB increase in the MAI level implies that the value of $P$ must be roughly incremented by one to maintain the same performance. In other words, loosening the power-control requirements significantly calls for only very minor increase in the required detector memory-length. It is seen from Fig. 3.6 that at lower signal-to-noise ratios the value $P = 4$ yields the same performance as the ideal IIR detector in all cases. From Figs. 3.7 and 3.8 it seen that similar conclusions can be drawn for a system with time-varying signature waveforms. However, the performance of the ideal IIR detector is slightly better with the time-invariant than with time-varying signature waveforms. This is understandable due to small crosscorrelations of the Gold sequences. On the other hand, a system with time-varying signature waveforms requires slightly smaller FIR detector memory-lengths than the system with time-invariant signature waveforms, particularly, at high signal-to-noise ratios. In [158], a similar behavior was observed and discussed for the noise-whitening detector. An intuitive explanation can be seen from (3.16). In systems with time-varying signature waveforms the elements in the matrix $\mathbf{R}_j(1)$ are (at least approximately) random variables with zero mean and are independent for different values of $j$. Thus, the elements of the matrix product $\mathbf{T}_{j,j}(j)\mathbf{R}_j(1)$ have also zero mean. In systems with time-invariant signature waveforms, on the other hand, the matrices $\mathbf{R}_j(1)$ are the same for different values of $j$ and there is "less randomness" in the elements of $\mathbf{T}_{j,j}(j)\mathbf{R}_j(1)$. Therefore, time-varying signature waveforms introduce more averaging out into the product in (3.16) and result in a faster convergence of the detector to a zero matrix

as the detector memory-length $N \to \infty$.

From Figs. 3.6 and 3.8 it is seen that the optimal FIR detectors perform slightly better at low signal-to-noise ratios than the truncated ones with small values of $P$. However, with moderate values of $P$ both are equivalent to the ideal IIR detectors, as is expected by Proposition 2. From Figs. 3.5 and 3.7 it seen that at high signal-to-noise ratios, on the other hand, the truncated decorrelating detector slightly outperforms the optimal FIR decorrelator. The reason can be understood from the expressions for AME. Although the contribution due to the symbols outside the processing window ($\mu_k^{(n)}(\boldsymbol{b}_e^{(n)})$) for the optimal FIR decorrelating detector in (3.24) is smaller than for the truncated FIR decorrelating detector in (3.26), the MAI due to other symbols $\boldsymbol{f}_k^\top \mathcal{A}^{(n)} \boldsymbol{b}^{(n)}$ in (3.24) is larger. Furthermore, the desired signal's energy per symbol $\sqrt{E_k}(\mathcal{F})_{(P+1)K+k,k}$ may be lower, and the enhanced additive white Gaussian noise $\sqrt{[\mathcal{D}_N^\top \mathcal{R}^{(n)} \mathcal{D}_N]_{kk}}$ in (3.24) may be larger than the corresponding quantities in (3.26) yielding lower asymptotic multiuser efficiency. Thus, the optimal FIR detectors do not yield any universal performance improvement in comparison to the truncated detectors.

It can be seen from Figs. 3.9 and 3.10 that the AME is degraded due to increased interference caused by multipath propagation. However, moderate memory-lengths ($P \leq 6$) are sufficient to obtain performance close to the ideal decorrelating detector except in the extreme cases of a severe near-far problem and/or high channel load ($K = 33$ and $L = 3$). The performance of the decorrelating detector with raised cosine chip waveform (Fig. 3.10) is in general better than with rectangular waveforms. The reason is the fact that filtering smoothes out the CDMA signals and reduces the crosscorrelations between the signature waveforms. However, for the high channel load ($K = 33$ and $L = 3$) case, the performance with raised cosine chip waveforms is poor. This is understandable due to bandwith limitation posed by filtering. In other words, the linear decorrelating detector is close to its ultimate capacity limit, when $K = 33$ and $L = 3$. The results in Figs. 3.9(a) and 3.10(a) confirm that the stability results in Figs. 3.3(a) and 3.4(a) can indeed be somewhat misleading, as predicted in Section 3.4.1. The truncated decorrelating detector is in the average unstable with the rectangular chip waveform and stable with the raised cosine chip waveform in the three-path case according to the results in Figs. 3.3(a) and 3.4(a). However, the corresponding power limited near-far resistance results in Figs. 3.9(a) and 3.10(a) give a contradicting result: the system with rectangular chip waveform outperforms the system with the raised cosine chip waveform.

The numerical examples show that moderate memory-lengths (roughly $N \leq 13$) give performance close to ideal IIR detectors in most cases. Even under a severe near-far problem ($E_{max}/E_{min} = 20$ dB) the optimal near-far resistance is obtained with detector memory-length $N = 13$ except with very high channel load. The use of FIR detectors loosens the required accuracy of the power-control significantly with very moderate detector memory-lengths.

## 3.5. Conclusions

Linear multiuser detectors in asynchronous multiuser systems, whose signature waveforms are allowed to be time-invariant or time-varying, have been discussed. Two classes of linear FIR multiuser detectors, namely the truncated and the optimal FIR detectors, approximating the ideal IIR detectors were defined. The truncated detectors were obtained by simply truncating the corresponding IIR detector, whereas the optimal FIR detectors were derived by optimizing the detector to the finite processing window model.

Numerical examples showed that the detectors are stable under relatively mild conditions. The stability was shown to imply asymptotic uniqueness of the limiting IIR detector also in the case of time-varying signature waveforms. The truncated and the optimal FIR detectors approach asymptotically the same IIR detector under relatively mild conditions.

The performance of the finite memory-length detectors was analyzed. It was shown that the truncated decorrelating, LMMSE, and data-aided noise-whitening detectors can be made near-far resistant under a given ratio between maximum and minimum received power of users by selecting an appropriate memory-length. Numerical examples demonstrated the fact that moderate memory-lengths of either truncated or optimal FIR detectors are sufficient to gain the performance of the ideal IIR detectors even under a severe near-far problem. At very high channel loads the decorrelating detector may become unstable, but the LMMSE detector is more robust. If the memory-lengths are small, the optimal FIR detectors outperform the truncated ones at low signal-to-noise ratios. However, at high signal-to-noise ratios the truncated detectors have better performance. The required memory-lengths tend to be smaller with time-varying than with time-invariant signature waveforms.

The use of FIR detectors instead of the IIR detectors makes the linear multiuser detection possible in CDMA systems in which the number of users, their propagation delays, or the signature waveforms change over time. An example of the time-varying signature waveforms is a CDMA system using spreading sequences longer than one symbol interval (an R-CDMA system). The truncated FIR detectors are easier to update to the changes in a communication system than the optimal FIR detectors. Because the optimal FIR detectors do not yield any universal performance improvement, the truncated detectors with appropriate memory-length are clearly the detectors of choice in practice. The required memory-length depends on other system parameters, especially on the ratio of maximum and minimum received powers. It should also be noted that the results give insight into the design of decentralized linear (adaptive LMMSE) detectors as well. Similar dependence of the performance on the memory-length is naturally valid also for them.

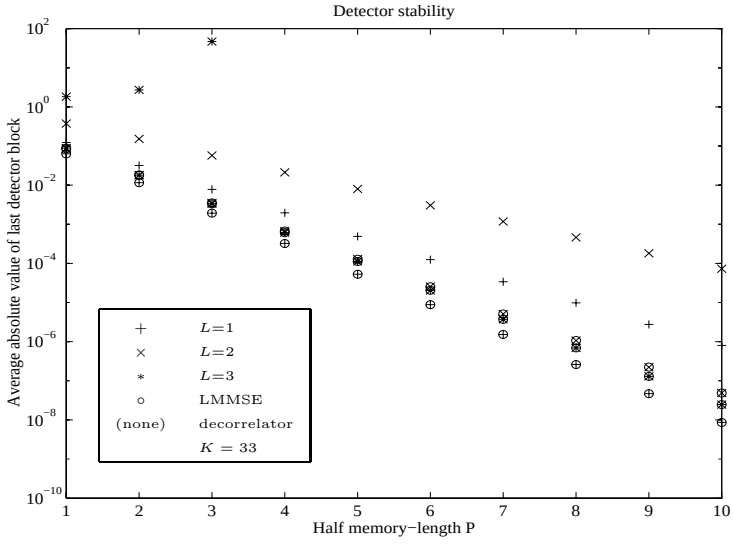


(a)

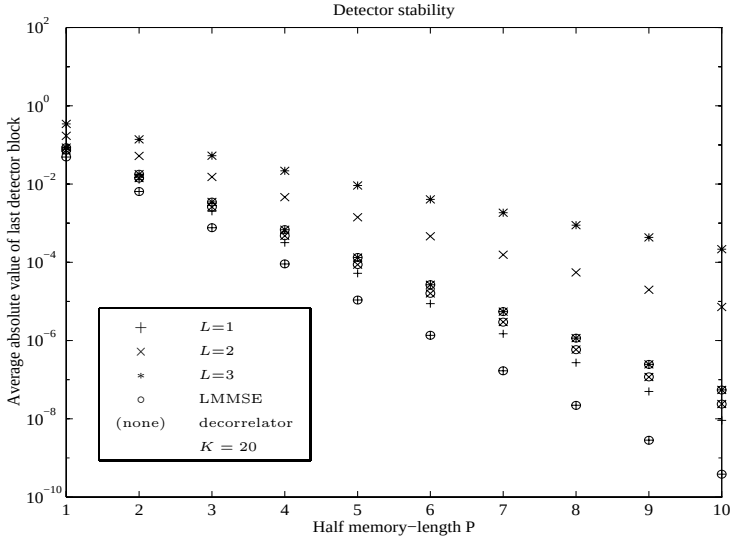


(b)

**Fig. 3.3**. **Mean absolute values of the edge detector blocks $\mathbf{D}(P)$ and $\mathbf{D}(-P)$ of truncated decorrelating and LMMSE detectors for different numbers of multipath components versus half memory-length $P$ with time-invariant signature waveforms and rectangular chip waveform; (a) $K = 33$, (b) $K = 20$. The curves marked by circles $\circ$ denote the LMMSE detector, and curves without circles denote the decorrelating detector.**

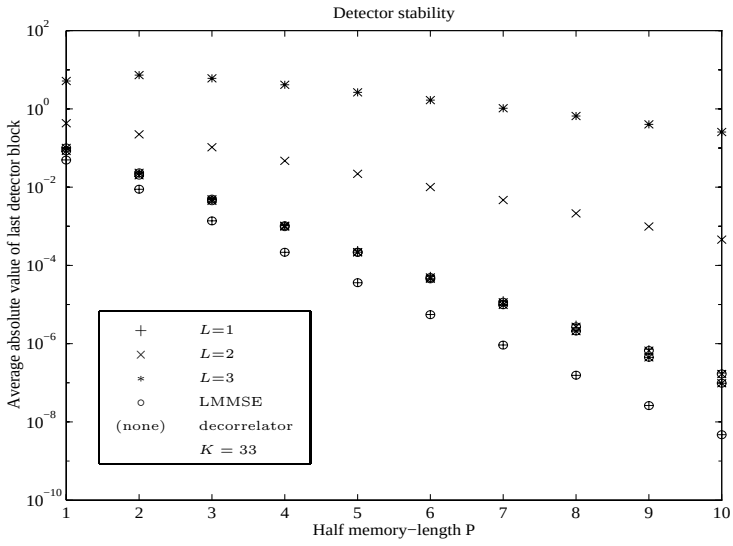


(a)

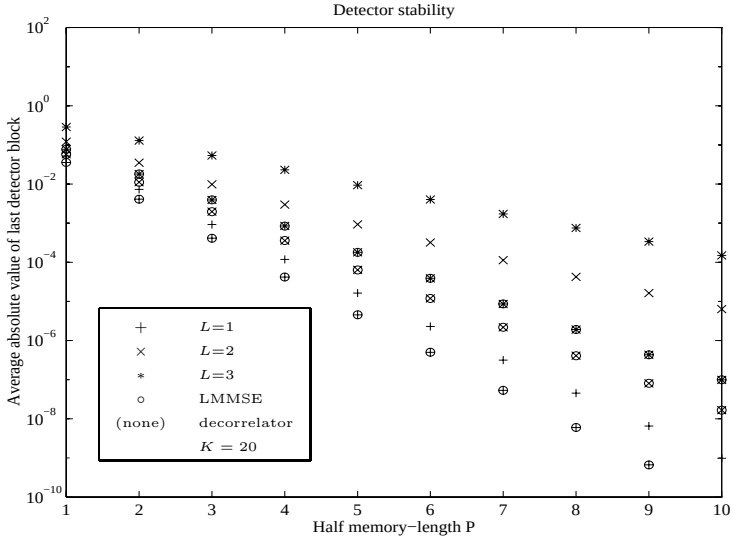


(b)

**Fig. 3.4. Mean absolute values of the edge detector blocks $\mathbf{D}(P)$ and $\mathbf{D}(-P)$ of truncated decorrelating and LMMSE detectors for different numbers of multipath components versus half memory-length $P$ with time-invariant signature waveforms and raised cosine chip waveform; (a) $K = 33$, (b) $K = 20$. The curves marked by circles $\circ$ denote the LMMSE detector, and curves without circles denote the decorrelating detector.**

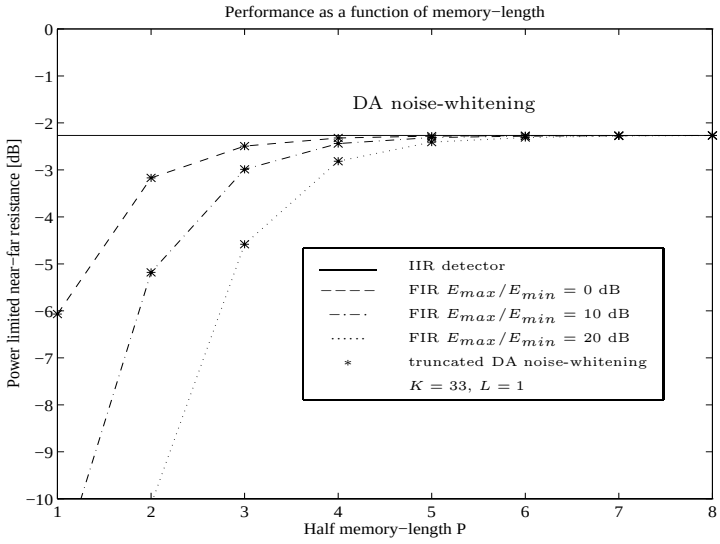


(a)

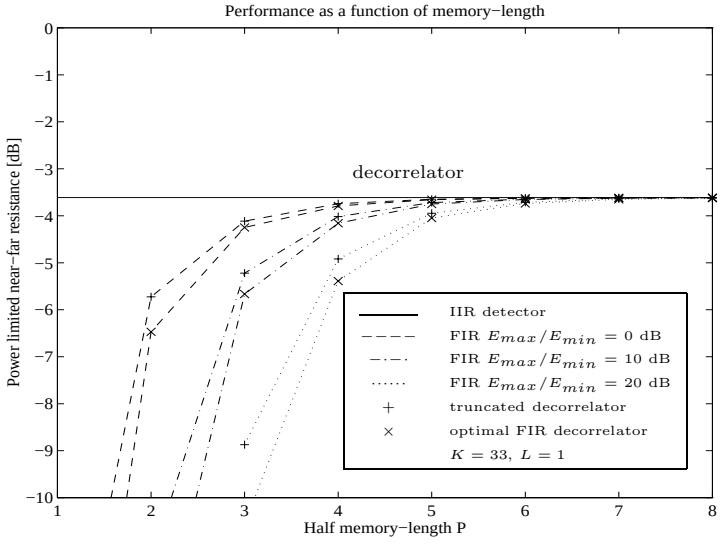


(b)

**Fig. 3.5. Power limited near-far resistances [dB] versus half memory-length $P$ with time-invariant signature waveforms and rectangular chip waveform; (a) DA truncated noise-whitening detector, (b) truncated and optimal FIR decorrelating detector.**

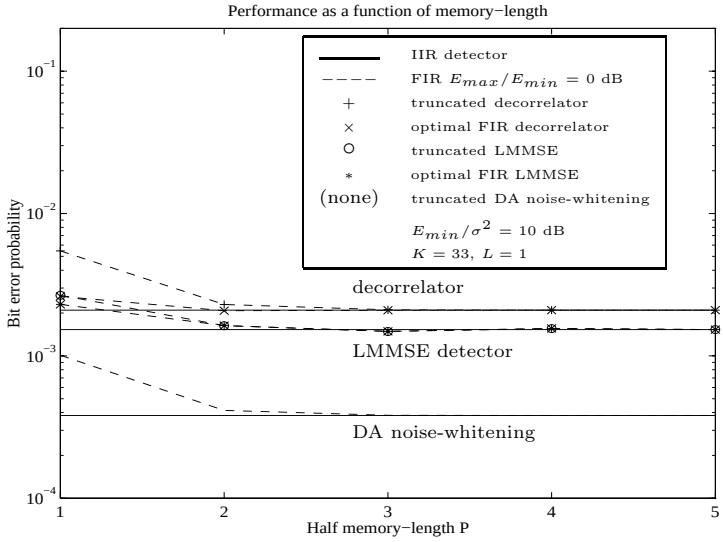
Performance as a function of memory−length
IIR detector
FIR $E_{max}/E_{min}$ = 0 dB
truncated decorrelator
optimal FIR decorrelator
truncated LMMSE
optimal FIR LMMSE
(none) truncated DA noise-whitening
$E_{min}/\sigma^2$ = 10 dB
$K = 33,\ L = 1$
decorrelator
LMMSE detector
DA noise-whitening
Bit error probability
Half memory−length P

(a)

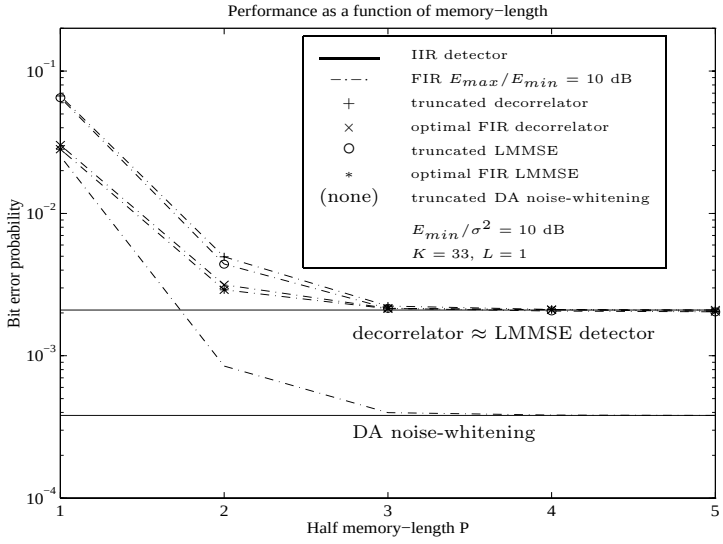
Performance as a function of memory−length
IIR detector
FIR $E_{max}/E_{min}$ = 10 dB
truncated decorrelator
optimal FIR decorrelator
truncated LMMSE
optimal FIR LMMSE
(none) truncated DA noise-whitening
$E_{min}/\sigma^2$ = 10 dB
$K = 33,\ L = 1$
decorrelator ≈ LMMSE detector
DA noise-whitening
Bit error probability
Half memory−length P

(b)

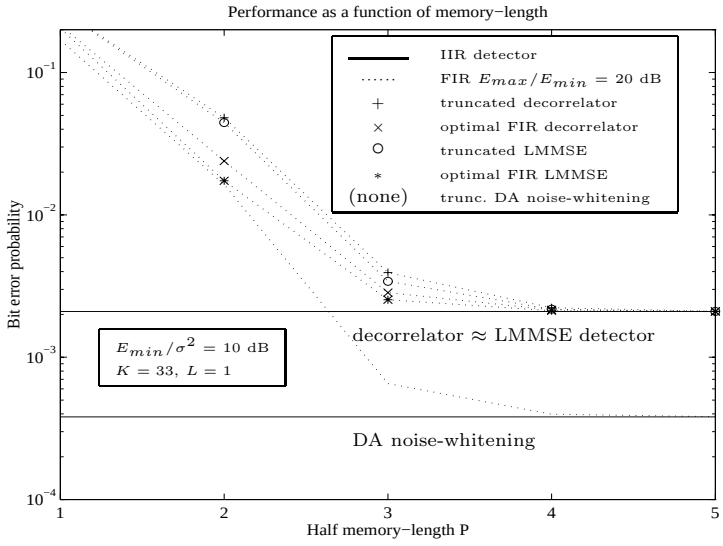


(c)

**Fig. 3.6. Probabilities of bit error versus half memory-length $P$ with time-invariant signature waveforms and rectangular chip waveform; (a) equal received energies $E_{max}/E_{min} =$ 0 dB, (b) near-far problem $E_{max}/E_{min} =$ 10 dB, (c) near-far problem $E_{max}/E_{min} =$ 20 dB.**

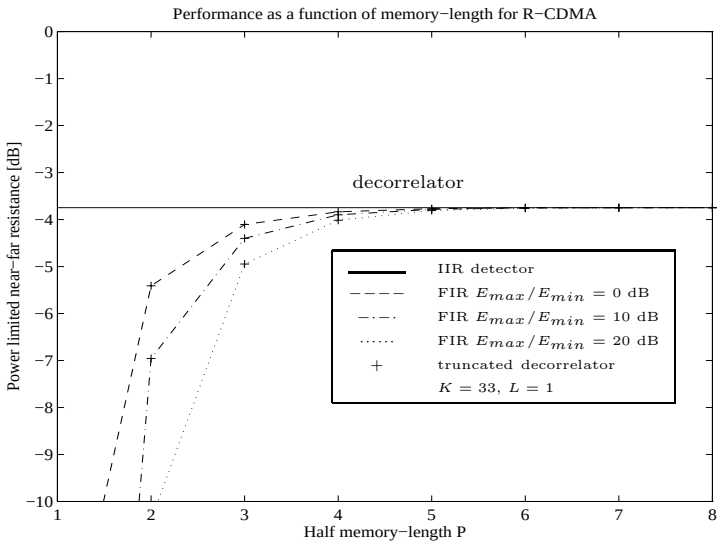


**Fig. 3.7**. **Power limited near-far resistances [dB] of the truncated decorrelating detector versus half memory-length $P$ with time-varying signature waveforms and rectangular chip waveform.**

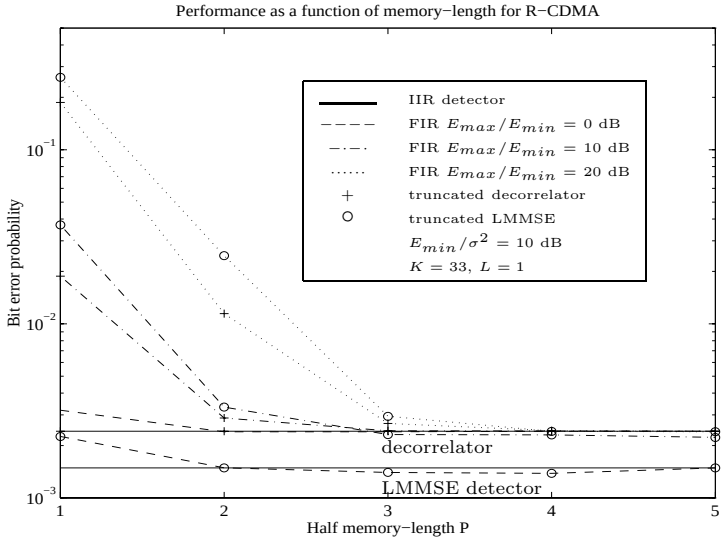


**Fig. 3.8. Probabilities of bit error of the truncated decorrelating detector versus half memory-length $P$ with time-varying signature waveform and rectangular chip waveform.**

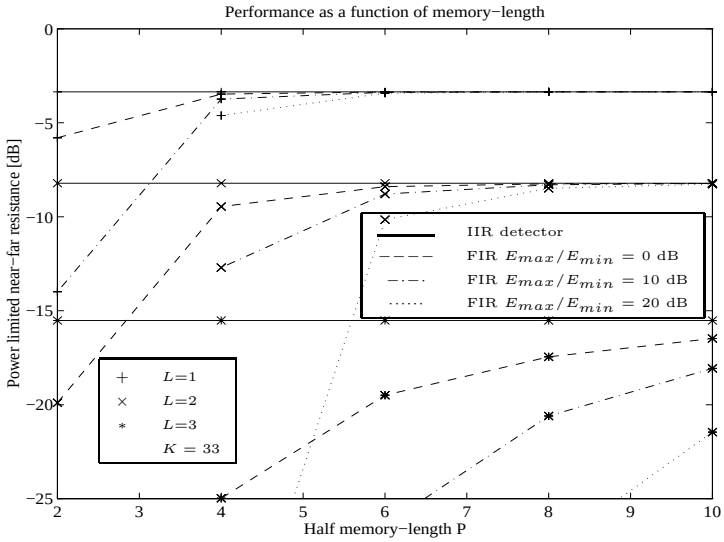


(a)

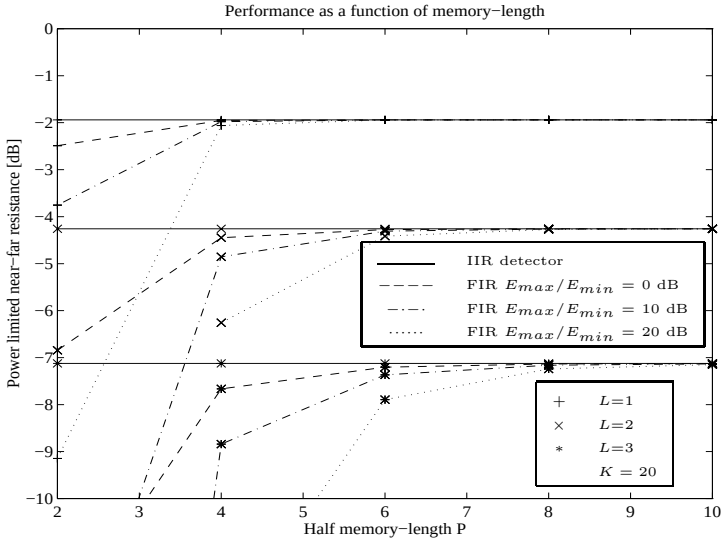


(b)

**Fig. 3.9. Power limited near-far resistances [dB] of the ideal (IIR) and truncated (FIR) decorrelating detector for different numbers of multipath components versus half memory-length $P$ with time-invariant signature waveforms and rectangular chip waveform; (a) $K = 33$, (b) $K = 20$.**

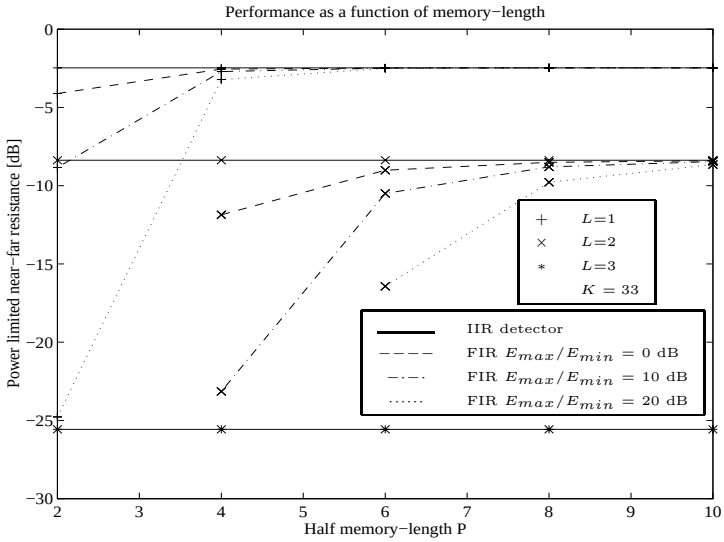


(a)

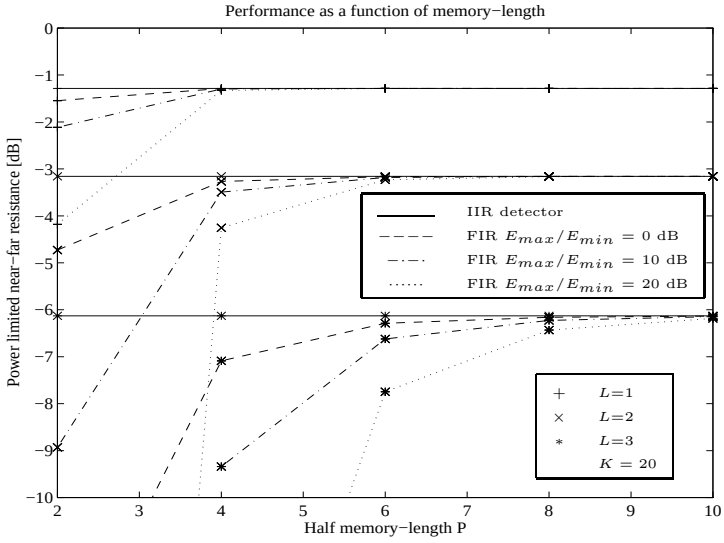


(b)

**Fig. 3.10**. **Power limited near-far resistances [dB] of the ideal (IIR) and truncated (FIR) decorrelating detector for different numbers of multipath components versus half memory-length $P$ with time-invariant signature waveforms and raised cosine chip waveform; (a) $K = 33$, (b) $K = 20$.**

# 4. Multiuser demodulation in Rayleigh fading channels

Multiuser demodulation in relatively fast fading channels is analyzed in this chapter. The goal is to find efficient receivers with moderate implementation complexity for multiuser demodulation. Coherent detection is considered to obtain a superior performance. Therefore, complex channel coefficient estimation is obviously a major problem to solve. Multiuser receivers for fading channels have been considered in the past, as discussed in Chapter 2. However, several open problems still exist. Even a clear presentation of the optimal demodulation technique for time-varying multipath channel is not available in the open literature. The performance of different proposed multiuser receivers has not been compared. Furthermore, the effect of various channel estimation algorithms to the receiver performance in general and to receiver performance differences in particular has gained very limited attention so far. For the parallel interference cancellation receiver it has been shown that the effect of complex channel coefficient estimation to the overall receiver performance is substantial [57]. Thus, the overall receiver design and especially the channel estimation problem in relatively fast Rayleigh fading channels are important problems.

In this chapter, the focus will be on the following three problems. First, the performance difference between optimal and suboptimal complex channel coefficient estimation is evaluated. Second, data-aided and decision-directed complex channel coefficient estimation are compared. Third, the bit error rates of the decorrelating and the parallel interference cancellation receivers are compared. The delays of the user signals are assumed to be perfectly known throughout the chapter.

The chapter is organized as follows. The optimal multiuser detector for unknown Rayleigh fading channels is presented in Section 4.1. Suboptimal decorrelating and parallel interference cancellation receivers with either DA or decision-directed complex channel coefficient estimation are considered in Section 4.2. In Section 4.3, performance of the suboptimal receivers is studied and numerical examples are presented. The results are summarized and discussed in Section 4.4.

## 4.1. Optimal receiver

The complete transmitted data block must be demodulated in the optimal MLSD multiuser receiver [47]. Therefore, the complete data block model (2.8) is considered. To find the optimal MLSD receiver for a frequency-selective Rayleigh fading channel the derivation by Kailath [84, 78] is extended to the multiuser detection problem. The covariance matrix $\mathbf{\Sigma}_{\boldsymbol{c}}$ of the channel coefficient vector $\boldsymbol{c}$ is assumed to be known in the detector derivation. The maximum likelihood sequence detector (often called maximum likelihood sequence estimator [23]) makes its decision as

$$\hat{\boldsymbol{b}}_{[MLSD]} = \arg \max_{\boldsymbol{b} \in \Xi^{N_b K}} p(\boldsymbol{y}|\boldsymbol{b}), \tag{4.1}$$

where $p(\boldsymbol{y}|\boldsymbol{b})$ is the probability density function (pdf) of the MF bank output vector $\boldsymbol{y}$ conditioned on the data vector $\boldsymbol{b}$. Since $\boldsymbol{c}$ and $\boldsymbol{w}$ are complex Gaussian random vectors independent of each other, $\boldsymbol{y}$ in (2.16) conditioned on $\boldsymbol{b}$ is a complex Gaussian random vector with zero mean and covariance matrix

$$\mathbf{\Sigma}_{\boldsymbol{y}|\boldsymbol{b}} = \mathcal{R}\mathbf{\Sigma}_{\boldsymbol{h}|\boldsymbol{b}}\mathcal{R} + \sigma^2\mathcal{R}, \tag{4.2}$$

where

$$\mathbf{\Sigma}_{\boldsymbol{h}|\boldsymbol{b}} = \mathcal{B}\mathbf{\Sigma}_{\boldsymbol{c}}\mathcal{B}^* \tag{4.3}$$

is the covariance matrix of $\boldsymbol{h} = \mathcal{C}\mathcal{A}\boldsymbol{b}$ conditioned on the data vector $\boldsymbol{b}$, and

$$\mathcal{B} = \operatorname{diag}\Big(A_1 b_1^{(0)}\mathbf{I}_L, A_2 b_2^{(0)}\mathbf{I}_L, \ldots, A_K b_K^{(0)}\mathbf{I}_L, A_1 b_1^{(1)}\mathbf{I}_L, \ldots, A_K b_K^{(N_b-1)}\mathbf{I}_L\Big)$$

$$\in \mathbb{C}^{N_b KL \times N_b KL}. \tag{4.4}$$

Note that the covariance matrix $\mathbf{\Sigma}_{\boldsymbol{c}}$ (2.45) of the channel coefficients (2.40) is insensitive to the data sequence $\boldsymbol{b}$. Thus, the pdf of $\boldsymbol{y}$ conditioned on $\boldsymbol{b}$ becomes

$$p(\boldsymbol{y}|\boldsymbol{b}) = \frac{1}{\pi^{N_b KL}\det(\mathbf{\Sigma}_{\boldsymbol{y}|\boldsymbol{b}})}\exp(-\boldsymbol{y}^{\mathrm{H}}\mathbf{\Sigma}_{\boldsymbol{y}|\boldsymbol{b}}^{-1}\boldsymbol{y}). \tag{4.5}$$

By substituting (4.5) into (4.1), the MLSD rule can be expressed in the form

$$\hat{\boldsymbol{b}}_{[MLSD]} = \arg \min_{\boldsymbol{b} \in \Xi^{N_b K}} \Big\{ \ln[\det(\mathbf{\Sigma}_{\boldsymbol{y}|\boldsymbol{b}})] + \boldsymbol{y}^{\mathrm{H}}\mathbf{\Sigma}_{\boldsymbol{y}|\boldsymbol{b}}^{-1}\boldsymbol{y}\Big\}, \tag{4.6}$$

where ln(.) is the natural logarithm. If constant envelope modulation is applied, $\det(\mathbf{\Sigma}_{\boldsymbol{y}|\boldsymbol{b}})$ does not depend on $\boldsymbol{b}$ [287] and can therefore be neglected in the minimization. In that case the MLSD rule becomes

$$\hat{\boldsymbol{b}}_{[MLSD]} = \arg \min_{\boldsymbol{b} \in \Xi^{N_b K}} \boldsymbol{y}^{\mathrm{H}}\mathbf{\Sigma}_{\boldsymbol{y}|\boldsymbol{b}}^{-1}\boldsymbol{y}. \tag{4.7}$$

By applying the matrix inversion lemma (A1.4) in (4.2) the inverse of the covariance matrix has the form

$$\mathbf{\Sigma}_{\boldsymbol{y}|\boldsymbol{b}}^{-1} = \sigma^{-2}\mathcal{R} - \sigma^{-2}(\mathcal{R} + \sigma^{-2}\mathbf{\Sigma}_{\boldsymbol{h}|\boldsymbol{b}}^{-1})^{-1}. \tag{4.8}$$

Since the first term $\sigma^{-2}\mathcal{R}$ in (4.8) does not depend on the data $\boldsymbol{b}$, the MLSD rule (4.7) becomes

$$\hat{\boldsymbol{b}}_{[MLSD]} = \arg \max_{\boldsymbol{b} \in \Xi^{N_b K}} \hat{\boldsymbol{h}}^{\mathrm{H}}_{[MMSE]} \boldsymbol{y}, \tag{4.9}$$

where

$$\hat{\boldsymbol{h}}_{[MMSE]} = (\mathcal{R} + \sigma^{-2}\boldsymbol{\Sigma}^{-1}_{\boldsymbol{h}|\boldsymbol{b}})^{-1}\boldsymbol{y} \tag{4.10}$$

is the minimum mean squared error estimate of the vector $\boldsymbol{h}$ [88] conditioned on the data. In other words, the optimal MLSD receiver estimates the received noiseless signal, and multiplies (correlates) the matched filter bank output with the estimated complex amplitude vector. In other words, the result is a generalization of the well-known estimator-correlator receiver [85, Chap. 2] to multiuser system with multiple propagation paths. Since the estimation and correlation must be performed for all possible data sequences, the MLSD receiver is prohibitively complex for practical implementation. Therefore, suboptimal multiuser detectors and channel estimators are studied in the following sections.

## 4.2. Suboptimal receivers

A natural way to approximate the optimal multiuser MLSD receiver is to detect the data detection by estimating the complex channel coefficients. The channel can be estimated from the received signal if the effect of the data symbols can be removed from the MF bank output. This is possible if known (pilot) symbols are available or if symbol decisions are utilized in channel estimation[1] [89].

By the analysis in Section 4.1, the optimal channel estimation strategy from detection point of view is the linear estimation minimizing the mean squared error of the complex channel coefficient estimate (4.10). However, the ideal LMMSE estimator is often impossible to implement, since the channel covariance matrix $\boldsymbol{\Sigma}_{\boldsymbol{c}}$ depends on the signal-to-noise ratios and the fade rates of all the users, and is usually unknown. Furthermore, the matrix inversion in (4.10) has high computational complexity. Adaptive versions of the LMMSE channel estimator have been proposed for single-user systems [103, 288]. For multiuser systems a multichannel adaptive receiver would be needed. Adaptation of such filters is difficult. Therefore, the LMMSE complex channel coefficient estimation appears to be impractical for most applications. A simplified channel estimator is obtained by decoupling the estimation of complex channel coefficients of the users from each other. In other words, the $N_b KL$-dimensional joint channel estimation problem can be approximated by $KL$ distinct channel estimation problems for $N_b$ symbol intervals[2].

[1] The received complex amplitudes $\mathcal{CA}$ are assumed to consist of the Rayleigh fading channel coefficients ($\mathcal{C}$) and much more slowly changing transmitted complex amplitudes ($\mathcal{A}$). Since the transmitted complex amplitudes are assumed to be known, the complex amplitude estimation is considered to be the estimation of the Rayleigh fading channel ($\mathcal{C}$) in the sequel.

[2] This is the standard approach which has been used in deriving most suboptimal multiuser receivers described in Chapter 2.

The implementation complexity is reduced in this way considerably, and real-time complex channel coefficient estimation becomes possible. Therefore, the considered receiver structure performs first the interference suppression, which separates the $N_bKL$ dimensional joint channel estimation and data detection problems to $KL$ distinct channel estimation and data detection problems for $N_b$ symbol intervals by reducing both multiple-access and intersymbol interference. Then the complex channel coefficients are estimated for all multipath components separately. Finally, the MF outputs are maximal ratio combined. The receiver structure is a generalization of the receivers in [127, 57], and it is illustrated in Fig. 4.1. In the rest of the chapter receivers with the structure as in Fig. 4.1 are studied. The alternatives for the channel estimation block in Fig. 4.1 are considered in Section 4.2.1, and for the interference suppression block in Section 4.2.2.

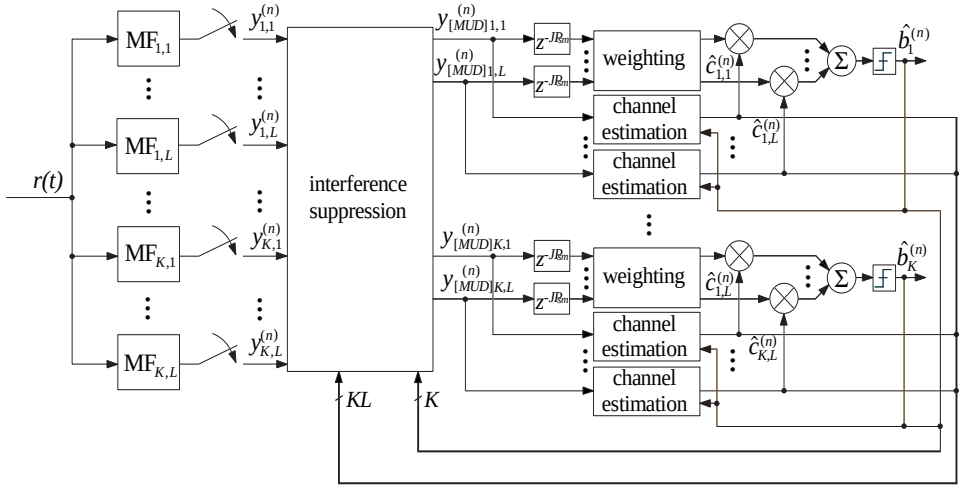


**Fig. 4.1. A multiuser receiver structure for a Rayleigh fading channel.**

## *4.2.1. Channel estimation*

In the considered receiver structure (Fig. 4.1) the channel estimation problems of users are separated from each other. Therefore, the channel estimation techniques of the single-user receivers can be applied. As in single-user receivers, the channel estimation blocks in Fig. 4.1 are assumed to include the a block removing of the effect of the data modulation and a channel estimation filter or several channel estimation filters. The effect of the data modulation can be removed by multiplying the interference suppression output by the complex conjugate of the current data symbol in data-aided or decision-directed channel estimation. Non-data-aided or blind channel estimation will not be considered in this chapter. Finite impulse

response channel estimation filters will be considered in the sequel, but infinite impulse response filters could also be applied in the receiver structure of Fig. 4.1. A general complex channel coefficient estimation filter structure is illustrated in Fig. 4.2. The symbol $J$ denotes the distance of the data or pilot symbols used in channel estimation. The symbols $P_{pr}$ and $P_{sm}$ denote the number of coefficients in the prediction and smoothing parts of the channel estimation filter [88, p. 400], respectively. Since the past samples are always available for channel estimation, it is assumed that $P_{pr} > 0$ in all cases. If $P_{sm} = 0$, and $v_{k,l}(0) = 0$, the channel estimation filter is a linear predictor, which uses only the past samples for complex channel coefficient estimation. If $P_{sm} = 0$, and $v_{k,l}(0) \neq 0$, the channel estimation filter is a linear "filter", which uses the past samples and the current sample for complex channel coefficient estimation. If $P_{sm} > 0$, the channel estimation filter is a linear smoother, which uses both the past and future samples for complex channel coefficient estimation. The current sample may ($v_{k,l}(0) \neq 0$) or may not ($v_{k,l}(0) = 0$) be used.

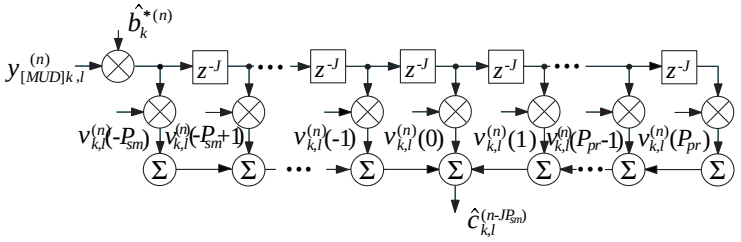


**Fig. 4.2. A general channel estimation filter structure.**

Let the channel estimation filter input vector for the $l$th path of user $k$ at time interval $n$ be denoted by $\mathbf{q}_{k,l}^{(n)}$. The corresponding channel estimation filter is denoted by vector $\mathbf{v}_{k,l}^{(n)}$. The channel estimate can then be expressed in the form

$$\hat{c}_{k,l}^{(n)} = \mathbf{v}_{k,l}^{\mathrm{H}(n)} \mathbf{q}_{k,l}^{(n)}. \tag{4.11}$$

The optimal channel estimation filter in the LMMSE sense for decoupled channel estimation is the Wiener filter [88, Sec. 12.4]

$$\mathbf{v}_{k,l}^{(n)} = \mathbf{\Sigma}_{\mathbf{q}_{k,l}^{(n)}}^{-1} \mathbf{\Sigma}_{\mathbf{q}_{k,l}^{(n)}, c_{k,l}^{(n)}}, \tag{4.12}$$

where $\mathbf{\Sigma}_{\mathbf{q}_{k,l}^{(n)}}$ is the covariance matrix of the channel estimation filter input vector, and $\mathbf{\Sigma}_{\mathbf{q}_{k,l}^{(n)}, c_{k,l}^{(n)}}$ is the covariance vector between the channel estimation filter input vector and the desired channel coefficient $c_{k,l}^{(n)}$ to be estimated. The optimal channel estimation filter depends naturally on the interference suppression scheme, since it determines the input correlation matrix $\mathbf{\Sigma}_{\mathbf{q}_{k,l}^{(n)}}$.

It is assumed that the channel statistics are constant over the observation window, which is a relatively mild assumption. Since the channel statistics depend on the vehicle speed, which is not known at the receiver, the optimal Wiener channel estimation filters require the estimation of the channel correlation function. The LMMSE channel estimation filters may also be approximated by adaptive channel estimation filters as in single-user communications [103, 288], or in a multiuser case [57].

In data-aided channel estimation the delay in Figs. 4.1 and 4.2 is set to $J = N_p$, where $N_p$ is the distance of the pilot symbols (Fig. 4.3). I.e., every $N_p$th symbol of the transmitted symbol stream is a pilot symbol known by the receiver. The channel is estimated by interpolating the samples at the pilot intervals. The channel estimation filter input vector for $i$th ($i \in \{1, 2, \ldots, N_p - 1\}$) data symbol in the frame[3] is

$$\mathbf{q}_{k,l}^{(n)} = \left(y_{[MUD]k,l}^{(n-i-P_{pr}N_p)}, \ldots, y_{[MUD]k,l}^{(n-i)}, y_{[MUD]k,l}^{(n+N_p-i)}, \ldots, y_{[MUD]k,l}^{(n+N_p-i+P_{sm}N_p)}\right)^{\top} \in \mathbb{C}^{P_{pr}+P_{sm}}, \tag{4.13}$$

and the corresponding channel estimation filter is

$$\mathbf{v}_{k,l}^{(n)} = \left(v_{k,l}^{(n)}(-P_{pr}), \ldots, v_{k,l}^{(n)}(-1), v_{k,l}^{(n)}(1), \ldots, v_{k,l}^{(n)}(P_{sm})\right)^{\top} \in \mathbb{C}^{P_{pr}+P_{sm}}. \tag{4.14}$$

The removal of the effect of the data, i.e., multiplication of $y_{[MUD]k,l}^{(n-i)}$ by $b_k^{*(n-i)}$ is neglected for notational convenience in (4.13). In other words, the channel is interpolated over past and future samples of the interference suppression output corresponding the $P_{pr}$ past and $P_{sm}$ future pilot symbols. The optimal channel estimation filter is naturally different for each data symbol in the data frame.

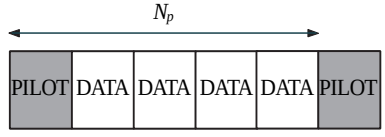


**Fig. 4.3. Data frame structure.**

In decision-directed channel estimation, the delay in Figs. 4.1 and 4.2 is set to $J = 1$. Since the future data symbol decisions are not available, a linear predictor with $P_{sm} = 0$, and $v_{k,l}(0) = 0$ is often applied. The channel estimation filter input vector is in that case

$$\mathbf{q}_{k,l}^{(n)} = \left(y_{[MUD]k,l}^{(n-P_{pr})}, \ldots, y_{[MUD]k,l}^{(n-1)}\right)^{\top} \in \mathbb{C}^{P_{pr}}, \tag{4.15}$$

[3]In other words, the symbol $b_k^{(n-i)}$ is the closest pilot symbol before the symbol $b_k^{(n)}$, and the symbol $b_k^{(n+N_p-i)}$ is the closest pilot symbol after the symbol $b_k^{(n)}$.

and the channel estimation filter is

$$\mathbf{v}_{k,l}^{(n)} = \left(v_{k,l}^{(n)}(-P_{pr}), \ldots, v_{k,l}^{(n)}(-1)\right)^{\top} \in \mathbb{C}^{P_{pr}}. \tag{4.16}$$

Channel estimation based on a smoother usually yields better results than the estimation based on a predictor, since more information on the channel coefficients can be utilized. A smoother can be applied with DD channel estimation if tentative data decisions are available for the current and future symbols. The channel estimation filter input vector is in that case

$$\mathbf{q}_{k,l}^{(n)} = \left(y_{[MUD]k,l}^{(n-P_{pr})}, \ldots, y_{[MUD]k,l}^{(n-1)}, y_{[MUD]k,l}^{(n)}, y_{[MUD]k,l}^{(n+1)}, \ldots, y_{[MUD]k,l}^{(n+P_{sm})}\right)^{\top} \in \mathbb{C}^{P_{pr}+P_{sm}+1}, \tag{4.17}$$

and the channel estimation filter is

$$\mathbf{v}_{k,l}^{(n)} = \left(v_{k,l}^{(n)}(-P_{pr}), \ldots, v_{k,l}^{(n)}(-1), v_{k,l}^{(n)}(0), v_{k,l}^{(n)}(1), \ldots, v_{k,l}^{(n)}(P_{sm})\right)^{\top} \in \mathbb{C}^{P_{pr}+P_{sm}+1}. \tag{4.18}$$

A technique to apply smoothers in DD channel estimation has been proposed for single-user communications in [103]. Tentative decisions can be obtained by using linear predictor for channel estimation. The decisions can then be delayed by $P_{sm}$ symbol intervals to be utilized in the smoother. In other words, the channel is estimated in two stages. The channel estimator structure is illustrated in Fig. 4.4. First, a linear predictor of length $P_{pr}$ using the inputs (4.15) is applied to obtain first stage channel estimates $\hat{c}_{k,l}^{(n)}(pr)$. They are then used in the maximal ratio combiner to produce tentative data decisions $\hat{b}_k^{(n)}(pr)$. The effect of data symbols is removed by using the past tentative decisions made based on the predicted complex channel coefficients. Second, the final channel estimates are obtained by using a linear smoother of length $P_{pr} + P_{sm} + 1$. The MUD outputs $y_{[MUD]k,l}^{(n-P_{pr}-P_{sm})}, \ldots, y_{[MUD]k,l}^{(n-1)}, y_{[MUD]k,l}^{(n)}$ are processed by the smoother to produce the final channel estimates $\hat{c}_{k,l}^{(n-P_{sm})}(sm)$. The effect of data symbols is removed by utilizing the delayed tentative decisions provided by the first stage predicted channel estimates. The channel estimates obtained from the smoother are applied in a maximal ratio combiner, and final data decisions $\hat{b}_k^{(n-P_{sm})}(pr)$ are made. The use of the smoother improves the channel estimation performance in comparison to the use of the predictor alone, since the memory of the fading channel can be utilized more efficiently. The smoother naturally causes an extra decision delay of $P_{sm}$ symbols, which may not be acceptable in some applications.

The DD channel estimation is sensitive to decision errors, which may cause hang-up (cycle slip), i.e., a locking to incorrect carrier phase with a 180 degree offset in comparison to the correct phase (with BPSK modulation). Usually some countermeasures to protect the channel estimator from hang-up are needed. The DD channel estimators require pilot symbols to be inserted into the data frame. Also some hang-up detection and correction scheme may be necessary. A simple way to detect hang-ups is to make decisions on the pilot symbols and to check

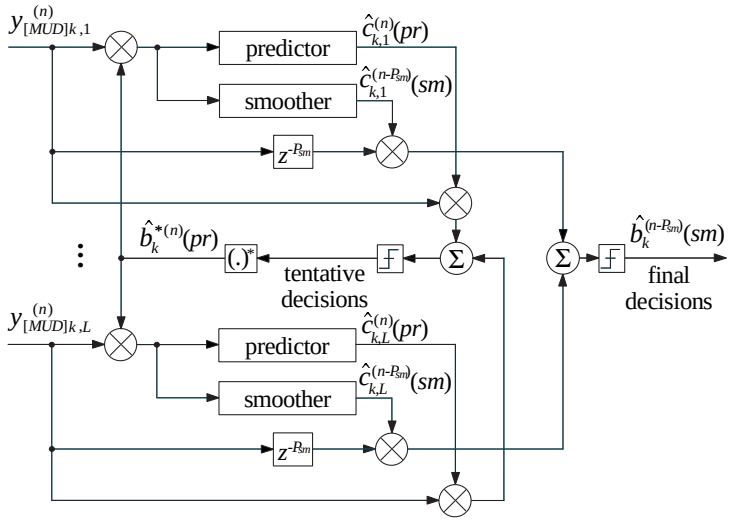


**Fig. 4.4. Two-stage DD channel estimator structure.**

whether the decisions are correct or not. If a decision error was made, an error-counter, which is set to zero at the beginning of the transmission, is incremented by one. If a correct decision was made, the error-counter is decremented by one, unless the value of the counter is zero. If the error-counter exceeds a pre-determined value, the channel estimator is declared to be in hang-up. Then the phase of the samples of the interference suppression output in the channel estimator is rotated 180 degrees (with BPSK modulation), and the error-counter is reset to zero.

The DA channel estimation is more robust than DD estimation, since decision errors are not a problem, and, thus, there are no hang-ups. Its drawback is that it may require a shorter pilot symbol distance $N_p$ than DD. The DA channel estimator also causes longer decision delay than DD channel estimation. The performance of DA and DD channel estimation is studied and compared in Section 4.3.

### *4.2.2. Interference suppression*

The interference suppression block in the receiver of Fig. 4.1 may in general apply any multiuser receiver algorithm capable to process $KL$ input propagation paths and provide $KL$ outputs. For continuous, unpacketized, asynchronous transmission the truncated decorrelating detector and the parallel interference canceler are among the most promising alternatives in relatively fast fading channels for centralized receivers from practical point of view, as discussed in Chapters 2 and 3.

The LMMSE detector of Chapter 3 is not considered any further, since it requires continuous updates due to complex channel coefficient variations in fading channels. Thus, the decorrelating and the PIC receivers are studied and compared in this chapter.

The truncated decorrelating detector described in Chapter 3 is used in the examples. The truncated decorrelator imposes a decision delay of $P$ symbols. Therefore, the total decision delay in conjunction with a smoother for channel estimation is $P + P_{sm}$ symbol intervals. Since the decorrelator needs neither complex channel coefficient estimates nor data decisions for MAI suppression, the feedback in Fig. 4.1 is not needed if the decorrelator is applied.

The PIC receiver needs both tentative complex channel coefficient estimates and data decisions to perform MAI suppression as seen from (2.61). The interference cancellation may be performed in several stages. The complex channel coefficient estimates may be formed independently in different stages or the complex channel coefficient of the last stage may be fed back to the former stages, for example. Therefore, there is a large variety of different PIC receiver versions available. The performance of some alternatives is studied in more detail in [289]. Based on those studies, a two-stage PIC receiver is applied in the sequel. It uses always the latest complex channel coefficient and data estimates that are available. In other words, for past symbol intervals the final symbol decisions and complex channel coefficient estimates are used in the interference cancellation. Tentative symbol decisions are used for the current and future symbol intervals. The latest final complex channel coefficient estimate is used for the current and future symbol intervals. Although this approach neglects changes in the complex channel coefficients, it has been shown to be superior to the use of tentative complex channel coefficient estimates [289].

## 4.3. Receiver performance analysis and results

The performance of multiuser receivers in Rayleigh fading channels is considered in this section. In Section 4.3.1, the performance of the linear receivers is analyzed. The ideal DA joint LMMSE channel estimator and decorrelator combined with decoupled channel estimator is compared. Bit error probability and channel capacity of the DA decorrelating receiver are also analyzed. Furthermore, the performance of the DA and DD decorrelating receivers is compared. The performance of the DD decorrelator and parallel interference canceler is compared in Section 4.3.2. The sensitivity of the bit error rate of the decorrelating and PIC receivers to channel estimation errors as well as the BER in an estimated channel are studied.

Numerical examples are considered. Some of them are obtained via theoretical analysis and the others are based on Monte-Carlo computer simulations. Simulations are used since the effect of decision errors to the performance of the DD channel estimation and the HD-PIC receivers is difficult to analyze. Direct-sequence spread-spectrum waveforms with BPSK data and spreading modulation are considered. A Gold sequence family with processing gain 31 is used. The delays of the

users and propagation paths are assumed to be uniformly distributed into $\big[0, T\big)$ and $\big[0, T_m\big)$, respectively. Delay spread is assumed to be $T_m = T/2$. One and two-path channel examples are considered. In the two-path channel case, equal power paths, i.e., $\mathrm{E}\Big(|c_{k,1}|^2\Big) = \mathrm{E}\Big(|c_{k,2}|^2\Big) = \frac{1}{2}$, are used. The vehicle speeds are equal for all users. The vehicle speed is 86 km/h (43 km/h in some examples in Section 4.3.1), the carrier frequency is 1.8 GHz, and the symbol rate is 16 kbits/s (i.e., $f_d T = 0.009$). The resulting normalized channel autocorrelation function is illustrated in Fig. 4.5. Both optimal and suboptimal channel estimation filters are considered. The optimal channel estimation filters are matched to the true channel correlation function (vehicle speed) and to the true average signal-to-noise ratio. The suboptimal channel estimation filters are Wiener filters optimized for a single-user channel and the autocorrelation function assuming vehicle speed of 50 km/h and an average SNR of 10 dB. The fixed, suboptimal channel estimation filters are used for all users and average SNR's. The data-aided channel estimators use an interpolator of length 6 ($P_{sm} = P_{pr} = 3$) (except in some examples in Section 4.3.1) and sample spacing of $J = N_p$. The decision-directed channel estimators use the two-stage channel estimation described in Section 4.2.1 with a predictor of length $P_{pr} = 10$ and a smoother of length 21 ($P_{sm} = P_{pr} = 10$). The sample spacing is $J = 1$ in both the predictor and smoother. In the simulations of the DD channel estimators every tenth symbol is a pilot symbol, i.e., $N_p = 10$. The hang-up detection scheme described in Section 4.2.1 with a threshold of 2 erroneous decisions on pilot symbols is also used. Simulations include examples with equal transmitted energies for all users, and examples with a near-far problem (about one third of the users have 10 dB larger transmitted energy per symbol than the other, desired users). The edge effect to the decorrelator due to a finite processing window (Chapter 3) is neglected in the analysis. However, the simulations include the edge effect, which was observed to be of minor importance.

## *4.3.1. Performance of linear receivers*

### *4.3.1.1. MSE of DA channel estimation*

The channel estimation performance assuming correct decisions on the data is analyzed to find the expression for the mean squared error of the channel estimators. The optimal joint estimation of all users' channels as in (4.10) is compared to the decoupled channel estimation as described in Section 4.2.1. For simplicity and to enable a fair comparison, a DA channel estimation with a data symbol interval $J = 1$ is applied in the examples. The data packet size is assumed to equal the processing window length, i.e., $N_b = N$. The decorrelator is applied as the interference suppression scheme in the decoupled channel estimation. Therefore, the input to the joint LMMSE estimator is $\boldsymbol{y} \in \mathbb{C}^{NKL}$, and the inputs to the decoupled channel estimators are $\mathbf{q}_{k,l}^{(n)} = \big(y_{[d]k,l}^{(0)}, y_{[d]k,l}^{(1)}, \ldots, y_{[d]k,l}^{(N)}\big)^{\top} \in \mathbb{C}^N$, $\forall\, k, l$.

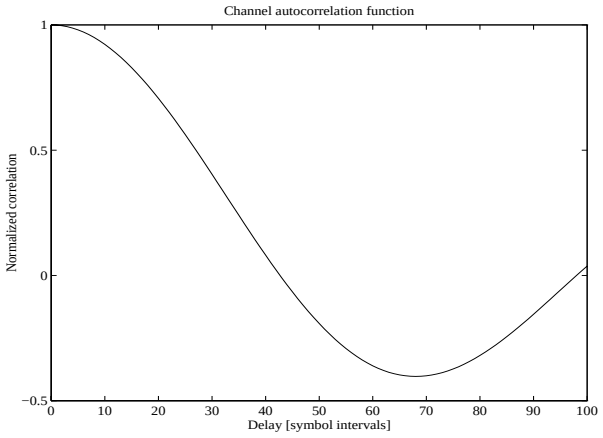


**Fig. 4.5. Channel autocorrelation function.**

The performance of the optimal joint LMMSE channel estimator of (4.10) is described by the error covariance matrix [88, p. 391]

$$\mathbf{\Sigma}_{\boldsymbol{h}-\hat{\boldsymbol{h}}_{[MMSE]}|\boldsymbol{b}} = (\mathbf{\Sigma}_{\boldsymbol{h}|\boldsymbol{b}}^{-1} + \sigma^{-2}\mathcal{R})^{-1}, \tag{4.19}$$

where each diagonal element of $\mathbf{\Sigma}_{\boldsymbol{h}-\hat{\boldsymbol{h}}_{[MMSE]}}$ is equal to the mean squared error of the optimal LMMSE estimator for that particular channel coefficient. The MSE of the decoupled channel estimator can be expressed in the form [88, p. 388]

$$\mathbf{MSE}_{[d]k,l} = \sigma^2_{h_{k,l}^{(n)}} - \mathbf{\Sigma}^{\mathrm{H}}_{\mathbf{q}_{k,l}^{(n)},h_{k,l}^{(n)}} \mathbf{\Sigma}^{-1}_{\mathbf{q}_{k,l}^{(n)}} \mathbf{\Sigma}_{\mathbf{q}_{k,l}^{(n)},h_{k,l}^{(n)}}, \tag{4.20}$$

where $\sigma^2_{h_{k,l}^{(n)}} = \mathrm{E}(|h_{k,l}^{(n)}|^2)$.

The optimal joint LMMSE channel estimator (4.10) utilizes the information embedded in the dependence of the channel noise components of the MF outputs of different users and multipath components, whereas the decoupled channel estimator neglects that information. If the optimal Wiener filter of (4.12) is applied at the decoupled channel estimator, the information of the fading process is utilized as efficiently as in the joint LMMSE estimator. Therefore, it can be conjectured that in several cases, the performance difference between the joint LMMSE and decoupled estimators is minor. This hypothesis is tested by evaluating the normalized MSE's of the joint LMMSE and decoupled channel estimators given in (4.19) and (4.20), respectively. The normalized MSE of the estimate $\hat{c}$ of some parameter $c$ is

$$MSE = \frac{\mathrm{E}\Big(|c-\hat{c}|^2\Big)}{\mathrm{E}\Big(|c|^2\Big)}. \tag{4.21}$$

The results are depicted in Figs. 4.6 and 4.7 for one and two-path channels, respectively. Two vehicle speeds (43 and 86 km/h) and processing window sizes ($N = N_b = 7$ and $N = N_b = 21$) are considered in the examples.

The channel estimation performance is worse in a two-path channel than in a one-path channel. There are two reasons for that. Firstly, an increase in the channel load $KL$ causes more linear dependence between the signals. Therefore, there is more noise enhancement in the decorrelating and joint LMMSE receivers. Secondly, in the examples the received power of a particular user is divided into two components, which both must be estimated independently, in a two-path channel. In a one-path channel, on the other hand, all the power can be utilized in the estimation of the single propagation path. In that sense, the normalization (2.41) is somewhat misleading, and the curves of Fig. 4.7 could be shifted 3 dB to the left.

It can be seen from the figures that the performance advantage of the joint LMMSE channel estimator over the decoupled channel estimator is indeed minor in most cases as predicted above. In the two-path channel with a small observation window ($N = 7$) the difference is the largest, roughly 1 dB. It can also be seen that the performance difference due to vehicle speed is very small, as long as optimal channel estimation filters are applied. Thus, it can be concluded that the decorrelating receiver is capable of providing near optimal channel estimation performance with significantly simpler implementation than the joint LMMSE estimator. If decision-directed channel estimation is applied, the result may be even more favorable for the channel estimator using decorrelator, since it is insensitive to the decisions of the other users, whereas the joint LMMSE estimator is not.

### *4.3.1.2. BEP of DA decorrelating receiver*

The performance of the data-aided decorrelating receiver is analyzed to obtain the expression for the average bit error probability. The analysis has similarities to [56, 123], where the channel was assumed to be known, or to [127], where error-free DD channel estimation[4] was considered. Here, DA detection with a pilot symbol distance larger than one ($N_p > 1$) is assumed. The decision variable of the decorrelating receiver for user $k$ after maximal ratio combining can be expressed in the form

$$y^{(n)}_{[d,MRC]k} = \tilde{\mathbf{c}}^{(n)\mathrm{H}}_k \mathbf{y}^{(n)}_{[d]k}, \tag{4.22}$$

where

$$\tilde{\mathbf{c}}^{(n)}_k = \left(\tilde{c}^{(n)}_{k,1}, \tilde{c}^{(n)}_{k,2}, \ldots, \tilde{c}^{(n)}_{k,L}\right) \in \mathbb{C}^L \tag{4.23}$$

is the combing vector, and

$$\mathbf{y}^{(n)}_{[d]k} = \left(y^{(n)}_{[d]k,1}, y^{(n)}_{[d]k,2}, \ldots, y^{(n)}_{[d]k,L}\right) \in \mathbb{C}^L \tag{4.24}$$

[4]Error-free DD channel estimation means actually DA channel estimation with pilot symbol distance one ($N_p = 1$).

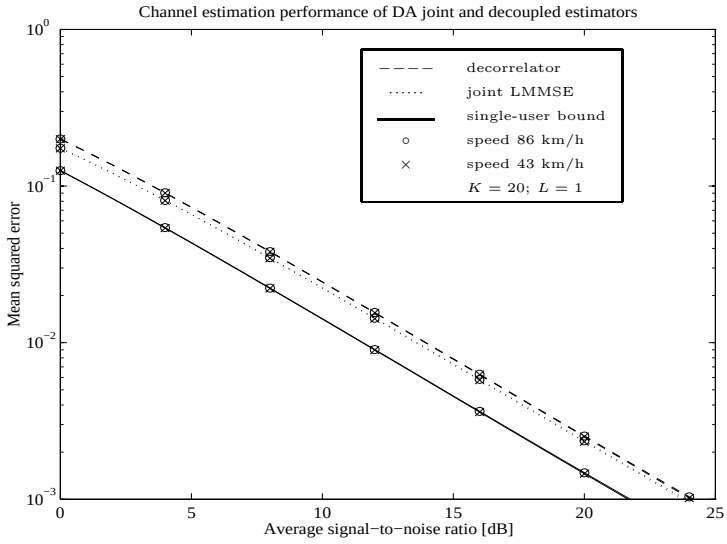


(a)

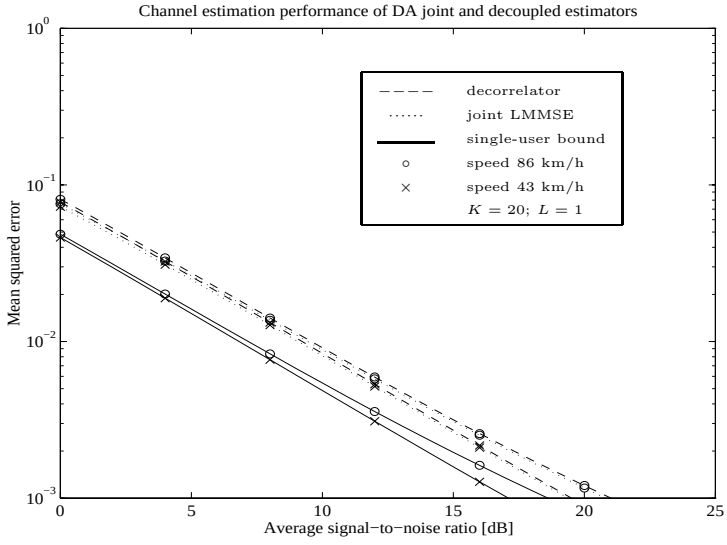


(b)

**Fig. 4.6. Mean squared errors of DA joint LMMSE and decoupled decorrelated channel estimators in a flat fading channel ($L = 1$) for two vehicle speeds; observation window is (a) $N = 7$, (b) $N = 21$.**

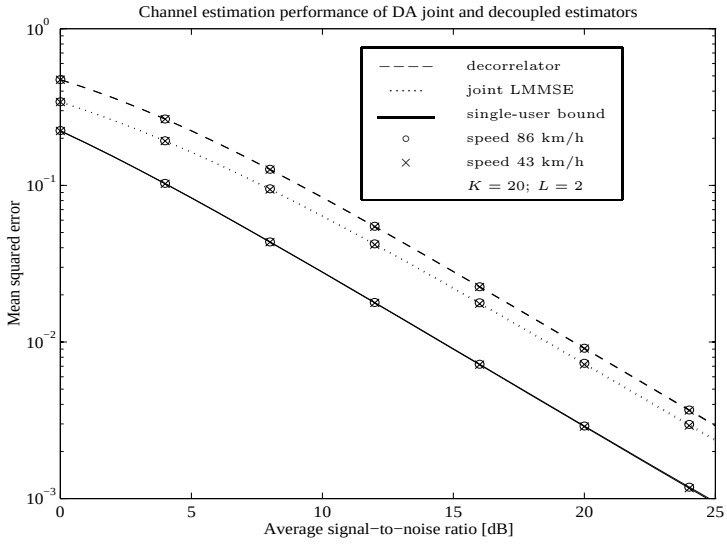


(a)

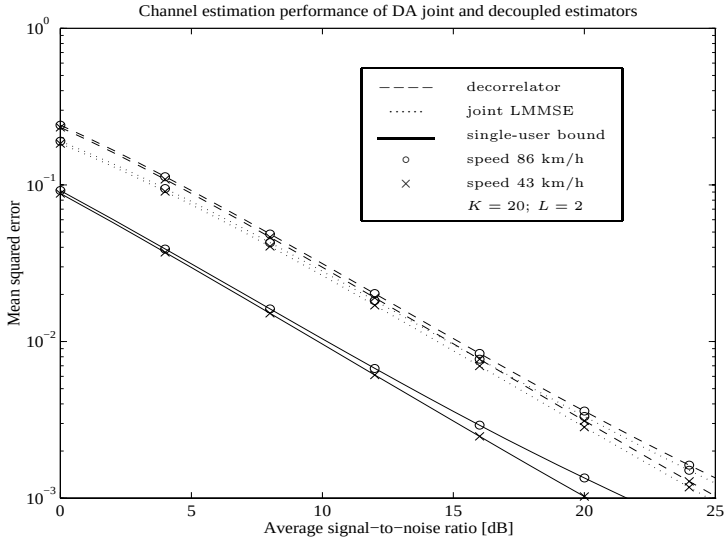


(b)

**Fig. 4.7**. **Mean squared errors of DA joint LMMSE and decoupled decorrelated channel estimators in a frequency-selective fading channel ($L = 2$) for two vehicle speeds; observation window is (a) $N = 7$, (b) $N = 21$.**

includes the decorrelator outputs for user $k$. The optimal choice for $\tilde{\mathbf{c}}_k^{(n)}$, given the complex channel coefficient estimate $\hat{\mathbf{c}}_k^{(n)}$, is $\tilde{\mathbf{c}}_k^{(n)} = \mathbf{D}_{[d]k,k}^{-1}(0)\hat{\mathbf{c}}_k^{(n)}$ (Section 3.3.2). Let

$$\mathbf{Q} = \frac{1}{2}\begin{pmatrix} \mathbf{0}_L & \mathbf{I}_L \\ \mathbf{I}_L & \mathbf{0}_L \end{pmatrix} \in \{0, \frac{1}{2}\}^{2L\times 2L}, \tag{4.25}$$

and

$$\boldsymbol{\nu} = (\tilde{\mathbf{c}}_k^{\top(n)}, \mathbf{y}_{[d]k}^{\top(n)})^{\top} \in \mathbb{C}^{2L}. \tag{4.26}$$

By rewriting (4.22) the decision variable $y_{[d,MRC]k}^{(n)}$ can be expressed in the form

$$y_{[d,MRC]k}^{(n)} = \boldsymbol{\nu}^{\mathrm{H}}\mathbf{Q}\boldsymbol{\nu}. \tag{4.27}$$

The decorrelator output vector $\mathbf{y}_{[d]k}^{(n)}$ conditioned on the data symbol $b_k^{(n)}$ is a complex Gaussian random vector. Assuming that the weight vector $\tilde{\mathbf{c}}_k^{(n)}$ is also Gaussian[5] the probability of bit error for user $k$ can be expressed in the case of BPSK modulation as [287]

$$P_k = \sum_{\substack{i=1 \\ \lambda_i<0}}^{2L} \prod_{\substack{j=1 \\ j\neq i}}^{2L} \frac{1}{1-\frac{\lambda_j}{\lambda_i}}, \tag{4.28}$$

where $\lambda_i, i = 1, 2, \ldots, 2L$ are the eigenvalues of the matrix $\boldsymbol{\Sigma}_{\boldsymbol{\nu}}$, and

$$\boldsymbol{\Sigma}_{\boldsymbol{\nu}} = \begin{pmatrix} \boldsymbol{\Sigma}_{\tilde{\mathbf{c}}_k^{(n)}} & \boldsymbol{\Sigma}_{\tilde{\mathbf{c}}_k^{(n)},\mathbf{y}_{[d]k}^{(n)}} \\ \boldsymbol{\Sigma}^{\mathrm{H}}_{\tilde{\mathbf{c}}_k^{(n)},\mathbf{y}_{[d]k}^{(n)}} & \boldsymbol{\Sigma}_{\mathbf{y}_{[d]k}^{(n)}} \end{pmatrix} \tag{4.29}$$

is the covariance matrix of the vector $\boldsymbol{\nu}$. The covariance matrix (4.29) depends on the channel estimation filter. Although the error probability expression in (4.28) is not very intuitive, it is extremely useful in computing numerical examples. The reason is that it can express the probability of bit error for any channel estimation filter.

The probability of error is computed for several values of the pilot symbol distance $N_p$ with interpolation, as described in Section 4.2.1. The length of the smoother satisfies $P_{pr} = P_{sm} = 3$, i.e., in total six consecutive pilot symbols are used to estimate the complex channel coefficients. Both optimal and suboptimal smoothers are applied. The results with the optimal channel estimation filter are presented in Fig. 4.8, and with the suboptimal channel estimation filter in Fig. 4.9.

The results show that with the optimal channel estimation filters the bit error probability performance is excellent even at large SNR's. A distance of $N_p < 30$ yields performance that is free of error probability saturation. A distance of $N_p > 45$ is so large that the error probability starts to saturate at high SNR's (SNR $>$ 30 dB). From low to moderate SNR's the performance loss due to increased pilot symbol distance is relatively low. For example, at error probability of $10^{-2}$

[5]Gaussian assumption holds for any DA linear channel estimation filter.

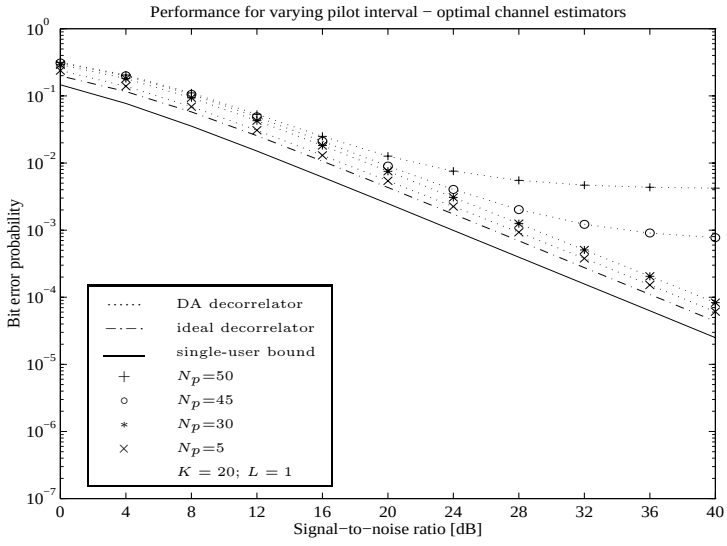


(a)

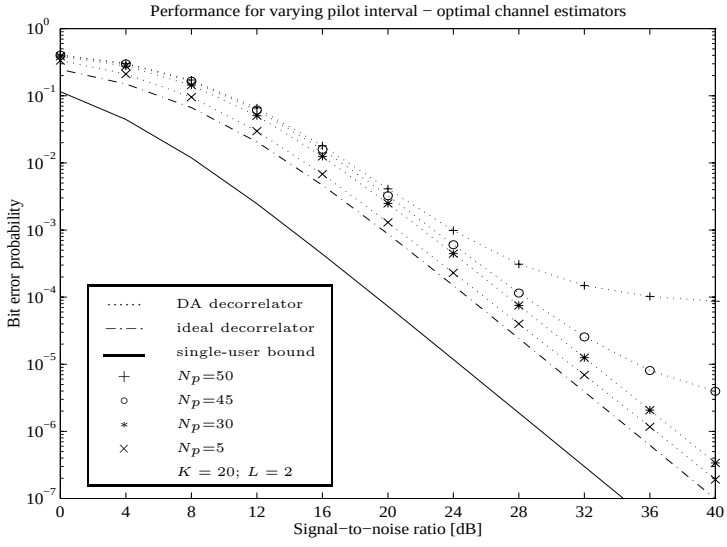


(b)

**Fig. 4.8. Bit error probabilities of DA decorrelating receiver for different pilot symbol distances with optimal channel estimation filters; (a) $L = 1$, (b) $L = 2$.**

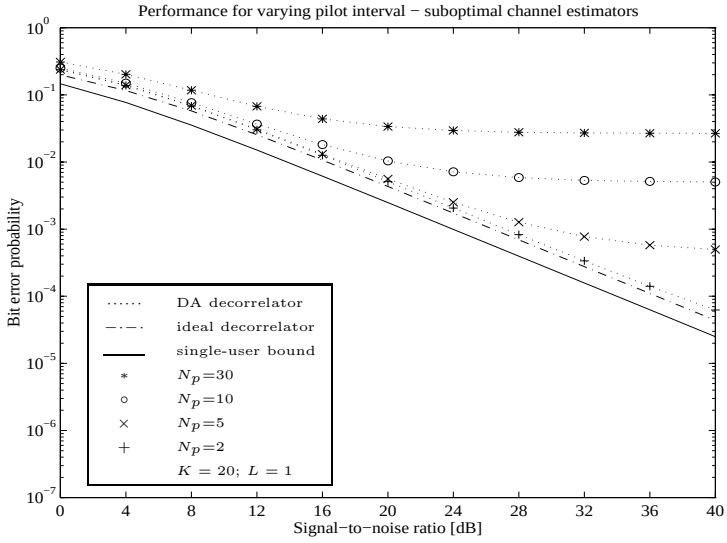


(a)

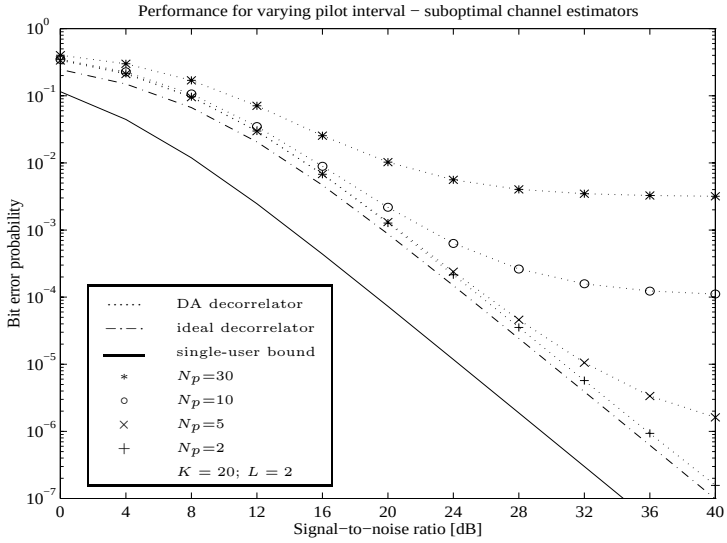


(b)

**Fig. 4.9. Bit error probabilities of DA decorrelating receiver for different pilot symbol distances with suboptimal channel estimation filters; (a) $L = 1$, (b) $L = 2$.**

the differences in the required SNR between $N_p = 5$ and $N_p = 50$ are about 4.5 dB and 3.5 dB for one and two-path channels, respectively. If suboptimal channel estimation filters are applied, the error floor is a significantly more severe problem. Even with a pilot symbol distance of $N_p = 5$, the bit error probability saturates at high SNR's. From low to moderate SNR's the performance loss due to increased pilot symbol distance is also larger than with optimal channel estimation filters. For example, at BER $= 10^{-2}$ the differences in the required SNR between $N_p = 5$ and $N_p = 30$ are $\infty$ dB and about 5 dB for one and two-path channels, respectively.

It can be concluded that superior performance can be obtained even with large pilot symbol distances if optimal channel estimation filters can be applied. The fixed, suboptimal channel estimation filters cause a severe performance loss at high SNR's. However, at low SNR's fairly good performance can be obtained even with a suboptimal channel estimation filter if the pilot symbol distance is small enough (roughly $N_p \leq 10$ in the examples).

#### *4.3.1.3. Channel capacity of DA decorrelating receiver*

The above analysis provided results on the bit error probability of the DA decorrelating receiver for different pilot symbol distances. The use of pilot symbols improves the bit error rate performance, but reduces the effective data rate. More specifically, if every $N_p$th symbol is a pilot symbol, the effective data rate is the nominal data rate multiplied by the factor $\frac{N_p-1}{N_p}$. Thus, the challenge is to select the pilot symbol distance so that the overall channel capacity is maximized. This problem is not easy to solve in practical examples, since the solution depends on the channel encoding and decoding schemes applied. Therefore, the pilot symbol distance should be jointly optimized with the complete signal design.

To give some insight into the pilot symbol distance optimization problem, the fundamental limit provided by the information theoretic Shannon's channel capacity is studied. For simplicity, it is assumed that the information bit stream is encoded, and transmitted through the fading multiple-access channel. It is assumed that the receiver consists of a decorrelating multiuser receiver and DA channel estimation, after which hard decision decoding is performed. Then the bit error probability analysis above applies to these hard decisions. The complete communications system can then be modeled as a binary symmetric channel [22, pp. 186-187] from a single-user point of view. In other words, from the coding point of view the channel of user $k$ is a binary symmetric channel with error probability $P_k$ given in (4.28). Thus, the Shannon capacity of the $k$th user is [22, pp. 14, 187], [23, p. 381]

$$CAP_k = \frac{N_p - 1}{N_p}\big[1 + P_k \log_2(P_k) + (1 - P_k)\log_2(1 - P_k)\big]. \qquad (4.30)$$

The Shannon capacity is the data rate at which a user can obtain an asymptotically error-free transmission as the signal-to-noise ratio approaches infinity, by applying

the very best encoding scheme that can exist with optimal decoding. The results provided by the Shannon capacity analysis are optimistic in the sense that the very best encoding scheme cannot be applied in practice, since the scheme is allowed to be arbitrarily complicated and there is no design rule to find that scheme. On the other hand, the capacity results are pessimistic in the sense that by applying soft decision decoding the performance can be improved.

The Shannon capacity (4.30) is evaluated for the bit error probability results presented in Figs. 4.8–4.9. The results are presented in Figs. 4.10 and 4.11. From the capacity results the optimal pilot symbol distances yielding the maximal Shannon capacity were determined. The optimal pilot symbol distances are illustrated versus SNR in Fig. 4.12.

The results demonstrate that the optimal pilot symbol distance depends strongly on the SNR. At low SNR's the optimal pilot symbol distance is rather low, whereas at high SNR's very large pilot symbol distances can be tolerated for maximal channel capacity if optimal channel estimation filters could be applied. The use of suboptimal channel estimation filters degrade the capacity, especially, at high SNR's. At low SNR's the differences in the capacity are significantly smaller. From Fig. 4.12, it can be seen that at SNR's of 16–20 dB and higher, the optimal pilot symbol distance depends heavily on the channel estimation.

It can be concluded based both on the bit error probability examples (Figs. 4.8–4.9) and on the capacity examples (Figs. 4.10–4.11) that the choice of the channel estimation filters is crucial in data transmission with very low bit error rate requirement. Thus, in data transmission systems there is clearly need for optimal or near-optimal channel estimation filters. In speech transmission, on the other hand, the fixed channel estimation filters can provide a satisfactory performance if the system requirements can tolerate a moderate pilot symbol distance ($N_p \approx 10$).

### *4.3.1.4. BER of DA and DD decorrelating receivers*

The bit error probability of the DA decorrelating receiver is compared to the bit error rate of the DD decorrelating receiver. Inspired by the results in Section 4.3.1.3, pilot symbol distance $N_p = 10$ is used. The results of the analysis (DA decorrelator) and Monte-Carlo computer simulations (DD decorrelator) are presented in Fig. 4.13.

It can be seen from Fig. 4.13 that the DA decorrelating receiver outperforms the DD decorrelating receiver by approximately 1 dB with optimal channel estimation filters both in the cases $L = 1$ and $L = 2$. Fig. 4.13(a) ($L = 1$) shows that the DA decorrelating receiver outperforms the DD decorrelating receiver by approximately 2.5 dB at BER $= 2 \times 10^{-2}$ with suboptimal channel estimation filters, and the performance difference increases with increasing SNR. Fig. 4.13(b) ($L = 2$) shows that in the two-path channel the performance difference between the DA and DD decorrelating receivers is significantly smaller than in the one-path channel. This is understandable, since the decisions are more reliable due to diversity, and the DD decorrelating receiver can also yield superior performance. At high SNR's,

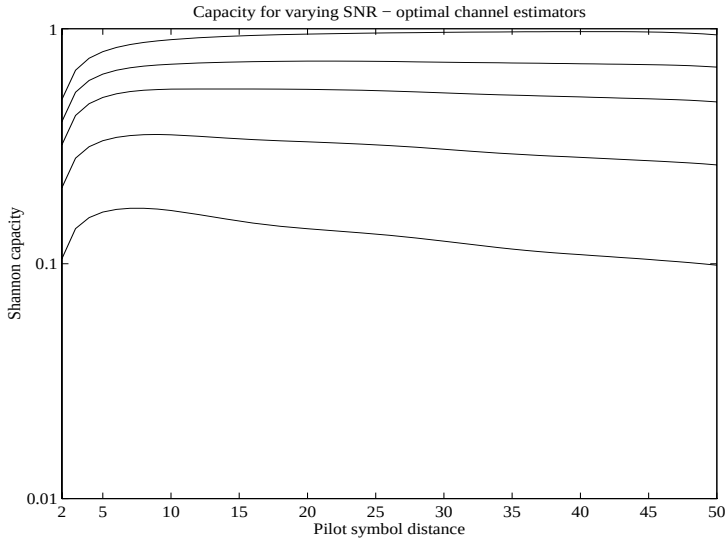


(a)

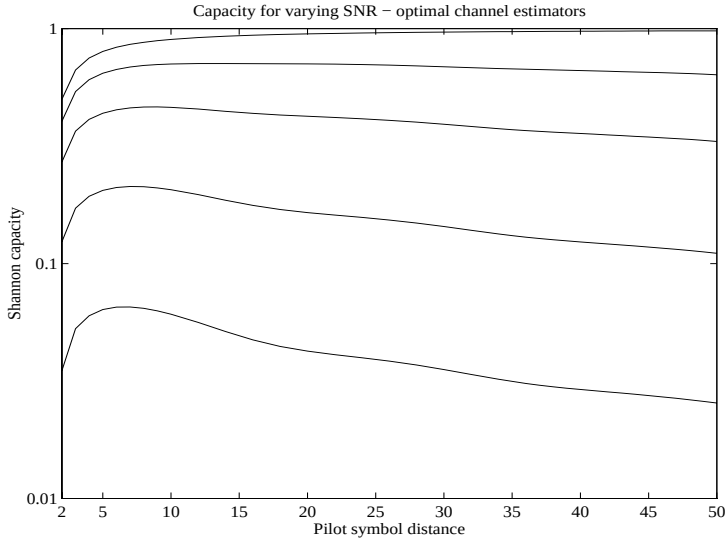


(b)

**Fig. 4.10. Channel capacities of DA decorrelating receiver for different signal-to-noise ratios (SNR = 0, 4, 8, 12, 40 dB from down to upwards) with optimal channel estimation filters; (a) $L = 1$, (b) $L = 2$.**

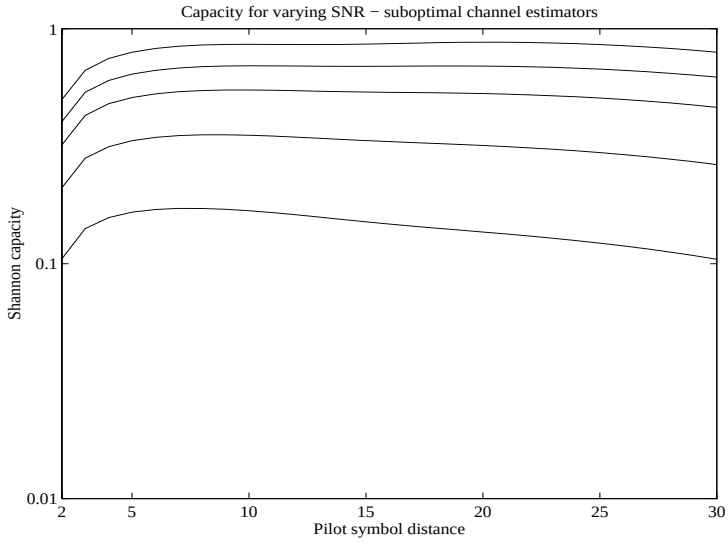


(a)

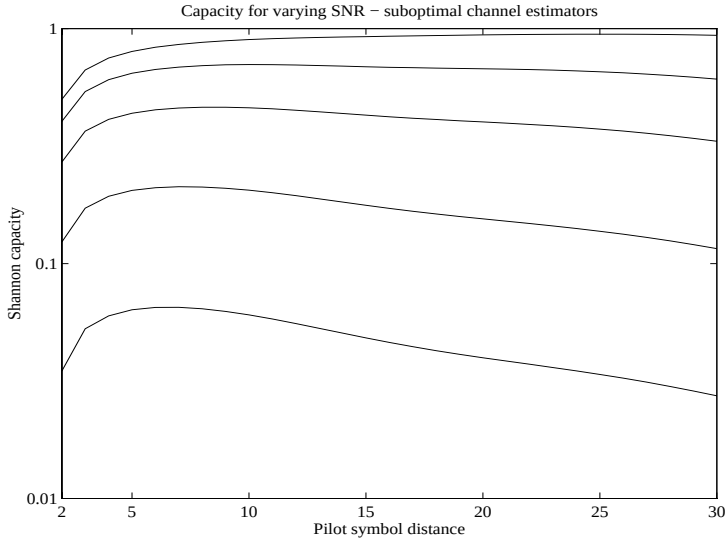


(b)

**Fig. 4.11. Channel capacities of DA decorrelating receiver for different signal-to-noise ratios (SNR = 0, 4, 8, 12, 40 dB from down to upwards) with suboptimal channel estimation filters; (a) $L = 1$, (b) $L = 2$.**

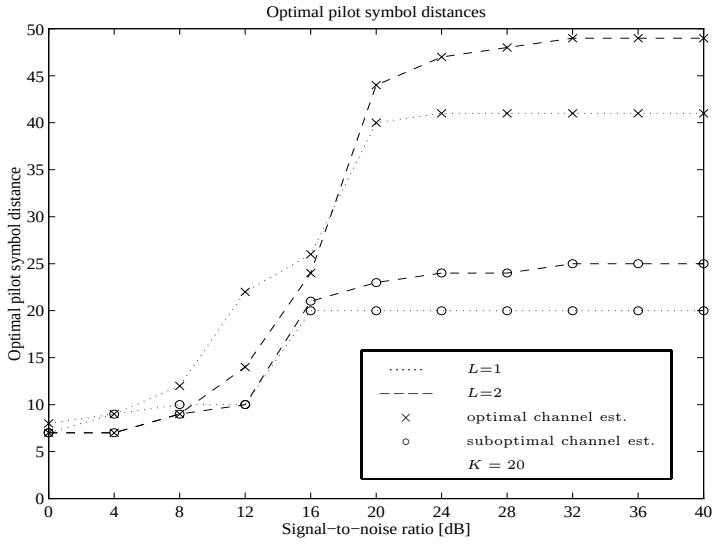


**Fig. 4.12. Optimal pilot symbol distances in Shannon capacity sense.**

however, the BER of the DD decorrelating receiver saturates if suboptimal channel estimation filters are be applied. It can be concluded that both the DA and DD decorrelating receivers provide relatively good performance if optimal channel estimation filters are applied. Furthermore, the DA decorrelating receiver is more robust to the channel estimation filter mismatch than the DD decorrelating receiver. In a two-path channel, where the decisions are rather reliable, the DD decorrelating receiver gives satisfactory performance also with suboptimal channel estimation filters.

## *4.3.2. Performance comparisons of decorrelating and PIC receivers*

### *4.3.2.1. Sensitivity of BER to channel estimation errors*

The sensitivity of the bit error rate to channel estimation errors is studied without simulating the channel estimation process implicitly. The detection with the decorrelating and the PIC receivers is simulated assuming that the channel estimates $\hat{c}_{k,l}^{(n)}$ with mean squared error $MSE$ are given. The estimates are generated in the simulations assuming a decomposition $\hat{c}_{k,l}^{(n)} = c_{k,l}^{(n)} + \Delta c_{k,l}^{(n)}$, where $\Delta c_{k,l}^{(n)}$

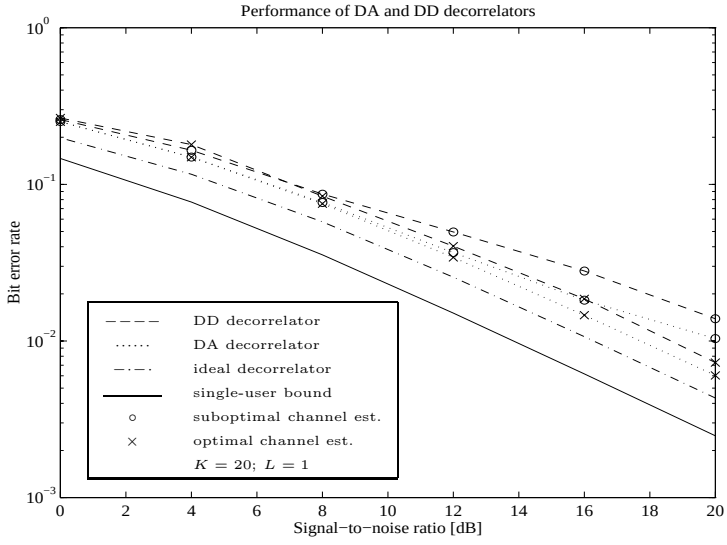


(a)

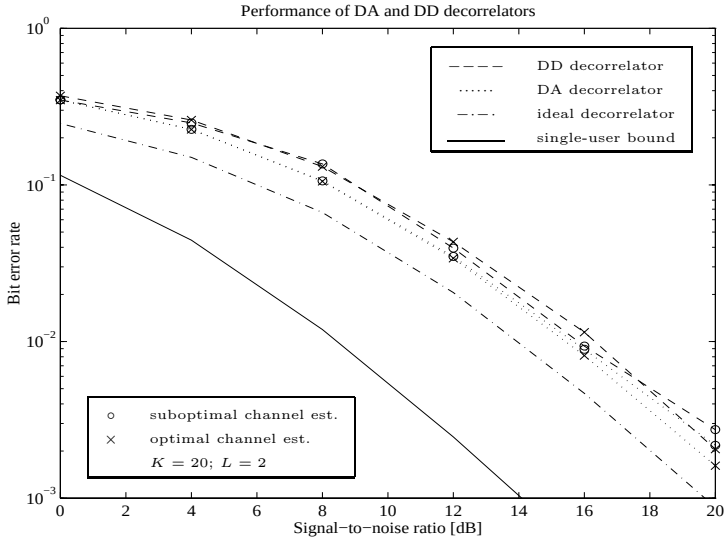


(b)

**Fig. 4.13**. **Bit error rates of DD and DA decorrelating receivers for $N_p = 10$; (a) $L = 1$, (b) $L = 2$.**

is the channel estimation error. It is further decomposed in the form $\Delta c_{k,l}^{(n)} = \Delta c_{k,l}^{(n)}(lag) + \Delta c_{k,l}^{(n)}(noise)$, where $\Delta c_{k,l}^{(n)}(lag)$ is the lag error due to channel variations and suboptimal channel estimation [23], and $\Delta c_{k,l}^{(n)}(noise)$ is the error due to the additive white Gaussian noise. In the examples, the absolute value of the lag error is assumed to be constant for one signal-to-noise ratio value, and the error due to the AWGN is assumed to be a complex Gaussian random variable with zero mean and variance $\sigma_{k,l}^2(noise)$, which is the variance of the AWGN at the output of the optimal channel predictor of length 10 ($P_{pr} = 10$, $J = 1$). The errors $\Delta c_{k,l}^{(n)}(noise)$ and $\Delta c_{k',l'}^{(n')}(noise)$ are assumed to be independent if $k \neq k'$ or $l \neq l'$ or $n \neq n'$. The absolute value of the lag error term is

$$|\Delta c_{k,l}^{(n)}(lag)| = \sqrt{MSE - \sigma_{k,l}^2(noise)}, \tag{4.31}$$

and its phase is assumed to be uniformly distributed into $[0, 2\pi)$.

An exactly known channel ($\Delta c_{k,l}^{(n)} = 0$ or $MSE = 0$), and three positive MSE levels ($MSE = MSE_{min}$, $MSE = 1.5MSE_{min}$, $MSE = 2MSE_{min}$), where $MSE_{min}$ is the mean squared error of the form (4.20) with the optimal predictor ($P_{pr} = 10$, $J = 1$) and no decision errors, are considered. The results are shown in Figs. 4.14 and 4.15 for one and two-path channels, respectively. Both the cases of equal received energies and a near-far problem are considered.

It can be seen from the Figs. 4.14 and 4.15 that in a perfectly known channel the PIC receiver clearly outperforms the decorrelating receiver, especially with diversity (Fig. 4.15). This is intuitive, since increasing the channel load $KL$ increases the noise enhancement in the decorrelator. Furthermore, the diversity offered by the two-path channel makes the decisions and MAI estimate in the PIC receiver more reliable. However, the PIC receiver is more sensitive to channel estimation errors than the decorrelating receiver, which is also understandable. The decorrelator completely decouples the reception of different users, whereas in the PIC receiver the channel estimation errors propagate to MAI estimates and degrade the performance for all users. In the single-path channel, the performance of the PIC and decorrelating receivers is nearly the same if the channel estimation error is large. In the two-path channel case, the PIC receiver outperforms the decorrelating receiver in the presence of channel estimation errors. An exception is the presence of a near-far problem and large channel estimation errors if the system operates at high SNR's (see Fig. 4.15(b)). It can be concluded that the PIC receiver yields often better performance than the decorrelating receiver. However, the decorrelating receiver is more robust to the channel estimation errors than the PIC receiver.

#### *4.3.2.2. BER in optimally estimated channel*

The decision-directed channel estimator structure is studied. Optimal channel estimation filters are applied. The simulations are performed for different numbers of active users ($K = 8, 20, 32$). The BER results are shown in Figs. 4.16 and

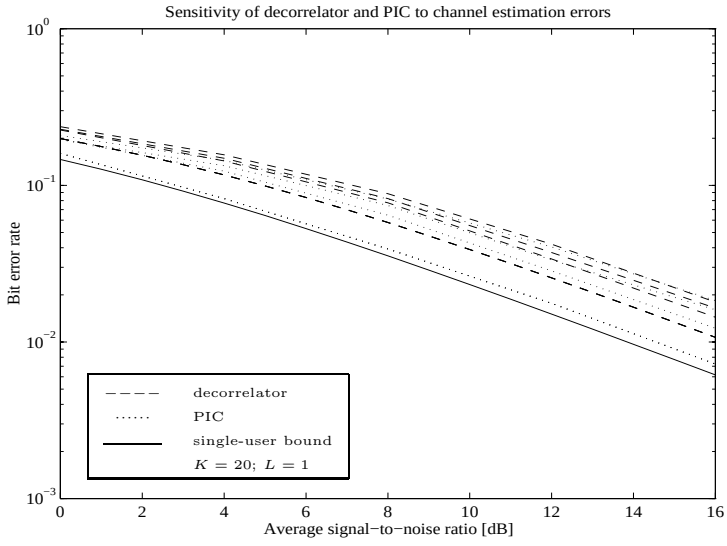


(a)

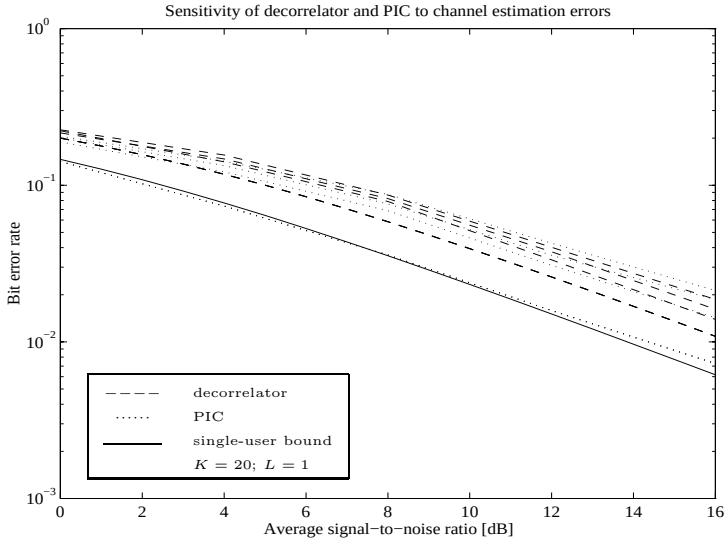


(b)

**Fig. 4.14. Sensitivity of BER to channel estimation errors in a flat fading channel ($L = 1$) for different MSE levels ($MSE = (0, 1, 1.5, 2) \times MSE_{min}$ from down to upwards); (a) equal received energies, (b) near-far problem.**

4.17 for one and two-path channels, respectively. Both the cases of equal received energies and a near-far problem are considered.

It can be seen from Fig. 4.16 that the PIC and the decorrelating receivers have nearly the same performance in a one-path channel. When comparing to Fig. 4.14, it is observed that the complex channel coefficient estimation is more challenging for the PIC receiver than for the decorrelating receiver. Fig. 4.17 demonstrates that the PIC receiver outperforms the decorrelating receiver in a two-path channel. This is understandable due to the increased noise enhancement in the decorrelating receiver caused by the larger channel load $KL$. However, in a heavily loaded CDMA system with $K = 32$ under a near-far problem ($K = 32$ in Figs. 4.16(b) and 4.17(b)), the BER of the PIC receiver saturates at high SNR's due to decision errors degrading the MAI estimates. The decorrelating receiver does not suffer from BER saturation. A similar phenomenon has been observed in an AWGN channel even with lower channel loads [248]. It can be concluded that, in general, the PIC receiver slightly outperforms the decorrelating receiver if optimal channel estimation filters are applied. However, at high SNR's and channel loads the PIC receiver suffers from BER saturation, whereas the decorrelating receiver does not.

#### *4.3.2.3. BER in suboptimally estimated channel*

The decision-directed channel estimators with suboptimal channel estimation filters are applied. The simulations are performed for $K = 20$ active users only to simplify simulations. The BER results are shown in Figs. 4.18 and 4.19 for one and two-path channels, respectively. Both the cases of equal received energies and a near-far problem are considered.

It can be seen from Fig. 4.18 that the PIC and the decorrelating receiver have nearly the same performance in a one-path channel also with suboptimal channel estimation filters. Fig. 4.19 demonstrates that the PIC receiver outperforms the decorrelating receiver in two-path channels with suboptimal channel estimation filters at relatively low SNR's. At high SNR's the performance loss due to suboptimal channel estimation is more severe for the PIC receiver than for the decorrelating receiver, as expected. The problem is of course even more severe under a near-far problem (Figs. 4.18(b) and 4.19(b)). It can be concluded that at high SNR's the PIC receiver suffers from the BER saturation, whereas the decorrelating receiver does not. Therefore, the PIC receiver has the potential to benefit more from adaptive channel estimation filters approximating the optimal channel estimation filters than the decorrelating receiver.

## 4.4. Conclusions

Multiuser demodulation in relatively fast Rayleigh fading channels has been studied in this chapter. The optimal maximum likelihood sequence detector was derived. It estimates the received noiseless signal and correlates the received signal with the estimate. The estimation-correlation must be performed for all possible received data sequences. Due to the prohibitive complexity of the optimal receiver, suboptimal demodulators were considered. They decouple the data detection and complex channel coefficient estimation from each other, and estimate the channel coefficients and detect the data for all users separately. Both data-aided and decision-directed complex channel coefficient estimation with optimal and suboptimal channel estimation filters were considered. The performance of the decorrelating and parallel interference cancellation receivers were compared.

The mean squared error of DA linear channel estimators was analyzed. It was shown that the decoupled complex channel coefficient estimation in the decorrelating receiver can achieve performance that is very close to that of the joint LMMSE estimator. The bit error probability and the channel capacity of the DA decorrelating receiver were analyzed. It was shown that very large pilot symbol distances can be tolerated with optimal channel estimation filters, whereas suboptimal channel estimation requires a significantly denser pilot symbol insertion. Based on the results of the chapter, it can be concluded that adaptive channel estimation filters [103, 288, 57] capable to approximate the optimal channel estimation filters are crucial in data transmission, where very low BER is required. In speech transmission, fixed channel estimation filters give satisfactory performance in most cases. However, the PIC receivers are rather sensitive to channel estimation errors, and they may need adaptive channel estimation filters also with a relatively high BER requirement.

The DA complex channel coefficient estimation is more robust than DD complex channel coefficient estimation, which may suffer from BER saturation caused by hang-ups at high SNR's. The DA channel estimation causes a longer decision delay than DD channel estimation. The DA channel estimation needs different channel estimation filters for different symbols in the data frame, whereas one filter (two filters in two-stage DD channel estimation) is enough for DD channel estimation. The adaptation of several channel estimation filters is more difficult than a single filter. On the other hand, DA channel estimation is less sensitive to channel estimation filter mismatch, and fixed filters may yield satisfactory performance with DA estimation, even though that was not the case with DD channel estimation. Thus, both DA and DD complex channel coefficient estimation appear as viable methods for multiuser receivers.

The PIC receiver achieves better performance in known channels than the decorrelating receiver, but it is more sensitive to complex channel coefficient estimation errors than the decorrelating receiver, and at high channel loads it suffers from BER saturation, whereas the decorrelating receiver does not. On the other hand, the decorrelating receiver's operation relies on exact delay estimation for all users [151], and it is probably more sensitive to delay estimation errors than the PIC receiver. Furthermore, at higher channel loads the decorrelator is rather sensitive

to the delay combinations of the users, as noted in some examples in Chapter 3. Therefore, a further study considering delay estimators is required to get a more realistic comparison on the performance of the PIC and the decorrelating receivers. With the existing knowledge both the decorrelating and the PIC receivers seem to be possible alternatives for multiuser receivers from the performance point of view.

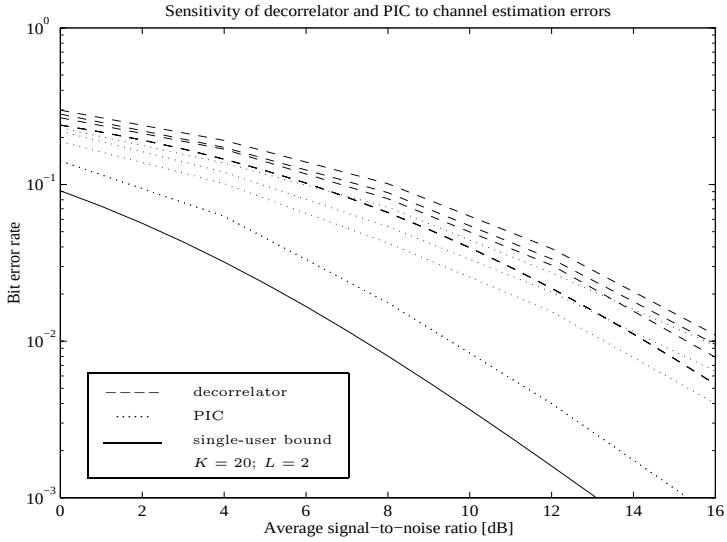


(a)

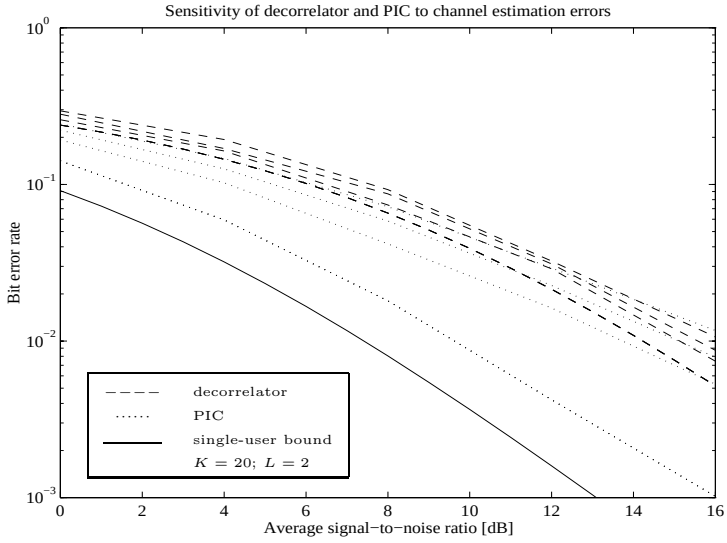


(b)

**Fig. 4.15. Sensitivity of BER to channel estimation errors in a frequency-selective fading channel ($L = 2$) for different MSE levels ($MSE = (0, 1, 1.5, 2) \times MSE_{min}$ from down to upwards); (a) equal received energies, (b) near-far problem.**

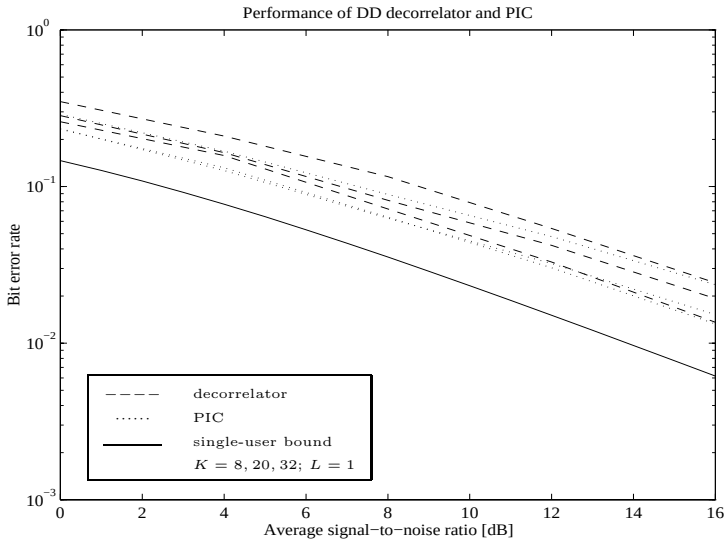


(a)

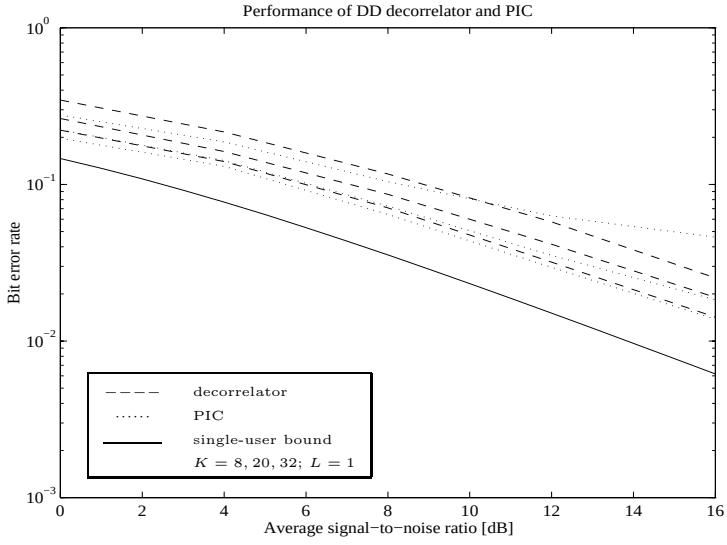


(b)

**Fig. 4.16. Bit error rates with DD channel estimation and optimal channel estimation filters in a flat fading channel ($L = 1$) for different numbers of users ($K = 8, 20, 32$ from down to upwards); (a) equal received energies, (b) near-far problem.**

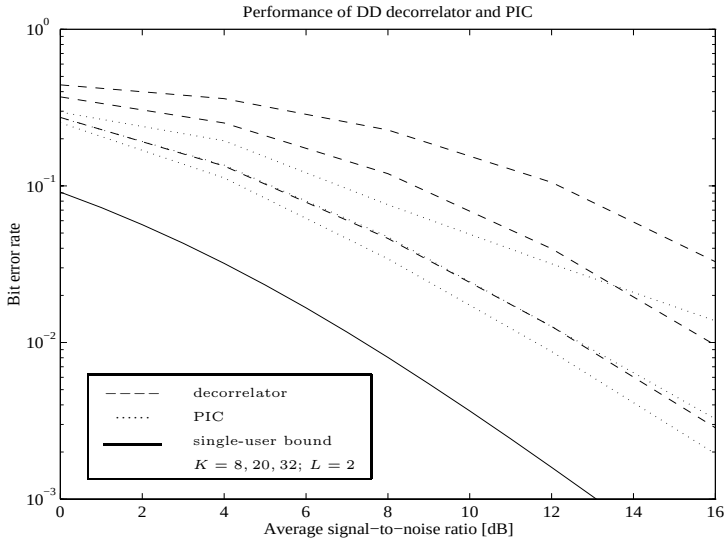


(a)

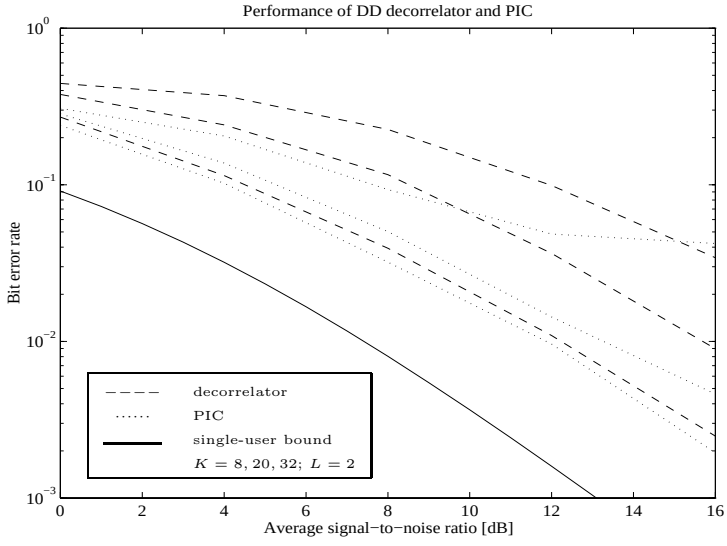


(b)

**Fig. 4.17**. **Bit error rates with DD channel estimation and optimal channel estimation filters in a frequency-selective fading channel ($L = 2$) for different numbers of users ($K = 8, 20, 32$ from down to upwards); (a) equal received energies, (b) near-far problem.**

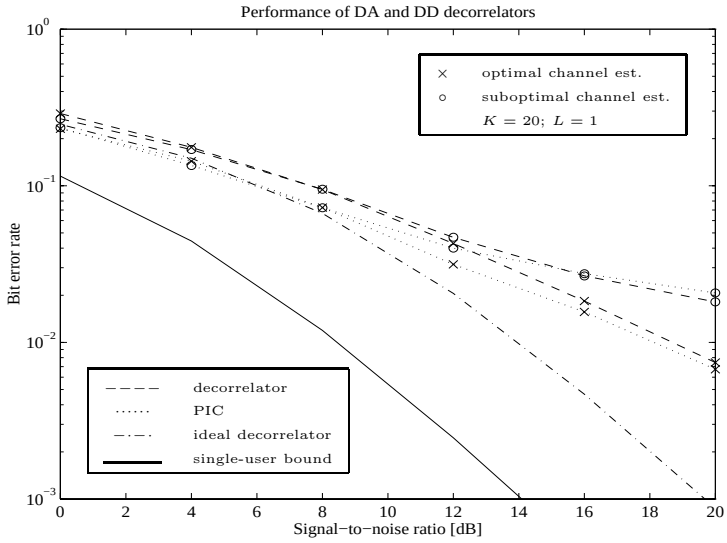


(a)

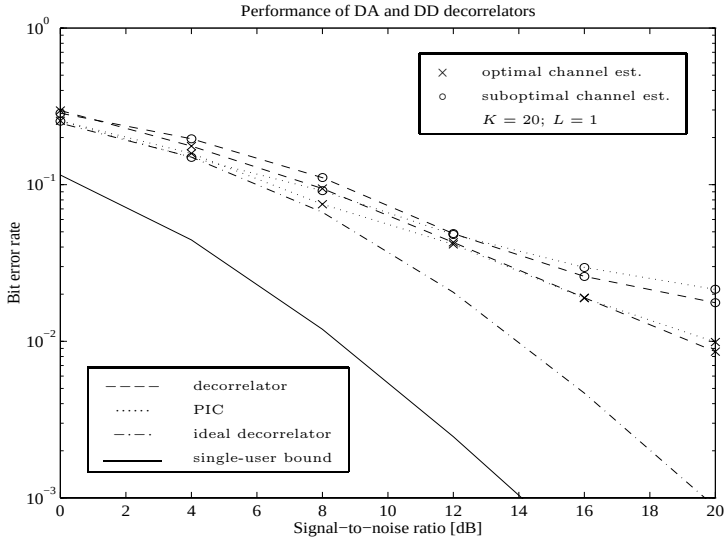


(b)

**Fig. 4.18. Bit error rates with DD channel estimation in a flat fading channel ($L = 1$) for different channel estimation filters; (a) equal received energies, (b) near-far problem. Ideal decorrelator refers to the decorrelating receiver in a known channel.**

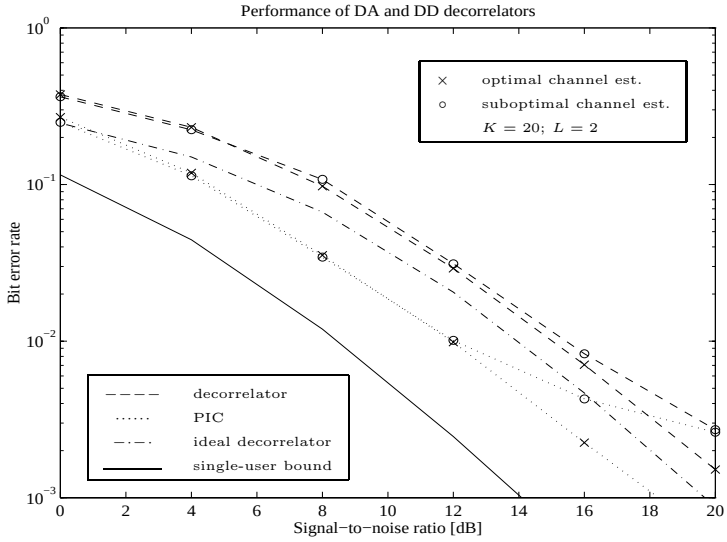


(a)

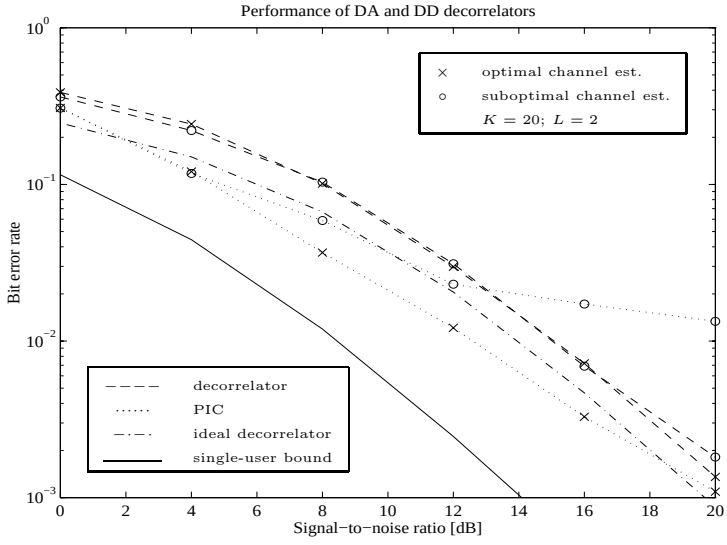


(b)

**Fig. 4.19. Bit error rates with DD channel estimation in a frequency-selective fading channel ($L = 2$) for different channel estimation filters; (a) equal received energies, (b) near-far problem. Ideal decorrelator refers to the decorrelating receiver in a known channel.**

# 5. Multiuser detection in dynamic CDMA systems

Multiuser receiver implementation algorithms are considered in this chapter. The problem is treated at the matrix algorithm level, and detailed algorithms or architectures are not considered. The objective is to find efficient detection or detector update algorithms for dynamic CDMA systems where the detectors must be updated frequently due to changes in the number of users, in the signature waveforms, in the delays, or in the received amplitudes. The goals are to find the most efficient algorithms that exist and to analyze their implementation complexity and performance. The attention is limited to two linear receivers, namely to the truncated decorrelating and LMMSE detectors, and the hard-decision parallel interference cancellation receiver. The algorithm implementation complexity is analyzed in terms of flops[1] and the number of clock cycles[2] required by synchronous DSP hardware[3]. The number of flops describes the computational burden of the algorithms and the number of clock cycles illustrates to what extent the operations can be performed in parallel.

Fixed single-path channels ($L = 1$) are assumed in the algorithm derivations and numerical examples in this chapter. The choice is due to notational convenience and to make the computer simulations feasible. The generalization of the algorithms to the multipath case is straightforward. The implementation complexity expression for the multipath case will then be obtained by substituting $KL$ for $K$ in the expressions in Sections 5.1–5.2. The complexity expressions are summarized with $K$ replaced by $KL$ in Section 5.3. The linear detection algorithms are presented for the truncated decorrelating detector. Due to the similarity of decorrelating and LMMSE detection, the generalization of the algorithms to the LMMSE detection is obvious. Both time-invariant and time-varying signature waveforms are considered

[1] A floating point operation (flop) is defined to be a multiplication or an addition [156, p. 19].

[2] Required clock cycles are defined to be the minimum number of computation steps that are required in the sense that the results of the previous computation step are needed in the following step. A computation step is assumed to include all operations that can be performed independent of each other. A multiplication followed by an addition are assumed to require two clock cycles in total. The actual number of required clock cycles depends on implementation details and the estimates given in this thesis are a lower bound to that.

[3] Synchronous DSP refers to the existence of a global clock which paces the computation flow in the signal processing system.

in this chapter. However, the superscript $n$ describing the symbol interval is left out from the correlation matrices $\mathbf{R}^{(n)}(i)$ due to notational convenience throughout the chapter.

The major problem is to find practical algorithms for linear multiuser detection. The obvious reason for this is the fact that linear detectors are characterized as inverses of some form of correlation matrices, and matrix inversion is a computationally intensive operation. Implementation of linear detection is considered in the first two sections. Ideal linear detection and detector update algorithms, which implement the multiuser detectors exactly (the effect of rounding errors is neglected throughout the chapter), are studied in Section 5.1. Iterative algorithms, which approximate the ideal linear detectors, are proposed in Section 5.2. In Section 5.3, the implementation complexity of the decorrelating and PIC receivers is compared. The results are summarized and discussed in Section 5.4.

## 5.1. Ideal linear detection

Ideal truncated linear detection is considered in this section. Detection algorithms and their complexity are analyzed in Section 5.1.1. Detector computation algorithms for synchronous and asynchronous CDMA systems are considered in Sections 5.1.2 and 5.1.3, respectively. The synchronous case is studied, since the update algorithms can be later utilized in conjunction with iterative detection as described in Section 5.2.

### *5.1.1. Detection algorithms*

If the truncated linear detector $\mathcal{D}_N$ is known, the detection can be performed as expressed in (3.3). The detector $\mathcal{D}_N$ is a $NK \times K$ matrix, i.e., it has $NK^2$ elements. Vector $\boldsymbol{y}^{(n)}$ has $NK$ elements. The product $\mathcal{D}_N^\top \boldsymbol{y}^{(n)}$ in (3.3) is equivalent to the inner products of $K$ vectors with $NK$ elements each. One inner product requires $NK$ multiplications of a complex number by a real number (i.e., $2NK$ real multiplications) and $NK-1$ complex (i.e., $2(NK-1)$ real) additions. Thus, one inner product requires $O[4NK]$ flops, where $O[cx^n]$ denotes a polynomial function of $x$ with order $n$ and coefficient $c$ for the highest order term[4]. The overall computational load is $O[4NK^2]$ flops. One inner product consists of $NK$ inner products, which can be computed in parallel, if sufficient hardware is available. Thus, the multiplications need one clock cycle. If a $NK$ input summing device is available, another clock cycle is needed for additions. The $K$ inner products are independent of each other allowing parallel implementation. Thus, 2 clock cycles are needed in

[4]In addition to the dominant term $x^n$ the coefficients $c$ in front of it need to be taken into consideration in the computational complexity expressions. The constants are needed to make distinctions to the complexities of some algorithms.

total. As mentioned above, the clock cycle estimates are definitely optimistic, but they yield lower bounds assuming that a multiplication and an addition take one clock cycle each. The following implementation complexity calculations follow the same principles as above and will not be presented.

The detector can be computed by solving the defining matrix equation. For the truncated decorrelating detector (3.6) needs to be solved. The detector can be solved by Cholesky factoring the correlation matrix $\mathcal{R}^{(n)}$. Then (3.6) becomes

$$\mathcal{L}^{\top(n)}\mathcal{L}^{(n)}\mathcal{D}_{[d]N} = \mathcal{U}_N. \tag{5.1}$$

The solution of (5.1) by backward and forward substitutions [156] requires $O[6NK^3]$ flops, $O[\frac{3}{2}NK^2]$ divisions, and $5NK$ clock cycles.

The detection can also be performed without directly computing the detector $\mathcal{D}_N$ itself, but by solving a linear matrix equation instead. For the truncated decorrelating detector the equation

$$\mathcal{R}^{(n)}\boldsymbol{y}_{[d]}^{(n)} = \boldsymbol{y}^{(n)} \Leftrightarrow \mathcal{L}^{\top(n)}\mathcal{L}^{(n)}\boldsymbol{y}_{[d]}^{(n)} = \boldsymbol{y}^{(n)} \tag{5.2}$$

must be solved, and after that $KL$ elements in the middle of the vector $\boldsymbol{y}_{[d]}^{(n)}$ are extracted to obtain $\mathbf{y}_{[d]}^{(n)}$. The solution of (5.2) by backward and forward substitutions [156] requires $O[16NK^2]$ flops $O[NK]$ divisions and $5NK$ clock cycles.

The computation of the linear detector $\mathcal{D}_{[d]N}$, as well as the solution of the detector output vector $\boldsymbol{y}_{[d]}^{(n)}$ without explicit detector computation, requires the knowledge of the Cholesky factor $\mathcal{L}^{(n)}$ of the correlation matrix $\mathcal{R}^{(n)}$. Thus, the algorithms for the Cholesky factor computation will be the core of the ideal linear multiuser detection in dynamic CDMA systems. Cholesky factor computation will be analyzed in Section 5.1.3 after considering the equivalent problem for the easier synchronous CDMA systems in Section 5.1.2.

### *5.1.2. Detector update in synchronous systems*

The detection in synchronous CDMA systems is significantly simpler than that in asynchronous systems, since a one-shot detector is optimal. Because $\mathbf{R}(i) = \mathbf{0}, \forall i > 1$, it is sufficient to update the Cholesky factor $\tilde{\mathbf{L}} \in \mathbb{R}^{K\times K}$ of $\mathbf{R}(0) \in (-1,1]^{K\times K}$ instead of the Cholesky factor of $\mathcal{R}^{(n)}$. It is also possible to update the inverse $\mathbf{T} = \mathbf{R}^{-1}(0) \in \mathbb{R}^{K\times K}$ of $\mathbf{R}(0)$. The algorithms can also be applied straightforwardly to update the inverse or the Cholesky factor of $\mathbf{R}(0)$ to correlation changes of one path of one user in asynchronous systems in multipath channels.

It is assumed that the correlations of one user change, while the other correlations remain constant[5]. In other words, if the correlations of user $k$ change, the elements of the $k$th row and the $k$th column of the matrix $\mathbf{R}(0)$ are altered. The

[5]The algorithms in this Section 5.1.2 are designed for systems with time-invariant signature waveforms only.

inverse or the Cholesky factor of $\mathbf{R}(0)$ are updated by computing the inverse or the Cholesky factor of the reduced $\mathbf{R}(0)$ ($(K-1)\times(K-1)$ matrix) which is obtained by removing the $k$th row and column from the old $\mathbf{R}(0)$. Based on that tentative result, the new inverse or Cholesky factor of the true new $\mathbf{R}(0)$ is computed by "adding" the $k$th row and column of the new $\mathbf{R}(0)$ to the reduced $\mathbf{R}(0)$. Therefore, update algorithms are described below for the case of a new user entering the system (the number of active users is incremented by one from $K$ to $K+1$), and for the case of an old user leaving the system (the number of active users is decremented by one from $K+1$ to $K$). To make the expressions describing the changing number of users precise, a super-index of the form $\mathbf{R}^{(K)}(0)$ and $\mathbf{T}^{(K)} = (\mathbf{R}^{(K)}(0))^{-1}$ indicating the number of users $K$ is included in subsequent matrix symbols in this Section 5.1.2.

### *5.1.2.1. Inverse update*

The key tools used in recursive inverse computations are the following two matrix inversion formulae, which are special cases of (A1.4) and (A1.5), [88, pp. 571-572]. Woodbury's identity is the rank one update

$$(\mathbf{A}+\mathbf{v}\mathbf{v}^\top)^{-1} = \mathbf{A}^{-1} - \frac{\mathbf{A}^{-1}\mathbf{v}\mathbf{v}^\top\mathbf{A}^{-1}}{1+\mathbf{v}^\top\mathbf{A}^{-1}\mathbf{v}}, \tag{5.3}$$

where $\mathbf{A}$ is a nonsingular square matrix and $\mathbf{v}\neq\mathbf{0}$ is a column vector with the same dimension. Under the same conditions as above, we also have the order update formula

$$\begin{pmatrix} 1 & \mathbf{v}^\top \\ \mathbf{v} & \mathbf{A} \end{pmatrix}^{-1} = \begin{pmatrix} (1-\mathbf{v}^\top\mathbf{A}^{-1}\mathbf{v})^{-1} & -(1-\mathbf{v}^\top\mathbf{A}^{-1}\mathbf{v})^{-1}\mathbf{v}^\top\mathbf{A}^{-1} \\ -(\mathbf{A}-\mathbf{v}\mathbf{v}^\top)^{-1}\mathbf{v} & (\mathbf{A}-\mathbf{v}\mathbf{v}^\top)^{-1} \end{pmatrix}. \tag{5.4}$$

**As a new user enters the CDMA network**, a row and a column must be added to the correlation matrix. The new user will be indexed to be user 1 and the indices of old users remaining in the network will be incremented by one. Let the new user's correlation vector $\boldsymbol{\rho}$ be

$$\boldsymbol{\rho} = (R_{12}(0), R_{13}(0), \ldots, R_{1,K+1}(0))^\top \in (-1,1)^K. \tag{5.5}$$

Now $\mathbf{R}^{(K+1)}(0)$ can be partitioned as

$$\mathbf{R}^{(K+1)}(0) = \begin{pmatrix} 1 & \boldsymbol{\rho}^\top \\ \boldsymbol{\rho} & \mathbf{R}^{(K)}(0) \end{pmatrix} \in (-1,1]^{(K+1)\times(K+1)}. \tag{5.6}$$

The new inverse matrix $\mathbf{T}^{(K+1)} = (\mathbf{R}^{(K+1)}(0))^{-1}$ can be found by Gaussian elimination, but an order-recursive algorithm is more efficient. The inverse of $\mathbf{R}^{(K+1)}(0)$ is partitioned as

$$\mathbf{T}^{(K+1)} = \begin{pmatrix} t & \mathbf{t}^\top \\ \mathbf{t} & \mathbf{T} \end{pmatrix}, \tag{5.7}$$

where $\mathbf{T} \in \mathbb{R}^{K\times K}$, $\mathbf{t} \in (0,\infty)^K$, and $t \in \mathbb{R}$. By using (5.3) and (5.4) the following algorithm is obtained

$$t = \frac{1}{1-\boldsymbol{\rho}^\top \mathbf{T}^{(K)}\boldsymbol{\rho}}, \tag{5.8}$$

$$\mathbf{T} = \mathbf{T}^{(K)} + t\mathbf{T}^{(K)}\boldsymbol{\rho}\boldsymbol{\rho}^\top\mathbf{T}^{(K)} = \mathbf{T}^{(K)} + \frac{1}{t}\mathbf{t}\mathbf{t}^\top, \tag{5.9}$$

$$\mathbf{t} = -\mathbf{T}\boldsymbol{\rho} = -t\mathbf{T}^{(K)}\boldsymbol{\rho}. \tag{5.10}$$

(5.8) follows directly from (5.4). From (5.4) it follows that

$$\begin{aligned}\mathbf{T} &= (\mathbf{R}^{(K)}(0) - \boldsymbol{\rho}\boldsymbol{\rho}^\top)^{-1} \\ &= \mathbf{T}^{(K)} + \frac{\mathbf{T}^{(K)}\boldsymbol{\rho}\boldsymbol{\rho}^\top\mathbf{T}^{(K)}}{1-\boldsymbol{\rho}^\top\mathbf{T}^{(K)}\boldsymbol{\rho}} \\ &= \mathbf{T}^{(K)} + t\mathbf{T}^{(K)}\boldsymbol{\rho}\boldsymbol{\rho}^\top\mathbf{T}^{(K)},\end{aligned} \tag{5.11}$$

where the second equation follows by applying (5.3) to the first one. The third equation follows by substituting (5.8) to the second. Both forms of (5.10) follow directly from (5.4) and the fact that $\mathbf{R}^{(K)}(0)$ and $\mathbf{T}^{(K)}$ are symmetric. By substituting $\mathbf{T}^{(K)}\boldsymbol{\rho} = -\frac{1}{t}\mathbf{t}$ from (5.10) back to (5.11) the last form of (5.9) follows.

As a new user enters the system, the operations in (5.8) require $O[2K^2]$ flops, and one division. Solution of (5.9) demands $O[K^2]$ flops; (5.10) does not require extra computations after (5.9) has been calculated. In total $O[3K^2]$ flops, and one division are required. The minimum number of clock cycles to compute (5.8)–(5.10) is 9.

**As a user is leaving the CDMA network**, the problem is opposite to the one discussed above. Now the detector matrix $\mathbf{T}^{(K+1)}$ is known and it has a partition as in (5.7). The detector matrix $\mathbf{T}^{(K)}$ must be computed. Assume that user 1 leaves the system. From (5.9) it follows that

$$\mathbf{T}^{(K)} = \mathbf{T} - \frac{1}{t}\mathbf{t}\mathbf{t}^\top. \tag{5.12}$$

The updating algorithm in the case the user indexed 1 leaves the system is described in (5.12). On the other hand, if user $k \in \{2,3,\ldots,K+1\}$ leaves the system, the updating problem is a bit more complicated. The original correlation matrix has the following partition

$$\mathbf{R}^{(K+1)}(0) = \begin{pmatrix} \mathbf{R}_{11} & \boldsymbol{\rho}_1 & \mathbf{R}_{12} \\ \boldsymbol{\rho}_1^\top & 1 & \boldsymbol{\rho}_2^\top \\ \mathbf{R}_{12}^\top & \boldsymbol{\rho}_2 & \mathbf{R}_{22} \end{pmatrix}, \tag{5.13}$$

where $\mathbf{R}_{11} \in \mathbb{R}^{k-1\times k-1}$, $\mathbf{R}_{12} \in \mathbb{R}^{k-1\times K-k+1}$ and $\mathbf{R}_{22} \in \mathbb{R}^{K-k+1\times K-k+1}$, $\boldsymbol{\rho}_1 \in \mathbb{R}^{k-1}$, and $\boldsymbol{\rho}_2 \in \mathbb{R}^{K-k+1}$. The new detector matrix can be found by virtually changing the indexing of users so that the leaving user is indexed to be 1. The equivalent correlation matrix is then

$$\tilde{\mathbf{R}}^{(K+1)} = \mathbf{U}_k^\top \mathbf{R}^{(K+1)}(0)\mathbf{U}_k, \tag{5.14}$$

where $\mathbf{U}_k$ is a unitary permutation matrix of the form

$$\mathbf{U}_k = \begin{pmatrix} \mathbf{u}_k & \mathbf{u}_1 & \cdots & \mathbf{u}_{k-1} & \mathbf{u}_{k+1} & \cdots & \mathbf{u}_{K+1} \end{pmatrix} \tag{5.15}$$

where the elements of the column vector $\mathbf{u}_k \in \{0,1\}^{K+1}$ are $(\mathbf{u}_k)_i = \delta_{k,i}$, $\forall\, i \in \{1,2,\ldots,K\}$ and $\delta_{k,i}$ is the discrete Kronecker delta function. Thus, the equivalent inverse becomes

$$\tilde{\mathbf{T}}^{(K+1)} = \mathbf{U}_k^{\top} \mathbf{T}^{(K+1)} \mathbf{U}_k. \tag{5.16}$$

The detector matrix $\mathbf{T}^{(K)}$ can be computed by using matrix $\tilde{\mathbf{T}}^{(K+1)}$ in (5.12).

As an old user leaves the system, $O[K^2]$ flops, and $K$ divisions are needed in (5.12). At least 3 clock cycles are needed.

### *5.1.2.2. Cholesky factor update*

**As a new user enters the CDMA network**, the Cholesky factorization

$$\mathbf{R}^{(K)}(0) = (\tilde{\mathbf{L}}^{(K)})^{\top} \tilde{\mathbf{L}}^{(K)} \tag{5.17}$$

is assumed to be known and the new factorization

$$\mathbf{R}^{(K+1)}(0) = (\tilde{\mathbf{L}}^{(K+1)})^{\top} \tilde{\mathbf{L}}^{(K+1)} \tag{5.18}$$

should be found in a recursive form. Let

$$\tilde{\mathbf{L}}^{(K+1)} = \begin{pmatrix} l & \mathbf{0}_{1\times K} \\ \mathbf{l} & \mathbf{L} \end{pmatrix}, \tag{5.19}$$

where $\mathbf{L} \in \mathbb{R}^{K\times K}$ is a lower triangular matrix, $\mathbf{l} \in \mathbb{R}^K$, and $l \in \mathbb{R}$.

By substituting (5.19) into (5.18) we get

$$(\tilde{\mathbf{L}}^{(K+1)})^{\top} \tilde{\mathbf{L}}^{(K+1)} = \begin{pmatrix} l^2 + \mathbf{l}^{\top}\mathbf{l} & \mathbf{l}^{\top}\mathbf{L} \\ \mathbf{L}^{\top}\mathbf{l} & \mathbf{L}^{\top}\mathbf{L} \end{pmatrix}. \tag{5.20}$$

By equating the corresponding parts in the above equation and in (5.6) the following algorithm is obtained

$$\mathbf{L} = \tilde{\mathbf{L}}^{(K)}, \tag{5.21}$$

$$\text{solve } \mathbf{L}^{\top}\mathbf{l} = \boldsymbol{\rho} \text{ for } \mathbf{l}, \tag{5.22}$$

$$l = \sqrt{1 - \mathbf{l}^{\top}\mathbf{l}}. \tag{5.23}$$

The operation in (5.22) is a linear matrix equation with an upper triangular coefficient matrix. Its solution demands $O[K^2]$ flops, and $K$ divisions. The computation in (5.23) requires $K$ multiplications and additions, and one square root. In total $O[K^2]$ flops, $K$ divisions, and one square root are required. The number of required clock cycles is $3K$.

As an alternative to the above algorithm we will also consider the Cholesky factorization update based on QR factorization of the code matrix $\mathbf{S}(0)$ [156]. It is assumed that the QR factorization

$$\mathbf{S}^{(K)}(0) = \mathbf{Q}^{(K)}\tilde{\mathbf{L}}^{(K)} \tag{5.24}$$

is known. Now we are interested in computing the new $\tilde{\mathbf{L}}^{(K+1)}$ for

$$\mathbf{S}^{(K+1)}(0) = \begin{pmatrix} \mathbf{s} & \mathbf{S}^{(K)}(0) \end{pmatrix}, \tag{5.25}$$

where $\mathbf{s}$ is the new spreading sequence. By (5.21)–(5.23) it is seen that only the first column of $\tilde{\mathbf{L}}^{(K+1)}$ needs to be computed[6]. In other words, the QR factorization of the $N_s \times K$ matrix

$$\begin{pmatrix} \mathbf{s} & \mathbf{0}_{(N_s-K)\times K} \\ & \tilde{\mathbf{L}}^{(K)} \end{pmatrix}$$

must be computed. The result is

$$\tilde{\mathbf{Q}} \begin{pmatrix} \mathbf{s} & \mathbf{0}_{(N_s-K)\times K} \\ & \tilde{\mathbf{L}}^{(K)} \end{pmatrix} = \begin{pmatrix} \mathbf{0}_{(N_s-K-1)\times 1} & \mathbf{0}_{(N_s-K-1)\times K} \\ l & \mathbf{0}_{1\times K} \\ \mathbf{l} & \tilde{\mathbf{L}}^{(K)} \end{pmatrix}, \tag{5.26}$$

where $\tilde{\mathbf{Q}}$ is unitary. The computation can be performed efficiently by applying $(N_s-K-1)$ Givens rotations [156], which requires $9(N_s-K-1)$ flops, $2(N_s-K-1)$ divisions, and $(N_s-K-1)$ square roots. The computational complexity of the QR factorization based Cholesky update is in general significantly lower than that of the update based on correlation matrix. This is not true, however, if the number of users is much smaller than the number of samples per symbol interval $N_s$. The QR factorization based computation does not require the correlation computation. That gives a further advantage in terms of computational complexity. It also reduces the effect of rounding errors, which are otherwise introduced while rounding the correlation coefficients after their computation.

**As a user is leaving the CDMA network**, the factorization

$$\mathbf{R}^{(K+1)}(0) = (\tilde{\mathbf{L}}^{(K+1)})^{\top}\tilde{\mathbf{L}}^{(K+1)} \tag{5.27}$$

is assumed to be known and the factorization

$$\mathbf{R}^{(K)}(0) = (\tilde{\mathbf{L}}^{(K)})^{\top}\tilde{\mathbf{L}}^{(K)} \tag{5.28}$$

needs to be computed. Let

$$\tilde{\mathbf{L}}^{(K+1)} = \begin{pmatrix} \mathbf{L}_{11} & \mathbf{0} & \mathbf{0} \\ \mathbf{l}_1^{\top} & l_3 & \mathbf{0} \\ \mathbf{L}_{21} & \mathbf{l}_2 & \mathbf{L}_{22} \end{pmatrix}, \tag{5.29}$$

[6]The fact that only the first column changes can also be easily seen by properties of QR factorizations [156]. This actually provides another proof for (5.21).

where $\mathbf{L}_{11} \in \mathbb{R}^{k-1\times k-1}$ and $\mathbf{L}_{22} \in \mathbb{R}^{K-k+1\times K-k+1}$ are lower triangular matrices, $\mathbf{L}_{21} \in \mathbb{R}^{K-k+1\times k-1}$, $\mathbf{l}_1 \in \mathbb{R}^{k-1}$, $\mathbf{l}_2 \in \mathbb{R}^{K-k+1}$ are column vectors, and $l_3 \in \mathbb{R}$ is a scalar. By (5.29) and definition of $\mathbf{R}^{(K)}(0) = (\tilde{\mathbf{L}}^{(K)})^\top \tilde{\mathbf{L}}^{(K)}$ it follows that

$$\begin{aligned}\mathbf{R}^{(K)}(0) &= \begin{pmatrix} \mathbf{L}_{11}^\top \mathbf{L}_{11} + \mathbf{l}_1\mathbf{l}_1^\top + \mathbf{L}_{21}^\top \mathbf{L}_{21} & \mathbf{L}_{21}^\top \mathbf{L}_{22} \\ \mathbf{L}_{22}^\top \mathbf{L}_{21} & \mathbf{L}_{22}^\top \mathbf{L}_{22} \end{pmatrix} \\ &= \begin{pmatrix} \mathbf{L}_0^\top & \mathbf{L}_{21}^\top \\ \mathbf{0} & \mathbf{L}_{22}^\top \end{pmatrix} \begin{pmatrix} \mathbf{L}_0 & \mathbf{0} \\ \mathbf{L}_{21} & \mathbf{L}_{22} \end{pmatrix},\end{aligned}$$

where $\mathbf{L}_0 \in \mathbb{R}^{k-1\times k-1}$ is a lower triangular matrix such that $\mathbf{L}_0^\top \mathbf{L}_0 = \mathbf{L}_{11}^\top \mathbf{L}_{11} + \mathbf{l}_1\mathbf{l}_1^\top$. Thus, the matrix $\tilde{\mathbf{L}}^{(K)}$ is

$$\tilde{\mathbf{L}}^{(K)} = \begin{pmatrix} \mathbf{L}_0 & \mathbf{0} \\ \mathbf{L}_{21} & \mathbf{L}_{22} \end{pmatrix}. \tag{5.30}$$

The result states that the Cholesky factorization cannot be updated totally recursively, but the computation of a new factor of a $(k-1)\times(k-1)$ positive definite matrix is necessary. Because the matrix to be Cholesky factored has the special structure of the form $\mathbf{L}_{11}^\top \mathbf{L}_{11} + \mathbf{l}_1\mathbf{l}_1^\top$, the computation can be performed effectively by QR factorization [290]. Let

$$\mathbf{A} = \mathbf{L}_{11}^\top \mathbf{L}_{11} + \mathbf{l}_1\mathbf{l}_1^\top = \begin{pmatrix} \mathbf{l}_1 & \mathbf{L}_{11}^\top \end{pmatrix} \begin{pmatrix} \mathbf{l}_1^\top \\ \mathbf{L}_{11} \end{pmatrix}. \tag{5.31}$$

Let the QR factorization of $\left(\mathbf{l}_1, \mathbf{L}_{11}^\top\right)^\top$ be

$$\begin{pmatrix} \mathbf{l}_1^\top \\ \mathbf{L}_{11} \end{pmatrix} = \mathbf{Q}' \begin{pmatrix} \mathbf{0}^\top \\ \mathbf{L}_0 \end{pmatrix}, \tag{5.32}$$

where $\mathbf{Q}' \in \mathbb{R}^{k\times k}$ is unitary. By substituting (5.32) into (5.31) it is seen that

$$\mathbf{A} = \begin{pmatrix} \mathbf{l}_1 & \mathbf{L}_{11}^\top \end{pmatrix} \begin{pmatrix} \mathbf{l}_1^\top \\ \mathbf{L}_{11} \end{pmatrix} = \mathbf{L}_0^\top \mathbf{L}_0. \tag{5.33}$$

Thus, $\mathbf{L}_0$ may be computed by QR factorizing the matrix $\left(\mathbf{l}_1, \mathbf{L}_{11}^\top\right)^\top$, which can be accomplished by applying $K$ Givens rotations. Because $\mathbf{L}_{11}$ is already lower triangular, this requires in total $6(k-1)^2 + 2(k-1)$ flops, $2(k-1)$ divisions, and $(k-1)$ square roots [156].

The Cholesky factorization could again be computed by QR factoring the code matrix $\mathbf{S}^{(K)}(0)$. This does not, however, offer any simplification to the computations. (It would stop the accumulation of rounding errors.)

The drawback of the Cholesky factorization is that computing it requires square roots, which may be a problem in some applications. The square roots can be partly avoided by using a $\mathrm{L}^\top\mathrm{DL}$ factorization instead of Cholesky factorization [156].

### *5.1.3. Detector computation in asynchronous systems*

As in Section 3.2, a subindex is added to $\mathcal{R}^{(n)}$ to denote its dimension yielding $\mathcal{R}_N \in (-1,1]^{NK\times NK}$. In the upcoming *order-recursive* derivations we will let the dimension take the values $m = 1, 2, \ldots, N$. In other words, $\mathcal{R}_m$ is $\mathcal{R}^{(n)}$ with dimension $mK \times mK$. Note that $\mathcal{R}_m$ can be partitioned as (compare to A1.1)

$$\mathcal{R}_m = \begin{pmatrix} \mathbf{R}(0) & \boldsymbol{\gamma}_{m-1}^\top \\ \boldsymbol{\gamma}_{m-1} & \mathcal{R}_{m-1} \end{pmatrix} \in \mathbb{R}^{mK\times mK}, \tag{5.34}$$

where

$$\boldsymbol{\gamma}_{m-1} = \begin{pmatrix} \mathbf{R}^\top(1) & \mathbf{0}_K & \cdots & \mathbf{0}_K \end{pmatrix}^\top \in \mathbb{R}^{(m-1)K\times K}. \tag{5.35}$$

The Cholesky factor $\mathcal{L}_m$ of $\mathcal{R}_m$ can be partitioned as [156]

$$\mathcal{L}_m = \begin{pmatrix} \mathbf{L}_{11}(m) & \mathbf{0}^\top \\ \boldsymbol{\zeta}_{m-1} & \mathcal{L}_{m-1} \end{pmatrix} \in \mathbb{R}^{mK\times mK}, \tag{5.36}$$

where $\mathcal{L}_{m-1} \in \mathbb{R}^{(m-1)K\times(m-1)K}$ is the Cholesky factor of $\mathcal{R}_{m-1}$,

$$\boldsymbol{\zeta}_{m-1} = \begin{pmatrix} \mathbf{L}_{21}^\top(m) & \mathbf{0}_K & \cdots & \mathbf{0}_K \end{pmatrix}^\top \in \mathbb{R}^{(m-1)K\times K}, \tag{5.37}$$

$\mathbf{L}_{ij}(m) \in \mathbb{R}^{K\times K}$ is the $ij$th block of $\mathcal{L}_m$, and $\mathbf{0}$ denotes a $mK \times K$ matrix with zero elements. In other words, the blocks that must be computed at the $m$th step are $\mathbf{L}_{11}(m)$ and $\mathbf{L}_{21}(m)$. Note that

$$\mathcal{L}_m^\top\mathcal{L}_m = \begin{pmatrix} \mathbf{L}_{11}^\top(m)\mathbf{L}_{11}(m) + \boldsymbol{\zeta}_{m-1}^\top\boldsymbol{\zeta}_{m-1} & \boldsymbol{\zeta}_{m-1}^\top\mathcal{L}_{m-1} \\ \mathcal{L}_{m-1}^\top\boldsymbol{\zeta}_{m-1} & \mathcal{L}_{m-1}^\top\mathcal{L}_{m-1} \end{pmatrix}. \tag{5.38}$$

By equating the corresponding parts in (5.38) and in (5.34) and using the definitions of $\boldsymbol{\gamma}_{m-1}$ and $\boldsymbol{\zeta}_{m-1}$ it is found that we must solve

$$\mathbf{L}_{11}^\top(m-1)\mathbf{L}_{21}(m) = \mathbf{R}(1) \quad \text{for} \quad \mathbf{L}_{21}(m) \tag{5.39}$$

$$\mathbf{L}_{11}^\top(m)\mathbf{L}_{11}(m) = \mathbf{R}(0) - \mathbf{L}_{21}^\top(m)\mathbf{L}_{21}(m) \quad \text{for} \quad \mathbf{L}_{11}(m), \tag{5.40}$$

for all $m \in \{2, 3, \ldots, N\}$.

Solving $\mathbf{L}_{21}(m)$ in (5.39) corresponds to solving $(K-1)$ matrix equations each giving one column of $\mathbf{L}_{21}(m)$. The solution of $\mathbf{L}_{21}(m)$ can be parallelized to $(K-1)$ separate linear equations. Each of the solutions requires $O[K^2]$ flops, $K$ divisions and at least $3K$ clock cycles due to backward substitutions. Thus, in total $O[NK^3]$ flops, $NK$ divisions, and $3NK$ clock cycles are required to compute all blocks $\mathbf{L}_{21}(m)$.

Solving $\mathbf{L}_{11}(m)$ in (5.40) requires Cholesky factorization of the $K \times K$ matrix $\mathbf{R}(0) - \mathbf{L}_{21}^\top(m)\mathbf{L}_{21}(m)$. A QR factorization based approach to solve $\mathbf{L}_{11}(m)$ is derived below. Let $\tilde{\mathbf{L}}$ be the Cholesky factor of $\mathbf{R}(0)$. Thus,

$$\mathbf{R}(0) - \mathbf{L}_{21}^\top(m)\mathbf{L}_{21}(m) = \tilde{\mathbf{L}}^\top\tilde{\mathbf{L}} - \mathbf{L}_{21}^\top(m)\mathbf{L}_{21}(m) =$$

$$\begin{pmatrix} j\mathbf{L}_{21}^\top(m) & \tilde{\mathbf{L}}^\top \end{pmatrix} \begin{pmatrix} j\mathbf{L}_{21}^\top(m) & \tilde{\mathbf{L}}^\top \end{pmatrix}^\top, \tag{5.41}$$

where $j^2 = -1$. Let the QR factorization of $\begin{pmatrix} j\mathbf{L}_{21}^\top(m) & \tilde{\mathbf{L}}^\top \end{pmatrix}^\top$ be

$$\begin{pmatrix} j\mathbf{L}_{21}(m) \\ \tilde{\mathbf{L}} \end{pmatrix} = \mathbf{Q} \begin{pmatrix} \mathbf{0}_K \\ \mathbf{L} \end{pmatrix}, \tag{5.42}$$

where $\mathbf{Q}$ is unitary, and $\mathbf{L}$ is lower-triangular. Substituting (5.42) into (5.41) yields

$$\mathbf{R}(0) - \mathbf{L}_{21}^\top(m)\mathbf{L}_{21}(m) = \mathbf{L}^\top\mathbf{L}, \tag{5.43}$$

or $\mathbf{L}_{11}(m) = \mathbf{L}$. In other words, $\mathbf{L}_{11}(m)$ can be computed by QR factoring $\begin{pmatrix} j\mathbf{L}_{21}^\top(m) & \tilde{\mathbf{L}}^\top \end{pmatrix}^\top$. The QR factorization can be computed by Householder reflections or Givens rotations [156], for example. The Householder reflections require in total $4K$ clock cycles, and $O[4K^3]$ flops and $K$ square roots [156, 41]. In total, the computation of all blocks $\mathbf{L}_{11}(m)$ requires $O[4NK^3]$ flops, $NK$ square roots, and at least $4NK$ clock cycles.

The computational requirements to complete the Cholesky factorization of $\mathcal{R}^{(n)}$ are found by summing the requirements to solve (5.39) and (5.40) for all values of $m$. Thus, the computation of $\mathcal{L}^{(n)}$ requires $O[5NK^3]$ flops, $NK$ square roots, $NK$ divisions, and at least $7NK$ clock cycles.

The "skinny" QR factorization of the sample matrix $\mathcal{S}$ can be represented in the form $\mathcal{S} = \mathcal{Q}\mathcal{L}^{(n)}$, where $\mathcal{Q} \in \mathbb{R}^{(N+1)N_s \times NK}$ is an orthogonal matrix [156, p. 217]. In other words, the Cholesky factor $\mathcal{L}^{(n)}$ can be computed by QR factoring $\mathcal{S}$. The resulting computational requirements are difficult to analyze exactly. However, they are lower bounded by $O[NN_sK^2]$ flops. Since $N_s$ is assumed to be greater than the number of users $K$ to guarantee the positive-definiteness of $\mathcal{R}^{(n)}$, the QR factorization of the sample matrix $\mathcal{S}$ is usually computationally more intensive than correlation matrix based approach. The QR factorization is numerically superior, since the rounding errors introduced in the correlation computation are avoided. The number of clock cycles is at least $4NK$.

The computational requirements of solving the decorrelating detector are the sum of the requirements to compute the Cholesky factor $\mathcal{L}^{(n)}$ and to solve the detector $\mathcal{D}_{[d]}$ in (5.1). Thus, $O[11NK^3]$ flops, $NK$ square roots, and $O[\frac{3}{2}NK^2]$ divisions are required to solve the decorrelating detector. Implementation by synchronous digital signal processing requires at least $12NK$ clock cycles. The computational requirements are linearly related to $N$, which was obtained by the use of the sparsity of the matrices. The computational requirements are still large having a cubic dependence on the number of users. If the number of users is large, the computational burden of the detector update is substantial, and the operations cannot be parallelized very effectively. At least in systems with time-varying signature waveforms, the proposed order-recursive algorithm may still be impractical for the current DSP hardware in many applications.

## 5.2. Iterative linear detection

To alleviate the implementation complexity of the ideal detector update described in Section 5.1, iterative implementation of the decorrelating and the LMMSE detectors will be studied in this section. The decorrelating detection can be represented as a linear equation (5.2), which can be solved by several iterative methods. Their advantage is the potential of offering significant savings in computational complexity, since there is no need to invert or Cholesky factorize the matrix $\mathcal{R}^{(n)}$ explicitly prior to $\boldsymbol{y}_{[d]}^{(n)}$ being solved. Some of the iterative algorithms will be considered in Section 5.2.1. In Section 5.2.2, an efficient way to initialize an iterative algorithm for a multiuser detector is proposed. In Section 5.2.3, the performance of the iterative detectors is studied.

### *5.2.1. Iterative algorithms*

The most popular iterative algorithms to solve (5.2) include the steepest descent (SD) and the conjugate gradient (CG) methods[7] [156, 291, 292]. Both the SD and CG methods utilize the fact that solving (5.2) is equivalent to minimizing the function

$$\Omega(\boldsymbol{h}) = \frac{1}{2}\boldsymbol{h}^{\mathrm{H}}\mathcal{R}^{(n)}\boldsymbol{h} - \boldsymbol{h}^{\mathrm{H}}\boldsymbol{y}^{(n)}. \tag{5.44}$$

In other words, the decorrelator output

$$\boldsymbol{y}_{[d]}^{(n)} = \min_{\boldsymbol{h}\in\mathbb{C}^{NK}} \Omega(\boldsymbol{h}) \tag{5.45}$$

can be viewed as an estimate of the data-amplitude product vector $\boldsymbol{h}$. The algorithms start with some initial guess $\hat{\boldsymbol{h}}(0)$, from which the estimate of the minimum of $\Omega(\boldsymbol{h})$ is improved by iterative steps. The $m$th estimate is computed in the form $\hat{\boldsymbol{h}}(m) = \hat{\boldsymbol{h}}(m-1) + \alpha(m)\boldsymbol{p}(m)$, where $\boldsymbol{p}(m)$ is the new search direction, and the coefficient $\alpha(m)$ is chosen so that $\Omega(\hat{\boldsymbol{h}}(m))$ is minimized given $\hat{\boldsymbol{h}}(m-1)$ and $\boldsymbol{p}(m)$. Different strategies to choose the search directions $\boldsymbol{p}(m)$ result in different iterative algorithms. Since $\Omega(\hat{\boldsymbol{h}}(m))$ decreases most rapidly in the direction of the negative gradient

$$\boldsymbol{q}(m) \hat{=} -\frac{\partial\Omega(\boldsymbol{h})}{\partial\boldsymbol{h}}\Big|_{\boldsymbol{h}=\hat{\boldsymbol{h}}(m)} = \boldsymbol{y}^{(n)} - \mathcal{R}^{(n)}\hat{\boldsymbol{h}}(m), \tag{5.46}$$

choosing $\boldsymbol{p}(m)$ as a function of $\boldsymbol{q}(m-1)$ has proved out to be efficient yielding a family of the so called gradient algorithms, such as the steepest descent and the conjugate gradient algorithms.

[7] There are also several other simple iterative algorithms (e.g., Jacobi or Gauss-Seidel methods) available. The Gauss-Seidel algorithm was also tested, but it yielded significantly worse results.

### *5.2.1.1. Steepest descent and conjugate gradient algorithms*

In the SD method the search direction is chosen simply to be the negative gradient [156], i.e., $\boldsymbol{p}(m) = \boldsymbol{q}(m-1)$. The choice implies that the search directions may be linearly dependent, even if $m < NK$ and $\boldsymbol{q}(m) \neq \boldsymbol{0}$, resulting in redundant minimization of the function $\Omega(\boldsymbol{h})$. In the CG method the new search direction $\boldsymbol{p}(m)$ is chosen so that it satisfies [156]

$$\boldsymbol{p}(m) = \arg \min_{\tilde{\boldsymbol{p}} \in \mathcal{V}_{m-1}^{\perp}} \|\tilde{\boldsymbol{p}} - \boldsymbol{q}(m-1)\|, \tag{5.47}$$

where $\mathcal{V}_m$ is the space spanned by vectors $\mathcal{R}^{(n)}\boldsymbol{p}(1), \ldots, \mathcal{R}^{(n)}\boldsymbol{p}(m)$, and $\mathcal{V}^{\perp}$ denotes the space orthogonal to $\mathcal{V}$. It is easy to see that $\boldsymbol{p}(m)$ is $\mathcal{R}^{(n)}$-*conjugate* or $\mathcal{R}^{(n)}$-*orthogonal* to the previous search directions, i.e.,

$$\boldsymbol{p}^{\mathrm{H}}(m)\mathcal{R}^{(n)}\boldsymbol{p}(i) = 0, \forall i < m. \tag{5.48}$$

This condition guarantees that the search directions are linearly independent as long as $\boldsymbol{q}(m-1) \neq \boldsymbol{0}$, since $\mathcal{R}^{(n)}$ is positive definite [156]. Thus, the algorithm results in the exact solution (neglecting the rounding errors) in $NK$ steps or faster. Moreover, in many cases a significantly smaller number of iterations yields solutions that are close to the ideal one.

The computationally most complex operation in both SD and CG algorithms is a matrix-vector multiplication of the form $\mathcal{R}^{(n)}\boldsymbol{p}(m)$. Due to the sparsity of $\mathcal{R}^{(n)}$ this requires $O[2NK^2]$ multiplications of a complex number by a real number and $O[2NK^2]$ complex additions, i.e., in total $O[8MNK^2]$ flops are required, where $M$ is the number of iterations performed. Since the matrix-vector multiplication consists of $NK$ separate vector inner products, it lends itself to a fully parallel implementation. The required number of clock cycles is found to be $11M$ for the SD algorithm, and $14M$ for the CG algorithm by [156].

The correlation coefficients in the matrix $\mathcal{R}^{(n)}$ must also be computed as a change in the signature waveforms or in their timing occurs. A computation of one coefficient requires $2N_s$ flops. If the signature waveforms are time-varying, all the $K^2$ new correlation coefficients need to be computed, and $O[2N_sK^2] \leq O[2K^3]$ flops would be required on every symbol interval. In other words, the correlation computation would be significantly more complicated than the iterative detection. Thus, the whole method would loose much of its advantages. The applicability to a highly parallel implementation would be the only one to remain. Fortunately, there is another way to implement the CG algorithm [291, p. 610]. It is mathematically equivalent to the CG algorithm described above. However, its input is the sampled received waveform $\boldsymbol{r}$ instead of $\boldsymbol{y}^{(n)}$, and it does not require the correlation matrix computation. It solves the least-squares problem $\hat{\boldsymbol{h}} = \arg\min_{\boldsymbol{h}} \|\mathcal{S}\boldsymbol{h} - \boldsymbol{r}\|$. Thus, it will be referred to as CGL (conjugate gradient for solving least-squares problems) algorithm. The details of the CGL algorithm can be found in [291, p. 610]. The algorithm requires matrix-vector products of the form $\mathcal{S}\boldsymbol{p}(m)$ and $\mathcal{S}^{\top}\boldsymbol{\xi}(m)$ on each iteration, where $\boldsymbol{\xi}(m) \in \mathbb{C}^{(N+1)N_s}$ is a vector needed in the CGL iteration [291, p. 610]. Thus, it requires in total $O[8MNN_sK]$ flops. The computational complexity of the CGL algorithm is higher than that of CG algorithm. Since the correlation

computation is not required separately, the overall complexity is lower with time-varying signature waveforms or with rapidly changing delays. The required number of clock cycles in the CGL algorithm is found to be $10M$ by [291, p. 610]. The CG algorithm can be straightforwardly applied to LMMSE detection by replacing the matrix $\mathcal{R}^{(n)}$ by $\mathcal{R}^{(n)} + \sigma^2\mathcal{E}^{-1}$. However, the application of the CGL algorithm to LMMSE detection is not possible, since LMMSE detection does not have a least-squares problem interpretation.

### *5.2.1.2. Preconditioned conjugate gradient algorithm*

The convergence speed of the conjugate gradient algorithm is determined by the condition number $\kappa$ of $\mathcal{R}^{(n)}$, which is defined as the eigenvalue ratio

$$\kappa(\mathcal{R}^{(n)}) = \frac{\lambda_{max}\left(\mathcal{R}^{(n)}\right)}{\lambda_{min}\left(\mathcal{R}^{(n)}\right)}, \tag{5.49}$$

where $\lambda_{max}(\mathbf{A})$ and $\lambda_{min}(\mathbf{A})$ denote the eigenvalues of a matrix $\mathbf{A}$ with the largest and smallest absolute value, respectively. The larger the ratio, the slower the convergence [156]. The convergence speed can be improved by a *preconditioning* strategy [156]. The idea is to replace (5.2) by an equivalent equation

$$\check{\mathcal{R}}\check{\boldsymbol{h}}_d = \check{\boldsymbol{y}}^{(n)}, \tag{5.50}$$

where $\check{\mathcal{R}} = \mathcal{G}^{-1}\mathcal{R}^{(n)}\mathcal{G}^{-1}$, $\check{\boldsymbol{h}}_d = \mathcal{G}\boldsymbol{y}^{(n)}_{[d]}$, $\check{\boldsymbol{y}}^{(n)} = \mathcal{G}^{-1}\boldsymbol{y}^{(n)}$, and $\mathcal{G} \in \mathbb{R}^{NK\times NK}$ is a symmetric, positive definite matrix used to improve the condition number. If the QR factorization of $\mathcal{G}$ is $\mathcal{G} = \mathcal{Q}\mathcal{H}$, and $\mathcal{H} \approx \mathcal{L}$ ($\mathcal{L}$ is the Cholesky factor of $\mathcal{R}^{(n)}$), we have $\check{\mathcal{R}} \approx \mathbf{I}_{NK}$ [156]. This means that the condition number $\kappa(\check{\mathcal{R}}) \approx 1$. In other words, the application of the preconditioning strategy requires finding a matrix $\mathcal{H}$ that is in some sense close to the Cholesky factor $\mathcal{L}$. The resulting algorithm does not include explicit reference to matrix $\mathcal{G}$. The only extra complication that is introduced to CG algorithm is the solution of a system of the form

$$\mathcal{H}^\top\mathcal{H}\boldsymbol{z} = \boldsymbol{q}(m-1) \Leftrightarrow \boldsymbol{z} = (\mathcal{H}^\top\mathcal{H})^{-1}\boldsymbol{q}(m-1), \tag{5.51}$$

see [156, pp. 527–529] for details.

The preconditioned conjugate gradient (PCG) algorithm is proposed for systems in which the signature waveforms are time-invariant. A simple preconditioning matrix is

$$\mathcal{H} = \mathrm{diag}(\tilde{\mathbf{L}}, \ldots, \tilde{\mathbf{L}}) \in \mathbb{R}^{NK\times NK}, \tag{5.52}$$

where $\tilde{\mathbf{L}}$ is the Cholesky factor of $\mathbf{R}(0)$. The choice implies

$$(\mathcal{H}^\top\mathcal{H})^{-1} = \mathrm{diag}(\mathbf{R}^{-1}(0), \ldots, \mathbf{R}^{-1}(0)) \in \mathbb{R}^{NK\times NK}. \tag{5.53}$$

The inverse matrix $\mathbf{R}^{-1}(0)$ can be updated to correlation changes with computational complexity $O[4K^2]$ flops by applying the algorithms described in Section 5.1.2. The solution of the system (5.51) requires $O[4NK^2]$ flops so that the overall computational complexity is $O[12MNK^2]$ flops. The PCG algorithm requires $16M$ clock cycles by [156], i.e., two more per iteration than the standard CG algorithm.

### 5.2.2. Iterative sliding window detection

Both the steepest descent and the conjugate gradient algorithms converge to the correct solutions with any initial guess under relatively mild conditions. A usual choice for the initial guess is a zero vector if no a priori information of the correct solution is available [156]. Since there is information about the vector $\boldsymbol{h}$, it can be expected that the zero vector is not the best possible initial guess. For example, the matched filter output vector $\boldsymbol{y}^{(n)}$ is clearly closer to the correct $\boldsymbol{h}$ than a zero vector. For the case of truncated detection, where the data symbols in the middle time interval of the observation window are detected, a *sliding window algorithm* is now proposed. It uses as an initial guess the values computed during previous symbol interval. More specifically, assume that a vector $\hat{\boldsymbol{h}}^{(n_0)}(M) \in \mathbb{C}^{NK}$ was computed and $\hat{\mathbf{h}}^{(n_0)}(M) \in \mathbb{C}^K$ was obtained from the middle components of $\hat{\boldsymbol{h}}^{(n_0)}(M)$. On the following symbol interval, where $\mathbf{h}^{(n_0+1)}$ is estimated, the last $(N-1)K$ elements of $\hat{\boldsymbol{h}}^{(n_0)}(M)$ computed on the previous symbol interval are substituted to be the first $(N-1)K$ elements of the new initial guess $\hat{\boldsymbol{h}}^{(n_0+1)}(0)$. The last $K$ elements of the new initial guess are substituted to be the matched filter outputs, i.e., the last $K$ element of $\boldsymbol{y}^{(n_0+1)}$.

### 5.2.3. Numerical performance evaluation

It is not possible to find useful analytical expressions for the average bit error probability or mean squared error of the iterative detectors. For that reason Monte-Carlo computer simulations are carried out. A 31-chip Gold sequence family used in the simulation for the system with time-invariant signature waveforms. Random signature sequences of length 6200 chips are used in the simulation for the system with time-varying signature waveforms. A rectangular chip waveform is applied. The number of users is $K = 33$. BPSK data and spreading modulation with coherent detection are used. The carrier phases of users are set to zero. The delays of the users are fixed, randomly selected, and they are the same in all simulations. The interfering users have equal energies (marked by $E_k$ in the illustrations). Most of the simulations use the sliding window algorithm described in Section 5.2.2 with window length $N = 2P + 1 = 7$. For purposes of comparison the SD, CG, and PCG algorithms approximating both the decorrelating and LMMSE detectors are simulated.

First, a system with data block length $N_b = 1$ (processing window naturally had length $N = N_b = 1$) is simulated so that there is no need for the sliding window algorithm, since the whole data block can be processed in the detector. In Figs. 5.1(a) and 5.1(b) the simulated mean squared errors of the estimates $\hat{\mathbf{h}}^{(n)}$ are plotted versus the number of iterations, $M$. The effect of the initial guess is also illustrated by using both a zero vector and the MF output vector as the initial guess. In Fig. 5.1(a) the received energies are the same, whereas in Fig. 5.1(b) the

near-far problem is emulated, since the desired user's ($k = 1$) energy per symbol is 10 dB weaker than the energies of the interfering users. The signal-to-noise ratio in the simulations is $E_1/\sigma^2 = 8$ dB.

The results in Fig. 5.1(a) indicate that a moderate number of iterations yields a performance close to that of the ideal detectors. The convergence of the CG algorithm to the final solution is faster than that of the SD algorithm, as expected. From Fig. 5.1(b) it is seen that in the case with a severe near-far problem more iterations are required to get the ideal detector performance, and the CG algorithm is superior to the steepest descent algorithm. It is noted from Figs. 5.1(a) and 5.1(b) that the matched filter output is a better initial guess than a zero vector, as is expected. It can also be seen that the initial guess does not have an adverse effect on the convergence, however, with a poor initial guess more iterations are required to obtain a certain performance level.

The performance of the sliding window algorithms versus the number of iterations per symbol interval is depicted in Figs. 5.2–5.3 and 5.4–5.5 for time-invariant and time-varying signature waveforms, respectively. The mean squared errors are presented in Figs. 5.2 and 5.4, and the bit error rates for the same example in Figs. 5.3 and 5.5. The signal-to-noise ratio in the simulations is again $E_1/\sigma^2 = 8$ dB. The results are similar to those described above. The number of required iterations in the sliding window algorithms is relatively small. For the CG algorithm four iterations per symbol are required to reach the minimum mean squared error performance in the examples with a near-far problem and time-invariant signature waveforms. A few more iterations are required in the examples with time-varying signature waveforms. One more iteration is required to obtain the optimal bit error rate than the optimal mean squared error, especially for the LMMSE detector. It is also noted that the CG algorithm is clearly superior to the SD algorithm, as expected. Preconditioning speeds up the convergence to the exact solution even further.

The mean squared errors versus the signal-to-noise ratio per symbol for the steepest descent, the conjugate gradient, and the preconditioned conjugate gradient algorithms with time-invariant signature waveforms are illustrated in Figs. 5.6, 5.7, and 5.8, respectively. It can be seen that at signal-to-noise ratios of practical interest ($\leq$ 16 dB) the CG decorrelator requires only two iterations to reach the MSE of the ideal decorrelator in the examples of equal received energies. It is noted that at very high signal-to-noise ratio the CG algorithm requires more than five iterations to achieve the minimum MSE in the examples with a near-far problem. The MSE of the PCG algorithm differs only marginally from the MSE of the ideal decorrelator even if only four iterations are performed when there is a near-far problem.

An interesting result seen in the figures is that there are some iteration steps where the iterative decorrelators "perform" better than the ideal decorrelator at low signal-to-noise ratios. This is possible, since the decorrelating detector is not optimal in the minimum mean squared error sense. The solutions provided by iterative decorrelators do finally converge to the exact decorrelating solution, as expected. During the iterative process the length of the error vector $\boldsymbol{\varepsilon}_d(m)$ is

reduced at each step of the CG algorithm, where

$$\boldsymbol{\varepsilon}_d(m) = \boldsymbol{y}_{[d]}^{(n)} - \hat{\boldsymbol{h}}(m) \tag{5.54}$$

is the error vector between the true decorrelating solution $\boldsymbol{y}_{[d]}^{(n)}$ and the estimate $\hat{\boldsymbol{h}}(m)$ computed by the iterative algorithm. In other words, it is guaranteed that the estimates computed by the CG decorrelator converge to the correct solution $\boldsymbol{y}_{[d]}^{(n)}$ and on each iteration the solution $\hat{\boldsymbol{h}}(m)$ gets closer to $\boldsymbol{y}_{[d]}^{(n)}$. In the simulation, on the other hand, the elementwise mean squared values of the error vector

$$\boldsymbol{e}(m) = \boldsymbol{h} - \hat{\boldsymbol{h}}(m) \tag{5.55}$$

are measured. Vector $\boldsymbol{e}(m)$ is the deviation between the true value of the received data-amplitude product vector $\boldsymbol{h}$ and the estimate $\hat{\boldsymbol{h}}(m)$ computed by the iterative algorithm. Reduction of the mean squared value of $\boldsymbol{e}(m)$ at each step is not guaranteed. The iterative schemes also perform always worse than the LMMSE detector, as expected. The phenomenon is discussed further in Appendix 2.

In Chapter 3 it was noted that the length of the decorrelating detector and the ratio $E_{max}/E_{min}$ of maximum and minimum energies are design parameters, and a trade-off between them needs to be made. The same conclusion can be made between the ratio $E_{max}/E_{min}$ and the number of iterations in the iterative implementation of the linear multiuser detectors.

All the numerical examples indicate a convergence to the exact solution after a few iterations while there are $NK = 231$ unknown variables. The fast convergence of the algorithms is to a large extent due to the initial guess as described in Section 5.2.2. As predicted, the performance of the iterative detectors is highly dependent on the number of iterations performed. On the other hand, the implementation complexity is also directly proportional to the number of iterations. Thus, the iterative detectors provide a trade-off between the implementation complexity and the performance of the detectors.

## 5.3. Complexity comparisons

The implementation of the parallel interference cancellation receiver is relatively straightforward on the algorithm level considered in this work. The interference cancellation in (2.62) requires $O[4MK^2]$ flops and $4M$ clock cycles, where $M$ is the number of cancellation stages. If the interference cancellation is performed for the received spread-spectrum signal (i.e., for the MF input), the corresponding cancellation requires $O[4MN_sK]$ flops and 4 clock cycles. The only update that is needed (in addition to amplitude estimation) is the correlation computation as a change in the communication system occurs.

### 5.3.1. Summary of implementation complexities

The implementation complexity of some of the algorithms of this chapter are summarized in Table 5.1. The detection given $\mathcal{L}$ refers to solving (5.2) by backward and forward substitutions without computing the detector $\mathcal{D}_N$. Both the total number of flops and the number of flops per detected symbol are shown for the detection methods. The total number of flops only is presented for ideal detector computation methods, since the detector is updated occasionally and the number of flops per symbol would not be a sensible measure of complexity. It should be noted that the computational burden of the computation of the correlations between users' signature waveforms is excluded from the comparisons. To obtain a better understanding of the complexity of different schemes an example is considered below.

*Table 5.1. Summary of total implementation requirements of different algorithms.*

| | flops | flops/$KL$ | clock cycles |
|---|---|---|---|
| Cholesky factorization of $\mathcal{R}$ | $O[5N(KL)^3]$ | — | $7NKL$ |
| QR factorization of $\mathcal{S}$ | $O[NN_s(KL)^2]$ | — | $4NKL$ |
| Detector computation given $\mathcal{L}$ | $O[6N(KL)^3]$ | — | $5NKL$ |
| Matched filtering | $O[4N_sKL]$ | $O[4N_s]$ | 2 |
| Lin. detection given $\mathcal{D}$ | $O[4N(KL)^2]$ | $O[4NKL]$ | 2 |
| Lin. detection given $\mathcal{L}$ | $O[16N(KL)^2]$ | $O[16NKL]$ | $5NKL$ |
| Lin. SD detection | $O[8MN(KL)^2]$ | $O[8MNKL]$ | $11M$ |
| Lin. CG detection | $O[8MN(KL)^2]$ | $O[8MNKL]$ | $14M$ |
| Lin. CGL detection | $O[8MNN_sKL]$ | $O[8MNN_s]$ | $10M$ |
| Lin. PCG detection | $O[12MN(KL)^2]$ | $O[12MNKL]$ | $16M$ |
| HD-PIC MF-OUT detection | $O[4M(KL)^2]$ | $O[4MKL]$ | $4M$ |
| HD-PIC MF-IN detection | $O[4MN_sKL]$ | $O[4MN_s]$ | $4M$ |

### 5.3.2. An example

The complexity of the update based on the ideal Cholesky factoring is determined by the rate of delay changes and the frequency of changes in the number of users or their signature waveforms. A mobile radio system example with the system parameters from the FRAMES project [34] is presented to provide reasonable numerical values for the parameters. Assume that the number of users is $K = 256$, the number of multipath components is $L = 4$, the number of chips per symbol (the processing gain) is $N_c = 256$, number of samples per chip is 5 to guarantee that $KL < N_s$. This yields a total number of samples per symbol $N_s = 1280$. It is assumed that the users have average vehicle speed of 80 $\frac{\text{km}}{\text{h}}$. Assume also that

the angle $\theta$ between the direction of the mobile unit movement with a line from a vehicle to the base station is uniformly distributed into $[0, \pi)$. The effective speed causing distance change from the mobile to the base station is then $80\ \frac{\text{km}}{\text{h}}\ |\cos(\theta)|$, which results in an average value $v \approx 51\ \frac{\text{km}}{\text{h}}$.

On a time-interval $\Delta t$ the delay of a user changes $\Delta\tau = \frac{v\Delta t}{c_{light}}$. A delay change is said to be significant if it exceeds a predetermined level $T_\delta$. It is assumed here $T_\delta = \frac{T}{2N_s} = \frac{T_c}{10}$, which is a strict synchronization requirement, but is supported by the results in [151]. Thus, the number of symbols transmitted between significant delay changes for any of the $K$ users is on the average $\frac{c_{light}T_\delta}{vKT} = \frac{c_{light}}{8vKN_c} \approx 32$. Assume that the symbol rate is 20.3 kbaud, i.e., the symbol interval is $T = 49.261\ \mu$s. To estimate the frequency of handovers, it is assumed that mobile users are driving through a cell of diameter 1 km after which a handover occurs. Then the average number of symbols transmitted between two handovers for any of the $K$ users is $\frac{1000\ \text{m}}{KvT} = 5597$. Therefore, the delay changes are more common than handovers so that the effect of the handovers on the implementation complexity can be neglected.

Assume that it is required that the detector is updated within 10 symbol intervals ($10T$) from a delay change. (Thus, the detector is updated during one frame [34]). Referring to Table 5.1, the detector computation requires at least $12NKL$ clock cycles. Thus, the DSP hardware must have at least $12NKL$ clock cycles in time $10T$, and the minimum clock frequency becomes $\frac{7NKL}{10T} \approx 320$ MHz, if $N = 13$. Since the detector update requires $O[11N(KL)^3]$ flops as seen from Table 5.1, the DSP hardware must be able to perform about $11N(KL)^3$ flops in time $10T$. In other words, the DSP must have speed $\frac{11N(KL)^3}{10T} \approx 310$ Tflops/s. If the CG detection applies $M = 124$ iterations[8] per symbol interval, the clock frequency $14M/T = 35$ MHz is required by Table 5.1. The required number of arithmetic operations is $\frac{8MN(KL)^2}{T} \approx 280$ Tflops/s. The corresponding clock frequency requirement for the CGL algorithm is $10M/T = 25$ MHz, and the number of arithmetic operations $\frac{8MNN_sKL}{T} \approx 340$ Tflops/s, as is easy to see from Table 5.1. If the PCG method applies $M = 62$ iterations on a symbol interval, it requires the clock frequency $16M/T = 20$ MHz, and the required number of arithmetic operations is $\frac{12MN(KL)^2}{T} \approx 210$ Tflops/s. Assuming two ($M = 2$) multistage iterations (as in the examples of Chapter 4) the HD-PIC receiver requires a speed of $4M/T = 160$ kHz, and a computation power of $4M(KL)^2 = 8.4$ Mflops/s. If the HD-PIC receiver processes the received wideband signal, the DSP speed of $4MN_sKL = 10$ Mflops/s is required. Finally, to put the above numbers into perspective it is noted that the matched filtering requires the minimum clock frequency of $2/T = 41$ kHz, and the number of arithmetic operations $4N_sKL \approx 5.2$ Mflops/s. The results are summarized in Table 5.2.

The example illustrates that due to the higher degree of parallelism, the DSP clock frequency requirements of the iterative algorithms are significantly less stringent than those of the ideal detection. The number of flops required is also smaller.

[8]The number of required iterations was estimated by assuming that the number of necessary iterations divided by the number of unknown variables is the same as in the numerical examples. Since $M = 4$ iterations yield an excellent performance for $K = 33$ unknown variables in Section 5.2.3, it is assumed that $M = \frac{4}{33} \times KL \approx 124$ iterations are needed in the current example.

*Table 5.2. Results of the example.*

| | flops | | flops/$KL$ | | clock freq. | |
|---|---|---|---|---|---|---|
| Matched filtering | 5.2 | Mflops/s | 5.1 | kflops/s | 41 | kHz |
| Detector computation | 310 | Tflops/s | 300 | Gflops/s | 320 | MHz |
| Lin. CG detection | 280 | Tflops/s | 270 | Gflops/s | 35 | MHz |
| Lin. CGL detection | 340 | Tflops/s | 340 | Gflops/s | 25 | MHz |
| Lin. PCG detection | 210 | Tflops/s | 200 | Gflops/s | 20 | MHz |
| HD-PIC MF-OUT detection | 8.4 | Mflops/s | 8.2 | kflops/s | 160 | kHz |
| HD-PIC MF-IN detection | 10 | Mflops/s | 10 | kflops/s | 160 | kHz |

The iterative algorithms use the computation resources steadily, whereas the ideal detector computation requires high computation peaks for detector computation. The PCG algorithm is the simplest in terms of both required DSP clock frequency and number of flops required. The CGL algorithm would clearly be the simplest algorithm for linear multiuser detection in an R-CDMA system with time-varying signature waveforms. The example also quantifies the well-known fact that the parallel interference cancellation receivers are significantly simpler to implement than the linear equalizer type receivers. The number of arithmetic operations that needs to be performed in decorrelating receiver in a unit of time is roughly $2 \times 10^7$ times the corresponding number for the HD-PIC receiver. The corresponding ratio for the clock frequency is approximately 100. The number of arithmetic operations required by the parallel interference cancellation is roughly twice the number required by the matched filter bank. The clock frequency is approximately four times that of the MF bank. In that sense the parallel interference cancellation can be considered to be a relatively simple technique to improve the performance of the CDMA systems.

The linear detector implementation requires a very large number of flops per second. The requirements for the processor clock frequency, on the other hand, are moderate. Furthermore, the number of flops per second is not a perfect measure of the implementation complexity, if an application specific integrated circuit (ASIC) is used. In other words, if all the potential for parallelism (measured by the minimum clock frequency) can be applied, the implementation of linear detectors will become feasible in the future.

## 5.4. Conclusions

Implementation of multiuser receivers in synchronous and asynchronous CDMA systems has been discussed. It was assumed that the delays, the signature waveforms, or the number of users may change over time. Algorithms for the ideal linear decorrelating or LMMSE detector computation were derived. The detector computation based on an order-recursive Cholesky factorization of the correlation

matrix was shown to require $O[11N(KL)^3]$ flops and $NKL$ square roots, and at least $12NKL$ clock cycles. The computational load is huge, since it has cubic dependence on the number of users times the number of multipath components. Iterative detectors were investigated to reduce the complexity of the linear detectors. Steepest descent and conjugate gradient algorithms were proposed for the decorrelating and the LMMSE detector implementation. The computational requirements of the algorithms are $O[8M(KL)^2]$ flops and at least $14M$ clock cycles. Preconditioned conjugate gradient algorithm was studied to obtain faster convergence. It requires $O[12MN(KL)^2]$ flops, and at least $16M$ clock cycles. A conjugate gradient algorithm not requiring separate correlation computation was proposed to be applied in CDMA systems with time-varying signature waveforms. A sliding window algorithm utilizing the values computed on the previous symbol interval was developed to reduce the required number of iterations. Simulation results demonstrate that moderate number of iterations with the CG or the PCG algorithm gives the essentially the same performance as the ideal detectors have. The results show that the preconditioned conjugate gradient algorithm yields the fastest convergence.

In the mobile communication example the preconditioned conjugate gradient algorithm was found to be the simplest linear detection scheme for D-CDMA system with time-invariant signature waveforms. The CGL version of the conjugate gradient algorithm is found to be the simplest linear detection scheme for R-CDMA system with time-varying signature waveforms. It was also noted that the parallel interference cancellation receivers are significantly simpler to implement than the linear receivers, as can be expected. The example demonstrated that the required clock frequency for linear receivers is roughly 100 times that for HD-PIC receiver. The corresponding factor for number of arithmetic operations is $2 \times 10^7$. The parallel interference cancellation requires twice as many arithmetic operations as the matched filter bank. The clock frequency requirement is four times that of the MF bank. Thus, the PIC multiuser receivers are significantly more desirable from the implementation point of view than the linear equalizer type multiuser receivers. Furthermore, the PIC receivers are only moderately more complex to implement than the conventional MF receivers.

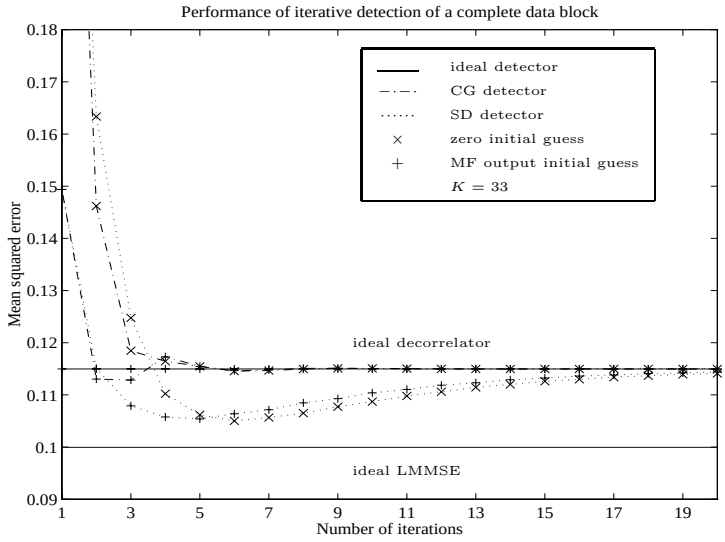


(a)

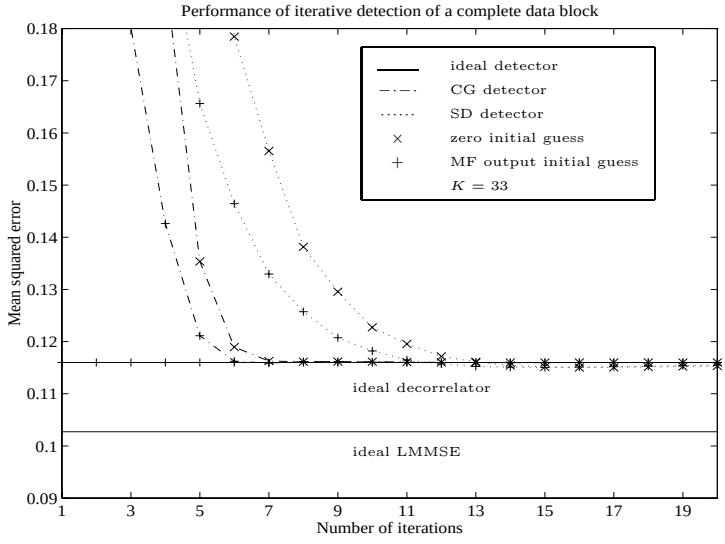


(b)

**Fig. 5.1. Mean squared errors of the iterative decorrelating detectors with time-invariant signature waveforms, $N_b = N = 1$, and SNR = 8 dB; (a) equal received energies, (b) near-far problem.**

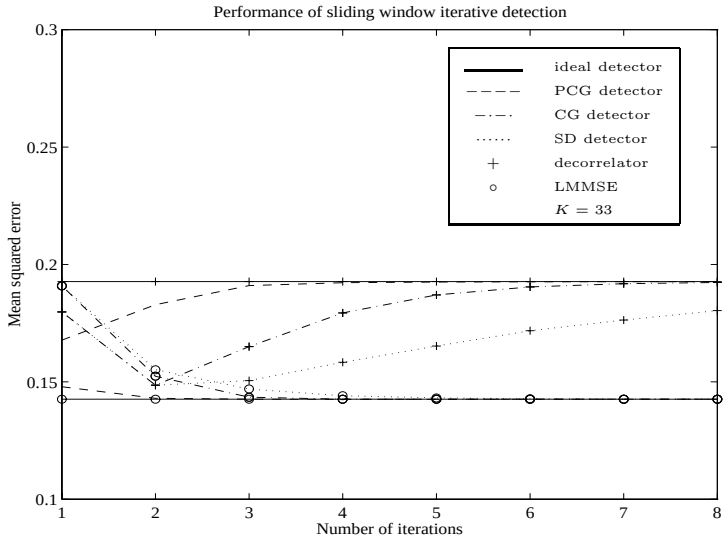


(a)

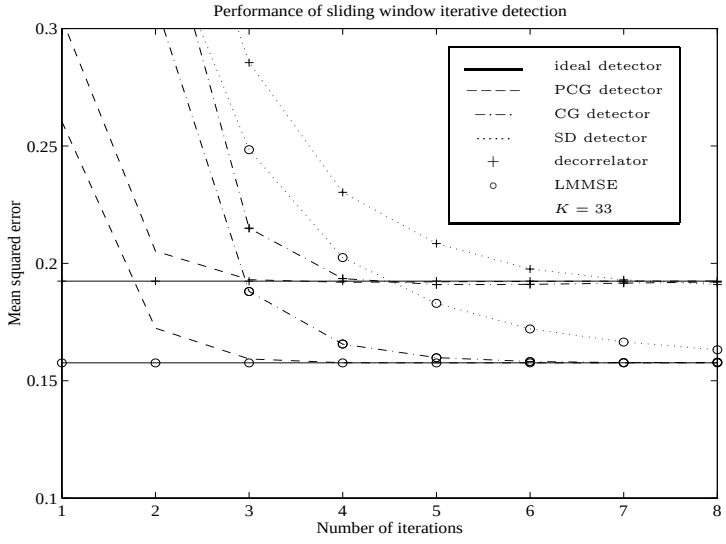


(b)

**Fig. 5.2**. **Mean squared errors of the iterative decorrelating and LMMSE sliding window detectors with time-invariant signature waveforms, $N_b = 200$, $N = 7$, and SNR = 8 dB; (a) equal received energies, (b) near-far problem.**

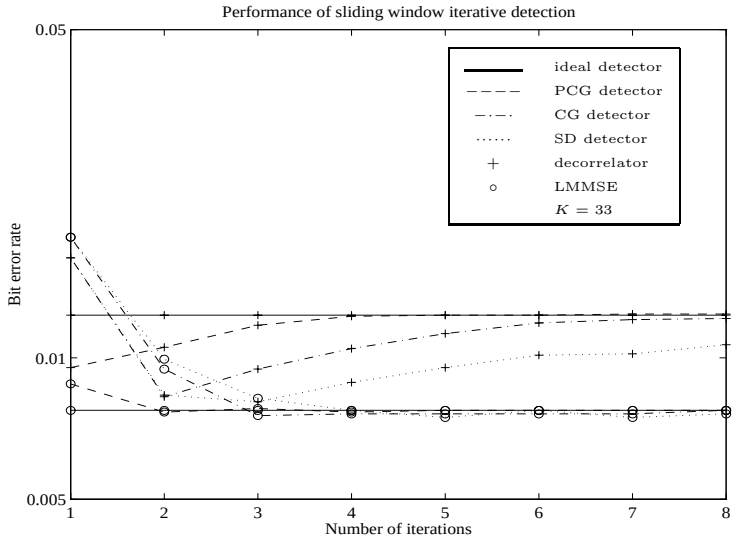


(a)

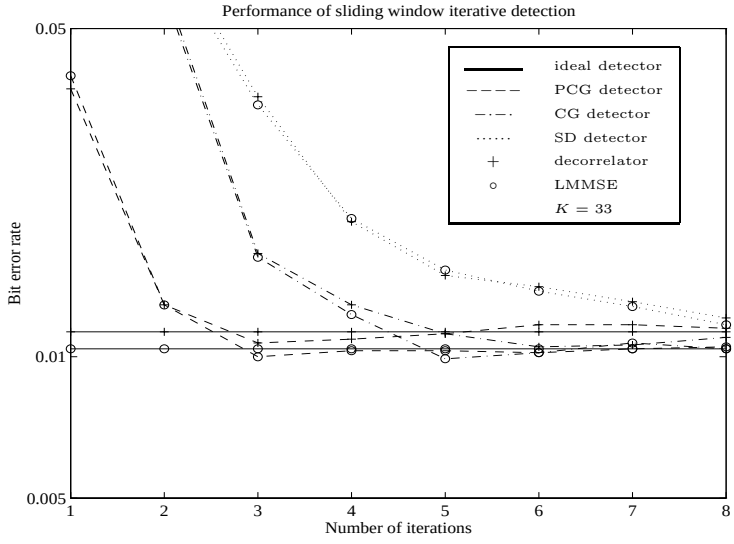


(b)

**Fig. 5.3**. **Bit error rates of the iterative decorrelating and LMMSE sliding window detectors with time-invariant signature waveforms, $N_b = 200$, $N = 7$, and SNR = 8 dB; (a) equal received energies, (b) near-far problem.**

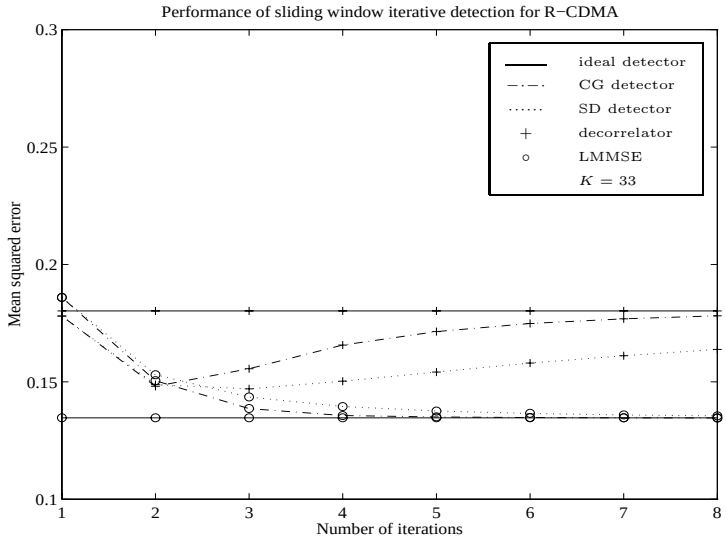


(a)

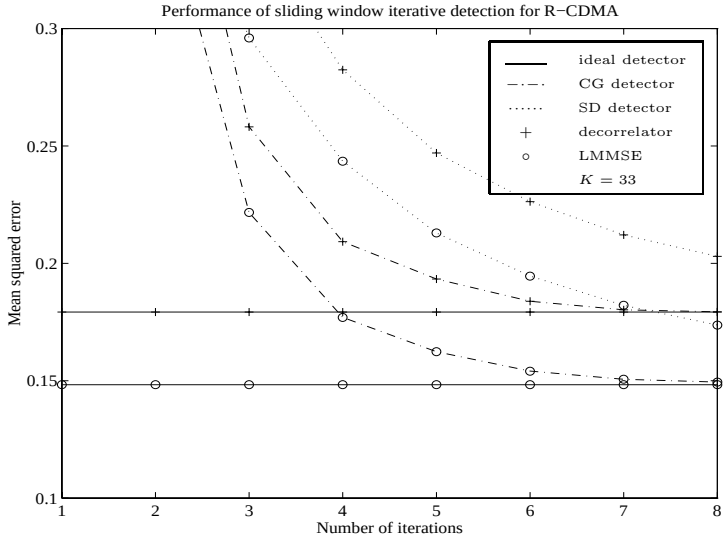


(b)

**Fig. 5.4. Mean squared errors of the iterative decorrelating and LMMSE sliding window detectors with time-varying signature waveforms, $N_b = 200$, $N = 7$, and SNR = 8 dB; (a) equal received energies, (b) near-far problem.**

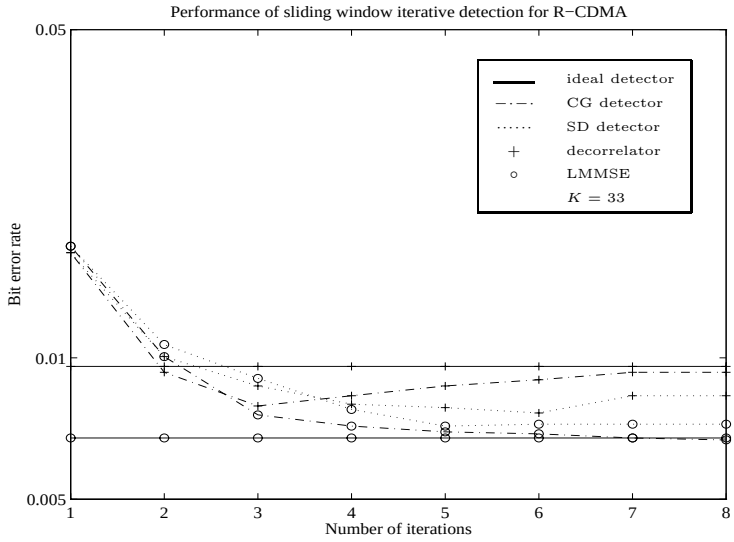


(a)

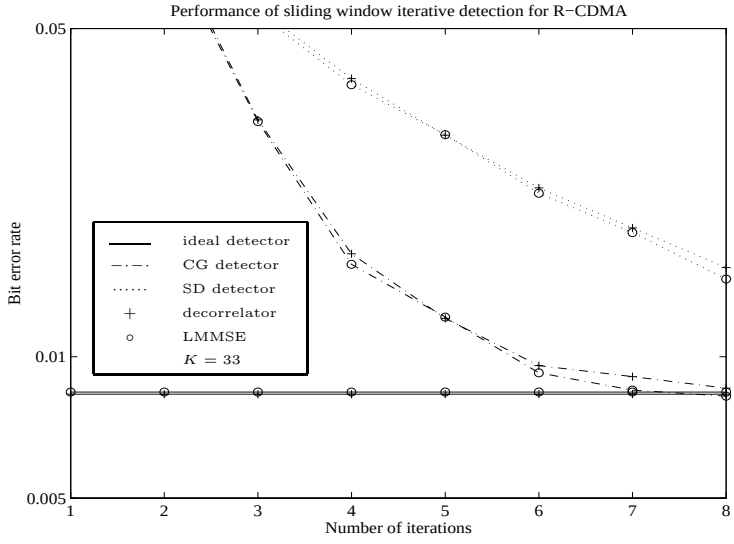


(b)

**Fig. 5.5. Bit error rates of the iterative decorrelating and LMMSE sliding window detectors with time-varying signature waveforms, $N_b = 200$, $N = 7$, and SNR = 8 dB; (a) equal received energies, (b) near-far problem.**

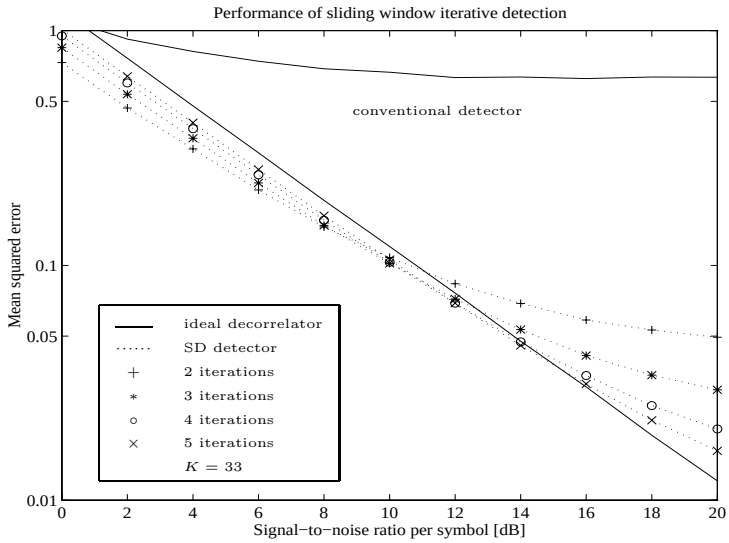


(a)

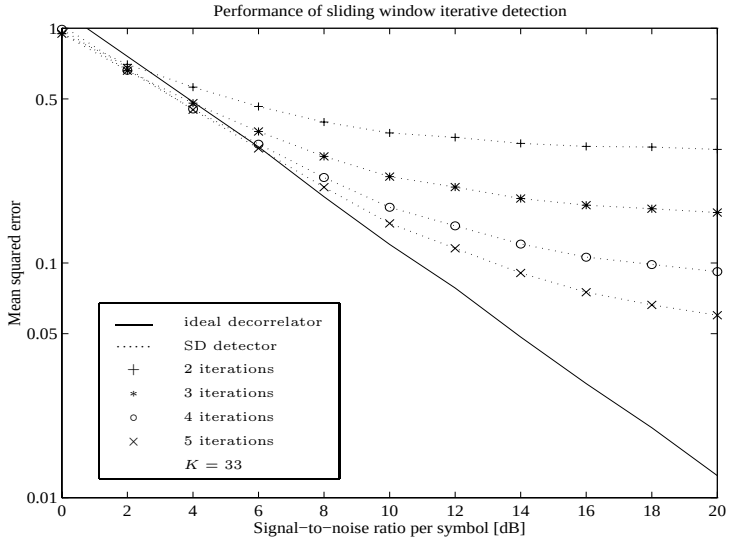


(b)

**Fig. 5.6. Mean squared errors of the decorrelating steepest descent sliding window detector for different numbers of iterations with time-invariant signature waveforms, $N_b = 200$, and $N = 7$; (a) equal received energies, (b) near-far problem.**

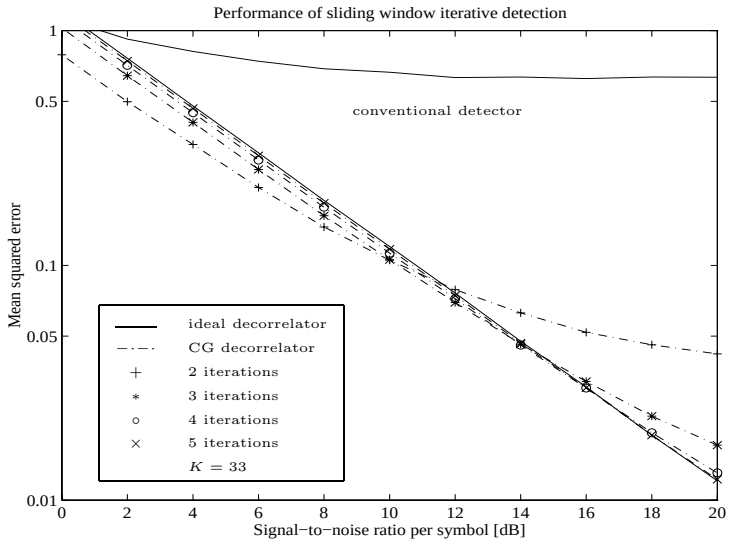


(a)

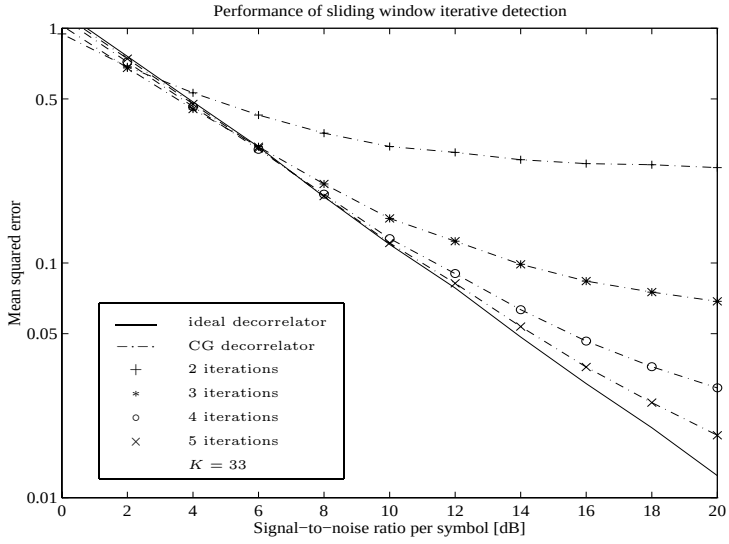


(b)

**Fig. 5.7**. **Mean squared errors of the decorrelating conjugate gradient sliding window detector for different numbers of iterations with time-invariant signature waveforms, $N_b = 200$, and $N = 7$; (a) equal received energies, (b) near-far problem.**

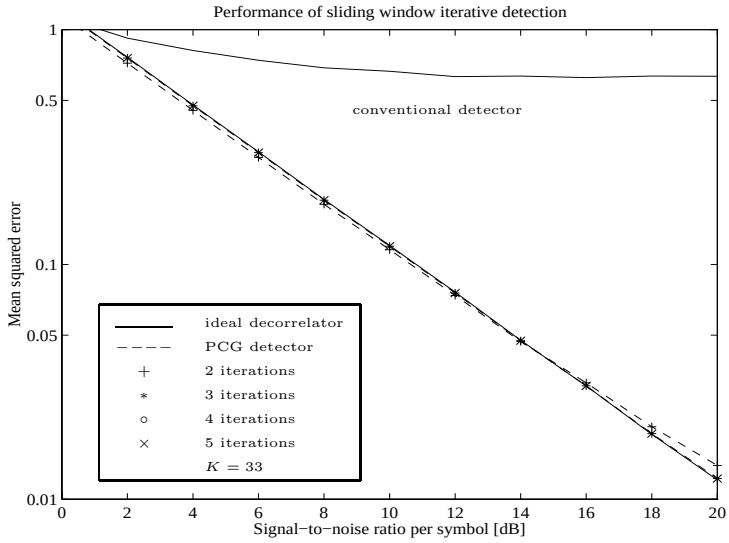


(a)

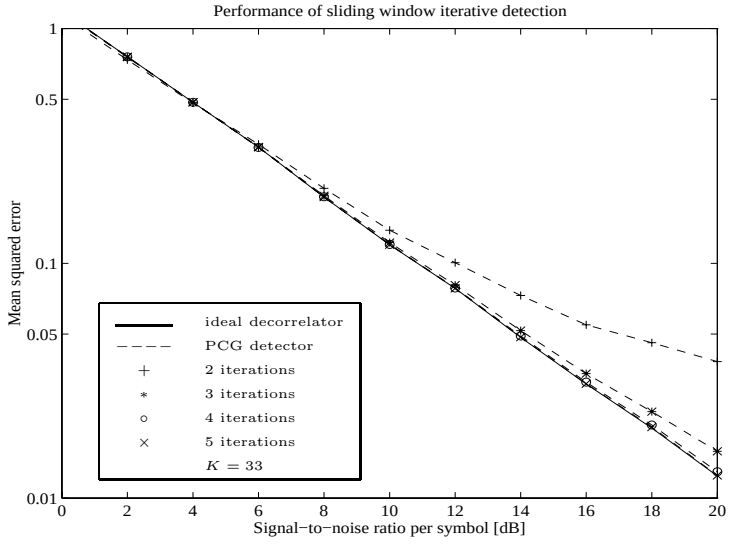


(b)

**Fig. 5.8. Mean squared errors of the decorrelating preconditioned conjugate gradient sliding window detector for different numbers of iterations with time-invariant signature waveforms, $N_b = 200$, and $N = 7$; (a) equal received energies, (b) near-far problem.**

# 6. Conclusions

## 6.1. Summary

Multiuser demodulation algorithms for centralized receivers of asynchronous DS-CDMA systems in frequency-selective fading channels were considered. The literature on single-user fading channel receivers and on multiuser demodulation was reviewed in Chapter 2. The problems to be analyzed in more detail were identified based on the review.

The approximation of ideal infinite memory-length linear multiuser detectors by finite memory-length detectors in asynchronous CDMA systems was considered in Chapter 3. The performance of the finite memory-length detectors was analyzed. It was shown that the FIR detectors can be made near-far resistant under a given ratio between maximum and minimum received power of users by selecting an appropriate memory-length. Numerical examples demonstrated the fact that moderate memory-lengths of the FIR detectors are sufficient to achieve the performance of the ideal IIR detectors even under a severe near-far problem. The required memory-length was shown to depend on other system parameters, especially on the ratio of maximum and minimum received powers.

Multiuser demodulation in relatively fast fading channels was the topic of Chapter 4. The optimal maximum likelihood sequence detector was derived. Due to the prohibitive complexity of the optimal receiver, suboptimal demodulators were considered. They decouple the data detection and complex channel coefficient estimation and estimate the channel coefficients for all users separately after suppressing the MAI. Decorrelating and parallel interference cancellation multiuser receivers were considered. The results show that the decoupled complex channel coefficient estimation yields excellent performance in comparison to joint LMMSE estimation. Furthermore, it was concluded that optimal or near-optimal channel estimation filters are crucial in data transmission where very low BER is required. In speech transmission, fixed channel estimation filters were shown to give satisfactory performance in most cases. The DA complex channel coefficient estimation was shown to be more robust than the DD complex channel coefficient estimation, which may suffer from BER saturation caused by hang-ups at high SNR's. The DD complex channel coefficient estimation was noted to be somewhat simpler to

be implemented than the DA complex channel coefficient estimation. The PIC receiver was demonstrated to achieve better performance in known channels than the decorrelating receiver, but it was observed to be more sensitive to complex channel coefficient estimation errors than the decorrelating receiver. At high channel loads the PIC receiver was seen to suffer from BER saturation, whereas the decorrelating receiver was demonstrated to be free of the BER saturation.

The implementation issues of the multiuser receivers in dynamic CDMA systems were analyzed in Chapter 5. Implementation of linear multiuser detectors in synchronous and asynchronous CDMA systems was studied. Algorithms for ideal linear decorrelating or LMMSE detector computation were derived. The detector computation was shown to have a cubic dependence on the number of users times the number of multipath components. Iterative detectors were investigated to reduce the complexity of the linear detectors. Steepest descent, conjugate gradient, and preconditioned conjugate gradient algorithms were proposed for decorrelating and LMMSE detector implementation. The computational requirements for one iteration were shown to be a quadratic function of the number of users times the number of multipath components. Furthermore, the iterative detectors were proved to be more applicable to parallel implementation than the ideal ones. A sliding window algorithm utilizing the values computed on the previous symbol interval was developed to reduce the number of required iterations. Simulation results demonstrated that a moderate number of iterations gives the same performance as the ideal detectors have. In the mobile communication example the well-known fact that the parallel interference cancellation receivers are significantly simpler to implement than the linear equalizer type receivers was quantified. What is more, it was demonstrated that the PIC receiver is only moderately more complex to implement than the conventional matched filter receiver.

## 6.2. Discussion

The results of the thesis show that the decorrelating multiuser receiver has often a performance advantage over the hard decision parallel interference cancellation receiver. This is especially true at high signal-to-noise ratios and/or with a poor channel complex coefficient estimation accuracy. The price for the performance advantages of the decorrelating receiver over the PIC receiver is the considerably higher implementation complexity. The choice between the two receivers depends clearly on the cost of DSP circuits. As the DSP techniques develop, the implementation cost may become insignificant sometimes in the future, and the choice of receiver algorithms can be based on the performance only. However, the parallel interference cancellation is clearly the choice as long as today's or the next decade's technology is concerned. It should also be noted that the superior performance of the decorrelating receiver requires very accurate estimation of the delays of the received signal, which poses another strict implementation requirement. Furthermore, the performance of the PIC algorithms can probably be improved with a moderate increase in complexity by the partial cancellation [226, 227, 228] men-

tioned in Section 2.2.3.2.

Although the HD-PIC receivers are more suitable for practice than the linear equalizer type receivers, the study of linear receivers has been and still is invaluable. Since the linear receivers are easy to analyze, significant information and insight about the multiuser demodulation problem can be obtained by studying them.

The attention in this thesis was limited to the linear equalizer type and hard decision parallel interference cancellation multiuser receivers, since they appeared to be among the most promising multiuser receiver techniques from the practical point of view. Therefore, the choice of the PIC receiver is based on the comparison to the linear equalizer type receivers only. Adaptive decentralized implementations of the linear equalizer type receivers are significantly simpler than the centralized ones. If the convergence problems associated to the adaptive receivers can be overcome in the future, they may appear as one alternative for practical multiuser receivers. However, the PIC receiver appears to be the most promising one for the first generation of multiuser receivers. Notably the same principle has been proposed for several evolving CDMA system standards, as mentioned in Section 1.1.

## 6.3. Future research directions

There are several interesting open problems in multiuser receivers requiring further study. Some of them are discussed here in short.

The performance of the parallel interference cancellation receivers can possibly be improved in some cases. As mentioned in Chapter 2, one alternative is to weight the cancellation according to the reliability of the MAI estimates [227, 228]. However, a simple and robust way to measure the reliability and to determine the cancellation weights remains to be found. Since the reliability depends on the state of the communication channel, the weights should be adapted to the changes in complex channel coefficients. That poses strict requirements to the speed of such weight determination. Thus, simple adaptive weighting, as proposed in [225], may not be fast enough in fading channels.

The thesis has concentrated on the reception of transmissions without forward error correction coding. This was reasonable, since the emphasis was on the receiver algorithms to achieve coherent detection, i.e., to estimate the fading channel coefficients reliably. From the data detection point of view channel encoding should be taken into consideration. The encoded transmission and reception for CDMA systems utilizing multiuser receivers are important research problems. The overall signal design (design of modulation and coding) for multiuser channels with some efficient low complexity joint decoding algorithms for all users would be of major interest. The goal could be to design a superior signal structure yielding the best possible performance with a given degree of decoding complexity. That would solve the spreading-coding tradeoff problem for the particular scenario. The problem is probably intractable, but an iterative process towards that goal should be continued.

The impact of several system level aspects to the multiuser receiver performance would be worth investigating. The same applies also vice versa. The impact of multiuser receivers on the overall system capacity has not been analyzed thoroughly yet. For example, the effect of the existence of multiple cells is often neglected in the multiuser receiver analysis. Multiuser receivers could naturally handle the intracell MAI by exploiting some ordinary multiuser receiver, e.g., a PIC receiver. The intercell MAI, on the other hand, could be compressed by some decentralized receiver technique. Multiuser receiver design and receiver performance in CDMA systems with multiple data rates in realistic fading channels has been studied very little. The application of groupwise multiuser receivers, where grouping could be based on the data rates of the users, appears as an interesting alternative [249]. The performance of multiuser receivers with antenna arrays should also be taken into consideration in the studies.

Centralized multiuser receivers have been considered in this thesis. There are, however, several applications (e.g., downlink receiver of a mobile communication system), where decentralized receivers need to be applied. There has been a considerable amount of interest in decentralized adaptive receivers, as discussed in Chapter 2. Several open problems still exist. A most severe problem is the fact that there are convergence problems associated with most adaptive receivers due to the large number of taps required by direct form FIR filters. Therefore, there is room for further work on dimension reduction techniques to reduce the number of filter taps needed, as well as for work on efficient adaptive algorithms to enhance the convergence.

The effect of optimal and suboptimal channel estimation filters to the multiuser receiver performance was studied in this thesis. However, there are only preliminary results on the application of adaptive channel estimation filters in conjunction with multiuser receivers [57]. More work on the performance of different adaptive algorithms is required. In general, the impact of various practical nonidealities (e.g., delay estimation errors and quantization in DSP hardware) to the performance of the receivers should be considered. The performance of the multiuser receivers with more realistic channel models and system parameters should be studied. The analysis of all real-life nonidealities is impossible, and Monte-Carlo computer simulations of nonidealities are intractable due to long simulation times and incomplete models for nonidealities. Thus, it will be necessary to carry out hardware simulations and construct testbeds and trial systems to determine the practical feasibility of multiuser demodulation for future communication systems.

# References


[1] Lee WCY (1991) Overview of cellular CDMA. IEEE Transactions on Vehicular Technology 40(2): p 291–302.

[2] Scholtz RA (1977) The spread spectrum concept. IEEE Transactions on Communications 25(8): p 748–755.

[3] Pickholtz RL, Schilling DL & Milstein LB (1982) Theory of spread-spectrum communications — a tutorial. IEEE Transactions on Communications 30(5): p 855–884.

[4] Simon MK, Omura JK, Scholtz RA & Levitt BK (1994) Spread Spectrum Communications Handbook. McGraw-Hill, New York City, New York, USA.

[5] Dixon RC (1994) Spread Spectrum Systems with Commercial Applications. John Wiley and Sons, New York City, New York, USA.

[6] Peterson RL, Ziemer RE & Borth DE (1995) Introduction to Spread Spectrum Systems. Prentice-Hall, Englewood Cliffs, New Jersey, USA.

[7] Viterbi AJ (1995) CDMA: Principles of Spread Spectrum Communication. Addison-Wesley, Reading, Massachusetts, USA.

[8] Scholtz RA (1982) The origins of spread-spectrum communications. IEEE Transactions on Communications 30(5): p 822–854.

[9] Scholtz RA (1983) Notes on spread-spectrum history. IEEE Transactions on Communications 31(1): p 82–84.

[10] Scholtz RA (1983) Further notes and anecdotes on spread-spectrum origins. IEEE Transactions on Communications 31(1): p 85–97.

[11] Prasad R & Hara S (1996) An overview of multi-carrier CDMA. Proc. IEEE International Symposium on Spread Spectrum Techniques and Applications (ISSSTA), Mainz, Germany, 1: p 107–114.

[12] Learned RE, Krim H, Claus B, Willsky AS & Karl WC (1994) Wavelet-packet-based multiple access communication. Proc. SPIE International Symposium on Optics, Imaging, and Instrumentation.

[13] Medley M, Saulnier G & Das P (1994) Applications of the wavelet transform in spread spectrum communications systems. Proc. SPIE International Symposium on Optics, Imaging, and Instrumentation, Princeton, New Jersey, USA, 2242 Wavelet Applications: p 54–68.

[14] Livingston JN & Tung CC (1996) Bandwidth efficient PAM signaling using wavelets. IEEE Transactions on Communications 44(12): p 1629–1631.

[15] Learned RE, Willsky AS & Boroson DM (1997) Low complexity optimal joint detection for oversaturated multiple access communications. IEEE Transactions on Signal Processing 45(1): p 113–123.

[16] Wornell GW (1995) Spread-signature CDMA: Efficient multiuser communication in the presence of fading. IEEE Transactions on Information Theory 41(5): p 1418–1438.

[17] Wornell GW (1996) Spread-response precoding for communication over fading channels. IEEE Transactions on Information Theory 42(2): p 488–501.

[18] Bingham JAC (1990) Multicarrier modulation for data transmission: An idea whose time has come. IEEE Communications Magazine 28(5): p 5–14.

[19] Viterbi AJ (1994) The orthogonal-random waveform dichotomy for digital mobile personal communication. IEEE/ACM Personal Communications 1(1): p 18–24.

[20] Vembu S & Viterbi AJ (1996) Two different philosophies in CDMA — a comparison. Proc. IEEE Vehicular Technology Conference (VTC), Atlanta, Georgia, USA, p 869–873.

[21] Verdú S (1997) Demodulation in the presence of multiuser interference: Progress and misconceptions. In: Docampo D, Figueiras-Vidal A & Perez-Gonzalez F (eds) Intelligent Methods in Signal Processing and Communications, Birkhauser, Boston, Massachusetts, USA, p 15–44.

[22] Cover TM & Thomas JA (1991) Elements of Information Theory. John Wiley and Sons, New York City, New York, USA.

[23] Proakis JG (1995) Digital Communications. McGraw-Hill, New York City, New York, USA, 3rd edn.

[24] Pickholtz RL, Milstein LB & Schilling DL (1991) Spread spectrum for mobile communications. IEEE Transactions on Vehicular Technology 40(2): p 313–322.

[25] Gilhousen KS, Jacobs IM, Padovani R, Viterbi AJ, Weaver LA & Wheatley III CEW (1991) On the capacity of a cellular CDMA system. IEEE Transactions on Vehicular Technology 40(2): p 303–312.

[26] Schilling DL, Milstein LB, Pickholtz RL, Bruno F, Kanterakis E, Kullback M, Erceg V, Biederman W, Fishman D & Salerno D (1991) Broadband CDMA for personal communications systems. IEEE Communications Magazine 29(11): p 86–93.

[27] Jung P, Baier PW & Steil A (1993) Advantages of CDMA and spread spectrum techniques over FDMA and TDMA in cellular mobile radio applications. IEEE Transactions on Vehicular Technology 42(3): p 357–364.

[28] De Gaudenzi R, Giannetti F & Luise M (1996) Advances in satellite CDMA transmission for mobile and personal communications. Proceedings of the IEEE 84(1): p 18–39.

[29] Telecommunication Industry Association (1993) Mobile Station–Base Station Compatibility Standard for Dual-Mode Wideband Spread Spectrum Cellular Systems.

[30] Ross AHM & Gilhousen KS (1996) CDMA technology and the IS-95 north american standard. In: Gibson JD (ed) The Mobile Communications Handbook, CRC Press, chap 27, p 430–447.

[31] Ojanperä T, Rikkinen K, Häkkinen H, Pehkonen K, Hottinen A & Lilleberg J (1996) Design of a 3rd generation multirate CDMA systems with multiuser detection, MUD-CDMA. Proc. IEEE International Symposium on Spread Spectrum Techniques and Applications (ISSSTA), Mainz, Germany, 1: p 334–338.

[32] Hottinen A & Pehkonen K (1996) A flexible multirate CDMA concept with multiuser detection. Proc. IEEE International Symposium on Spread Spectrum Techniques and Applications (ISSSTA), Mainz, Germany, 2: p 556–560.

[33] Ojanperä T, Castro J, Emmer D, Gudmundson M, Jung P, Klein A, Kramer G, Pirhonen R, Rademacher L, Sköld J & Toskala A (1996) FRAMES – hybrid multiple access technology. Proc. IEEE International Symposium on Spread Spectrum Techniques and Applications (ISSSTA), Mainz, Germany, 1: p 320–324.

[34] Ovesjö F, Dahlman E, Ojanperä T, Toskala A & Klein A (1997) FRAMES multiple access mode 2 — wideband CDMA. Proc. IEEE International Symposium on Personal, Indoor, and Mobile Radio Communications (PIMRC), Helsinki, Finland, 1: p 42–46.

[35] Ohno K, Sawahashi M & Adachi F (1995) Wideband coherent DS-CDMA. Proc. IEEE Vehicular Technology Conference (VTC), Chicago, Illinois, USA, p 779–783.

[36] Adachi F, Sawahashi M, Dohi T & Ohno K (1996) Coherent DS-CDMA: Promising multiple access for wireless multimedia mobile communications. Proc. IEEE International Symposium on Spread Spectrum Techniques and Applications (ISSSTA), Mainz, Germany, 1: p 351–358.

[37] Fukasawa A, Sato T, Takizawa Y, Kato T, Kawabe M & Fisher RE (1996) Wideband CDMA system for personal radio communications. IEEE Communications Magazine 34(10): p 116–123.

[38] Pichna R & Wang Q (1996) Power control. In: Gibson JD (ed) The Mobile Communications Handbook, CRC Press, chap 23, p 370–380.

[39] Kärkkäinen K (1996) Code Families and Their Performance Measures for CDMA and Military Spread-Spectrum Systems. Acta Universitatis Ouluensis C89, University of Oulu Press, Oulu, Finland.

[40] Batra A & Barry JR (1995) Blind cancellation of co-channel interference. Proc. IEEE Global Telecommunication Conference (GLOBECOM), Singapore, 1: p 157–162.

[41] Haykin S (1991) Adaptive Filter Theory Prentice Hall, Englewood Cliffs, New Jersey, USA, 2nd edn.

[42] Widrow B & Stearns SD (1985) Adaptive Signal Processing. Prentice-Hall, Englewood Cliffs, New Jersey, USA.

[43] Schneider KS (1979) Optimum detection of code division multiplexed signals. IEEE Transactions on Aerospace and Electronic Systems 15(1): p 181–185.

[44] Kashihara TK (1980) Adaptive cancellation of mutual interference in spread spectrum multiple access. Proc. IEEE International Conference on Communications (ICC), p 44.4.1–44.4.5.

[45] Kohno R, Imai H & Hatori M (1983) Cancellation technique of co-channel interference in asynchronous spread-spectrum multiple-access systems. IEICE Transactions on Communications 65-A: p 416–423.

[46] Verdú S (1984) Optimum multiuser signal detection. Ph.D. thesis, Department of Electrical and Computer Engineering, University of Illinois at Urbana-Champaign, Urbana, Illinois, USA.

[47] Verdú S (1986) Minimum probability of error for asynchronous Gaussian multiple-access channels. IEEE Transactions on Information Theory 32(1): p 85–96.

[48] Verdú S (1986) Optimum multiuser asymptotic efficiency. IEEE Transactions on Communications 34(9): p 890–897.

[49] Verdú S (1993) Multiuser detection. In: Advances in Statistical Signal Processing. JAI Press, Greenwich, Connecticut, USA, 2: p 369–409.

[50] Duel-Hallen A, Holtzman J & Zvonar Z (1995) Multiuser detection for CDMA systems. IEEE/ACM Personal Communications 2: p 46–58.

[51] Moshavi S (1996) Multi-user detection for DS-CDMA communications. IEEE Communications Magazine 34(10): p 124–137.

[52] Jung P & Alexander PD (1996) A unified approach to multiuser detectors for CDMA and their geometrical interpretations. IEEE Journal on Selected Areas in Communications 14(8): p 1595–1601.

[53] Pursley MB (1977) Performance evaluation for phase-coded spread-spectrum multiple-access communication–Part I: System analysis. IEEE Transactions on Communications 25(8): p 795–799.

[54] Lupas R & Verdú S (1990) Near-far resistance of multiuser detectors in asynchronous channels. IEEE Transactions on Communications 38(4): p 496–508.

[55] Varanasi MK & Aazhang B (1990) Multistage detection in asynchronous code-division multiple-access communications. IEEE Transactions on Communications 38(4): p 509–519.

[56] Zvonar Z (1993) Multiuser detection for Rayleigh fading channels. Ph.D. thesis, Department of Electrical and Computer Engineering, Northeastern University, Boston, Massachusetts, USA.

[57] Latva-aho M & Lilleberg J (1998) Parallel interference cancellation in multiuser CDMA channel estimation. Wireless Personal Communications, Kluwer Academic Publishers, in press.

[58] Parsons JD (1992) The Mobile Radio Propagation Channel. Pentech Press, London, U.K.

[59] Ranta PA, Hottinen A & Honkasalo ZC (1995) Co-channel interference cancelling receiver for TDMA mobile systems. Proc. IEEE International Conference on Communications (ICC), Seattle, Washington, USA, 1: p 17–21.

[60] Blanz J, Klein A, Nasshan M & Steil A (1994) Performance of a cellular hybrid C/TDMA mobile radio system applying joint detection and coherent receiver antenna diversity. IEEE Journal on Selected Areas in Communications 12(4): p 568–579.

[61] Kramer G, Loher U, Ruprecht J & Jung P (1996) A comparison of demodulation techniques for code time division multiple access. Proc. IEEE Global Telecommunication Conference (GLOBECOM), London, U.K., 1: p 525–529.

[62] Mabuchi T, Kohno R & Imai H (1994) Multiuser detection scheme based on canceling cochannel interference for MFSK/FH-SSMA system. IEEE Journal on Selected Areas in Communications 12(4): p 593–604.

[63] Halford KW & Brandt-Pearce M (1996) Performance of a multistage multiuser detector for a frequency hopping multiple-access system. Proc. Conference on Information Sciences and Systems (CISS), Princeton University, Princeton, New Jersey, USA, 1: p 605–610.

[64] Haimovich A & Bar-Ness Y (1996) On the performance of a stochastic gradient-based decorrelation algorithm for multiuser multicarrier CDMA. Wireless Personal Communications, Kluwer Academic Publishers 2(4): p 357–371.

[65] Rasmussen LK & Lim TJ (1996) Detection techniques for direct sequence & multicarrier variable rate broadband CDMA. Proc. IEEE International Conference on Communication Systems and IEEE International Workshop on Intelligent Signal Processing & Communication Systems (ICCS/ISPACS), Singapore, 3: p 1526–1530.

[66] Sanada Y & Nakagawa M (1996) A multiuser interference cancellation technique utilizing convolutional codes and orthogonal multicarrier modulation for wireless indoor communications. IEEE Journal on Selected Areas in Communications 14(8): p 1500–1509.

[67] Vandendorpe L & van de Wiel O (1996) Performance analysis of linear joint equalization and multiple access interference cancellation for multitone CDMA. Wireless Personal Communications, Kluwer Academic Publishers 3(1-2): p 17–36.

[68] Beheshi S & Wornell GW (1997) Interference cancellation and decoding in spread-signature CDMA systems. Proc. IEEE Vehicular Technology Conference (VTC), Phoenix, Arizona, USA, 1: p 26–30.

[69] Lupas R (1989) Near-far resistant linear multiuser detection. Ph.D. thesis, Department of Electrical Engineering, Princeton University, Princeton, New Jersey, USA.

[70] Lupas R & Verdú S (1989) Linear multiuser detectors for synchronous code-division multiple-access channels. IEEE Transactions on Information Theory 34(1): p 123–136.

[71] Zvonar Z & Brady D (1994) Multiuser detection in single-path fading channels. IEEE Transactions on Communications 42(2/3/4): p 1729–1739.

[72] Vasudevan S & Varanasi MK (1996) Achieving near-optimum asymptotic efficiency and fading resistance over the time-varying Rayleigh-faded CDMA channel. IEEE Transactions on Communications 44(9): p 1130–1143.

[73] Varanasi MK & Vasudevan S (1994) Multiuser detectors for synchronous CDMA communication over non-selective Rician fading channels. IEEE Transactions on Communications 42(2/3/4): p 711–722.

[74] Vasudevan S & Varanasi MK (1994) Optimum diversity combiner based multiuser detection for time-dispersive Ricean fading CDMA channels. IEEE Journal on Selected Areas in Communications 12(4): p 580–592.

[75] Turin GL (1980) Introduction to spread-spectrum antimultipath techniques and their application to urban digital radio. Proceedings of the IEEE 68(3): p 328–353.

[76] Stein S (1987) Fading channel issues in system engineering. IEEE Journal on Selected Areas in Communications 5(2): p 68–89.

[77] Schwartz M, Bennett WR & Stein S (1966) Communication Systems and Techniques. McGraw-Hill, New York City, New York, USA.

[78] Mämmelä A (1995) Diversity Receivers in a Fast Fading Multipath Channel. VTT Publications 253, Technical Research Centre of Finland, Oulu, Finland.

[79] Price R & Green PE (1958) A communication technique for multipath channels. Proceedings of the IRE 46: p 555–570.

[80] Forney GD (1972) Maximum-likelihood sequence estimation of digital sequences in the presence of intersymbol interference. IEEE Transactions on Information Theory 18(3).

[81] Forney GD (1973) The Viterbi algorithm. Proceedings of the IEEE 61(3): p 268–278.

[82] Stojanovic M, Proakis JG & Catipovic JA (1995) Analysis of the impact of channel estimation errors on the performance of a decision-feedback equalizer in fading multipath channels. IEEE Transactions on Communications 43(2/3/4): p 877–886.

[83] Kam PY (1991) Optimal detection of digital data over the nonselective Rayleigh fading channel with diversity reception. IEEE Transactions on Communications 39(2): p 214–219.

[84] Kailath T (1960) Correlation detection of signals perturbed by a random channel. IRE Transactions on Information Theory 6(3): p 361–366.

[85] Van Trees HL (1971) Detection, Estimation, and Modulation Theory, Part III. John Wiley and Sons, New York City, New York, USA.

[86] Haeb R & Meyr H (1989) A systematic approach to carrier recovery and detection of digitally phase modulated signals on fading channels. IEEE Transactions on Communications 37(7): p 748–754.

[87] Tong L (1995) Blind sequence estimation. IEEE Transactions on Communications 43(12): p 2986–2994.

[88] Kay S (1993) Fundamentals of Statistical Signal Processing: Estimation Theory. Prentice-Hall, Englewood Cliffs, New Jersey, USA.

[89] Gardner FM (1990) Demodulator reference recovery techniques suited for digital implementation. Technical Report, ESTEC Contract no. 6847/86/NL/DG, European Space Agency.

[90] Davarian F (1989) Mobile digital communications via tone calibration. IEEE Transactions on Vehicular Technology 36(2): p 55–62.

[91] Cavers JK (1991) Performance of tone calibration with frequency offset and imperfect pilot filter. IEEE Transactions on Vehicular Technology 40(2): p 426–434.

[92] Li HWH & Cavers JK (1991) An adaptive filtering technique for pilot-aided transmission systems. IEEE Transactions on Vehicular Technology 40(3): p 532–545.

[93] Moher ML & Lodge JH (1989) TCMP — a modulation and coding strategy for Ricean fading channels. IEEE Journal on Selected Areas in Communications 7(9): p 1347–1355.

[94] Aghamohammadi A, Meyr H & Ascheid G (1991) A new method for phase synchronization and automatic gain control of linearly modulated signals on frequency-flat fading channels. IEEE Transactions on Communications 39(1): p 25–29.

[95] Cavers JK (1991) An analysis of pilot symbol assisted modulation for Rayleigh fading channels. IEEE Transactions on Vehicular Technology 40(4): p 686–693.

[96] Lo NWK, Falconer DD & Sheikh AUH (1991) Adaptive equalization and diversity combing for mobile radio using interpolated channel estimates. IEEE Transactions on Vehicular Technology 40(3): p 636–645.

[97] Irvine GT & McLane PJ (1992) Symbol-aided plus decision-directed reception for PSK/TCM modulation on shadowed mobile satellite fading channels. IEEE Journal on Selected Areas in Communications 10(8): p 1289–1299.

[98] Fechtel SA & Meyr H (1994) Optimal parametric feedforward estimation of frequency-selective fading radio channels. IEEE Transactions on Communications 42(2/3/4): p 1639–1650.

[99] Mämmelä A & Kaasila VP (1997) Smoothing and interpolation in diversity reception. International Journal of Wireless Information Networks, in press.

[100] Kam PY & Teh CH (1983) Reception of PSK signals over fading channels via quadrature amplitude estimation. IEEE Transactions on Communications 31(8): p 1024–1027.

[101] Kam PY & Teh CH (1984) An adaptive receiver with memory for slowly fading channels. IEEE Transactions on Communications 32(6): p 654–659.

[102] Kam PY & Teh CH (1987) Adaptive diversity reception over a slow nonselective fading channel. IEEE Transactions on Communications 35(5): p 572–574.

[103] Liu Y & Blostein SD (1995) Identification of frequency non-selective fading channels using decision feedback and adaptive linear prediction. IEEE Transactions on Communications 43(2/3/4): p 1484–1492.

[104] Viterbi AJ & Viterbi AM (1983) Nonlinear estimation of PSK-modulated carrier phase with application to burst digital transmission. IEEE Transactions on Information Theory 29(4): p 543–551.

[105] Xu G, Liu H, Tong L & Kailath T (1995) A least-squares approach to blind channel identification. IEEE Transactions on Signal Processing 43(12): p 2982–2993.

[106] Zeng HH & Tong L (1995) Blind channel estimation: Comparison studies and a new algorithm. Proc. IEEE International Conference on Communications (ICC), Seattle, Washington, USA, 1: p 12–16.

[107] Tsatsanis MK (1995) Time-varying system identification and channel equalization using wavelets and higher-order statistics. In: Leondes CT (ed) Control and Dynamic Systems: Advances in Theory and Applications, Academic Press, San Diego, California, USA, 68: p 333–394.

[108] Zvonar Z (1996) Multiuser detection in asynchronous CDMA frequency-selective fading channels. Wireless Personal Communications, Kluwer Academic Publishers 3(3–4): p 373–392.

[109] Lu L & Sun W (1997) The minimal eigenvalues of a class of block-tridiagonal matrices. IEEE Transactions on Information Theory 43(2): p 787–791.

[110] Schlegel C & Wei L (1997) A simple way to compute the minumum distance in multiuser CDMA systems. IEEE Transactions on Communications 45(5): p 532–535.

[111] Fawer U & Aazhang B (1996) Multiuser receivers for code-division multiple-access systems with trellis-based modulation. IEEE Journal on Selected Areas in Communications 14(8): p 1602–1609.

[112] Giallorenzi TR & Wilson SG (1996) Multiuser ML sequence estimator for convolutionally coded asynchronous DS-CDMA systems. IEEE Transactions on Communications 44(8): p 997–1007.

[113] Gray SD, Kocic M & Brady D (1995) Multiuser detection in mismatched multiple-access channels. IEEE Transactions on Communications 43(12): p 3080–3089.

[114] Poor HV (1989) On parameter estimation in DS/SSMA formats. In: Porter WA & Kak SC (eds) Advances in Communications and Signal Processing, Springer-Verlag, Berlin–Heidelberg, Germany, vol 129 of Lecture Notes in Control and Information Sciences, p 59–70.

[115] Xie Z, Rushforth CK, Short RT & Moon TK (1993) Joint signal detection and parameter estimation in multiuser communications. IEEE Transactions on Communications 41(7): p 1208–1216.

[116] Hagmanns FJ & Hespelt V (1994) On the detection of bandlimited direct-sequence spread-spectrum signals transmitted via fading multipath channels. IEEE Journal on Selected Areas in Communications 12(5): p 891–899.

[117] Sung PA & Chen KC (1996) A linear minimum mean square error multiuser receiver in Rayleigh-fading channels. IEEE Journal on Selected Areas in Communications 14(8): p 1583–1594.

[118] Lilleberg J, Nieminen E & Latva-aho M (1996) Blind iterative multiuser delay estimator for CDMA. Proc. IEEE International Symposium on Personal, Indoor, and Mobile Radio Communications (PIMRC), Taipei, Taiwan, 2: p 565–568.

[119] Poor HV & Verdú S (1988) Single-user detectors for multiuser channels. IEEE Transactions on Communications 36(1): p 50–60.

[120] Klein A & Baier PW (1993) Linear unbiased data estimation in mobile radio systems applying CDMA. IEEE Journal on Selected Areas in Communications 11(7): p 1058–1066.

[121] Varanasi MK & Aazhang B (1991) Optimally near-far resistant multiuser detection in differentially coherent synchronous channels. IEEE Transactions on Information Theory 37(4): p 1006–1018.

[122] Varanasi MK (1993) Noncoherent detection in asynchronous multiuser channels. IEEE Transactions on Information Theory 39(1): p 157–176.

[123] Zvonar Z & Brady D (1995) Suboptimal multiuser detector for frequency-selective Rayleigh fading synchronous CDMA channels. IEEE Transactions on Communications 43(2/3/4): p 154–157.

[124] Klein A (1996) Multi-user detection of CDMA signals – algorithms and their application to cellular mobile radio. VDI-Verlag, Düsseldorf, Germany.

[125] Zvonar Z & Brady D (1995) Differenially coherent multiuser detection in asynchronous CDMA flat Rayleigh fading channels. IEEE Transactions on Communications 43(2/3/4): p 1252–1255.

[126] Stojanovic M & Zvonar Z (1996) Linear multiuser detection in time-varying multipath fading channels. Proc. Conference on Information Sciences and Systems (CISS), Princeton University, Princeton, New Jersey, USA, 1: p 349–354.

[127] Stojanovic M & Zvonar Z (1996) Performance of linear multiuser detectors in time-varying multipath fading CDMA channels. Proc. Communication Theory Mini-Conference (CTMC) in conjunction with IEEE Global Telecommunication Conference (GLOBECOM), London, U.K., p 163–167.

[128] Kawahara T & Matsumoto T (1995) Joint decorrelating multiuser detection and channel estimation in asynchronous CDMA mobile communications channels. IEEE Transactions on Vehicular Technology 44(3): p 506–515.

[129] Huang HC (1996) Combined multipath processing, array processing, and multiuser detection for DS-CDMA channels. Ph.D. thesis, Department of Electrical Engineering, Princeton University, Princeton, New Jersey, USA.

[130] Miller SY (1989) Detection and estimation in multiple-access channels. Ph.D. thesis, Department of Electrical Engineering, Princeton University, Princeton, New Jersey, USA.

[131] Miller SY & Schwartz SC (1995) Integrated spatial-temporal detectors for asynchronous Gaussian multiple-access channels. IEEE Transactions on Communications 43(2/3/4): p 396–411.

[132] Jung P, Blanz J, Nasshan M & Baier PW (1994) Simulation of the uplink of JD-CDMA mobile radio systems with coherent receiver antenna diversity. Wireless Personal Communications, Kluwer Academic Publishers 1(2): p 61–89.

[133] Jung P & Blanz J (1995) Joint detection with coherent receiver antenna diversity in CDMA mobile radio systems. IEEE Transactions on Vehicular Technology 44(1): p 76–88.

[134] Brown T & Kaveh M (1995) A decorrelating detector for use with antenna arrays. International Journal of Wireless Information Networks 2(4): p 239–246.

[135] Zvonar Z (1996) Combined multiuser detection and diversity reception for wireless CDMA systems. IEEE Transactions on Vehicular Technology 45(1): p 205–211.

[136] Kandala S, Sousa ES & Pasupathy S (1995) Multi-user multi-sensor detectors for CDMA networks. IEEE Transactions on Communications 43(2/3/4): p 946–957.

[137] Kandala S, Sousa ES & Pasupathy S (1995) Decorrelators for multi-sensor systems in CDMA networks. European Transactions on Telecommunications 6(1): p 29–40.

[138] Juntti MJ & Lilleberg JO (1997) Comparative analysis of conventional and multiuser detectors in multisensor receivers. Proc. IEEE Military Communications Conference (MILCOM), Monterey, California, USA.

[139] Saquib M, Yates R & Mandayam N (1996) Decorrelating detectors for a dual rate synchronous DS/CDMA system. Proc. IEEE Vehicular Technology Conference (VTC), Atlanta, Georgia, USA, 1: p 377–381.

[140] Juntti MJ & Lilleberg JO (1997) Linear FIR multiuser detection for multiple data rate CDMA systems. Proc. IEEE Vehicular Technology Conference (VTC), Phoenix, Arizona, USA, 2: p 455–459.

[141] Chen DS & Roy S (1994) An adaptive multiuser receiver for CDMA systems. IEEE Journal on Selected Areas in Communications 12(6): p 808–816.

[142] Mitra U & Poor HV (1996) Analysis of an adaptive decorrelating detector for synchronous CDMA channels. IEEE Transactions on Communications 44(2): p 257–268.

[143] Mitra U & Poor HV (1996) Adaptive decorrelating detectors for CDMA systems. Wireless Personal Communications, Kluwer Academic Publishers 2(4): p 415–440.

[144] Giallorenzi TR & Wilson SG (1996) Suboptimum multiuser receivers for convolutionally coded asynchronous DS-CDMA systems. IEEE Transactions on Communications 44(9): p 1183–1196.

[145] Kajiwara A & Nakagawa M (1994) Microcellular CDMA system with a linear multiuser interference canceler. IEEE Journal on Selected Areas in Communications 12(4): p 605–611.

[146] Van Heeswyk F, Falconer DD & Sheikh AUH (1996) Decorrelating detectors for quasi-synchronous CDMA. Wireless Personal Communications, Kluwer Academic Publishers 3(1-2): p 129–147.

[147] Van Heeswyk F, Falconer DD & Sheikh AUH (1996) A delay independent decorrelating detector for quasi-synchronous CDMA. IEEE Journal on Selected Areas in Communications 14(8): p 1619–1626.

[148] Iltis RA & Mailaender L (1996) Multiuser detection of quasisynchronous CDMA signals using linear decorrelators. IEEE Transactions on Communications 44(11): p 1561–1571.

[149] Iltis RA (1996) Demodulation and code acquisition using decorrelator detectors for QS-CDMA. IEEE Transactions on Communications 44(11): p 1553–1560.

[150] Zheng FC & Barton SK (1995) On the performance of near-far resistant CDMA detectors in the presence of synchronization errors. IEEE Transactions on Communications 43(12): p 3037–3045.

[151] Parkvall S, Ström E & Ottersten B (1996) The impact of timing errors on the performance of linear DS-CDMA receivers. IEEE Journal on Selected Areas in Communications 14(8): p 1660–1668.

[152] Paris BP (1994) Finite precision decorrelating receiver for multiuser CDMA communication systems. IEEE Transactions on Communications 44(4): p 496–507.

[153] Bulumulla S & Venkatesh SS (1996) On the quantized input decorrelating detector. Proc. Conference on Information Sciences and Systems (CISS), Princeton University, Princeton, New Jersey, USA, 1: p 595–598.

[154] Duel-Hallen A (1995) A family of multiuser decision-feedback detectors for asynchronous code-division multiple-access channels. IEEE Transactions on Communications 43(2/3/4): p 421–434.

[155] Duel-Hallen A (1993) Decorrelating decision-feedback multiuser detector for synchronous code-division multiple-access channel. IEEE Transactions on Communications 41(2): p 285–290.

[156] Golub GH & van Loan CF (1989) Matrix Computations. The Johns Hopkins University Press, Baltimore, Maryland, USA, 2nd edn.

[157] Wei L & Schlegel C (1994) Synchronous DS-SSMA system with improved decorrelating decision-feedback multiuser detection. IEEE Transactions on Vehicular Technology 43(3): p 767–772.

[158] Wei L & Rasmussen LK (1996) A near ideal noise whitening filter for an asynchronous time-varying CDMA system. IEEE Transactions on Communications 44(10): p 1355–1361.

[159] Schlegel C, Roy S, Alexander PD & Xiang ZJ (1996) Multiuser projection receivers. IEEE Journal on Selected Areas in Communications 14(8): p 1610–1618.

[160] Madhow U & Honig ML (1994) MMSE interference suppression for direct-sequence spread-spectrum CDMA. IEEE Transactions on Communications 42(12): p 3178–3188.

[161] Xie Z, Short RT & Rushforth CK (1990) A family of suboptimum detectors for coherent multiuser communications. IEEE Journal on Selected Areas in Communications 8(4): p 683–690.

[162] Klein A, Kaleh GK & Baier PW (1996) Zero forcing and minimum mean-square-error equalization for multiuser detection in code-division multiple access channels. IEEE Transactions on Vehicular Technology 45(2): p 276–287.

[163] Wu WC & Chen KC (1996) Linear multiuser detectors for synchronous CDMA communication over Rayleigh fading channels. Proc. IEEE International Symposium on Personal, Indoor, and Mobile Radio Communications (PIMRC), Taipei, Taiwan, p 578–582.

[164] Bernstein X & Haimovich AM (1996) Space-time optimum combining for CDMA communications. Wireless Personal Communications, Kluwer Academic Publishers 3(1-2): p 73–89.

[165] Gray SD, Preisig JC & Brady D (1997) Multiuser detection in a horizontal underwater acoustic channel using array observations. IEEE Transactions on Signal Processing 45(1): p 148–160.

[166] Honig ML & Veerakachen W (1996) Performance variability of linear multiuser detection for DS/CDMA. Proc. IEEE Vehicular Technology Conference (VTC), Atlanta, Georgia, USA, 1: p 372–376.

[167] Poor HV & Verdú S (1997) Probability of error in MMSE multiuser detection. IEEE Transactions on Information Theory 43(3): p 858–871.

[168] Rapajic PB & Vucetic BS (1994) Adaptive receiver structures for asynchronous CDMA systems. IEEE Journal on Selected Areas in Communications 12(4): p 685–697.

[169] Rapajic PB & Vucetic BS (1995) Linear adaptive transmitter-receiver structures for asynchronous CDMA systems. European Transactions on Telecommunications 6(1): p 21–27.

[170] Miller SL (1995) An adaptive direct-sequence code-division multiple-access receiver for multiuser interference rejection. IEEE Transactions on Communications 43(2/3/4): p 1746–1755.

[171] Miller SL (1996) Training analysis of adaptive interference suppression for direct-sequence code-division multiple-access systems. IEEE Transactions on Communications 44(4): p 488–495.

[172] Lee KB (1996) Orthogonalization based adaptive interference suppression for direct-sequence code-division multiple-access systems. IEEE Transactions on Communications 44(9): p 1082–1085.

[173] Woodward G, Rapajic P & Vucetic BS (1996) Adaptive algorithms for asynchronous DS-CDMA receivers. Proc. IEEE International Symposium on Personal, Indoor, and Mobile Radio Communications (PIMRC), Taipei, Taiwan, p 583–587.

[174] Latva-aho M & Juntti M (1997) Modified adaptive LMMSE receiver for DS-CDMA systems in fading channels. Proc. IEEE International Symposium on Personal, Indoor, and Mobile Radio Communications (PIMRC), Helsinki, Finland, 2: p 554–558.

[175] Veeravalli VV & Aazhang B (1996) On the coding-spreading tradeoff in CDMA systems. Proc. Conference on Information Sciences and Systems (CISS), Princeton University, Princeton, New Jersey, USA, 2: p 1136–1141.

[176] Oppermann I & Vucetic BS (1996) Capacity of a coded direct sequence spread spectrum system over fading satellite channels using an adaptive LMS-MMSE receiver. IEICE Transactions on Fundamentals of Electronics Communications and Computer Sciences E79-A(12): p 2043–2049.

[177] Chu LC & Mitra U (1996) Improved MMSE-based multi-user detectors for mismatched delay channels. Proc. Conference on Information Sciences and Systems (CISS), Princeton University, Princeton, New Jersey, USA, 1: p 326–331.

[178] Honig ML, Madhow U & Verdú S (1995) Blind adaptive multiuser detection. IEEE Transactions on Information Theory 41(3): p 944–960.

[179] Schodorf JB & Williams DB (1997) A constrained optimization approach to multiuser detection. IEEE Transactions on Signal Processing 45(1): p 258–262.

[180] Tsatsanis MK (1997) Inverse filtering criteria for CDMA systems. IEEE Transactions on Signal Processing 45(1): p 102–112.

[181] Wang X & Poor HV (1997) Multiuser diversity receivers for frequency-selective Rayleigh fading CDMA channels. Proc. IEEE Vehicular Technology Conference (VTC), Phoenix, Arizona, USA, 1: p 198–202.

[182] Madhow U (1997) Blind adaptive interference suppression for the near-far resistant acquisition and demodulation of direct-sequence CDMA. IEEE Transactions on Signal Processing 45(1): p 124–136.

[183] Mangalvedhe NR & Reed JH (1997) Blind CDMA interference rejection in multipath channels. Proc. IEEE Vehicular Technology Conference (VTC), Phoenix, Arizona, USA, 1: p 21–25.

[184] Rupf M, Tarkoy F & Massey JL (1994) User-separating demodulation for code-division multiple-access systems. IEEE Journal on Selected Areas in Communications 12(6): p 786–795.

[185] Monk AM, Davis M, Milstein LB & Helstrom CW (1994) A noise-whitening approach to multiple access noise rejection–Part I: Theory and background. IEEE Journal on Selected Areas in Communications 12(5): p 817–827.

[186] Davis M, Monk A & Milstein LB (1996) A noise whitening approach to multiple-access noise rejection–Part II: Implementation issues. IEEE Journal on Selected Areas in Communications 14(8): p 1488–1499.

[187] Yoon YC & Leib H (1996) Matched filters with interference suppression capabilities for DS-CDMA. IEEE Journal on Selected Areas in Communications 14(8): p 1510–1521.

[188] Mailander L & Iltis R (1996) Single user CDMA detection using the whitened matched filter. Proc. Conference on Information Sciences and Systems (CISS), Princeton University, Princeton, New Jersey, USA, 2: p 846–851.

[189] Zheng FC & Barton SK (1995) Near-far resistant detection of CDMA signals via isolation bit insertion. IEEE Transactions on Communications 43(2/3/4): p 1313–1317.

[190] Moshavi S, Kanterakis EG & Schilling DL (1996) Multistage linear receivers for DS-CDMA systems. International Journal of Wireless Information Networks 3(1): p 1–17.

[191] Wijayasuriya SSH, Norton GH & McGeehan JP (1996) A sliding window decorrelating receiver for multiuser DS-CDMA mobile radio networks. IEEE Transactions on Vehicular Technology 45(3): p 503–521.

[192] Kajiwara A & Nakagawa M (1991) Crosscorrelation cancellation in SS/DS block demodulator. IEICE Transactions on Communications E 74(9): p 2596–2602.

[193] Tsatsanis MK & Giannakis GB (1996) Optimal decorrelating receivers for DS-CDMA systems: A signal processing framework. IEEE Transactions on Signal Processing 44(12): p 3044–3055.

[194] Wijayasuriya SSH, Norton GH & McGeehan JP (1993) A novel algorithm for dynamic updating of decorrelator coefficients in mobile DS-CDMA. Proc. IEEE International Symposium on Personal, Indoor, and Mobile Radio Communications (PIMRC), Yokohama, Japan p 292–296.

[195] Yang LL & Scholtz RA (1996) $\delta$-adjusted $m$th order multiuser detector. Proc. IEEE Global Telecommunication Conference (GLOBECOM), London, U.K., 3: p 1555–1560.

[196] Varanasi MK (1989) Multiuser detection in code-division multiple-access communications. Ph.D. thesis, Department of Electrical and Computer Engineering, Rice University, Houston, Texas, USA.

[197] Varanasi MK & Aazhang B (1991) Near-optimum detection in synchronous code-division multiple-access systems. IEEE Transactions on Communications 39(5): p 725–736.

[198] Mowbray RS, Pringle RD & Grant PM (1992) Increased CDMA system capacity through adaptive cochannel interference regeneration and cancellation. IEE Proceedings I 139(5): p 515–524.

[199] Tachikawa S (1992) Characteristics of M-ary/spread spectrum multiple access communication systems using co-channel interference cancellation techniques. IEICE Transactions on Communications E76-B(8): p 941–946.

[200] Abrams BS, Zeger AE & Jones TE (1995) Efficiently structured CDMA receiver with near-far immunity. IEEE Transactions on Vehicular Technology 44(1): p 1–13.

[201] Sanada Y & Wang Q (1996) A co-channel interference cancellation technique using orthogonal convolutional codes. IEEE Transactions on Communications 44(5): p 549–556.

[202] Kohno R, Imai H, Hatori M & Pasupathy S (1990) Combination of an adaptive array antenna and a canceller of interference for direct-sequence spread-spectrum multiple-access system. IEEE Journal on Selected Areas in Communications 8(4): p 675–682.

[203] Yoon YC, Kohno R & Imai H (1993) Cascaded co-channel interference cancellating and diversity combining for spread-spectrum multi-access system over multipath fading channels. IEICE Transactions on Communications E76-B(2): p 163–168.

[204] Yoon YC, Kohno R & Imai H (1993) A spread-spectrum multiaccess system with cochannel interference cancellation for multipath fading channels. IEEE Journal on Selected Areas in Communications 11(7): p 1067–1075.

[205] Saifuddin A, Kohno R & Imai H (1995) Integrated receiver structures of staged decoder and CCI canceller for CDMA with multilevel coded modulation. European Transactions on Telecommunications 6(1): p 9–19.

[206] Saifuddin A & Kohno R (1995) Performance evaluation of near-far resistant receiver DS/CDMA cellular system over fading multipath channel. IEICE Transactions on Communications E78-B(8): p 1136–1144.

[207] Fawer U & Aazhang B (1995) A multiuser receiver for code division multiple access communications over multipath channels. IEEE Transactions on Communications 43(2/3/4): p 1556–1565.

[208] Sanada Y & Wang Q (1997) A co-channel interference cancellation technique using orthogonal convolutional codes on multipath Rayleigh fading channel. IEEE Transactions on Vehicular Technology 46(1): p 114–128.

[209] Hottinen A, Holma H & Toskala A (1995) Performance of multistage multiuser detection in a fading multipath channel. Proc. IEEE International Symposium on Personal, Indoor, and Mobile Radio Communications (PIMRC), Toronto, Ontario, Canada, 3: p 960–964.

[210] Holma H, Toskala A & Hottinen A (1996) Performance of CDMA multiuser detection with antenna diversity and closed loop power control. Proc. IEEE Vehicular Technology Conference (VTC), Atlanta, Georgia, USA, 1: p 362–366.

[211] Latva-aho M & Lilleberg J (1996) Parallel interference cancellation in multiuser detection. Proc. IEEE International Symposium on Spread Spectrum Techniques and Applications (ISSSTA), Mainz, Germany, 3: p 1151–1155.

[212] Saifuddin A & Kohno R (1996) Performance evaluation of DS/CDMA scheme with diversity coding and MUI cancellation over fading multipath channel. IEICE Transactions on Fundamentals of Electronics Communications and Computer Sciences E79-A(12): p 1994–2001.

[213] Hottinen A, Holma H & Toskala A (1996) Multiuser detection for multirate CDMA communications. Proc. IEEE International Conference on Communications (ICC), Dallas, Texas, USA.

[214] Latva-aho M & Lilleberg J (1996) Parallel interference cancellation based delay tracker for CDMA receivers. Proc. Conference on Information Sciences and Systems (CISS), Princeton University, Princeton, New Jersey, USA, 2: p 852–857.

[215] Latva-aho M & Lilleberg J (1996) Delay trackers for multiuser CDMA receivers. Proc. IEEE International Conference on Universal Personal Communications (ICUPC), Boston, Massachusetts, USA, 1: p 326–330.

[216] Buehrer RM, Kaul A, Striglis S & Woerner BD (1996) Analysis of DS-CDMA parallel interference cancellation with phase and timing errors. IEEE Journal on Selected Areas in Communications 14(8): p 1522–1535.

[217] Buehrer RM, Correal NS & Woerner BD (1996) A comparison of multiuser receivers for cellular CDMA. Proc. IEEE Global Telecommunication Conference (GLOBECOM), London, U.K., 3: p 1571–1577.

[218] Agashe P & Woerner B (1996) Interference cancellation for a multicellular CDMA environment. Wireless Personal Communications, Kluwer Academic Publishers 3(1-2): p 1–15.

[219] Chen DW, Siveski Z & Bar-Ness Y (1994) Synchronous multiuser CDMA detector with soft decision adaptive canceler. Proc. Conference on Information Sciences and Systems (CISS), Princeton University, Princeton, New Jersey, USA, 1: p 139–143.

[220] Bar-Ness Y & Sezgin N (1995) Adaptive threshold setting for multiuser CDMA signal separators with soft tentative decisions. Proc. Conference on Information Sciences and Systems (CISS), The Johns Hopkins University, Baltimore, Maryland, USA, p 174–179.

[221] Vanghi V & Vojcic B (1996) Soft interference cancellation in multiuser communications. Wireless Personal Communications, Kluwer Academic Publishers 3(1-2): p 111–128.

[222] Bar-Ness Y, Siveski Z & Chen DW (1994) Bootstrapped decorrelating algorithm for adaptive interference cancelation in synchronous CDMA communications systems. Proc. IEEE International Symposium on Spread Spectrum Techniques and Applications (ISSSTA), Oulu, Finland, 1: p 162–166.

[223] Zhu B, Ansari N & Siveski Z (1995) Convergence and stability analysis of a synchronous adaptive CDMA receiver. IEEE Transactions on Communications 43(12): p 3073–3079.

[224] Bar-Ness Y & Punt JB (1996) Adaptive 'bootstrap' CDMA multi-user detector. Wireless Personal Communications, Kluwer Academic Publishers 3(1-2): p 55–71.

[225] Elders-Boll H, Herper M & Busboom A (1997) Adaptive receivers for mobile DS-CDMA communication systems. Proc. IEEE Vehicular Technology Conference (VTC), Phoenix, Arizona, USA, 3: p 2128–2132.

[226] Divsalar D & Simon M (1995) Improved CDMA performance using parallel interference cancellation. Technical Report, Jet Propulsion Laboratory, California Institute of Technology, Pasadena, California, USA.

[227] Divsalar D & Simon M (1996) A new approach to parallel interference cancellation for CDMA. Proc. IEEE Global Telecommunication Conference (GLOBECOM), London, U.K., 3: p 1452–1457.

[228] Correal NS, Buehrer RM & Woerner BD (1997) Improved CDMA performance through bias reduction for parallel interference cancellation. Proc. IEEE International Symposium on Personal, Indoor, and Mobile Radio Communications (PIMRC), Helsinki, Finland, 2: p 565–569.

[229] Radović A & Aazhang B (1993) Iterative algorithms for joint data detection and delay estimation for code division multiple access communication systems. Proc. Annual Allerton Conference on Communications, Control, and Computing, Allerton House, Monticello, Illinois, USA.

[230] Nelson LB & Poor HV (1996) Iterative multiuser receivers for CDMA channels: An EM-based approach. IEEE Transactions on Communications 44(12): p 1700–1710.

[231] Dahlhaus D, Fleury H & Radović A (1998) A sequential algorithm for joint parameter estimation and multiuser detection in DS/CDMA systems with multipath propagation. Wireless Personal Communications, Kluwer Academic Publishers, in press.

[232] Dahlhaus D, Jarosch A, Fleury H & Heddergott R (1997) Joint demodulation in DS/CDMA systems exploiting the space and time diversity of the mobile radio channel. Proc. IEEE International Symposium on Personal, Indoor, and Mobile Radio Communications (PIMRC), Helsinki, Finland, 1: p 47–52.

[233] Viterbi AJ (1990) Very low rate convolutional codes for maximum theoretical performance of spread-spectrum multiple-access channels. IEEE Journal on Selected Areas in Communications 8(4): p 641–649.

[234] Patel P & Holtzman J (1994) Analysis of a simple successive interference cancellation scheme in a DS/CDMA system. IEEE Journal on Selected Areas in Communications 12(10): p 796–807.

[235] Soong ACK & Krzymien WA (1995) Performance of a reference symbol assisted multistage successive interference cancelling receiver in a multi-cell CDMA wireless systems. Proc. IEEE Global Telecommunication Conference (GLOBECOM), Singapore, 1: p 152–156.

[236] Soong ACK & Krzymien WA (1996) A novel CDMA multiuser interference cancellation receiver with reference symbol aided estimation of channel parameters. IEEE Journal on Selected Areas in Communications 14(8): p 1536–1547.

[237] Nesper O & Ho P (1996) A reference symbol assisted interference cancelling hybrid receiver for an asynchronous DS/CDMA system. Proc. IEEE International Symposium on Personal, Indoor, and Mobile Radio Communications (PIMRC), Taipei, Taiwan, 1: p 108–112.

[238] Nesper O & Ho P (1996) A pilot symbol assisted interference cancellation scheme for an asynchronous DS/CDMA system. Proc. IEEE Global Telecommunication Conference (GLOBECOM), London, U.K., 3: p 1447–1451.

[239] Soong ACK & Krzymien WA (1997) Performance of a reference symbol assisted multi-stage successive interference cancelling receiver with quadriphase spreading. Proc. IEEE Vehicular Technology Conference (VTC), Phoenix, Arizona, USA, 2: p 460–464.

[240] Johansson AL & Svensson A (1995) Successive interference cancellation in multiple data rate DS/CDMA systems. Proc. IEEE Vehicular Technology Conference (VTC), Chicago, Illinois, USA, p 704–708.

[241] Johansson AL & Svensson A (1996) Multistage interference cancellation in multirate DS/CDMA on a mobile radio channel. Proc. IEEE Vehicular Technology Conference (VTC), Atlanta, Georgia, USA, 2: p 666–670.

[242] Cheng FC & Holtzman JM (1994) Effect of tracking error on DS/CDMA successive interference cancellation. Technical Report, WINLAB-TR-90 WINLAB, Rutgers University, Piscataway, New Jersey, USA.

[243] Soong ACK & Krzymien WA (1996) Robustness of the reference symbol assisted multistage successive interference cancelling receiver with imperfect parameter estimates. Proc. IEEE Vehicular Technology Conference (VTC), Atlanta, Georgia, USA, 2: p 676–680.

[244] Oon TB, Steele R & Li Y (1997) Performance of an adaptive successive serial-parallel CDMA cancellation scheme in flat Rayleigh fading channels. Proc. IEEE Vehicular Technology Conference (VTC), Phoenix, Arizona, USA, 1: p 193–197.

[245] Van der Wijk F, Janssen GMJ & Prasad R (1995) Groupwise successive interference cancellation in a DS/CDMA system. Proc. IEEE International Symposium on Personal, Indoor, and Mobile Radio Communications (PIMRC), Toronto, Ontario, Canada, 2: p 742–746.

[246] Haifeng W, Lilleberg J & Rikkinen K (1997) A new sub-optimal multiuser detection approach for CDMA systems in Rayleigh fading channel. Proc. Conference on Information Sciences and Systems (CISS), The Johns Hopkins University, Baltimore, Maryland, USA, 1: p 276–280.

[247] Alexander PD, Rasmussen LK & Schlegel C (1997) A linear receiver for coded multiuser CDMA. IEEE Transactions on Communications 45(5): p 605–610.

[248] Juntti MJ (1998) Multiuser detector performance comparisons in multirate CDMA systems. Proc. IEEE Vehicular Technology Conference (VTC), Ottawa, Canada, submitted.

[249] Juntti MJ (1997) Performance of multiuser detection in multirate CDMA systems. Wireless Personal Communications, Kluwer Academic Publishers, submitted.

[250] Varanasi MK (1995) Group detection in synchronous Gaussian code-division multiple-access channels. IEEE Transactions on Information Theory 41(3): p 1083–1096.

[251] Varanasi MK (1995) Parallel group detection for synchronous CDMA communication over frequency-selective Rayleigh fading channels. IEEE Transactions on Information Theory 41(3): p 1083–1096.

[252] Abdulrahman M, Sheikh AUH & Falconer DD (1994) Decision feedback equalization for CDMA in indoor wireless communications. IEEE Journal on Selected Areas in Communications 12(4): p 698–706.

[253] Hafeez A & Stark WE (1996) Combined decision-feedback multiuser detection/soft-decision decoding for CDMA channels. Proc. IEEE Vehicular Technology Conference (VTC), Atlanta, Georgia, USA, 1: p 382–386.

[254] Xie Z, Rushforth CK & Short R (1990) Multiuser signal detection using sequential decoding. IEEE Transactions on Communications 38(5): p 578–583.

[255] Wu B & Wang Q (1996) New suboptimal multiuser detectors for synchronous CDMA systems. IEEE Transactions on Communications 44(7): p 782–785.

[256] Juntti MJ, Schlösser T & Lilleberg JO (1997) Genetic algorithms for multiuser detection in synchronous CDMA. Proc. IEEE International Symposium on Information Theory (ISIT), Ulm, Germany, p 492.

[257] Iltis RA & Mailaender L (1994) Multiuser code acquisition using parallel decorrelators. Proc. Conference on Information Sciences and Systems (CISS), Princeton, New Jersey, USA, 1: p 109–114.

[258] Ström EG, Parkvall S, Miller SL & Ottersen BE (1996) Propagation delay estimation in asynchronous direct-sequence code-division multiple access systems. IEEE Transactions on Communications 44(1): p 84–93.

[259] Steiner B & Jung P (1994) Optimum and suboptimum channel estimation for the uplink of CDMA mobile radio systems with joint detection. European Transactions on Telecommunications 5(1): p 39–50.

[260] Ström EG, Parkvall S, Miller SL & Ottersten BE (1996) DS-CDMA synchronization in time-varying fading channels. IEEE Journal on Selected Areas in Communications 14(8): p 1636–1642.

[261] Bensley SE & Aazhang B (1996) Subspace-based channel estimation for code division multiple access communication systems. IEEE Transactions on Communications 44(8): p 1009–1019.

[262] Parkvall S, Ström EG & Milstein LB (1996) Coded asynchronous near-far resistant DS-CDMA receivers operating without synchronization. Proc. Communication Theory Mini-Conference (CTMC) in conjunction with IEEE Global Telecommunication Conference (GLOBECOM), London, U.K., p 183–187.

[263] Torlak M & Xu G (1997) Blind multiuser channel estimation in asyncronous CDMA systems. IEEE Transactions on Signal Processing 45(1): p 137–147.

[264] Joutsensalo J, Lilleberg J, Hottinen A & Karhunen J (1996) A hierarchic maximum likelihood method for delay estimation in CDMA. Proc. IEEE Vehicular Technology Conference (VTC), Atlanta, Georgia, USA, 1: p 188–192.

[265] Zheng D, Li J, Miller SL & Ström EG (1997) An efficient code-timing estimator for DS-CDMA signals. IEEE Transactions on Signal Processing 45(1): p 82–89.

[266] Iltis RA & Mailaender L (1996) An adaptive multiuser detector with joint amplitude and delay estimation. IEEE Transactions on Communications 44(11): p 1561–1571.

[267] Lim TJ & Rasmussen LK (1997) Adaptive symbol and parameter estmation in asynchronous multiuser CDMA detectors. IEEE Transactions on Communications 45(2): p 213–220.

[268] Steinberg Y & Poor HV (1994) Sequential amplitude estimation in multiuser communications. IEEE Transactions on Information Theory 40(1): p 11–20.

[269] Steinberg Y & Poor HV (1994) On sequential delay estimation in wideband digital communication systems. IEEE Transactions on Information Theory 40(5): p 1327–1333.

[270] Moon TK, Xie Z, Rushforth CK & Short RT (1994) Parameter estimation in a multi-user communication system. IEEE Transactions on Communications 42(8): p 2553–2560.

[271] Halford KW & Brandt-Pearce M (1994) User identification and multiuser detection of $l$ out of $k$ users in a CDMA system. Proc. Conference on Information Sciences and Systems (CISS), Princeton University, Princeton, New Jersey, USA, 1: p 115–120.

[272] Halford KW & Brandt-Pearce M (1995) Maximum likelihood detection and estimation for new users in CDMA. Proc. Conference on Information Sciences and Systems (CISS), The Johns Hopkins University, Baltimore, Maryland, USA, 1: p 193–198.

[273] Mitra U & Poor HV (1996) Activity detection in a multi-user environment. Wireless Personal Communications, Kluwer Academic Publishers 3(1-2): p 149–174.

[274] Joutsensalo J (1996) A subspace method for model order estimation in CDMA. Proc. IEEE International Symposium on Spread Spectrum Techniques and Applications (ISSSTA), Mainz, Germany, 2: p 688–692.

[275] Liu H & Xu G (1996) A subspace method for signature waveform estimation in synchronous CDMA systems. IEEE Transactions on Communications 44(10): p 1346–1354.

[276] Johnson DH, Lee YK, Kelly OE & Pistole JL (1996) Type-based detection for unknown channels. Proc. IEEE International Conference on Acoustics, Speech, and Signal Processing (ICASSP), Atlanta, Georgia, USA, p 2475–2478.

[277] Djuric PM & Guo M (1997) A novel approach to multiuser detection for CDMA systems. Proc. IEEE Vehicular Technology Conference (VTC), Phoenix, Arizona, USA, 2: p 563–566.

[278] Lee YK, Johnson DH & Kelly OE (1997) Type-based detection for spread spectrum. Proc. IEEE International Conference on Communications (ICC), Montreal, Canada.

[279] Aazhang B, Paris BP & Orsak G (July 1992) Neural networks for multiuser detection in code-division multiple access systems. IEEE Transactions on Communications 40(7): p 1212–1222.

[280] Mitra U & Poor HV (1995) Adaptive receiver algorithms for near-far resistant CDMA. IEEE Transactions on Communications 43(2/3/4): p 1713–1724.

[281] Hottinen A (1994) Self-organizing multiuser detection. Proc. IEEE International Symposium on Spread Spectrum Techniques and Applications (ISSSTA), Oulu, Finland, 1: p 152–156.

[282] Mitra U & Poor HV (1994) Neural network techniques for adaptive multi-user demodulation. IEEE Journal on Selected Areas in Communications 12(9): p 1460–1470.

[283] Miyajima T, Hasegawa T & Haneishi M (1993) On the multiuser detection using a neural network in code-division multiple-access communications. IEICE Transactions on Communications E76-B(9): p 961–968.

[284] Miyajima T & Hasegawa T (1996) Multiuser detection using a Hopfield network for asynchronous code-division multiple-access systems. IEICE Transactions on Fundamentals of Electronics Communications and Computer Sciences E79-A(12): p 1963–1971.

[285] Proakis JG & Manolakis DG (1992) Digital Signal Processing: Principles, Algorithms and Applications Macmillan, New York City, New York, USA, 2nd edn.

[286] Ludyk G (1985) Stability of Time-Variant Discrete-Time Systems. In: Hartmann I (ed) Advances in Control Systems and Signal Processing, vol 5, Friedr. Vierweg & Sohn, Braunschweig, Germany.

[287] Barrett MJ (1987) Error probability for optimal and suboptimal quadratic receivers in rapid Rayleigh fading channels. IEEE Journal on Selected Areas in Communications 5(2): p 302–304.

[288] Mämmelä A & Kaasila VP (1994) Prediction, smoothing and interpolation in adaptive diversity reception. Proc. IEEE International Symposium on Spread Spectrum Techniques and Applications (ISSSTA), Oulu, Finland, p 475–478.

[289] Latva-aho M, Juntti M & Heikkilä M (1997) Parallel interference cancellation receiver for DS-CDMA systems in fading channels. Proc. IEEE International Symposium on Personal, Indoor, and Mobile Radio Communications (PIMRC), Helsinki, Finland, 2: p 559–564.

[290] Pan CT & Plemmons RJ (1989) Least squares modifications with inverse factorizations: parallel implications. Journal of Computational and Applied Mathematics 27: p 109–127.

[291] Stoer J & Bulirsch R (1993) Introduction to Numerical Analysis. Springer-Verlag, New York City, New York, USA.

[292] Hestenes MR & Stiefel E (1952) Methods of conjugate gradients for solving linear systems. Journal of Research of the National Bureau of Standards 49(6): p 409–436.

# Stability analysis of linear detectors

**Proof of equations (3.14) and (3.15):** We define partitions

$$\mathcal{R}_N = \begin{pmatrix} \mathcal{R}_{N-1} & \boldsymbol{\gamma}_{N-1} \\ \boldsymbol{\gamma}_{N-1}^\top & \mathbf{R}_N(0) \end{pmatrix} \in \mathbb{R}^{NK \times NK}, \tag{A1.1}$$

where $\mathcal{R}_{N-1} \in \mathbb{R}^{(N-1)K \times (N-1)K}$,

$$\boldsymbol{\gamma}_{N-1} = \begin{pmatrix} \mathbf{0}_K & \cdots & \mathbf{0}_K & \mathbf{R}_N(1) \end{pmatrix}^\top \in \mathbb{R}^{(N-1)K \times K}, \tag{A1.2}$$

and

$$\mathcal{T}_N = \mathcal{R}_N^{-1} = \begin{pmatrix} \mathcal{C}_{N-1} & \boldsymbol{\alpha}_{N-1} \\ \boldsymbol{\alpha}_{N-1}^\top & \mathbf{T}_{N,N}(N) \end{pmatrix} \in \mathbb{R}^{NK \times NK}, \tag{A1.3}$$

where $\mathcal{C}_{N-1} \in \mathbb{R}^{(N-1)K \times (N-1)K}$, and $\boldsymbol{\alpha}_{N-1} \in \mathbb{R}^{(N-1)K \times K}$.

By applying the matrix inversion formulae [88, pp. 571-572]

$$(\mathbf{A} + \mathbf{BCD})^{-1} = \mathbf{A}^{-1} - \mathbf{A}^{-1}\mathbf{B}(\mathbf{DA}^{-1}\mathbf{B} + \mathbf{C}^{-1})^{-1}\mathbf{DA}^{-1}, \tag{A1.4}$$

$$\begin{pmatrix} \mathbf{A} & \mathbf{B} \\ \mathbf{C} & \mathbf{D} \end{pmatrix}^{-1} =$$

$$\begin{pmatrix} (\mathbf{A} - \mathbf{BD}^{-1}\mathbf{C})^{-1} & -(\mathbf{A} - \mathbf{BD}^{-1}\mathbf{C})^{-1}\mathbf{BD}^{-1} \\ -(\mathbf{D} - \mathbf{CA}^{-1}\mathbf{B})^{-1}\mathbf{CA}^{-1} & (\mathbf{D} - \mathbf{CA}^{-1}\mathbf{B})^{-1} \end{pmatrix}, \tag{A1.5}$$

and the fact that $\mathcal{R}_N$ and $\mathcal{T}_N$ are symmetric we obtain the following recursion formulae

$$\mathcal{C}_{N-1} = \mathcal{T}_{N-1} + \mathcal{T}_{N-1}\boldsymbol{\gamma}_{N-1}\mathbf{T}_{N,N}(N)\boldsymbol{\gamma}_{N-1}^\top\mathcal{T}_{N-1}, \tag{A1.6}$$

$$\boldsymbol{\alpha}_{N-1}^\top = -\mathbf{T}_{N,N}(N)\boldsymbol{\gamma}_{N-1}^\top\mathcal{T}_{N-1}. \tag{A1.7}$$

Now (3.14) and (3.15) follow by the definitions of $\mathcal{T}_{N-1}$, $\boldsymbol{\gamma}_{N-1}$, and $\boldsymbol{\alpha}_{N-1}$. $\diamond$

**Proof of Proposition 1**: Assume that the decorrelating detector is stable, and assume that integer $j$ is such that $N \to \infty$ implies $(N - j) \to \infty$[1]. Then

[1]Condition states that $j$ is such that its distance to $N$ approaches infinity as $N$ approaches infinity. The condition is satisfied, e.g., if $N = cj$, where $c$ is an arbitrary constant. For example, since $N = 2P + 1$, it follows that $N \to \infty \Rightarrow P \to \infty$.

we have by the stability of the decorrelating detector $\mathbf{T}_{N-1,j}(N-1) \to \mathbf{0}_K$, as $N \to \infty$. Assume that both $i$ and $j$ are such that $N \to \infty$ implies $(N-i) \to \infty$ and $(N-j) \to \infty$. Then the increment part in (3.14) approaches zero matrix as $N \to \infty$, since both $\mathbf{T}_{N-1,i}(N-1)$ and $\mathbf{T}_{N-1,j}(N-1) \to \mathbf{0}_K$, as $N \to \infty$. This guarantees the existence of a unique asymptotic limit for $\mathbf{T}_{i,j}(N-1)$. Thus, the uniqueness of the blocks $\mathbf{T}_{i,P+1}(N-1)$, $i = -P, \ldots, P$ follows. Since the decorrelating detector $\mathcal{D}_N$ consists of the blocks $\mathbf{T}_{i,P+1}(N-1)$, $i = -P, \ldots, P$ the uniqueness of the IIR decorrelating detector has been shown. The uniqueness of the LMMSE detector follows with exactly similar arguments. The uniqueness of the noise-whitening detector follows easily from the uniqueness of the decorrelating detector by analyzing the Cholesky factor of $\mathcal{T}_N$ as $N \to \infty$. $\diamond$

**Proof of Proposition 2**: The result follows by manipulation of (3.11). By the definition of $\bar{\mathcal{R}}^{(n)}$, i.e., by $\bar{\mathcal{R}} = \left(\boldsymbol{\zeta}_1, \mathcal{R}^{(n)}, \boldsymbol{\zeta}_2\right) \in \mathbb{R}^{NK \times (N+2)K}$, we can write

$$\bar{\mathcal{R}}^{(n)\top}(\mathcal{R}^{(n)})^{-1}\bar{\mathcal{R}}^{(n)} = \begin{pmatrix} \boldsymbol{\zeta}_1^\top(\mathcal{R}^{(n)})^{-1}\boldsymbol{\zeta}_1 & \boldsymbol{\zeta}_1^\top & \boldsymbol{\zeta}_1^\top(\mathcal{R}^{(n)})^{-1}\boldsymbol{\zeta}_2 \\ \boldsymbol{\zeta}_1 & \mathcal{R}^{(n)} & \boldsymbol{\zeta}_2 \\ \boldsymbol{\zeta}_2^\top(\mathcal{R}^{(n)})^{-1}\boldsymbol{\zeta}_1 & \boldsymbol{\zeta}_2^\top & \boldsymbol{\zeta}_2^\top(\mathcal{R}^{(n)})^{-1}\boldsymbol{\zeta}_2 \end{pmatrix}. \tag{A1.8}$$

Thus, except for the edges (the first and last $K$ columns and rows) the matrix

$$\bar{\mathcal{H}}^{(n)} = (\bar{\mathcal{R}}^{(n)\top}(\mathcal{R}^{(n)})^{-1}\bar{\mathcal{R}}^{(n)} + \sigma^2\bar{\mathcal{E}}^{-1}) \tag{A1.9}$$

is the same as

$$\mathcal{H} = (\mathcal{R}^{(n)} + \sigma^2(\mathcal{E}^{(n)})^{-1}). \tag{A1.10}$$

If the assumptions of the Proposition 2 are valid, $\mathbf{T}_{N,1}(N) \to 0$, as $N \to \infty$, and

$$\boldsymbol{\zeta}_1^\top(\mathcal{R}^{(n)})^{-1}\boldsymbol{\zeta}_2 = \mathbf{R}^{(n-P-1)}(1)\mathbf{T}_{N,1}^\top\mathbf{R}^{\top(n+P+1)}(1) \to 0, \text{ as } N \to \infty. \tag{A1.11}$$

By utilizing the fact that the mathematical structure of the decorrelating and the LMMSE detectors is similar, it can be seen from (3.14) that the effect of the first and the last diagonal blocks of $\bar{\mathcal{H}}^{(n)}$ on the middle block column of $(\bar{\mathcal{H}}^{(n)})^{-1}$ goes to zero as $N \to \infty$. Thus, we have shown that

$$\text{mbc}\left\{(\bar{\mathcal{H}}^{(n)})^{-1}\right\} \to \text{mbc}\left\{\mathcal{H}^{-1}\right\}, \text{ as } N \to \infty. \tag{A1.12}$$

Recall that the optimal FIR LMMSE detector is the middle block column of $(\mathcal{R}^{(n)})^{-1}\bar{\mathcal{R}}^{(n)}(\bar{\mathcal{H}}^{(n)})^{-1}$ by (3.11). It is easy to verify by definitions that

$$(\mathcal{R}^{(n)})^{-1}\bar{\mathcal{R}}^{(n)} = \begin{pmatrix} (\mathcal{R}^{(n)})^{-1}\boldsymbol{\zeta}_1 & \mathbf{I}_{NK} & (\mathcal{R}^{(n)})^{-1}\boldsymbol{\zeta}_2 \end{pmatrix}. \tag{A1.13}$$

Matrix $(\mathcal{R}^{(n)})^{-1}\bar{\mathcal{R}}^{(n)}$ is now identity except the first and last block columns. By the stability assumptions the first and last blocks of the middle block column of $(\bar{\mathcal{H}}^{(n)})^{-1}$ approach zero so that the effect of the first and last block of matrix $(\mathcal{R}^{(n)})^{-1}\bar{\mathcal{R}}^{(n)}$ vanishes asymptotically. Thus, $(\mathcal{R}^{(n)})^{-1}\bar{\mathcal{R}}^{(n)}$ acts asymptotically ($N \to \infty$) as an identity to the middle block column of the matrix $(\mathcal{R}^{(n)})^{-1}\bar{\mathcal{R}}^{(n)}\bar{\mathcal{H}}^{(n)}$. Proposition 2 is now proved by the above and (A1.12). $\diamond$

**Discussion on expression (3.19) to be valid**: First note that by the definition of $\bar{\mathcal{R}}^{(n)}$, we have

$$\bar{\mathcal{R}}^{(n)}\bar{\mathcal{R}}^{(n)\top} = \mathcal{R}^2 + \boldsymbol{\zeta}_1\boldsymbol{\zeta}_1^\top + \boldsymbol{\zeta}_2\boldsymbol{\zeta}_2^\top. \tag{A1.14}$$

The structure of the matrix $\bar{\mathcal{R}}^{(n)}\bar{\mathcal{R}}^{(n)\top}$ is similar to that of $\mathcal{R}^{(n)}$. Furthermore, the matrix is the same as $\mathcal{R}^2$ except the perturbations caused by $\boldsymbol{\zeta}_1\boldsymbol{\zeta}_1^\top$ and $\boldsymbol{\zeta}_2\boldsymbol{\zeta}_2^\top$ to the first and last diagonal blocks. Now it easy to understand, that under conditions similar to (3.17) being true the middle block row (or column) of $(\bar{\mathcal{R}}^{(n)}\bar{\mathcal{R}}^{(n)\top})^{-1}$ approaches the middle block row (or column) of $\mathcal{R}^{-2}$. If, on the other hand, that is the case, it is easy to see from (3.10) that $\bar{\mathcal{D}}_{[d]N} \to \mathcal{D}_{[d]N}$, as $N \to \infty$, because the zero blocks of $\bar{\mathcal{R}}^{(n)}$ remove the effect of perturbations caused by $\boldsymbol{\zeta}_1\boldsymbol{\zeta}_1^\top$ and $\boldsymbol{\zeta}_2\boldsymbol{\zeta}_2^\top$ to the first and last diagonal blocks of $\bar{\mathcal{R}}^{(n)}\bar{\mathcal{R}}^{(n)\top}$ as $N$ is sufficiently large.

# Eigenanalysis of detection based on conjugate gradient algorithm

Let the correlation matrix (2.37) be presented with the eigenvalue decomposition [291, Chap. 6]

$$\mathcal{R}^{(n)} = \mathcal{U}\mathbf{\Lambda}\mathcal{U}^{\top}, \tag{A2.1}$$

where

$$\mathbf{\Lambda} = \mathrm{diag}(\lambda_1, \lambda_2, \ldots, \lambda_{NK}), \tag{A2.2}$$

$\lambda_i, i = \{1, 2, \ldots, NK\}$ are the eigenvalues of $\mathcal{R}^{(n)}$, and the matrix $\mathcal{U} \in \mathbb{R}^{NK \times NK}$ includes the corresponding orthonormal eigenvectors in its columns. Let $\mathbf{u}_i$ be the $i$th column of $\mathcal{U}$. Let the estimation error vector of the decorrelating detector output be

$$\boldsymbol{\epsilon}_d = \hat{\boldsymbol{h}}_d - \boldsymbol{y} = \Big[(\mathcal{R}^{(n)})^{-1} - \mathbf{I}_{NK}\Big]\boldsymbol{y} = \sum_{i=1}^{NK}(\frac{1}{\lambda_i} - 1)(\mathbf{u}_i^{\top}\boldsymbol{y})\mathbf{u}_i, \tag{A2.3}$$

and similarly the estimation error vector of the LMMSE detector output

$$\boldsymbol{\epsilon}_{ms} = \hat{\boldsymbol{h}}_{ms} - \boldsymbol{y}. \tag{A2.4}$$

To explain the better performance of the CG method in comparison to the ideal decorrelating detector it is first justified, why

$$\|\boldsymbol{\epsilon}_{ms}\| < \|\boldsymbol{\epsilon}_d\| \tag{A2.5}$$

tend to be true, when there is no near-far problem. The result in (A2.5) states that the LMMSE detector is a compromise between the conventional single user matched filter detector and the decorrelating detector. Assume that the energies satisfy $E_k = E_l, \forall k, l$ and

$$\gamma = \frac{E_k}{\sigma^2}. \tag{A2.6}$$

Then it follows from (A2.3)

$$\|\boldsymbol{\epsilon}_d\|^2 = \sum_{i=1}^{NK}(\frac{1}{\lambda_i} - 1)^2(\mathbf{u}_i^{\top}\boldsymbol{y})^2 = \sum_{i=1}^{NK} f(\lambda_i)(\mathbf{u}_i^{\top}\boldsymbol{y})^2, \tag{A2.7}$$

where $f(x) = (\frac{1}{x} - 1)^2$. Since the LMMSE detector is similar to the decorrelating detector $\mathcal{R}^{-1(n)}$ replaced by $(\mathcal{R}^{(n)} + \gamma \mathbf{I}_{NK})^{-1}$, it follows that

$$\|\boldsymbol{\epsilon}_{ms}\|^2 = \sum_{i=1}^{NK} (\frac{1}{\lambda_i + \gamma^{-1}} - 1)^2 (\mathbf{u}_i^\top \boldsymbol{y})^2 = \sum_{i=1}^{NK} f(\lambda_i + \gamma^{-1})(\mathbf{u}_i^\top \boldsymbol{y})^2, \tag{A2.8}$$

By its derivative

$$\frac{df(x)}{dx} = 2(\frac{1}{x^2} - \frac{1}{x^3}) \tag{A2.9}$$

it is easy to see that $f(x)$ decreases very fast, when $x < 1$, and increases slowly, when $x > 1$. Usually some of the eigenvalues $\lambda_i$ are greater than 1 and some are smaller than 1. This implies that the values $f(\lambda_i + \gamma^{-1})$ tend to be much smaller than values $f(\lambda_i)$, when $\lambda_i < 1$. Similarly, the values $f(\lambda_i + \gamma^{-1})$ tend to be only slightly larger than values $f(\lambda_i)$, when $\lambda_i > 1$ justifying

$$\|\boldsymbol{\epsilon}_{ms}\| < \|\boldsymbol{\epsilon}_d\|. \tag{A2.10}$$

The CG method used for decorrelating detection reduces distance

$$\boldsymbol{\varepsilon}(m) = \hat{\boldsymbol{h}}(m) - \hat{\boldsymbol{h}}_d. \tag{A2.11}$$

at each iteration by smoothly increasing the subspace in which $\Omega(\boldsymbol{h})$ is minimized. Assume that the initial guess is

$$\hat{\boldsymbol{h}}(0) = \boldsymbol{y}. \tag{A2.12}$$

The LMMSE detector output is geometrically between the MF bank and decorrelating detector output vectors. Therefore, it is understandable that there exists $m$ such that for the $m$th iteration the estimate $\hat{\boldsymbol{h}}(m)$ is closer to $\hat{\boldsymbol{h}}_{ms}$ than to $\hat{\boldsymbol{h}}_d$. The CG estimate in a way sweeps through the LMMSE estimate.